UNIVERSITY OF TORONTO

JULS

Journal of Undergraduate Life Sciences

Science in a Global Age

Volume 5 • Issue 1 • Spring 2011

McMaster School of Biomedical Engineering

Take the Next Step:
Graduate Studies in Biomedical Engineering

A new type of professional is needed to help meet the health care needs of tomorrow, one able to work at the intersect of science, medicine and engineering. The McMaster School of Biomedical Engineering offers studies at the Master's and Ph.D. levels to help develop that expertise. If you have a background in science, health care or engineering, and are interested in working on leading-edge research, in state-of-the-art facilities, with world-renowned faculty, take the next step and contact us today.

- **biomaterials and tissue engineering**
- **medical imaging**
- **biomedical devices and instrumentation**
- **medical robotics**
- **biophotonics**
- **bioprocessing**

www.msbe.mcmaster.ca

McMaster University

Learn more about engineering graduate studies at McMaster by visiting: www.mcmaster.ca/graduatestudies

Volume 5 • No. 1 • Spring 2011

JULS

Contents

JULS
Spring 2011

JULS
Journal of Undergraduate Life Sciences
University of Toronto

Call for Submissions

The *University of Toronto Journal of Undergraduate Life Sciences (JULS)* is always looking for submissions that showcase the research achievements of undergraduate life science students. We welcome manuscripts in the form of Research Articles or Reviews. Submissions must come from University of Toronto undergraduate students or undergraduate students outside of U of T who have conducted research for at least three months under the supervision of a faculty member at U of T.

Research articles should present original research and address an area of the life sciences. Mini-reviews should focus on a specific scientific topic of interest or related to the research work of the author. Research articles should be between 2,000-3,000 words and mini-reviews between 1,500-2,000 words. All works must not have been previously submitted or published in another undergraduate journal. The deadline for submissions for each issue will appear on the JULS website at http://juls.library.utoronto.ca.

Contact Us

JULS is always looking for contributions from writers, artists, designers, and editors. Please contact JULS at juls@utoronto.ca if you are interested in joining the JULS team, or have any questions regarding any matter pertaining to the journal, or visit our websites: http://juls.sa.utoronto.ca or http://jps.library.utoronto.ca/index.php/juls.

© 2011 University of Toronto Journal of Undergraduate Life Sciences (JULS). Authors retain all rights to their work published in JULS except the right to publish in another undergraduate journal. The content and/or opinions expressed in this publication are expressively those of the authors and do not necessarily reflect the views of the University of Toronto or JULS.

Staff List

Editor-in-Chief
Tayyaba Jiwani
Jong Park

Senior Editors
Nicole Choi
John Janetzko
Siyang Li
Nancy Song

News Editor
Ana Komparic

Review Board Managers
Richard Cheng
Katarzyna Swica

Layout Managers
Maggie Siu
Ellen Wong

External Affairs Managers
Allen Jian
Qiudi (Henry) Zeng

Editorial Review Board
Karan Joshua Abraham
Ahmed Aly
Sinead Brady
Jingwei Chen
Katherine Li
Tina Binesh Marvasti
Jin Suk Park
Eric Pun
Matthew Purser
Asha Sardar
Shalini Sivathasan
Supreet Sunil
Natalie Yavorska
Matthew Yu
Dun (Roddy) Zhou

Layout Associates
Jin Liu
Victor Liu
Deanna Lue
Rehana Siddiqi
Andrea Wu

Faculty Review Board
Dr. Cathy Barr
Dr. David Dansereau
Irwin Adam Eydelnant
Dr. Anthony Gramolini
Dr. Claire Healy
Dr. Tony Harris
Dr. Ayal Schaffer
Dr. Stephen Scherer
Dr. Jeremy Schofield
Dr. Doug Templeton
Dr. Aaron Wheeler
Dr. Melanie Woodin

Cover Photo Credits
Modified from Flickr:
Cyberchemist, "Carbon Monoxide"

Volume 5 • No. 1 • Spring 2011

Letter From the Editors

Dear reader,

It is our pleasure to present to you the 2011 issue of the University of Toronto *Journal of Undergraduate Life Sciences (JULS)*. This year we are celebrating our fifth anniversary, an important milestone that represents the vision and dedication of everyone involved in the journal since its founding. Without the countless hours of work put in by our past and current editors, review board members, layout associates, and external affairs staff, as well as the contributions from our authors, commentators, and sponsors, you would not be holding this beautiful edition in your hands right now.

Our theme for the issue reflects this spirit of collaboration and support. We are now living in a global age: a time when scientists must be particularly mindful of the ramifications of their research, and where progress in the life sciences can no longer occur in isolation. The undergraduate students publishing in our journal are investigating the cancer fighting properties of Chinese herbal medicine and the changing coral reef ecosystems in Barbados. The reporters for our news section are highlighting groundbreaking advances here at the University of Toronto, Canada's premiere institution for biomedical research. And the senior staff, who had the privilege to interview some of the 2010 Canada Gairdner Award Laureates, are describing the lives of world renowned scientists in the United Kingdom, Thailand, and the United States.

Browsing through this issue, we hope that you will be as excited as we are to explore science in a global age.

Sincerely,

Tayyaba Jiwani and Jong Park
Co-Editors-in-Chief, 2010-2011

NOTE: All articles in this issue as well as supplementary information are freely available online at http://juls.library.utoronto.ca/. If you would like to join the JULS team, submit an article or have any comments or suggestions, please feel free to contact us as at juls@utoronto.ca.

Endoglin Identified as a Potential Diagnostic Tool for Preeclampsia

Jessica Ebrahimi

Preeclampsia is a life-threatening pregnancy condition and the leading cause of maternal and fetal mortality and morbidity.

The complications during pregnancy appear to be primarily related to the placenta as evidenced by the gradual cessation of disease symptoms soon after delivery. Affected newborns may be born with devastating conditions such as cerebral palsy, blindness, deafness, and epilepsy. Both mother and infant are also at increased susceptibility for developing hypertension, cardiac problems and diabetes later in life. Dr. Isabella Caniggia at the Samuel Lunenfeld Institute is the leading authority on preeclampsia research. She seeks to investigate the molecular basis of the disease and to find innovative therapeutic strategies for early risk assessment and treatment of expectant mothers.

Normal placental development requires successful invasion of the maternal vasculature by placental epithelial cells known as trophoblasts. One of the key regulators of trophoblast invasion is transforming growth factor beta-3 (TGFβ3), a protein that controls cellular differentiation and proliferation. In preeclampsia, an up-regulation of TGFβ3 and its co-receptor, endoglin, are believed to be responsible for shallow trophoblast invasion and consequently impaired and hypoxic placental conditions [1].

To investigate endoglin as a potential indicator of preeclampsia, the Caniggia lab examined the effect of oxygen and TGFβ3 expression on endoglin levels using in vitro cultures of placental villous explants. They found that exposure of explants to low oxygen concentrations (3% O2) resulted in increased endoglin expression in comparison to control conditions (20% O2) [2]. Furthermore, inhibition of TGFβ3 using anti-sense technology prevented hypoxia-induced endoglin overexpression and restored trophoblast invasive capabilities. Taken together, these findings suggest that the hypoxic conditions mediated by elevated TGFβ3 levels in preeclampsia cause an overproduction of endoglin, which inhibits trophoblast invasion and ultimately leads to an impaired placental environment for fetal development. In the mother, the excess endoglin in the circulation exacerbates vascular damage, leading to the disease symptoms of hypertension and proteinuria (the presence of excess proteins in urine).

Dr. Isabella Caniggia at the Samuel Lunenfeld Institute is the leading authority on preeclampsia research.

Consistent with in vitro observations, Dr. Caniggia reported that women diagnosed with preeclampsia have elevated endoglin levels throughout pregnancy, as opposed to normal pregnancies in which endoglin elevation is present only during early gestation. This finding has established endoglin as an important biomarker, and has since enticed biomedical companies to work alongside Dr. Caniggia to use endoglin as a diagnostic tool to assess preeclampsia risk in expectant mothers. Since a cure has yet to be found, early detection is the most promising therapeutic strategy which could potentially lead to improved health outcomes for both mother and infant.

The next steps in Dr. Caniggia's research will be to validate the endoglin biomarker in clinical trials and to achieve a greater understanding of other mechanisms that may play a role in abnormal trophoblast regulation in preeclampsia.

References

1. Caniggia, I., Taylor, C.V., Ritchie, J.W.K., Lye, S.J., and M. Letarte. Endoglin regulates trophoblast differentiation along the invasive pathway in human placental villous explants. Endocrinology, 1997. 138: p. 4977–4988.
2. Yinon, Y., Nevo, O., Xu, J., Many, A., Rolfo, A., Todros, T., Post, M., and I. Caniggia. Severe intrauterine growth restriction pregnancies have increased placental endoglin levels: hypoxic regulation via transforming growth factor-β3. Am J Pathol, 2008. 172(1): p. 77–85.

Research on Engineering Photoactive Yellow Proteins Aims to Discover its Function

Charmaine Ross

In previous years, neurobiology research focused predominantly on how electrophysiological techniques could measure and manipulate neuron activity.

Recently however, optical techniques have become useful due to the development of newly synthesized photosensitive tools. The general strategy for making a photosensitive tool is to couple a photoisomerizable molecule, or "photoswitch," with an ordinary ion channel or receptor to make it sensitive to light. For reversible photocontrol, a light-sensitive system that undergoes reversible photochemistry is required.

Dr. Andrew Woolley's research on Photoactive Yellow Proteins (PYPs) is very important in this regard. PYPs are among the most common naturally-occurring photoswitches that undergo reversible photochemistry [1,2]. They are small, 125-residue, water-soluble, light sensitive proteins that contain the chromophore p-hydroxycinnamic acid. In the dark, the chromophore is in the trans, deprotonated state and the protein is well folded. This state absorbs in the blue light spectrum, so it appears yellow when visualized. When a blue photon is absorbed, the chromophore can isomerize to the cis state and become protonated. Since the cis state absorbs near 350 nm, the protein now appears colourless. Moreover, in the cis, protonated state, the protein partially unfolds. Finally, when the blue light source is removed, the protein spontaneously refolds and the chromophore re-isomerizes to the trans form [2].

When PYP is used as a genetically encoded light switch and made to fuse to transcription factors such as GCN4, it can control their activity. In 2010, Morgan et al. reported a structure-based design of a photocontrolled bZIP-type DNA binding protein based on PYP. The bZIP- type DNA binding protein, GCN4Δ25PYP-v2, was a hybrid of the ideal homodimeric bZIP protein GCN4 and PYP, created from the fusion of the C-terminal zipper region of GCN4-bZIP with the N-terminal cap of PYP [2].

Morgan et al. found that the designed fusion protein is monomeric in the dark since fluorescence, circular dichroism, NMR and analytical ultracentrifugation data indicated that the zipper domain is hidden. This discovery suggests that designed bZIP-PYP fusions could lead to a range of opto-genetic tools for the manipulation of bZIP proteins. Morgan et al. also used the photocontrolled folding or unfolding process of PYP to sterically prevent or allow an interaction required for function. This allows the possibility of determining the function of PYP by selectively activating or inactivating these proteins in a spatially and temporally precise manner. Further research by the Woolley lab seeks to investigate the possibility of a family of related photocontrolled proteins for manipulating bZIP activity [2] and to suggest ways to improve designed photocontrolled transcription factors.

References

1.Kramer HR, Fortin LD, Trauner D, New photochemical tools for controlling neuronal activity. Curr Opin Neurobiol, 2009. 19 (5): 544 – 552.
2.Morgan SA, Al-Abdul-Wahid S, Woolley GA, Structure-Based Design of a Photocontrolled DNA Binding Protein. Journal of Molecular Biology, 2010. 399 (1): 94 - 112.

Development of an Array of Hypothalamic Neuronal Cell Models

Matthew Purser

Dr. Denise Belsham is a Professor and Principal Investigator in the Department of Physiology at the University of Toronto.

Her lab seeks to understand the integrated nature of how signals from the body control neuroendocrinology by studying the hypothalamus, a vital brain centre and the body's key regulator of reproduction, temperature control and feeding.

The lack of information available concerning the molecular mechanisms by which the hypothalamus achieves its diverse functions is in part due to the difficulty of performing mechanistic studies in whole brain or animal models, given the complex structure of the hypothalamus. The "absence of appropriate models" by which to investigate the direct regulation and signal transduction of specific neuropeptides in the hypothalamus prompted Dr. Belsham to develop her own models. What began as an effort to immortalize only Neuropeptide Y neurons, has since expanded into an extensive array of immortalized, clonal hypothalamic neuronal cell lines from embryonic and adult mouse hypothalamii, which are now employed in research labs around the world [1, 2]. These cell lines are the first available models which permit the analysis of neuropeptide gene regulation and signal transduction events involved in the direct hormonal control of the hypothalamus at the level of an individual neuron.

Since developing these lines, Dr. Belsham has enjoyed much

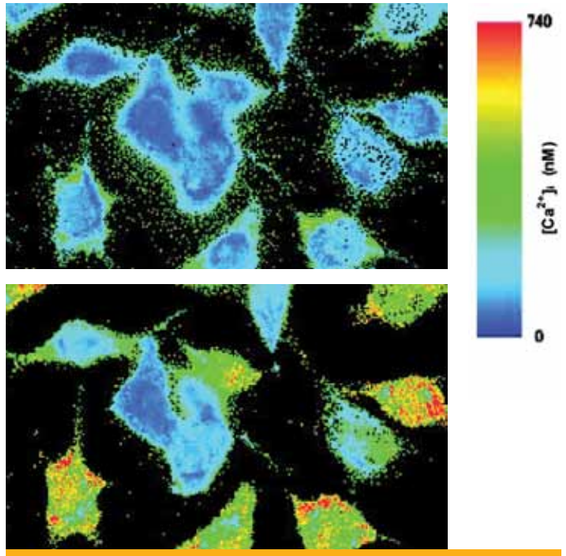

Depolarization of N-38 nueroendocrine cells causes a significant increase in intracellular calcium levels [1].

success following many seminal discoveries. Once thought to be incapable of cell division, she has shown that adult neurons are able to replicate themselves following their immortalization through the induction of neurogenesis [2]. Her lab was also one of the first to elucidate the molecular events in the development of cellular insulin resistance in an in vitro model system [3].

Currently, the lab is focused on studying the development of insulin and leptin resistance, generating new models for specific neuropeptidergic neurons, and elucidating the link between reproduction, energy homeostasis, and other neuroendocrine systems. Dr. Belsham's cell lines are also repeatedly used as models in drug development and in the generation of therapies for chronic diseases such as obesity and diabetes.

In the future, Dr. Belsham plans to address the need for more human-based cell models of the brain. At the moment, the only available cell models are derived from tumours, which exhibit numerous differences from endogenous cell populations. The creation of immortalized, clonal human hypothalamic cell lines will serve to uncover previously unrecognized differences between human and rodent cell signalling by comparing mechanistic studies performed on human lines with those already performed in the mouse hypothalamus. This has the potential to affect how numerous labs that employ mice view their data when considering the implications for humans.

References

1. D. D. Belsham et al. Generation of a phenotypic array of hypothalamic neuronal cell models to study complex neuroendocrine disorders. Endocrinology, 2004. 145:393-400.
2. D.D. Belsham et al. Ciliary neurotrophic factor recruitment of glucagon-like peptide-1 mediates neurogenesis, allowing immortalization of adult murine hypothalamic neurons. FASEB J., 2009. 23(12): 4256-65.
3. C.M. Mayer and D.D. Belsham. Central insulin signaling is attenuated by long-term insulin exposure via insulin receptor substrate-1 serine phosphorylation, proteasomal degradation, and lysosomal insulin receptor degradation. Endocrinology, 2010. 151(1): 75-84.

Cells on Demand

Mihir Soparkar

Fifty years after McCulloch and Till pioneered stem cell research at the University of Toronto, Dr. Peter Zandstra, a bioengineer at the Donnelly Centre for Cellular and Biomolecular Research, is working to harness its potential for cell-based therapies through bioprocess engineering.

The value of stem cells lies in their ability to self-renew and differentiate into different types of functionally mature cells. Zandstra is specifically interested in pluripotent stem cells (PSCs), which can be obtained from the inner cell mass of a pre-implantation blastocyst, or may be generated through reprogramming technologies, and are characterized by their ability to differentiate into any type of somatic cell [1]. However, the therapeutic utility of PSCs depends on the availability of useful cell quantities. According to Zandstra, his developments in increasing cell production and optimizing growth conditions will allow for the generation of pure populations of desired cell types [2]. "[If] we can one day produce cells like we now produce drugs... cells would be a permanent cure to many diseases if we could manufacture them in a way that they were robust, [and in] large numbers" says Zandstra. For example, a more effective solution for Type 1 diabetes, rather than insulin injections, could be to grow insulin-secreting cells, and then to transplant them into patients.

However, researchers face unique difficulties since the cells themselves are the desired product, instead of proteins isolated from them [3]. PSCs are sensitive to variations in their cellular microenvironment, or niche, and are commonly grown as a single layer on tissue-culture plastic. This method rapidly exhausts cultivation area and thus requires frequent intervention by the user which increases the risk of contamination. Additionally, this approach does not allow for adequate control of physiological parameters resulting in disparities between niches, thus causing uncontrolled cell differentiation [4].

Although PSCs and their differentiated counterparts are dependent on cell-cell aggregation for propagation, Zandstra has developed a technology that regulates cell-cell interactions in scalable culture by mass encapsulation of PSCs in agarose. The encapsulated cells can be placed in a stirred-suspension bioreactor, which simulates a physiological niche and suspends the cells in a liquid medium to grow large quantities in a finely controlled environment. This type of bioreactor homogenizes growth conditions by stirring the medium in which the cells live and allows for easy measurement and control of glucose, cytokine and oxygen concentrations as well as pH [2]. Combining this technique with low oxygen conditions known to promote PSC proliferation results in significantly increased cell output. In a separate project, Zandstra demonstrated that the trajectories and rate of PSC differentiation can be manipulated by patterning PSCs onto adhesive islands with defined colony diameters and distances between colonies [1].

By integrating successful strategies such as stirred-suspension bioreactors, colony size control, and hypoxic conditions, Zandstra has made headway toward producing clinically useful numbers of target cells [5]. He is now studying how transplanted cells interact with their environment and how their complex communication networks form to improve the next generation of cell-manufacturing technology.

References

1. Peerani, R., Rao, B.M., Bauwens, C., Yin, T., Wood, G.A., Nagy, A., Kumacheva, E., Zandstra, P.W., Niche-mediated control of human embryonic stem cell self-renewal and differentiation. The EMBO Journal, 2007. 26 (22): p. 4744-4755.
2. Dang, M.S., Gerecht-Nir, S., Chen, J., Itskovitz-Eldor, J., Zandstra, P.W., Controlled, Scalable Embryonic Stem Cell Differentiation Culture. Stem Cells, 2004. 22 (3): p. 275-282.
3. Kirouac, D.C., Zandstra, P.W., The systematic production of cells for cell therapies. Cell Stem Cell, 2008. 3 (4): p. 369-381.
4. Fok, E.Y.L., Zandstra, P.W., Shear-Controlled Single-Step Mouse Embryonic Stem Cell Expansion and Embryoid Body-Based Differentiation. Stem Cells, 2005. 23 (9): p. 1333-1342.
5. Niebruegge, S., Bauwens, C.L., Peerani, R., Thavandiran, N., Masse, S., Sevaptisidis, E., Zandstra, P.W., Generation of Human Embryonic Stem Cell-Derived Mesoderm and Cardiac Cells Using Size-Specified Aggregates in an Oxygen-Controlled Bioreactor. Biotechnology and Bioengineering, 2009. 102 (2): p. 493-507.

Female Bias of the *Dioecious Rumex hastatulus* Plant Species

Lisa St-Amant

Professor Spencer Barrett and his lab are conducting research on the evolution of plant reproductive systems, sexual dimorphisms, sex ratios and invasive species.

One of their current research projects involves the investigation of biased sex ratios in the dioecious plant populations of the Rumex hastatulus. Dioecious species possess separate male and female sexes and reproduce predominantly through outcrossing [1]. In nature, it is common to see a balanced 1:1 sex ratio in dioecious organisms [4]. According to Dr. Melinda Pickup, a postdoctoral fellow in Spencer Barrett's lab, "Approximately 6 % of plant species are dioecious, and only a small fraction of these exhibit biased sex ratios". Deviation from the more common 1:1 sex ratio can be indicative of potential selective pressures acting on a single sex [3].

The Barrett lab obtained samples from 46 populations across the United States to determine the extent of sexual bias in the Rumex hastatulus over a large geographic range and hence identify the cause of female bias. The plant samples were outcrossed to yield progeny for use in controlled experiments. The demographics of plants within different local mating environments were analyzed in relation to varying proximities of females to males.

Dr. Pickup explained that female plants within close proximity to males were found to exhibit greater bias than female plants that were located further away. While experimental analysis is ongoing to confirm the cause of female bias, two proposals have been made. First, pollen competition between females is presumed to be a factor in the correlation between female frequency and distance between sexes. This creates selective pressure on the female for genotypes that improve development of the pollen tubes in order to increase the prospect of fertilization. Second, female bias, which exhibits a lesser occurrence than male bias, is mainly observed in plant species where sex is determined by combinations of two or more forms of sex chromosomes [4]. The Rumex hastatulus plant species possesses the heteromorphic sex chromosomes XY (male) and XX (female) [3]. It is hypothesized that the degenerative Y chromosome, being less capable of recombination to dispel acquired mutations, is the cause for a lower male frequency in Rumex hastatulis species. This would affect the fitness of the male and, being in competition with the female for resources, would be a disadvantage for male survival.

Sex ratio analysis in different plant species provides the foundation for proper breeding of dioecious plants [1]. Knowledge of dioecious sex ratios can help foster improvements within the fields of biodiversity conservation, plant community restoration, biotechnology and agriculture [2]. Most agricultural plants are dioecious and knowledge of proper plant reproduction is therefore crucial in yielding large supplies of vegetative food for consumer use.

References

1. Barrett, S.C.H., et al., Ecological genetics of sex ratios in plant populations. Philosophical Transactions of the Royal Society B-Biological Sciences, 2010. 365 (1552): 2549-2557.
2. Barrett, S.C.H., Understanding plant reproductive diversity. Philosophical Transactions of the Royal Society B-Biological Sciences, 2010. 365 (1537): 99-109.
3. Conn, J.S. and U. Blum, Sex ratio of Rumex hastatulus: the effect of environmental factors and certation. Evolution, 1981. 35 (6): 1108-1116.
4. Lloyd, D.G., Female-predominant sex ratios in angiosperms. Heredity, 1974. 32 (1): 35-44.

JULS RESEARCH

Interactions of coral, algae, fish and abiotic factors on a eutrophic fringing reef in Barbados

Daniel Anstett[1], Mitalie Makhani[2], Yiqing Liang[3]

[1]Department of Ecology and Evolutionary Biology, University of Toronto St. George; [2]Department of Physical and Environmental Sciences, Department of Biological Sciences, University of Toronto Scarborough; [3]Department of Physical and Earth Sciences, University of Toronto Scarborough

Abstract

Many coral reefs worldwide have experienced deterioration due to increased anthropogenic disturbance and rising sea temperatures. Regardless of their complexity, fundamental patterns have been characterized for the reefs. While herbivorous fish can prevent harmful algal overgrowth, increases in macroalgae, depth, sedimentation and current strength have been linked to decline in corals. To better understand deteriorated reefs, we investigate these associations on two eutrophic fringing reefs near the Bellairs Research Institute in Barbados. Four transects were used to sample three depth zones, where coral and algae were quantified along with fish richness. Current and coral stress due to sedimentation were also assessed. We found that depth was not correlated with coral diversity or percent cover. However, the height of Porites astreoides coral colonies were significantly lower in shallow waters while herbivorous fish co-occurred with palatable algae at shallow depths. Furthermore, algae cover was positively correlated with coral diversity at medium depths, contrary to various other studies. Sedimentation was not found to be a significant predictor of coral distributions. Overall, the three-meter depth range examined in this study may not have been large enough to allow for variation in coral diversity across depths. P. astreoides may be shorter in shallower waters to prevent exposure to waves and air. At medium depths Porilithon pachydermum, a crustose algae, may be facilitating the initial establishment of corals rather than outcompeting them. Abiotic conditions favoring algal growth in shallow depths may maximize fish feeding. Overall, not all the expected patterns were seen. These differences may represent fundamentally altered patterns in reef ecosystem processes. Documenting these changing interactions across impacted reefs may help further understand their vulnerabilities.

Introduction

Coral reefs are becoming increasingly degraded worldwide due to human activities such as overfishing, coral mining and eutrophication (Hughes, 1994). El Niño-Southern Oscillation (ENSO) events and global climate change are also leading to increased ocean temperatures, resulting in coral bleaching (Glynn and WH, 1991). In the Caribbean, reef cover has been reduced from 50% to 10% in thirty years (Gardner et al., 2003). An understanding of the basic factors affecting reef sensitivities and coral distributions is fundamental in determining how to make these systems more resilient. Such expertise is critical for making informed conservation decisions and advancing effective management policies (Bellwood et al., 2004).

The distribution of coral species on a reef is the culmination of many biotic and abiotic factors. Species distributions are affected by unpredictable factors such as mortality due to disturbances or predators, climate change, and immigration (Karlson, 1998). On a smaller scale, local environmental variables, including light availability, competition, predation and habitat characteristics (such as current and sedimentation), affect species distribution (Karlson, 1998).

The existence of vertical reef zonation is evidence that depth is a major factor in coral distribution patterns. Light intensity and spectral quality decrease with increasing depth (Mundy, 1998) and individual coral species are often restricted to specific depth ranges depending on which light regimes and mechanical forces they are adapted to (Dana, 1976). Near the surface of the water, mechanical action and the risk of desiccation increases (Huston, 1985). Thus, coral richness is usually low near the surface, and then increases at medium depths, before declining at lower depths (Huston, 1985).

The presence of macroalgae on a reef is often associated with a lack of reef regeneration after disturbance (Foster, 1987). During such phase shifts, faster growing algae become the dominant growth form (Bellwood et al., 2004). The algae are capable of outcompeting the symbiotic algae living in the coral polyps (zooxanthellae) thereby overwhelming the corals (Tanner, 1995). Without adequate controls, these algae can cause significant levels of coral mortality. Algal growth can be controlled by herbivorous fish and urchins, which prevent smothering and coral loss (Ogden, 1978). In most areas of the Caribbean, the urchin *Diadema antillarum* served as the principle algae control agent of algae (Hay, 1984). However, due to habitat degradation and hurricane damage, its population has dropped by two orders of magnitude (Lessios, 1988). Herbivorous fish are critical to many Caribbean reefs (Bellwood et al., 2004) and they may be the only main remaining form of algal control. Consequently, their presence becomes even more important to the health of a reef.

Algal overgrowth can be associated with higher levels of sedimentation. Sedimentation effects coral diversity, species composition, and coverage by hindering their growth, recruitment, and recovery potential (Rogers, 1990). Particle suspension can reduce the amount of light reaching corals, and can also settle on coral surfaces, inhibiting both feeding and photosynthesis (Huston, 1985). This may result in a decline in growth rates and productivity as the corals allocate excess energy to sediment discharge (Diaz-Pulido, 2002). Thus, gradients in the distribution of coral species may exist due to different adaption responses to sedimentation. For example, corals can push sediments away using mucus secretion and ciliary action (Carlon, 1993). However, this expels the zooxanthellae in the process and results in an area of partial mortality, which is easily overgrown by algae (Carlon, 1993).

Oxygen concentration, salinity and temperature variation at the local scale have not been found to be important to coral distribution (Dana, 1976). However, current could either be beneficial, by flushing out sedimentation, or detrimental, by causing mechanical damage. It may also indirectly control coral distributions by affecting dispersal of coral larvae (Lewis, 1960). Current can thus lead to varied microclimatic conditions across the reef topography.

The study aims to identify factors that may affect coral distributions within a degraded reef. We investigate whether these factors are different from the aforementioned expected patterns. Apart from overall diversity, this study specifically examines *Porites astreoides* and *Favia fragum*, two common species of hard corals known to be abundant in Barbados (Dana, 1976). We also test the accuracy of using fish abundance as a predictor of palatable algae. We expect coral diversity to be highest at mid-depth zones, and corals to decrease with increasing currents, sedimentation stress and algal cover. As well, herbivorous fish should be attracted to areas with higher levels of palatable algae.

Materials and Methods

Study Site

Barbados is a non-volcanic island consisting largely of Pleistocene limestone. Coral reefs are only found on the western, leeward side (Lewis, 1960). Coral patches were studied on two fringing reefs off the coast of the Bellairs Research Institute. The reef was fairly shallow, with most coral colonies extending down to a maximum of three to four meters. We surveyed the study site for four days in February of 2010 during periods of low wave action. We found the reef to be fairly degraded. The limited, patchy distribution of coral was attributed to the recent hurricane damage and excess nutrients runoff due to agriculture and human habitation.

Study organisms

We studied species of coral, algae and herbivorous fish on the fringing reefs. Thirty-three species of scleractinian corals have been recorded from the island but only 13 were observed in this study, with the most common ones being *Porites astreoides* and *Favia fragum*. Also, two Millepora spp. and one species of gorgonian (*Erythropodium caribaeorum*) were observed. These were identified using the guide Reef Coral Identification (Humann, 2002). Eleven species of algae were observed, with representatives from the three most conspicuous phyla: green algae (Chlorophyta), brown algae (Phaeophyta), and red algae (Rhodophyta). These were identified using the guide Marine Plants of the Caribbean (Littler, 1989). One species of blue-green algae (Cyanophyta) was also present. Thirty-six species of herbivorous fish were observed at the study sites. These fish were identified using the guide Reef Fish Identification (Simpson, 1949).

Survey approach

Two transects were established on each reef. For every transect line, three quadrats each were randomly chosen for each of the three depth levels: shallow (<1 m), medium (1-2 m), and deep (2-3 m). In total, there were four transects and 36 quadrats. Each quadrat was 2x2 meters and established using a two-meter length of rope with rock weights on both ends, which acted as a visual guide to estimate the total square area. For each quadrat, percent cover by species was recorded for corals and algae. Coral species richness and species diversity were also estimated. The number and species of fish observed within each quadrat during a fifteen-minute time frame was recorded. The dimensions and heights of the most common coral, P. astreoides were also noted.

Sedimentation stress can be expressed as overgrowth of algae on coral individuals or partial mortality due to sediment deposition (Diaz-Pulido, 2002). Overgrowth was measured by quantifying algae percent cover. Coral sedimentation stress was estimated as percent mortality of corals in each quadrat. Current was measured for each quadrat using a ping-pong ball tied to a rock with fishing line. The currents were qualitatively described as still, slight, moderate, or strongly oscillating.

Statistical analyses

Coral diversity and distribution

The reciprocal of Simpsons diversity index (1/D) was computed (Simpson, 1949) using Microsoft Excel 2008. This number ranges upwards from one. A larger number signifies greater richness weighted by evenness. This index was calculated using coral percent cover for each reef (reef 1 and reef 2) and each depth zone (shallow, medium and deep). Coral species diversity within each reef and also between different depths was compared using a chi-square test.

A two-factor ANOVA was performed using Graph Pad Prism (version 5) to detect differences between depth and reef for five coral variables: total coral percent cover, coral species diversity, coral species richness, *Porites astreoides* height and area, and *Favia fragum* percent cover. We tested species-level differences for the height and area of the dominant species, which were present at most transects. There were a total of 36 replicates, with each transect being one unit of replication. This design was balanced in that the two reefs each had n=18 observations assigned to them and each depth had n=12 observations.

Coral distribution and algae cover

For each depth, the five coral variables were correlated against algae percent cover for that quadrat using Excel. Three regression lines on a single scatterplot were generated and tested for statistical significance using statistical analysis software SPSS 18.0 Student Version. The regression lines for the three depths were compared using three two-tailed t-tests using the formula

$$t = \frac{Slope_1 - Slope_2}{\sqrt{SE_{slope_1}^{\ 2} + SE_{slope_2}^{\ 2}}} \quad d.f. = (n_1 - 2) + (n_2 - 2)$$

where SE represents standard error, t is the t-statistic, n1 and n2 are the sample sizes of each regression. The correlations were repeated using coral

diversity (1/D) in place of coral percent cover. An additional analysis associating coral diversity on a species-specific level was done post-hoc using the crustose coralline algae *Porilithon pachydermum*.

Herbivorous fish and palatable algae

Palatable algae were identified by researching existing literature for known experiments and compiling data on edibility and palatability. Edibility differs from palatability in that an organism may be capable of eating a certain algae species but finds it unpalatable due to secondary metabolites or morphology (Diaz-Pulido, 2002). We correlated the total number of herbivorous fish in each quadrat against palatable algal percent cover using the aforementioned statistical procedure for coral distribution and algal cover.

Current and sedimentation stress

We correlated the five coral variables against a qualitative measurement of current and an estimation of the percent of corals experiencing sedimentation stress. The aforementioned correlation methods for coral distribution and algal cover were used.

In one case an influential outlier was removed from the calculation. This quadrat had a massive coral that occupied a larger portion of the quadrat and had an equally massive sedimentation stress area. This coral was not representative of the rest of the sampled coral colonies. It was removed as this one data point created a strong correlational pattern that was not representative of most of the data.

Results

Coral diversity and distribution

When both reefs were compared as a whole, reef 1 had a 1/D of 5.24 while reef 2 had a value of 5.65. Diversity was also compared between shallow (1/D=3.64), medium (1/D=7.02) and deep (I/D =4.74) depths. While the medium value appears to be the highest, this difference in diversity was not significant ($\chi^2 2=1.16$, p=0.56). The two reefs were not significantly different in terms of diversity ($\chi^2 1=5.6$, p=0.90).

Percent coral cover was log transformed as it severely violated the assumption of normality. There was no significant difference between reefs ($F_{1,35}=0.34$, p=0.57) and depths ($F_{2,35}=1.42$, p=0.26) in terms of total coral percent cover. Less variation was present in coral species richness, and again we found no significant difference between reefs ($F_{1,35}=0.09$, p=0.77) and depths (F2,35=0.67, p=0.52) for this variable. Mean richness (±s.e.) was 3.22 ± 0.03 among all quadrats

P. astreoides was present in 34 out of 36 quadrats, and was the most common coral species. There was no significant difference in height of *P. astreoides* colonies between reefs 1 and 2 (Figure 1, $F_{1,35}=2.7$, p=0.11). However, there was a significant difference across depths ($F_{2,35}=5.6$, p=0.0086). Tukey's HSD post-hoc tests between depths showed that the height of *P. astreoides* at shallow depths was significantly less than the height of P. astreoides at medium depths ($q_{23}=3.54$, p=0.0017) and deep depths (q=4.41, p=0.0002) (Figure 2). The heights of P. asteroides at medium and deep depths were not significantly different (q=0.87, p=0.39). The areas of P. astreoides colonies were not a significantly different between reefs 1 and 2 (Figure 3, F2,35=0.9, p=0.35). However, depth was marginally significant ($F_{1,35}=5.6$, p=0.0571). *F. fragum* percent cover was not significantly different across depths ($F_{1,35}=2.41$, p=0.107), but was marginally significant across reefs ($F_{2,35}=3.16$, p=0.067) (Figure 4).

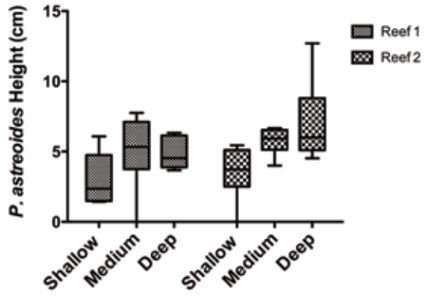

Figure 1: P. astreoides height compared across reefs and reef depth (n=36). Box and whisker plots show the data distributions. The bottom and top of the whiskers represent minimum and maximum values. Box edges represent the first and third quartiles, while the middle line shows the median. Reef was not a significant predictor ($F_{1,35}=2.7$, p=0.11), but depth was (F2,35=5.6, p=0.0086).

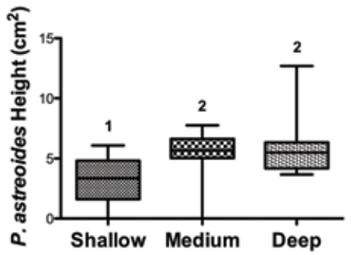

Figure 2: Multiple comparisons of P. astreoides height at different reef depths (n=36). The different number above the boxes signifies that the two compared groups are significantly different. The majority of shallow heights observed were below those seen in medium ($q_{23}=3.54$, p<0.05) and deep colonies ($q_{23}=4.41$, p>0.05). Medium and deep heights were statistically similar ($q_{23}=0.87$, p>0.05).

Coral distribution and algae cover

Percent algal cover was used as a predictor for percent coral cover and coral diversity. No significant correlations were found. Comparison of the regression lines from three, two-tailed t-tests also did not detect significant differences. When coral diversity was assessed within each quadrat, algae cover was found to be a significant predictor at medium depth levels (Figure 5, $R^2=0.47$, p=0.014). Shallow ($R^2<0.01$, p=0.96) and deep ($R^2<0.01$, p=0.83) regression lines were not significant. However, slope for the medium depth (slope=0.026) was significantly different from the slope of the shallow depth (slope=0.002, $t_{20}=0.72$, p=0.48), but only marginally significant from the slope of the deep depth (slope =0.002, $t_{20}=1.89$, p=0.073).

P. pachydermum percent cover and coral diversity were also positively correlated in the medium depth (Figure 6, $R^2=0.501$, p=0.01). However, there was no significant difference between the regression lines for depth (shallow and medium $t_{20}=-0.84$, p=0.41; medium and deep $t_{20}=1.30$, p=0.21; shallow and deep $t_{20}=0.20$, p=0.84).

Upon the removal of one major outlier, algal cover was not a significant predictor of *P. astreoides* height ($R^2=0.01$, p=0.53). *P. astreoides* area was not significantly correlated with algal coverage ($R^2=0.032$, p=0.30) either. However, *F. fragum* percent cover ($R^2=0.15$, p=0.018) was significantly correlated to algae cover (Figure 7).

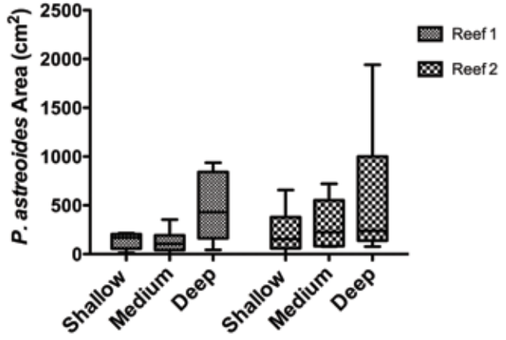

Figure 3: P. astreoides area across reefs and reef depths (n=36). While reef was not significant ($F_{2,35}=0.9$, p=0.35), the effect of depth was marginally significant ($F_{1,35}=5.6$, p=0.0571).

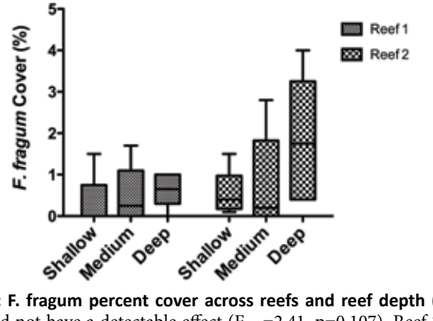

Figure 4: F. fragum percent cover across reefs and reef depth (n=36). Depth did not have a detectable effect ($F_{1,35}=2.41$, p=0.107). Reef 2 tends to have slightly higher values for F. fragum cover, but this pattern is only marginally significant. ($F_{1,35}=3.16$, p=0.067).

Herbivorous fish and palatable algae

Palatable algal percent cover was found to be a significant predictor for herbivorous fish at shallow depths (Figure 8, $R^2=0.68$, p=0.015). Medium ($R^2=0.035$, p=0.56) and deep ($R^2<0.01$, p=0.98) regression lines were not significant. The slope for the shallow depth (slope=0.38) was significantly higher than the slope of the deep depth (slope=0, $t_{23}=2.19$, p=0.04), but was not significantly different from the slope of the medium depth (slope=0.17, $t_{23}=0.68$, p=0.504).

Current and sedimentation stress

Coral percent cover, coral richness, *P. astreoides* height and area, and *F. fragum* percent cover were compared with current in a correlational analysis. However, significant correlations were only detected for coral richness, which was found to be positively correlated with current ($R^2=0.1$, p=0.0057) (Figure 9). Percent sedimentation stress was tested as a possible predictor for percent coral cover and richness, *P. astreoides* height and area, and *F. fragum* percent cover. After the removal of an outlier in the percent coral cover correlation, none of the correlations were found to be significant (Table 2).

Discussion

Coral diversity and distribution

Coral diversity and richness did not vary significantly across depth zones, unlike the findings in some other studies (Dana, 1976; Huston, 1985). However, previous studies that consider diversity across depths are often conducted using greater depth ranges. All three of the zones in this study could easily be classified as "shal-

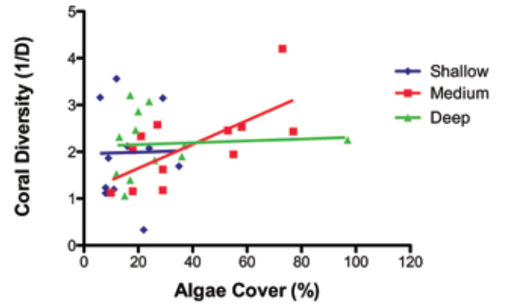

Figure 5: Coral diversity (SDI) regressed on algae cover at low, medium and deep depths (n=12 per depth). The medium regression accounted for 47% of the variation and was significant (p=0.014). The slope of medium regression was not significantly different from the shallow slope ($t_{20}=0.72$, p=0.48) and marginally significant from the deep slope ($t_{20}=1.89$, p=0.073).

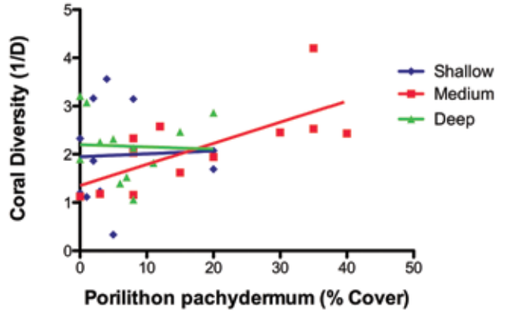

Figure 6: A scatterplot showing coral diversity correlated with the crustose coralline algae *Porilithon pachydermum* percent cover for three reef depths (n= 12 per depth). There was no significant correlation for the shallow quadrats ($R^2=0.002$, p=0.891) and deep quadrats ($R^2=0.002$, p=0.897). There was a significantly positive correlation for the medium quadrats ($R^2=0.501$, p=0.01). However, it was not significantly different from shallow ($t_{20}=-0.84$, p=0.41) and deep quadrats ($t_{20}=1.30$, p=0.21).

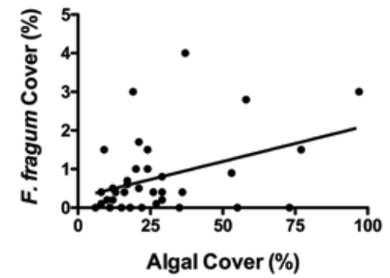

Figure 7: Algal percent cover as a predictor of F. fragum percent cover (n=36). 15% of the variability was explained by algal cover (p=0.018). The regression line had a slope of 0.019 and a y-intercept of 0.26. Considerable variability was seen throughout the regression.

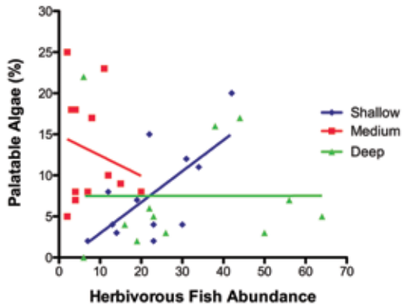

Figure 8: Percent palatable algae regressed on herbivorous fish abundance at low, medium and deep depths (n=36 per depth). The shallow regression accounted for 46% of the variation and was significant (p=0.015). The slope of shallow depth was higher than the deep slope (t_{23}=02.19, p=0.04) but was not different from the medium slope (t_{23}=0.68, p=0.504).

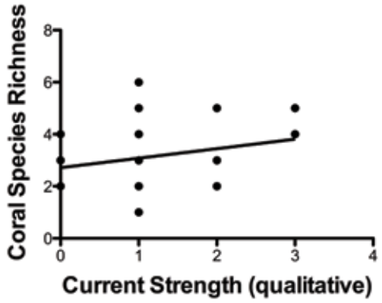

Figure 9: Current strength (assigned 0-3 for no current to strong current) correlated with coral percent cover. There is a significant correlation (R^2=0.1, p=0.006). Thirty-six replicates were analyzed. Due to the discrete nature of both variables, there were many repeats of both coordinates, giving the graphical impression of fewer replicates.

low" if depths below 10 m are considered as is done in studies considering larger reefs. This may explain some of the null results we recorded, as there just may not have been enough differences between the depth categories we used. However, the two reefs considered in this study were almost exclusively located within five meters from the surface, making this study particularly relevant to other shallow reefs.

Coral species have been shown to exhibit individual depth gradients (Dana, 1976). Thus pooling percent cover into one value per quadrat may have conflated the differential effects of each species. This may result in no evident relationship between percent cover and depth or diversity and depth. Even when differences across depths were considered within the two most common species, *P. astreoides* and *F. fragum*, the comparisons were significant for height, and only marginally significant for area. For this species, colonies in the shallow zone were shorter than those from medium and deep zones. This pattern may be due to the effect of mechanical stress from waves and desiccation during low tide, which may select against exposed coral. Overall, a larger sample size may result in the collection of more species-specific data (i.e. lengths, widths and height of all species) and also yield a more robust trend between depth and height of *P. astreoides.*

Coral distribution and algal cover

Algal growth should be negatively correlated with coral cover and diversity as algae can locally outcompete coral for resources (Ogden, 1978). However, we found no significant correlation between coral percent cover and algal percent cover and an unexpected positive correlation between coral diversity and algal percent cover at medium depths (Figure 5). A supplementary species-level correlational analysis between coral diversity and Porilithon pachydermum percent cover suggests that this species was contributing to the significant positive trend in the medium depth (Figure 6). *Porilithon pachydermum*, or reef cement, is a type of crustose coralline algae that can promote settlement of coral recruits (Vermeij, 2005) and help build reef structure by contributing calcium carbonate (Wai, 2005). In general, the abundance of crustose coralline algae correlates negatively with harmful turf algae and promotes coral settlement and health (Vermeij, 2008). This may explain the positive correlation with coral diversity in the present study.

Herbivorous fish and palatable algae

Herbivory is expected to be greatest in shallow depths, where algae are competitively superior to corals (Karleskint, 2010). This accounts for the significant positive correlation between percent algal cover and herbivorous fish abundance at shallow depths found in the present study. Although in some cases algal cover increases with depth as a result of low herbivore grazing (Brokovish, 2010), primary production is highest at shallow depths exposed to high light intensities and ultraviolet wavelengths (Carpenter, 1985). As algal production decreases with depth, declining herbivorous fish abundance has been reported (Brokovish, 2010). Previous studies have shown the importance of herbivorous fish in the regulation of algal abundance in shallow zones (Hay, 1984; Sotka, 2009). Sotka and Hay showed direct evidence of exclusion of herbivorous fish from shallow reef depths and macroalgal blooms (Sotka, 2009). Furthermore, a study by Morrison suggests that herbivory is largely responsible for the algal distribution patterns throughout the reef (Morrison, 1988). Thus, light intensity is a likely predictor of algal primary productivity, which in turn facilitates herbivorous fish abundance.

Table 1: Various estimates of coral coverage correlated against current. Only coral richness yielded significant results.

Variable correlated with current	R^2	p-value
Percent Coral Cover	0.057	0.16
Coral Richness	0.1	0.0057
P.astreoides Height	0	0.69
P. astreoides Area	0.02	0.40
F. fragum Percent Cover	0.068	0.12

Table 2: Coefficient of determination and p-values for correlations between coral variables and percent corals stressed due to sedimentation. Once the outlier was removed there were no significant correlations.

Variable correlated with sedimentation stress	R^2	p-value
Coral Cover (without outlier)	0	0.61
Coral Richness	0.014	0.5
P. astreoides Height	0.01	0.6
P. astreoides Area	0.003	0.76
F. fragum Percent Cover	0.04	0.26

Current and sedimentation stress

Coral percent cover and diversity is expected to be negatively correlated with percent of corals under sedimentation stress as coral stressors decrease the survivorship of corals (Rogers, 1990). Indeed, several studies show that rates of coral mortality were higher where there was more sedimentation (Nugues, 2003). However, the present results showed no correlation between coral diversity and sedimentation stress. It is probable that sedimentation is not a major stressor on the Bellairs reef. Current strength was positively correlated with coral species richness. This indicates that currents may have been capable of lowering sediment stress in some areas, but not strong enough to damage corals.

Results

The results did not support a direct pattern of coral distribution by depth or current. Sedimentation and algal coverage showed patterns differing from common expectations. Strange results often require investigation of species-specific interactions. Yet, due to the complexity of interactions at the biotic and abiotic level and at different spatial scales, it is difficult to test every relationship and to detect every trend. As one of our authors has previously found, it can be difficult to identify general community patterns without a better characterization of individual factors within the system (Liang, 2010). Within a degraded reef, it is especially hard to apply generalizations, given that such systems may function differently from many reefs where classical coral marine biology studies have been conducted.

Despite these limitations we have shown that the presence of coralline algae reef cement may be correlated with increased coral diversity, possibly due to its facilitation of coral establishment. Knowledge of such patterns is potentially important for reef regeneration as it establishes other species that are may be beneficial for successful coral establishment and perhaps recolonization. Such "helper" species may have to be given more consideration in conservation efforts. Similarly we have shown a positive correlation between algal cover and fish abundance, providing evidence that reef fish may be impeding algal dominance. With the sea urchins effectively removed, the system is less resilient. A similar crash in reef fish could prove to be catastrophic for corals.

Acknowledgements

We would like to thank Catherine Febria and Dudley Williams for their advice, logistical support and help with species identification. We also thank the staff at the Bellairs Research Institute for their hospitality.

References

Bellwood, D.R., Hughes, T.P., Folke, C., and Nystrom, M. (2004). Confronting the coral reef crisis. Nature 429, 827-833.
Brokovish, E., I. Ayalon, S. Einbinder, N. Segev, Y. Shaked, A. Genin, S. Kark, M. Kiflawi, (2010). Grazing pressure on coral reef decreases across a wide depth gradient in the Gulf of Aquba, Red Sea. Marine Ecology Progress Series 399, 69-80.
Carlon, D.B., Olson, R.R. (1993). Larval dispersal distance as an explanation for adult spatial pattern in two Caribbean reef corals. Journal of Experimental Marine Biology and Ecology 173, 247-263.
Carpenter, R.C. (1985). Relationships between primary production and irradiance in coral reef algal communities. Limnology and Oceanography 30, 784-793.
Dana (1976). Reef-coral dispersion patterns and environmental variables on a Caribbean coral reef. Bulletin of Marine Science 26, 1-13.
Diaz-Pulido, G.M., L.J. (2002). The fate of bleached corals: patterns and dynamics of algal recruitment. Marine Ecology Progress Series 232, 115-128.
Foster, S.A. (1987). The relative impacts of grazing by Caribbean coral reef fishes and Diadema: effects of habitat and surge. Journal of Experimental Marine Biology and Ecology 105, 1-20.
Gardner, T.A., Cote, I.M., Gill, J.A., Grant, A., and Watkinson, A.R. (2003). Long-term region-wide declines in Caribbean corals. Science 301, 958-960.
Glynn, P.W., and WH, D.E.W. (1991). Elimination of two reef-building hydrocorals following the 1982-83 el nino warming event. Science 253, 69-71.
Hay, M.E. (1984). Patterns of fish and urchins grazing on Caribbean coral reefs: are previous results typical? . Ecology 65, 446-454.
Hughes, T.P. (1994). Catastrophes, phase shifts, and large-scale degradation of a Caribbean coral reef. Science 265, 1547-1551.
Humann, P., DeLoach, N. (2002). Reef Coral Identification (Jacksonville, FL, New World Publications, Inc.).
Huston (1985). Patterns of species diversity on coral reefs. Annual Review Ecological Systematics 16, 149-177.
Karleskint, G., Turner, R., Small, J. (2010). Introduction to Marin Biology (3rd ed.) (Belmon, CA, Brooks/Cole Cengage Learning).
Karlson, R.H., Cornell, H.V. (1998). Scale-dependent variation in local vs. regional effects on coral species richness. Ecological Monographs 68, 259-274.
Lessios, H.A. (1988). Mass mortality of Diadema antillarum in the Caribbean: what have we learned? . Annual Review of Ecology Systematics 19, 371-393.
Lewis, J.B. (1960). The coral reefs and coral communities of Barbados. Canadian Journal of Zoology 38, 1133-1145.
Liang, Y., N. Waltho, (2010). Top-down trophic shifts in the subtidal habitats of Cuba and the role of herbivorous fish and urchins. Journal of Undergraduate Life Sciences 4, 12-17.
Littler, S.L., M.M. Littler, K.E. Bucher, J.N. Norris, (1989). Marine plants of the caribbean (Washington, DC, Smithsonian Institution Press).
Morrison, D. (1988). Comparing fish and urchin grazing in shallow and deeper coral reef algal communities. Ecology 69, 1367-1382.
Mundy, C.N., Babcock, R.C. (1998). Role of light intensity and spectral quality in coral settlement: Implications for depth-dependent settlement? Journal of Experimental Marine Biology and Ecology 223, 235-255.
Nugues, M.M., C.M. Roberts, (2003). Partial mortality in massive reef corals as an indicator of sediment stress on coral reefs. Marine Pollution Bulletin 46, 314-323.
Ogden, J.C., Lobel, P.S. (1978). The role of herbivorous fishes and urchins in coral reef communities. Environmental Biology of Fish 3, 49-63.
Rogers, C.S. (1990). Responses of coral reefs and reef organisms to sedimentation. Marine Ecology Progress Series 62, 185-202.
Simpson, E.H. (1949). Measurement of diversity. Nature 163, 688.
Sotka, E.E., M.E. Hay, (2009). Effects of herbivores, nutrient enrichment, and their interactions on macroalgal proliferation and coral growth. Coral Reefs 28, 555-568.
Tanner, J.E. (1995). Competition between scleractinian corals and macroalgae: an experimental investigation of coral growth, survival, and reproduction. Journal of Experimental Marine Biology and Ecology 190, 151-168.
Vermeij, M.J.A. (2005). Substrate composition and adult distribution determine recruitment patterns in a Caribbean brooding coral. Marine Ecology Progress Series 295, 123-133.
Vermeij, M.J.A., S.A. Sandin, (2008). Density-dependent settlement and mortality structure the earliest life phases of a coral population. Ecology 89, 1994-2004.
Wai, T., G.A. Williams, (2005). The relative importance of herbivore-induced effects on productivity of crustose coralline algae: Sea urchin grazing and nitrogen excretion. Journal of Experimental Marine Biology and Ecology 324, 141-156.

Pathogenic Copy Number Variants (pCNVs) in Individuals Diagnosed on the Autism Spectrum Disorder (ASD): A Closer look at Candidate Genes

Allan Dale Baniaga[1]

[1]University of British Columbia

Abstract

The genetic basis for autism spectrum disorders (ASDs) is well established, and its heterogenetic nature provides us with substantial evidence for the many chromosomal aberrations associated with this complex disorder. However, little is known about the genes that express the phenotypes associated with ASDs and the gene networks they participate in. Here, the author reports candidate genes that may be implicated with the observed clinical phenotypes of ASDs in 9 patients who are identified to have pathogenic copy number variants (pCNVs) through array-comparative genomic hybridization (CGH). Formal clinical assessments, which include a full physical examination, a medical history report, as well as a family history, were administered by a clinical geneticist unaware of the array-CGH results. Candidate genes were then compiled through the genome browser of the Database of Genomic Variants website and subsequently narrowed down utilizing the SUSPECTS database. Additional information on each candidate gene was obtained through the NCBI, iHOP, and metalife databases. The author's findings suggest a number of genes involved in neurodevelopment as well as craniofacial and systemic features that may account for the observed phenotypes in the 9 affected patients, most notably, the *CYFIP1* gene which is involved in maturation and maintenance of dendrites, the Gamma acid receptor family (*GABA*) which exhibit linkage disequilibrium with autistic disorders, and the *PHF8* and *WNK3* genes which have been shown to be associated with X-linked mental retardation (XLMR). Future studies need to be conducted in order to precisely determine the networks these genes participate in and how they are regulated to gain a deeper understanding in the roles they play in the clinical presentations of affected individuals with ASDs.

Abbreviations: ASD – Autism Spectrum Disorder; CGH – Comparative Genomic Hybridization; FISH – Fluorescence In Situ Hybridization; pCNVs – Pathogenic Copy Number Variants; qPCR – Quantitative Polymerase Chain Reaction

Introduction

Autism Spectrum Disorders (ASDs) are neurodevelopmental disorders characterized by impairments in communication, social interaction, and repetitive behavior, and have a prevalence as high as 60 per 10000 individuals by recent estimates (Baird et al., 2000; Bertrand et al., 2001; Chakrabarti and Fombonne, 2001; Chakrabarti and Fombonne, 2005; Coo et al., 2008). The heritability of ASD has also been well established over the years, particularly through comparing monozygotic (MZ) and dizygotic (DZ) concordance rates which, when taken collectively with family studies, clearly point to an important genetic liability for autism (Newschaffer et al., 2007). Although current estimates show that clinical genetic evaluation can positively identify a specific etiology in up to 40% of individuals with an ASD (Shaefer and Mendelsohn, 2008), little is understood in terms of the genotype-phenotype correlations for the vast majority of genetic abnormalities found in affected individuals. Genes responsible for specific clinical phenotypes of ASDs and the possible gene networks and interactions they participate in have yet to be clearly identified. To address this, this paper reports possible candidate genes associated with particular pathogenic copy number variants (pCNVs) in 3 pairs of individuals, of which 2 pairs had de novo changes, and a pair who inherited the same X-linked deletion from their unaffected mother. Three other individuals were also identified to have unique copy number changes not shared with other affected individuals in the cohort. Array-CGH, FISH, and RT-qPCR data were gathered from experiments, as well as detailed phenotypic descriptions of these affected individuals. From these, candidate genes in each unbalanced region were compiled through the use of various databases to provide a genetic basis for their clinical presentation. The major premise of the databases utilized is that genes associated with complex traits will participate in the same gene networks and exhibit similar expression patterns. To this end, the databases rank candidate genes according to their possible involvement with the trait of interest.

Methods and Materials

Array-CGH

PUREGENE DNA Isolation Kits (Gentra, Minneapolis, MN) were utilized to extract DNA from peripheral blood and were matched to normal male and female control DNAs (Promega, Madison, WI) as a reference. Both sample and reference DNAs were then subsequently hybridized using the 1-Mb BAC array (Tyson et al., 2005) [Spectral Genomics, Houston, TX] through dye swap methods. Spectralware 2 software (Spectral Genomics) was then utilized for data analysis, and clones bearing a significant gain or loss were identified through the use of the established values of 1.2 and 0.8, respectively, as cut-offs.

FISH

Deletions and duplications of BAC DNA clones identified by array-CGH were confirmed through FISH analyses (Rajcan-Separovic et al., 2007). A Zeiss Axioplan 2 fluorescence microscope and the MacProbe software (Applied Imaging, Santa Clara, CA) were then utilized to view the slides and capture the images, respectively.

Real-Time Quantitative PCR (RT-qPCR)

RT-qPCR (Qiao et al., 2007) was employed to confirm the pCNVs. The ABI Prism 7900HT system (Applied Biosystems) using SYBR Green I detection was utilized to assess the RT-qPCR products. The primers used can be made available upon request.

Phenotypic Data

A spectrum of clinical characteristics modified from the De Vries scoring method were taken into account, and included prenatal and postnatal growth abnormalities that are indicative of subtelomeric rearrangements, not in exclusion of other characteristics. A spectrum of clinical and physical characteristics was noted for each participant by a professional Clinical Geneticist (M.E.S.L.) blinded to the array results. These included micro- and macrocephaly, prenatal and postnatal growth abnormalities, craniofacial dysmorphisms, systemic anomalies, and the presentation of medical co-morbidities such as seizures, intellectual disabilities (ID), and gastro-intestinal (GI) problems. Pregnancy and postnatal histories were also collected at the time of the appointment.

Identification of Pathogenic Copy Number Variants (pCNVs)

A total of nine subjects were identified to have pCNVs through various genetic testing methods. These subjects were chosen from a case population for their unique presentation of pCNVs and were referred for genetic testing. Low resolution array-CGH findings were confirmed by FISH and RT-qPCR methods which were also used to refine breakpoints and determine the origins of the changes when parents were available for testing.

Individuals identified to harbor pCNVs found at genomic loci associated with other disorders fulfilled CNV criteria strongly suggesting their pathogenicity (Fan et al., 2007; Lee et al., 2007). Several criteria were used to distinguish benign CNVs (bCNVs) from potentially pathogenic ones (pCNVs), including: a de novo origin (or maternally inherited X-linked in male probands), the involvement of multiple genes not known to vary in databases, the overlap with a gene or region that leads to a clinical phenotype when unbalanced, or if the affected region is >1Mb and overlaps with well characterized genes (Fan et al., 2007; Lee et al., 2007). This is in contrast to benign CNVs (bCNVs) which were found in at least 2 healthy individuals in independent studies found on the Database of Genomic Variants website [http://projects.tcag.ca/variation/].

Identification of Candidate Genes

A general list of candidate genes were compiled for each proband through the Database of Genomic Variants website (http://projects.tcag.ca/variation/), and were subsequently narrowed down using the SUSPECTS database (http://www.genetics.med.ed.ac.uk/suspects/). Information on each candidate gene identified by SUSPECTS was collected through the NCBI website (http://www.ncbi.nlm.nih.gov/), specifically looking at the Entrez Gene record and the database of Genotype and Phenotype (dbGaP) entry (when available) for each gene. Further information regarding genotype-phenotype relationships was gathered from the iHOP website (http://www.ihop-net.org/UniPub/iHOP/) which compiles a list of all known functions, interactions, and diseases the gene of interest is associated with. The metalife database (http://www.phenomicdb.de/) was also utilized to complement the gene ontology information collected from the iHOP website. It gives an informative summary of all the research done on the gene of interest and links it to various associated phenotypes.

Results

Table 1 summarizes the candidate genes for each subject pair sharing the same pathogenic CNV, as well as the candidate genes for individuals bearing unique pCNVs. Known gene ontologies for each candidate gene are also listed in Table 1. A list of shared and unique phenotypes was also compiled in Table 2 for each pair and unique individuals bearing a particular pathogenic CNV. Figure 1 presents a schematic diagram summarizing all of the candidate genes found on the various chromosomes. All tables and figures can be found under the supplementary items section.

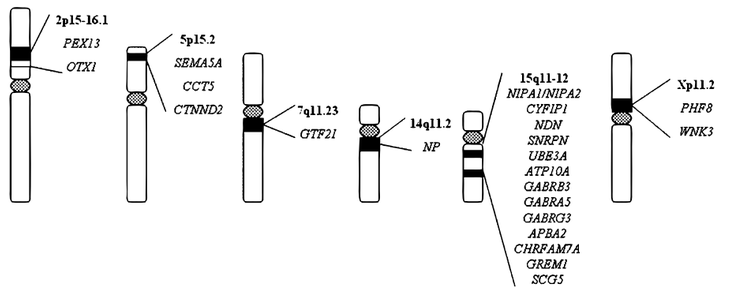

Figure 1: A schematic diagram portraying the candidate genes on different chromosomal positions. Black bars on chromosomes represent regions where candidate are located.

Table 1: Candidate genes identified by subject

Patient(s)	Genomic Region (bp)[2]	Pathogenic CNV(s) and cytoband(s)[2]	Origin	Candidate Gene(s)[1]	Gene Ontology[3]
A, B	A=56,800,000 – 63,200,000 B=55,500,000 – 63,400,000	Del 2p15 – 16.1	de novo	1.PEX13 2.OTX1	1.Peroxisome Biogenesis Disorders 2.Brain and sensory organ development, Inner ear morphogenesis
C, D	1. 19,570,792 – 20,341,734 2.20,536,416 – 30,830,821	1.del 14q11.2 2.dup 15q11 – 12	Both translocations	1a.NP 2a.NIPA1/NIPA2 b. CYFIP1 c. NDN d. SNRPN e. UBE3A f. ATP10A g. GABRB3 h. GABRA5 i. GABRG3 j. APBA2 k. CHRFAM7A l. GREM1 m. SCG5	1a.Purine nucleoside phosphorylase activity 2a.Prader-Willi/Angelman syndrome b.Nervous system development c. Neuron development d. RNA splicing, Prader-Willi Syndrome e. Brain development, Angelman Syndrome f. Angelman Syndrome g,h,i.GABA-A receptor activity j.Nervous system development k.Role in failure to thrive in infants l.Bone and Nervous System development m.Neuropeptide signaling, hormone secretion regulation
E, F	53,970,960 – 54,326,640	del Xp11.2 (relatively skewed X-inactivation)	familial inherited	1.PHF8 2.WNK3	1.X-linked mental retardation 2.Protein amino acid phosphorylation
G	1. 15,780,358 – 15,940,642 2. 9,334,790 – 11,738,791	1.del 3p24.2 – 25 2.del 5p15.2	1.de novo 2.de novo	2a.SEMA5A b.CCT5 c.CTNND2	2a.Axonal guidance, Nervous system development b.Chaperon protein binding c.Neuron adhesion, synaptic plasticity
H	72,200,000 – 73,767,523	dup 7q11.23	unknown origin	1.GTF2I	1.General transcription factor, Williams-Beuren syndrome
I	5,910,725 – 6,063,460	dup 18p11.3	de novo	1. L3MBTL4	1.Cell adhesion, platelet activation, integrin complex component

[1]Confirmed through Database of Genomic Variants website and subsequently narrowed down with SUSPECTS database
[2]Affected region confirmed by RT-qPCR and/or FISH
[3]Information gathered collectively from the NCBI, iHOP, and metalife databases

Subjects A and B

The affected, unrelated pair shares almost identical 2p15-16.1 deletions which are of de novo origin. The affected region has been further defined to be from positions 56,800,000 to 63,200,000 for subject A, and from positions 55,500,000 to 63,400,000 for subject B on chromosome 2 confirmed through RT-qPCR and FISH methods.

Candidate genes for both subjects within the overlapping regions include PEX13 and OTX1, which are involved in Peroxisome Biogenesis Disorders and brain and sensory organ development as well as inner ear morphogenesis, respectively.

Subjects C and D

Subject D is the aunt of subject C, and both individuals share the same deletion at the 14q11.2 locus and duplication at the 15q11-12 locus. An unbalanced product of a reciprocal cryptic 14q/15q translocation represents this finding. A perfect overlap at the 14q11.2 and 15q11-12 regions between both subjects was found (19,570,792 to 20,341,734 and 20,536,416 to 30,830,821, respectively).

Subjects E and F

Subjects E and F are brothers who share the same Xp11.2 deletion that is maternally inherited, and the precise genomic region of the deletion was found to be from 53,970,960 to 54,326,640 on the X chromosome. Of particular note, the mother was confirmed to have a relatively skewed X-inactivation, perhaps implying dosage imbalance problems in both siblings. Potential candidate genes in the affected region of both subjects E and F include PHF8, which is associated with X-linked mental retardation, as well as the WNK3 gene which is involved in protein amino acid phosphorylation.

Of particular note, several candidate genes are implicated with nervous system development, which include CYFIP1, NDN, UBE3A, APBA2, GREM1, and SCG5, all of which are found on the shared 15q11-12 site. Several candidate genes found on the same locus are also implicated with Angelman syndrome as well as Prader-Willi syndrome, including the NIPA1/NIPA2, SNRPN, UBE3A, and ATP10A genes.

Subject G

The affected individual harbors two deletions at the 3p24.3-25 and 5p15.2 regions, with both regions of de novo origin. The precise affected region for the chromosome 3 deletion was found to be from 15,780,358 to 15,940,642, and the chromosome 5 deletion is from 9,334,790 to 11,738,791, as confirmed by FISH and RT-qPCR.

In relation to the observed phenotypes, several candidate genes that may play a role in the pathogenesis of classical autism include SEMA5A and CTNND2, both of which are located on chromosome 5 and are involved in axonal guidance and neuron adhesion and synaptic plasticity, respectively. CCT5 was also identified by SUSPECTS to be another candidate gene on the same chromosome, and is involved with chaperon protein binding in neurons.

Subject H

Subject H is an individual with a unique 7q11.23 duplication of unknown origin that is not found in other subjects presenting with pathogenic CNVs. The affected genomic region was found to be from 72,200,000 to 73,767,523 through FISH and RT-qPCR methods. Of particular note, the GTF2I candidate gene was identified by the SUSPECTS database, which is known to be a general transcription factor, as well as being implicated in Williams-Beuren syndrome.

Table 2: Observed Clinical Phenotypes

Subject(s)	Shared Phenotypes	Unique Phenotypes
A, B	Severe ID[1], microcephaly (<2%), craniofacial dysmorphisms (short forehead, high and broad nasal root), other systemic dysmorphisms (bilaterally tight heel cords, oral motor dysfunction), abnormal brain imaging	A=Prenatal growth retardation, B=Seizure disorder, postnatal small stature (<5%)
C, D	Craniofacial dysmorphisms (strabismus, flat occiput, prominent alar cartilage), no other systemic dysmorphisms	C=Moderate ID, respiratory distress and poor suck and feeding difficulties (postnatal) D=Mild ID, seizure disorder, floppy infant (postnatal)
E, F	Moderate ID, craniofacial dysmorphisms (flat occiput, coarse asymmetric face [right side > left side fullness], micrognathia, unilateral cleft lip, other systemic dysmorphisms (pes planus, bone anomalies)	E=Prominent metopic suture, prominent finger pads F=Long slender fingers, macrocephaly at birth, mild hyperoptic refractive error
G	N/A	G=Moderate ID, seizure disorder, macrocephaly (>98%), postnatal large stature (>98%), craniofacial dysmorphisms (coarse facial features, frontal bossing, prominent supra-orbital ridge), other systemic dysmorphisms (prominent finger pads, bilateral tight heel cords, slight toe walking)
H	N/A	H=Moderate ID, craniofacial dysmorphism (plagiocephaly, brachycephaly, prognathia), other systemic dysmorphisms (GI unusual dark stool colour, walks on heels, occasional enuresis), normal brain imaging
I	N/A	I= Mild ID, heightened blood pressure (during pregnancy), craniofacial dysmorphisms (mild bilateral epicanthal folds, ears bilaterally protuberant slight malar flattening), other systemic dysmorphisms (slight metatarsus varus when walking)

[1]ID = Intellectual Disability

Subject I

This affected individual was identified to have a duplication of de novo origin at the 18p11.3 region, which was further refined to be from 5,910,725 to 6,063,460 on chromosome 18. L3MBTL4 was the sole candidate gene identified that may account for the observed phenotypes, and is known to be involved in cell adhesion, platelet activation, as well as being a component of the integrin complex.

Discussion

Subjects A and B: 2p15-16.1 deletion

Several characteristics shared by both subjects include intellectual disability as well as poor oral motor skills and poor muscle tone, which overlap with certain Peroxisome Biogenesis Disorder (PBD) phenotypes, thus making the PEX13 gene on chromosome 2 a possible culprit for the observed phenotypes. Since both subjects are alive well past the early childhood years, Refsum's disease is the most likely out of all the other PBDs since its prognosis indicates a high likelihood of living past the early childhood years. However, normal laboratory evidence of phytanic acid and long chain fatty acids, both of which are found in elevated levels in Refsum's affected individuals due to faulty enzymes during the alpha oxidation of phytanic acid and fatty acid oxidation, is found for both individuals harboring the overlapping 2p15-16.1 deletion (Rajcan-Separovic et al., 2007). Nonetheless, the possibility of PEX13 and other candidate genes in the deleted region contributing to part of the observed phenotypes, in particular those aspects involved with neurodevelopment (in keeping with microcephaly in both subjects) and poor muscle tone, cannot be completely ruled out.

Another candidate gene that may be responsible for neurodevelopment as well as sensory organ development is OTX1, a transcription factor that was recently found to be essential in cerebellum development (de Haas et al., 2006). The observed large ears, relative to the microcephaly in both subjects, may be in part due to the loss of function of the OTX1 gene. Furthermore, evidence suggests that the OTX1 gene dictates the segregation of the saccule and the utricle during inner ear morphogenesis (Beisel et al., 2005), and its loss of function due to the deletion may perhaps be responsible for the hyperacusis observed in subject A as well as the bilateral sensorineural loss (mild to moderate in the left ear and slight to mild in the right ear) observed in subject B.

Subjects C and D: 14q11.2 deletion and 15q11-12 duplication

Both subjects present strikingly similar characteristics, most notably sharing several craniofacial dysmorphisms (strabismus, flat occiput, prominent alar cartilage) and presentation of intellectual disability (subject C has moderate ID while subject D has mild ID). These findings suggest an underlying genomic basis that may be responsible for the shared pathogenesis. Indeed, both a deletion and a duplication arising through a reciprocal cryptic 14q/15q translocation were found whose affected genomic areas had perfect overlap between the two relatives (Table 1).

Candidate genes that may be implicated with cephalic development were found in the duplicated 15q11-12 region and as such, dosage effects may be at play here in terms of over-expression of a particular gene and/or altered regulation of a gene that may exert its effects on adjacent genes involved in the same gene network. The highly conserved CYFIP1 gene may be one such gene. Through co-localization experiments, there is evidence that the products of the CYFIP1 gene do indeed interact with FMRPs [Fragile X mental retardation proteins] (Schenck et al., 2001). Although the functions of the CYFIP1 proteins are currently unknown, the extraction of CYFIP1 proteins at the synaptosome of the distal portion of den-

drites suggests that they also interact with the small GTPase Rac1 where CYFIP1 proteins also localize (Schenck et al., 2001). Rac1 is known to be essential for dendritic spine maturation as well as maintenance (Nakayama et al., 2000), and a duplication of the CYFIP1 gene with whom it interacts may have direct or indirect effects on the maturation and maintenance of these structures. One possibility is that improper dosage of the CYFIP1 gene product could directly alter expression levels of Rac1 and other genes in the network involved in dendrite formation. This would have major implications for neurodevelopment and could thus be responsible for the shared ID and ASD observed in both subjects.

Several other candidate genes that may be responsible for the shared dysmorphisms include UBE3A and APBA2. Most notably, maternally derived duplications of the 15q11-13 region results in changes to UBE3A expression observed in autistic individuals, whereas the duplication is not present in normal individuals (Veenstra-VanderWeele et al., 1999). In addition, GREM1 may also be the culprit gene for the observed bone fractures in subject D and the ligamentous laxity in subject C, as over-expression of this gene in transgenic mice analogous to that of a duplication event resulted in a 20-30% reduction in bone mineral density as well as formation of bone fractures (Gazzerro et al., 2005). It has been well established that deletions in the 15q11-13 region result in Prader-Willi syndrome (PWS) as well as Angelman syndrome (AS) (Dittrich et al., 1992) in which several of the phenotypes overlap with those present in both subjects. These include reduced fetal movements, respiration and feeding difficulties, strabismus, and intellectual disability (Holm et al., 1993). NIPA1/NIPA2, NDN, SNRPN, UBE3A, ATP10A, and the Gamma acid receptor family (GABA) were identified by SUSPECTS in the duplicated 15q11-12 region to be implicated in the autistic disorder in both subjects. There is evidence that a marker in the gene for the gamma aminobutyric acid receptor subunit of GABRB3 was found to have linkage disequilibrium with autistic disorder, making this gene as well as other members of the gene family prime candidates (Cook et al., 1998). Furthermore, the role of benzodiazepines as GABA receptor agonists in treating autistic phenotypes such as anxiety disorders and seizures suggest a potential role of the GABA gene family in the presentation of these phenotypes beyond the normal inhibitory neurotransmitter GABA function (Cook et al., 1998). Additional studies need to be conducted in the future to precisely dissect the roles of the GABA gene family as well as others that exhibit linkage disequilibrium with autistic disorders.

Subjects E and F: Xp11.2 deletion

Both brothers share the same maternally inherited Xp11.2 deletion, and a possible candidate gene that may account for their shared moderate ID in relation to this critical linkage region on Xp11.2 is PHF8. The PHF8 gene encodes a PHD finger protein which has been shown through truncation mutation experiments to cause X-linked mental retardation (XLMR) with or without cleft lip/cleft palate presentation (Laumonnier et al., 2005). The PHD finger protein has also been thought to regulate and modify chromatin structure (Jensen et al., 2005), which has major implications in terms of altered transcription levels and neurodevelopment in individuals with mutations or deletions of the PHF8 gene.

Another candidate gene that may be implicated with the observed moderate ID in both subjects is WNK3, which is shown to occupy the critical linkage region on Xp11.2, and thus may also play a critical role in neurodevelopmental disorders such as XLMR (Ropers et al., 2003). However, future studies need to be conducted to determine whether the WNK3 deletions could account for the difference in autism occurrences in comparison to the PHF8 deletion cases, and whether deletion size differences between the WNK3 and PHF8 genes affect their interaction with neighboring genes.

Subject G: 3p24.3-25 and 5p15.2 deletions

Subject G is an affected individual identified to harbor unique deletions at the 3p24.3-25 and 5p15.2 regions. Several phenotypes unique to subject G in relation to these deletions include moderate ID, macrocephaly (>98%), postnatal large stature (>98%), and several craniofacial dysmorphisms (coarse facial features, frontal bossing). SEMA5A, a candidate gene identified by SUSPECTS, may account for the observed moderate ID and macrocephaly as it is known to be involved in axonal guidance and nervous system development (Adams et al., 1996). This gene occupies the 5p15.2 region and experimental evidence shows that axonal development and formation of synapses may be affected by changes in SEMA5A expression (Jones et al., 2002). Furthermore, deletions from the 5p band are also implicated with the Cri-du-chat phenotype, and haploinsufficiency of SEMA5A may be responsible for the intellectual disability in individuals exhibiting this phenotype (Simmons et al., 1998). A deletion at the 5p15.2 region may thus have major implications in SEMA5A expression levels as not enough products are made to maintain proper axonal development and synapse formation, possibly leading to the observed macrocephaly and moderate ID in subject G.

CCT5 is another candidate gene that was identified by SUSPECTS as likely to be involved in neurodevelopment since the chaperon protein product of CCT5 was found to have an additional role in polymerization as well as maintenance of cytoskeletal proteins in neurons (Bourke et al., 2002). Deletions in the 5p15.2 region would thus have profound effects on proper neurodevelopment due to a lack of CCT5 chaperone proteins essential for proper neuron functioning. The CTNND2 gene, which is also found on 5p15.2, was additionally identified as a possible candidate for the shared macrocephaly and moderate ID phenotypes. Mutational experiments suggest a specialized role for the CTNND2 protein as mutations in the gene result in learning and synaptic plasticity deficits (Israely et al., 2004). Furthermore, a strong correlation between a hemizygous deletion of the CTNND2 gene and severe mental retardation in individuals with Cri-du-chat syndrome (CDCS) (Medina et al., 2000) further outlines the critical role of CTNND2 in the intellectual disability of subjects manifesting a deletion in the 5p15.2 region. Moreover, delta catenin (the protein product of CTNND2) was also found to co-bind with kaiso to the promoter sites of rapsyn [a synapse protein necessary for segregating acetylcholine receptors at the neuromuscular area] (Rodova et al., 2004). Deletion of the CTNND2 gene on 5p15.2 would thus have adverse effects on proper rapsyn functioning, and this may attribute to the seizures, delays in motor milestones, and failure to thrive observed in the affected individual.

Subject H: 7q11.23 duplication

Subject H is an isolated case that does not share any pathogenic CNVs or cytogenetic bands with the other cases presented here, but several other abnormalities have been reported. A unique 7q11.23 duplication of unknown origin was found, and GTF2I was the sole candidate gene identified by SUSPECTS that may be implicated with the unique phenotype associated with the affected genomic region. Structural features of 7q11.23 render this region susceptible to genomic rearrangement and deletions, yielding various CNVs that are also involved with Williams-Beuren syndrome [WBS] (Cuscó et al., 2008). The subject shares several characteristics with WBS, including intellectual disability, hyperacusis, and genito-urinary problems (Sammour et al., 2006) [subject has a history of enuresis]. Furthermore, GTF2I was also shown to be involved in tooth development at the bud and early bell stage (Ohazama and Sharpe, 2007), and thus may also account for the carious and early loss of teeth in the subject. Moreover, hemizygosity of GTF2I was found to be sufficient to account for a number of features associated with WBS, including visuospatial deficits (Edelmann et al., 2007), which may contribute to the astigmatism and myopia observed in subject H.

Subject I: 18p11.3 duplication

The affected subject harbors a unique duplication at the 18p11.3 region of de novo origin and presents several phenotypes that may be associated with the duplication. Of particular note, the candidate L3MBTL4 gene is known to be involved in platelet activation, and a dosage imbalance arising through duplication may have direct or indirect consequences with regards to the observed heightened blood pressure during pregnancy. Furthermore, the role of the L3MBTL4 gene in cell adhesion, in particular as a component of the integrin complex which is known to be involved in mediating various intracellular signals, may indeed account for the craniofacial and systemic dysmorphisms as well as the mild ID observed in subject I. The implications of dosage effects through duplication of the 18p11.3 region need to be further investigated as well as the specific roles of L3MBTL4, as research on this region and its genes is too limited to make any conclusive statements regarding genotype-phenotype relationships at this time.

Conclusions

The identification of candidate genes on various chromosomes provided further insight as to how changes occurring at the gene level affects phenotype at the organismal level. Autism spectrum disorders present an especially daunting task, as its variability between different individuals suggests a multitude of genes that may interact with other candidate genes involved in the same or different gene networks. Due to time and resource constraints, the author of this paper was not able to experimentally investigate the gene interactions hypothesized in this paper, and so every effort was made to account for the clinical manifestations of the patients presenting with an ASD with their candidate genes through the extensive use of databases in order to hypothesize and explore their genotype-phenotype relationships. Additional experiments need to be conducted in the future so as to uncover the functions of these candidate genes, how their expression is regulated, and what gene networks they participate in. Only through understanding these finer details at the gene level can we then unravel the genetic bases of some of the phenotypes associated with classical autism.

Acknowledgements

The author would like to thank Noemie Riendeau and Ying Qiao at the Child and Family Research Institute (CFRI) wet lab for all of their help in assisting with the CNV data, as well as for their insightful comments. A warm thank-you also goes out to Priscilla Carrion and Lindsay Swinton at the dry lab for all of their help with the clinical files, all of which the author is grateful for having access to. Last, but certainly not least, the author would like to express his sincerest gratitude towards his mentor, Dr. Lewis, for allowing the author to undertake this directed studies project, as well as for all of her guidance without which this project would not have been possible.

References

Adams, R.H., Betz, H., and Puschel, A.W. (1996). A novel class of murine semaphorins with homology to thrombospondin is differentially expressed during early embryogenesis. Mech Dev. 57, 33–45.

Baird, G., Charman, T., Baron-Cohen, S., Cox, A., Swettenham, J., Wheelright, S., and Drew, A. (2000). A screening instrument for autism at 18 months of age: a 6-year follow up study. J. Am. Acad. Child Adolesc. Psychiatry 39, 694–702.

Beisel, K.W., Wang-Lundberg, Y., Maklad, A., and Fritzsch, B. (2005). Development and evolution of the vestibular sensory apparatus of the mammalian ear. Journal of Vestibular Research 15(5-6), 225-241.

Bertrand, J., Mars, A., Boyle, C., Bove, C., Yeargin-Allsopp, M., and Decoufle, P. (2001).Prevalence of autism in a United States population: the Brick Township, New Jersey, investigation. Pediatrics 108, 1155–1161.

Bourke, G.J., El Alami, W., Wilson, S.J., Yuan, A., Roobol, A., and Carden, M.J. (2002). Slow axonal transport of the cytosolic chaperonin CCT with Hsc73 and actin in motor neurons. J. Neurosci. Res. 68, 29–35.

Chakrabarti, S., and Fombonne, E. (2001). Pervasive developmental disorders in preschool children. JAMA 285, 3093–3099.

Chakrabarti, S., and Fombonne, E. (2005). Pervasive developmental disorders in preschool children: confirmation of high prevalence. Am. J. Psychiatry 162, 1133–1141.

Coo, H., Ouellette-Kuntz, H., Lloyd, J.E.V., Kasmara, L., Holden, J.J.A., and Lewis, M.E.S. (2008). Trends in Autism Prevalence: Diagnostic Substitution Revisited. J. of Autism and Dev. Disorders 38(6), 1036-1046.

Cook, E.H. Jr. et al. (1998). Linkage-Disequilibrium Mapping of Autistic Disorder, with 15q11-13 Markers. Am. J. Hum. Genet. 62, 1077–1083.

Cuscó, I., Corominas, R., Bayés, M., Flores, R., Rivera-Brugués, N., Campuzano, V., andPérez-Jurado, L.A. (2008). Copy number variation at the 7q11.23 segmental duplications is a susceptibility factor for the Williams-Beuren syndrome deletion. Genome Res. 18(5), 683-694.

Dittrich, B., Robinson, W.P., Knoblauch, H., Buiting, K., Schmidt, K., Gillessen-Kaesbach, G., and Horsthemke, B. (1992). Molecular diagnosis of the Prader-Willi and Angelman syndromes by detection of parent-of-origin specific DNA methylation in 15q11-13. Hum. Genet. 90, 313-315.

Edelmann, L. et al. (2007). An atypical deletion of the Williams–Beuren syndrome interval implicates genes associated with defective visuospatial processing and autism. J. Med. Genet. 44, 136-143.

Fan, Y.S., Jayakar, P., Zhu, H., Barbouth, D., Sacharow, S., Morales, A., Carver, V., Benke, P., Mundy, P., and Elsas, L.J. (2007). Detection of pathogenic gene copy number variations in patients with mental retardation by genome wide oligonucleotide array comparative genomic hybridization. Human mutation 28(11), 1124-1132.

Gazzerro, E., Pereira, R.C., Jorgetti, V., Olson, S., Economides, A.N., and Canalis, E. (2005). Skeletal Overexpression of Gremlin Impairs Bone Formation and Causes Osteopenia. Endocrinology 146(2), 655–665.

de Haas, T. et al. (2006). OTX1 and OTX2 Expression Correlates With the Clinicopathologic Classification of Medulloblastomas. Journal of Neuropathology & Experimental Neurology 65(2), 176-186.

Holm, V.A., Cassidy, S.B., Butler, M.G., Hanchett, J.M., Greenswag, L.R., Whitman, B.Y., and Greenberg, F. (1993). Prader-Willi Syndrome: Consensus Diagnostic Criteria. Pediatrics 91, 398-402.

Israely, I et al. (2004). The neuronal adherens-junction protein Delta-Catenin is critical for learning and synaptic plasticity. Curr. Biol. 14, 1657–1663.

Jensen, L.R. et al. (2005). Mutations in the JARID1C gene, involved in transcriptional regulation and chromatin remodeling, cause X-linked mental retardation. Am. J. Hum. Genet. 76, 227–236.

Jones, L., Lopez-Bendito, G., Gruss, P., Stoykova, A., and Molnar, Z. (2002). Pax6 is required for the normal development of the forebrain axonal connections. Development 129, 5041–5052.

Laumonnier, F. et al. (2005). Mutations in PHF8 are associated with X linked mental retardation and cleft lip/cleft palate. J. Med. Genet. 42, 780–786.

Lee, C., Iafrate, A.J., and Brothman, A.R. (2007). Copy number variations and clinical cytogenetic diagnosis of constitutional disorders. Nat. Genet. 39(7 Suppl), S48-S54.

Medina, M., Marinescu, R.C., Overhauser, J., Kosik, K.S. (2000). Hemizygosity of delta-catenin (CTNND2) is associated with severe mental retardation in cri-du-chat syndrome. Genomics 63(2), 157–164.

Nakayama, A.Y., Harms, M.B., and Luo, L. (2000). Small GTPases Rac and Rho in the Maintenance of Dendritic Spines and Branches in Hippocampal Pyramidal Neurons. The Journal of Neuroscience 20(14), 5329-5338.

Newschaffer, C.J. et al. (2007). The Epidemiology of Autism Spectrum Disorders. Annu. Rev. Public Health 28, 235–258.

Ohazama, A., and Sharpe, P.T. (2007). TFII-I Gene Family During Tooth Development: Candidate Genes for Tooth Anomalies in Williams Syndrome. Developmental Dynamics 236(10), 2884–2888.

Qiao, Y., Liu, X., Harvard, C., Nolin, S.L., Brown, W.T., Koochek, M., Holden, J.J.A., Lewis, M.E.S., and Rajcan-Separovic, E. (2007). Large-scale copy number variants (CNVs): distribution in normal subjects and FISH/real-time qPCR analysis. BMC genomics 8, 167.

Rajcan-Separovic, E. et al. (2007). Clinical and molecular cytogenetic characterisation of a newly recognised microdeletion syndrome involving 2p15 16.1. J. Med. Genet. 44(4), 269-276.

Rodova, M., Kelly, K.F., VanSaun, M., Daniel, J.M., and Werle, M.J. (2004). Regulation of the Rapsyn Promoter by Kaiso and Delta-Catenin. Mol. Cell Biol. 24(16), 7188–7196.

Ropers, H.H., Hoeltzenbein, M., Kalscheuer, V., Yntema, H., Hamel, B., Fryns, J.P., Chelly, J., Partington, M., Gecz, J., and Moraine, C. (2003). Nonsyndromic X-linked mental retardation: where are the missing mutations? Trends Genet. 19, 316-320.

Sammour, Z., Gomes, C., Duarte, R., Trigo-Rocha, F., Srougi, M. (2006). Voiding Dysfunction and the Williams-Beuren Syndrome: A Clinical and Urodynamic Investigation. The Journal of Urology 175(4), 1472-1476.

Schenck, A., Bardoni, B., Moro, A., Bagni, C., and Mandel, J.L. (2001). A highly conserved protein family interacting with the fragile X mental retardation protein (FMRP) and displaying selective interactions with FMRP-related proteins FXR1P and FXR2P. PNAS 98(15), 8844-8849.

Shaefer, G.B., and Mendelsohn, N.J. (2008). Clinical genetics evaluation in identifying the etiology of autism spectrum disorders. Genetics in Medicine 10(1), 4-12.

Simmons, A.D., Puschel, A.W., McPherson, J.D., Overhauser, J., and Lovett, M. (1998). Molecular cloning and mapping of human semaphorin F from the Cri-du-chat candidate inteval. Biochem. Biophys. Res. Commun. 242, 685–691.

Tyson, C. et al. (2005). Submicroscopic deletions and duplications in individuals with intellectual disability detected by array-CGH. Am. J. Med. Genet. A. 139(3), 173-185.

Veenstra-VanderWeele, J., Gonen, D., Leventhal, B.L., and Cook Jr E.H. (1999). Mutation screening of the UBE3A/E6-AP gene in autistic disorder. Molecular Psychiatry 4, 64-67.

JULS RESEARCH

A Putative Approach to Modeling Entropy-driven Protein Folding Applied to Undeca-alanine and Tal-1a

Michael Chong[1], Sinisa Vukovic[2], Imre G. Csizmadia[2]

[1]McMaster University, Department of Chemistry, 1280 Main Street West, Hamilton ON L8S 4L8
[2]University of Toronto, Department of Chemistry, 80 St. George Street, Toronto ON M5S 3H6

Abstract

An entropy-driven refinement of the conventional "straight-chain" method of computational modeling by molecular dynamics simulation is proposed. This refinement entails a step-wise amino acid by amino acid modeling, which more accurately mimics the process of in vivo protein synthesis and purposely and dramatically reduces the number of potential conformations produced. This study shows that nucleation trigger points "lock" certain motifs in place regardless of subsequent amino acid additions. This reduction in space exploration represents a purposeful reduction in entropy to arrive at native conformations more likely to be synthesized in the same step-wise process by the ribosome. Molecular dynamics simulations of Tal-1a and undeca-alanine peptides demonstrate the differences resulting from this approach. To date, no empirical visualizations of tal-1a by X-ray crystallography or atomic force microscopy (AFM) have been conducted, but it would be interesting to compare our computationally predicted conformations to these empirical ones. The results of our study evoke questions surrounding the validity of the conventional straight-chain method as the current paradigm of peptide molecular dynamics modeling and also the foundation of homology based studies.

Introduction

Conventionally, computational chemists model protein conformations by "stretching" the polypeptide into a straight chain prior to simulation of protein folding (Chasse, 2001). However, this methodology is a departure from the ribosome-facilitated, step-wise amino-acid polymerization process that occurs in all organisms (Barlow and Thornton, 1988). As the ribosome reads through the mRNA transcript, amino acids are added to the nascent chain one by one. Peptide bonds in a single sequence are formed sequentially and not simultaneously (Lodish, 2000). Accordingly, protein folding should be modeled sequentially and not simultaneously.

This study proposes an alternative molecular dynamics (MD) method for protein simulations. To our knowledge, there have been no reports of molecules that stabilize the nascent peptide into a straight chain *in vivo* (analogous to SSB proteins for DNA). Therefore, we hypothesize that step-wise protein folding more accurately predicts protein synthesis. Some global minima conformations computed from *ab initio* investigations do not correspond to native conformations observed through experimental methods, such as X-Ray crystallography and NMR (Brooks et al., 2001). These native conformations represent local energy minima and not global minima. The present study provides evidence that this could be explained by the path-dependent nature of protein synthesis.

Still, one cannot completely ignore the great finds of the conventional computational method in unraveling the native conformations of many proteins. For example, in 2002, Shea *et al.* modeled the protein folding of Src homology 3 (SH3) through molecular dynamics (Shea et al., 2002). They observed that not only the final conformation was congruent with conformations derived experimentally, but also that the transition state conformations corresponded with the experimentally determined transition states. Even though Shea *et al.* arrived at the "correct" folding path and final conformation, this is simply one path of many possible pathways. In order to refine this search of native conformers, we propose this sequential computational method.

The present study investigates the molecular synthesis of two peptides: an undeca-alanine (11 alanines) and the Tal-1a peptide. The Tal-1a peptide is the smallest, functional peptide reported in *Drosophila melanogaster* to date (Kondo et al., 2007), with a sequence of MAAYLDPTGQY. This diminutive peptide is an important regulator of tarsal (leg) and trichome (hair) development in *D. melanogaster* (Pi, 2009). Though its function has been elucidated, nothing is known about Tal-1a's secondary or tertiary structure.

The undeca-alanine peptide will also be investigated to isolate backbone interactions, free of the numerous side chain interactions which will inevitably be present with the MAAYLDPTGQY sequence of Tal-1a. This is due to alanine's small and non-polar methyl side chain, which eliminates steric and electronic effects. An alpha helix is the putative conformation of a chain of 4 or more alanines (Charkabartty, 2008), as a single alpha turn is comprised

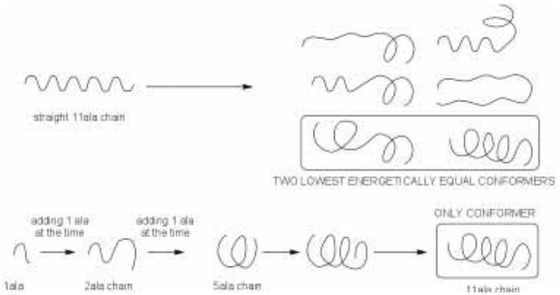

Schematic 1: All alanine peptides investigated, straight (left) and helical (right) peptides.

of 3.6 amino acids (Sun, 2010). Accordingly, we predict that all simulations will produce alpha helices. However, to refine this hypothesis, we predict that the straight-chain method does not produce this conformation as reliably as the sequential method.

We have opted to examine methodology, temperature, and time step as the variable parameters of our experiment. The two different methodologies have been explained *ad nauseam*, so only temperature and time step will be explained henceforth. All peptide folding simulations were computed at 300K and 350K. The conformations derived at 350K temperature serve as a negative control and we expect that these conformations will differ greatly from those derived at 300K. In layman's terms, time step is how much "freedom" you give to the molecule to "shake" during each step. If the time step is too high, then the simulation may condone even the breaking of covalent bonds. It was determined experimentally that time steps 0.001 and 0.002 were adequate to permit intramolecular hydrogen bonding, which is crucial to alpha helices formation in the undeca-alanine peptides.

Methods

For all molecular dynamics simulations, Amber ff99 was applied to the peptides. To visualize these simulations, the GUI "Molecular Operating Environment (MOE) 2007" was used. All nascent peptide chains were constructed in Gaussview and imported into MOE. All peptides were protected at the N-terminus with N-formyl groups and at the C-terminus as methyl amides.

The undeca-alanine peptide was simulated at 300K, time step 0.002 picoseconds, 0.005 RMS gradient, for 2000 picoseconds (all other parameters were set to their program defaults). In total, this simulation was conducted for 100 000 steps. The full length anti-anti undeca-alanine chain and the growing undeca-alanine chain were simulated. Step-wise simulation began with molecular dynamics simulation of two alanines until a stable conformation emerged. A conformation was considered stable once it had "settled" for approximately 10 000 steps. After stabilization, the last conformation was isolated and another alanine was added to this conformation and run again under a molecular dynamics simulation. This process of simulation, isolation, and addition was repeated until the full length peptide was synthesized. This entire process was repeated for the Tal-1a peptide and at different parameters of 350K, time step 0.001 picoseconds, 0.005 RMS, for 1000 picoseconds.

Table 1: Summary of eight Molecular Dynamics (MD) simulations.

Name	Sequence	Method	Parameters
1A	AAAAAAAAAAA	Conventional (simultaneous)	300K, 0.002TS, 2000 picoseconds
1B	AAAAAAAAAAA	Sequential (step-wise)	300K, 0.002TS, 2000 picoseconds
1C	AAAAAAAAAAA	Conventional	350K, 0.001TS, 1000 picoseconds
1D	AAAAAAAAAAA	Sequential	350K, 0.001TS, 1000 picoseconds
2A	MAAYLDPTGQY	Conventional	300K, 0.002TS, 2000 picoseconds
2B	MAAYLDPTGQY	Sequential	300K, 0.002TS, 2000 picoseconds
2C	MAAYLDPTGQY	Conventional	350K, 0.001TS, 1000 picoseconds
2D	MAAYLDPTGQY	Sequential	350K, 0.001TS, 1000 picoseconds
2E	MAAYLDPTGQY	Sequential	350K, 0.002TS, 2000 picoseconds
2F	MAAYLDPTGQY	Sequential	300K, 0.001TS, 1000 picoseconds

Results

All undeca-alanine simulations (at 350K and 300K with 0.001 and 0.002 TS) synthesized by the sequential method produced complete alpha helices with three complete turns (Figures 1B and 1D). The first full turn formed with the addition of the fourth amino acid, and all subsequent alanines appeared to "lock" into place, contributing to the formation of the subsequent turns. For the step-wise simulations of 5 to 11 alanines, conformations very rarely deviated from the helix structure. Slight deviation of the ends of the helix occurred, but the core of the helix always remained solidly intact. For example, at 300K, the N-formyl cap formed a 3-10 helix instead of the expected alpha helix (Figure 1B). Additionally at 350K, the last alanine at the C-terminus end did not "lock" into the alpha helices like the other amino acids (Figure 2D).

In contrast, undeca-alanine simulations using the conventional method never produced complete helices at 300K (Figure 1A). At 350K, the N-terminus end was observed to loop around to the middle of the peptide and form hydrogen bonds (Figure 1C). Also, it appeared as if the alpha helices attempted to form from the C-terminus end, but were not able to finish formation due to the stable interactions between the N- terminus and the middle of the peptide (Figure 1C).

To test the reliability of these results, these simulations were repeated with the exact same stipulations. For this second run, no alpha helices were formed at either 300K or 350K. Instead a similar phenomenon observed in the first run at 350K, in which the N-terminus end bent inwards to form hydrogen bonds with the middle of the backbone, was also observed in the second runs but at both 300 and 350K. However, instead of the N-terminus looping inwards, the C-terminus looped inwards to inhibit complete alpha helices formation throughout the entire sequence.

This phenomenon is apparent in simulation 1A, where the C-terminus end of the peptide bent inwards towards the middle of the peptide and the last carbonyl group of the peptide was stabilized by hydrogen bonding with surrounding N–H groups (Figure 1A). An alpha turn at the N-terminus did indeed form, but the helix appeared sterically stifled in propagating throughout the entire sequence by the C-terminus end interactions with the middle of the peptide. Thus, it appears that end-middle interactions of the backbone are the major obstacles to alpha helices formation using

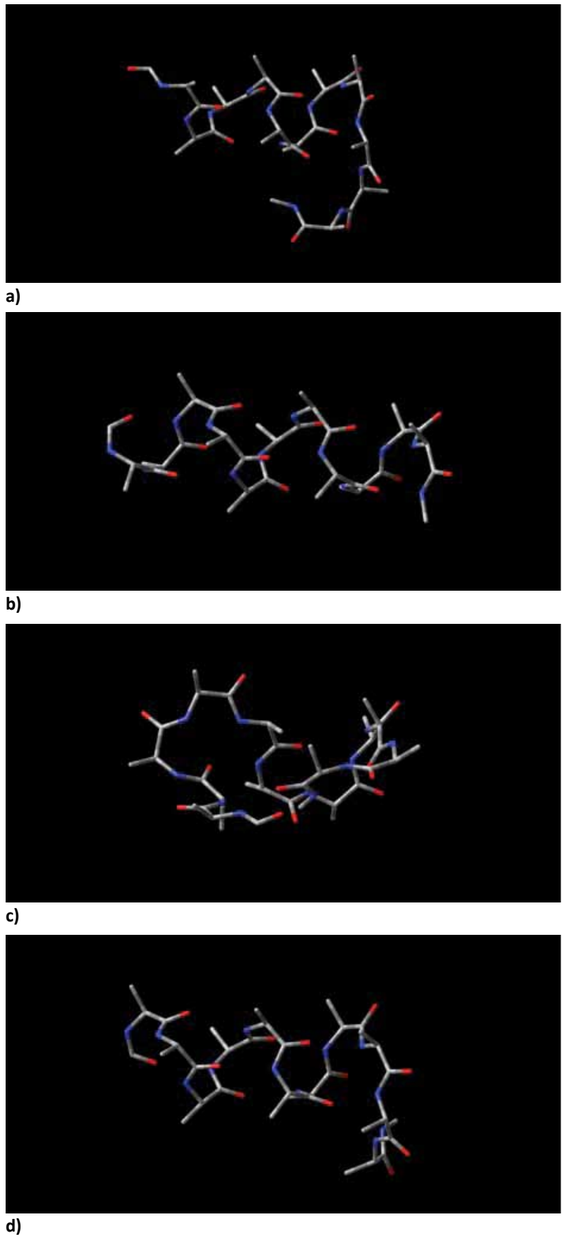

Figure 1: (a) Peptide backbone outline of undeca-alanine peptide conformation at 300K, time step 0.002, conventional method. Notice that the C- terminus end does not "lock" into the alpha helices as expected. **(b) Peptide backbone outline of undeca-alanine peptide conformation at 300K, time step 0.002, sequential method.** Notice that the N- terminus end forms a 3-10 helices instead of the expected alpha helices. **(c) Peptide backbone outline of undeca-alanine peptide conformation at 350K, time step 0.001, conventional method.** Notice that the N- terminus end loops towards the middle of the backbone inhibiting alpha helices formation. **(d) Peptide backbone outline of undeca-alanine peptide conformation at 350K, time step 0.001, sequential method.** The conformation is nearly a perfect alpha helices except that the C-terminus does not completely lock into place.
Figure Legend: Grey = Carbon, Red = Oxygen, Blue = Nitrogen, Yellow = Sulfur. Hydrogen atoms are omitted to better visualize backbone conformations.

this conventional method.

At an initial glance, all four Tal-1a final conformations appear to be completely distinct from one another; however, some characteristics are shared upon closer observation. Comparing Figures 2B and 2D, a MAAY motif where the sulfur of the methionine side chain interacts with hydrogen atoms of the first tyrosine backbone is shared (Figure 2B and 2D). The MAAY motif in the full-length peptide was also present in the earlier stages of the nascent peptide, beginning from MAAY itself. The conformation of the peptide experienced only one major conformational change after the addition of the PTG tripeptide. Even after the introduction of the proline kink, the MAAY motif persisted.

In contrast, it is apparent that the conventional methodology permitted interactions of the methionine side chain outside of the first four amino acids (Figures 2A and 2C). In Figure 2A, the methionine side chain interacts with the hydrogen atoms of the leucine residue (position 5 – MAAYL) (Figure 2A). Figure 2C upholds this pattern of methionine interacting beyond the fourth tyrosine residue (Figure 2C). Instead of dipolar interactions with the α-hydrogen atoms of the leucine side chain however, the sulfur of the methionine residue interacts with the α-hydrogen atoms of proline, the fifth amino acid in sequence. Thus, a MAAY motif can be found between sequentially derived Tal-1a peptides but, no such motif exists with the conventionally derived Tal-1a peptides.

The second major observation of the Tal-1a peptides was the differential location of the aspartic acid residue (position six in sequence). In the conventionally derived peptides, the aspartic acid side chain is located towards the outer edge of the molecule. Conversely, in the sequentially derived peptides, the aspartic acid side chain is located closer towards the centre of the molecule and stabilized by hydrogen bonding to several N–H moieties. At 300K, the aspartic acid side chain is stabilized by hydrogen bonding to five N–H groups and also an additional hydrogen bond between the O–H of the fourth tyrosine residue and the carbonyl of the aspartic acid side chain (Figure 2B). At 350K, the aspartic acid side chain is also stabilized by hydrogen bonding to five N–H groups and an additional hydrogen bond between the threonine O–H and the carbonyl of the aspartic acid side chain (position eight in sequence) (Figure 2D).

Another pair of simulations were conducted only using the step-wise methods at 300K/ TS 0.001 and 350K/TS 0.002, which represent the "cold" and "hot" conditions, respectively. In these two experiments, a similar MAAY motif was observed in Figure 2E and 2F to the one shared by Figures 2A and 2C. Additionally, the aspartic acid side chain was also stabilized by hydrogen bonding to five N–H bonds and located in the approximate centre of the peptide chain.

An overall comparison between the conformations produced from both methods shows that characteristic motifs are shared between conformations that are derived step-wise at both 300K and 350K. The MAAY motif and centralized aspartic acid residue with specific hydrogen bonding stabilization were the two central observations. Conversely, no such shared motifs existed between

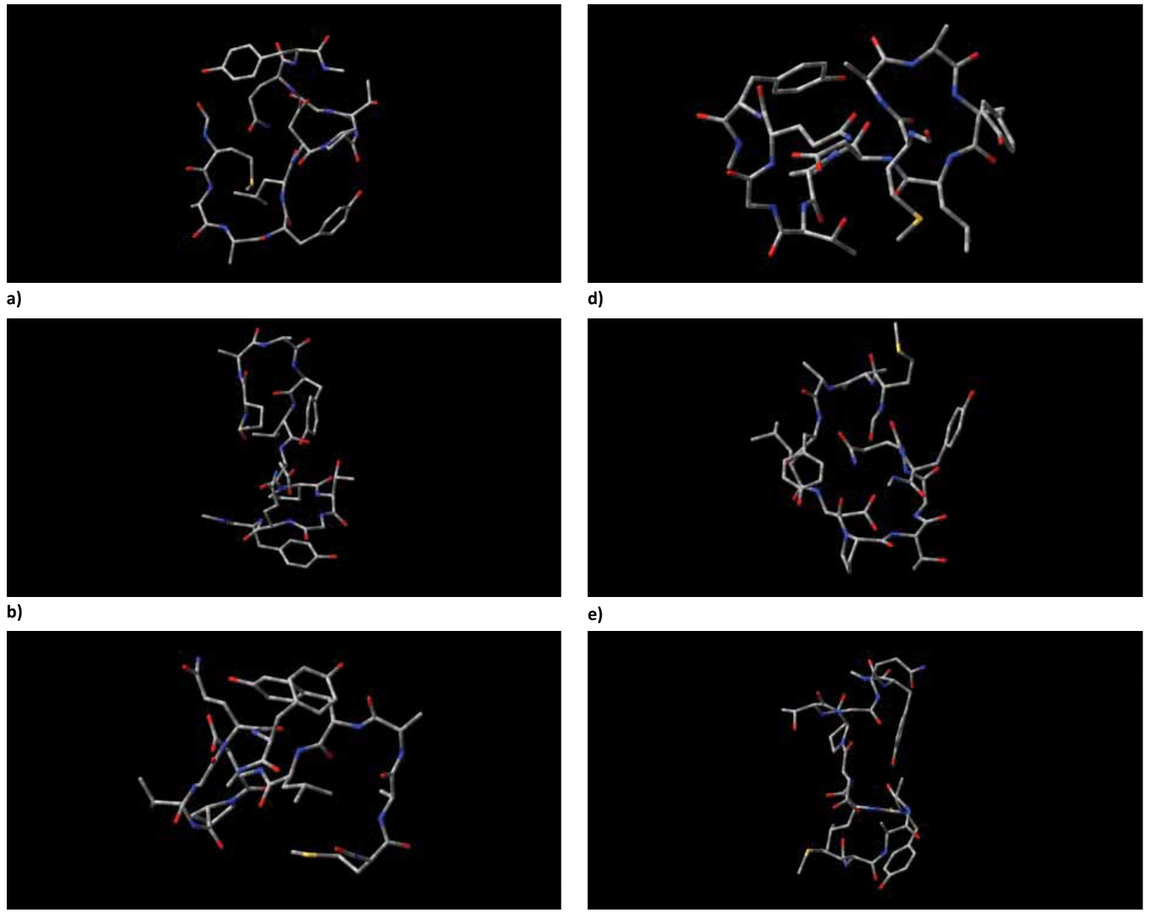

Figure 2: (a) Peptide backbone outline of Tal-1a peptide conformation at 300K, time step 0.002, conventional method. This conformation does not contain the characteristic MAAY loop nor the centralized aspartic acid as the sequentially derived Tal-1a peptides do. **(b) Peptide backbone outline of Tal-1a peptide conformation at 300K, time step 0.002, sequential method.** Notice the characteristic MAAY loop and centralized aspartic acid shared with Figures 2D, 2E, and 2F. **(c) Peptide backbone outline of Tal-1a peptide conformation at 350K, time step 0.002, conventional method.** This conformation does not contain the characteristic MAAY loop nor the centralized aspartic acid as the sequentially derived Tal-1a peptides do. **(d) Peptide backbone outline of Tal-1a peptide conformation at 350K, time step 0.001, sequential method.** Notice the characteristic MAAY loop and centralized aspartic acid shared with Figures 2B, 2E, and 2F. **(e) Peptide backbone outline of Tal-1a peptide conformation at 350K, time step 0.002, sequential method.** Notice the characteristic MAAY loop and centralized aspartic acid shared with Figures 2B, 2D, and 2F. **(f) Peptide backbone outline of Tal-1a peptide conformation at 300K, time step 0.001, sequential method.** Notice the characteristic MAAY loop and centralized aspartic acid shared with Figures 2B, 2D, and 2E.
Figure Legend: Grey = Carbon, Red = Oxygen, Blue = Nitrogen, Yellow = Sulfur. Hydrogen atoms are omitted to better visualize backbone conformations.

the 300K and 350K conventionally derived conformations. The consistency of the MAAY motif and the centralized aspartic acid residue through figures 2B, 2D, 2E, and 2F demonstrate that the final conformation is largely determined by the methodology irrespective of time step or temperature.

Discussion

Our goal was to demonstrate how the prevailing, conventional approach to MD might be inefficient when looking for the natural folding of a peptide/protein. We propose to consider mimicking the natural synthesis of a peptide and simulating its growth path. This way we allow a nascent peptide to fold without any consideration of what is coming later on in the sequence – which a typical MD simulation beginning with the full peptide sequence does not permit. It is not only that our methodology is more akin to *in vivo* peptide synthesis but also that it is more accurate and less computationally costly.

This study predicts the structure of Tal-1a to contain a MAAY loop motif and a centralized aspartic acid. The consistent manifestation of these "motifs" in all sequentially derived Tal-1a confor-

mations provides confidence for our prediction. Our confidence for this new method is also bolstered from correctly predicting the putative alpha helices fold of the undeca-alanine sequence. Moreover, this study demonstrates sequential molecular dynamics more reliably produces similar conformations compared to conventionally derived methods, which seem to exhibit a wide array of conformations. The step-wise process predicted undeca-alanine to be a complete alpha helix while the conventional method only produced a partial helix. Accordingly, we cannot trust this conventional approach for Tal-1a either. However, because the step-wise process for undeca-alanine was correct, then this instills confidence that step-wise molecular dynamics would better predict the natural fold of a peptide.

The notion that subsequent folding patterns are predicated on previous "locked" motifs is a major observation of this study. For example, comparing Figure 2B and 2D, the MAAY motifs are actually inverted in the two conformations, which may account for the drastically different conformation of the subsequent seven amino acids (Figure 2B and 2D). Also, the MAAY motif was consistently linked with a centralized aspartic acid residue, and thus the MAAY motif may contribute to the centralization of the aspartic acid. Future studies should explore the utilization of this sequential molecular dynamics methodology applied to much larger proteins. Tal-1a is the smallest functional peptide discovered *in vivo*, and thus the implications of our proposed methodology may not extend to larger peptides. Perhaps there are specific "locking motifs" which constrain the peptides to specific folding pathways.

Interestingly, temperature was not observed to alter the conformation as much as expected. It was unexpected that the MAAY loop motifs and centralized aspartic acid persisted in all sequentially derived conformations regardless of temperature (Figure 2B, 2D, 2E, and 2F). Temperature appeared to have a bigger effect on undeca-alanine chains. For the undeca-alanine peptides, modeling at 300K more consistently produced "fuller" alpha helices (Figure 1A and 1B) when compared to their 350K counterparts (Figure 1C and 1D). This is consistent with the fact that the bond energy for intramolecular hydrogen bonds is relatively weak (6-8 kcal/mol) compared to the stronger side-chain–side-chain or side-chain–backbone interactions within the Tal-1a peptide (Rupp, 2009).

The next logical step is to characterize the 3-D structure of Tal-1a by X-ray crystallography or atomic force microscopy (Galindo et al., 2007; Giessibl, 2003). As aforementioned, Tal-1a has not been characterized beyond its primary amino acid sequence, and this is admittedly the biggest limitation of our study. However, this is extremely exciting because we may actually be predicting the peptide's conformation – instead of confirming a putative conformation determined by experimental methods, it is these methods which will stand to either validate or invalidate our computationally derived conformations.

The consequences of our findings are important when evaluating the role of a single amino acid within the context of a protein's functionality. Classically, residues can be subject to covalent modification, such as phosphorylation, methylation, etc., all of which are potential mediators of wildtype function. In this study, we have shown that individual residues may also be components of critical upstream motifs that affect downstream folding of an important active site. Thus, the question is how can we discern between these two roles of a single amino acid?

Homology-based substitution studies and *in vivo* mutagenesis studies facilitate this type of investigation. Both studies observe the influence of changing an amino acid within an active cavity; however, the subtle difference is noticeable once we consider the methodologies themselves. Namely, substitution experiments maintain the tertiary structure of the wildtype protein and exchange the wildtype for mutant amino acid. Mutagenesis also exchanges an amino acid but the process of creating a tertiary structure is repeated in a stepwise process, which we conveyed depends on the surrounding sequence; however, there is no way of visualizing this *in vivo*. Conversely, computational substitution experiments can be visualized but do not properly "re-synthesize" the polypeptide in a step-wise manner, thus eliminating the effect of that single residue in the formation of crucial upstream motifs that may predetermine downstream folding patterns. Instead, one should synthesize the wildtype protein and mutant protein via our putative MD methodology. Ultimately, this would be the framework for a "step-wise MD mutagenesis experiment."

Conclusion

Overall, the sequential methodology proposed here yielded more consistent representations of *in vivo* protein folding when compared to the conventional straight-chain approach, but it remains to be seen whether they more accurately depict the native conformations since Tal-1a peptides have yet to be characterized by experimental methods, such as X-ray crystallography. To fully mimic the environment of ribosomal synthesis, additional factors must be considered including solvation effects within the cytoplasm of the cell as well as steric crowding by the ribosome itself or macromolecular crowding. Essentially, to properly model peptide folding, the process of ribosomal synthesis and the environment in which it occurs must be taken into consideration. It is clear that additional structures will enormously increase the complexity of the simulation, but the conformational space available to the protein being formed (folded) will be dramatically reduced by an entropy effect.

Acknowledgements

In addition to professors Csizmadia and Vukovic, who provided me with great guidance throughout the project, I would like to thank Dr. Paul Ayers of McMaster University who made this inter-university collaboration possible, and also Dr. Dave Setiadi for his ongoing encouragement and support.

References

Barlow, D.J., and Thornton, J.M. (1988). Helix geometry in proteins. J Mol Biol 201, 601-619.
Brooks, C.L., 3rd, Onuchic, J.N., and Wales, D.J. (2001). Statistical thermodynamics. Taking a walk on a landscape. Science 293, 612-613.
Charkabarrty, A., Kortemme, T., Baldwin, R.L. (2008). Helix propensities of the amino acids measured in alanine-based peptides without helix-stabilizing side-chain interactions. Protein Science 3, 843-852.
Chasse, G.A. (2001). Peptide and Protein Folding. Journal of Molecular Structure: THEOCHEM 53, 319-361.
Galindo, M.I., Pueyo, J.I., Fouix, S., Bishop, S.A., and Couso, J.P. (2007). Peptides encoded by short ORFs control development and define a new eukaryotic gene family. PLoS Biol 5, e106.
Giessibl, F.J. (2003). Advances in atomic force microscopy. Rev Mod Phys 75, 949-983.
Kondo, T., Hashimoto, Y., Kato, K., Inagaki, S., Hayashi, S., and Kageyama, Y. (2007). Small peptide regulators of actin-based cell morphogenesis encoded by a polycistronic mRNA. Nat Cell Biol 9, 660-665.
Lodish, H. (2000). Molecular Cell Biology (New York, W.H. Freeman).
Pi, H. (2009). New insights into polycistronic transcripts in eukaryotes. Chang Gung Medical Journal 32, 494-498.
Rupp, B. (2009). Biomolecular crystallography: principles, practice and application to structural biology (New York, Garland Science).
Shea, J.E., Onuchic, J.N., and Brooks, C.L., 3rd (2002). Probing the folding free energy landscape of the Src-SH3 protein domain. Proc Natl Acad Sci U S A 99, 16064-16068.
Sun, C., Wang C. (2010). Estimation on the intramolecular hydrogen-bonding energies in proteins and peptides by the analytical potential energy function. THEOCHEM 956, 38-43.

GRADUATE STUDIES
ANATOMY & CELL BIOLOGY
Schulich MEDICINE & DENTISTRY
www.uwo.ca/anatomy

Looking for research opportunities in cell biology or neurobiology?

Get a graduate degree (MSc/PhD) in Anatomy & Cell Biology at Western

- World-class research programs in cancer, cardiovascular disease, musculoskeletal health, cell communication, schizophrenia, reward and addiction, circadian rhythms and neuroendocrinology
- Direct-entry PhD available
- Individualized training and career development to meet the needs of students
- Students with a background in science, health science or psychology accepted
- Generous stipend support

Application deadline: June 1, 2011
www.uwo.ca/anatomy
Western

JULS RESEARCH

The Case of Fly Sex Combs: Using a Model Organism to Infer Mechanisms of Morphological Evolution

Jiwon Lee, Juan Nicolas Malagon, Ellen Larsen

Department of Cell & Systems Biology, University of Toronto, 25 Harbord St, Toronto, ON Canada M5S 3G5

Abstract

Secondary sexual characteristics evolve rapidly in many animals. To elucidate possible mechanisms of rapid evolution, we investigated a secondary sexual characteristic in *Drosophila* males called sex combs; a group of thickened bristles found distally on the front legs. We studied the arrangement and classification of bristles in wild type and mutant flies by comparing numbers of sex comb teeth, tarsal segmental location and vertical position. We included several *Drosophila* species in our analyses, and our results suggest that mutations in *Drosophila melanogaster* can mimic aspects of sex comb morphology and rotation in other species. Also, the perturbations of bristle number alter the localization of sex comb teeth to positions normally occupied by other bristle types in wild type *D. melanogaster*. The existence of *D. melanogaster* mutants which mimic sex comb bristle patterns in related species suggest that there may be a basic "ground plan" in developing tarsal segments that can be rapidly shifted during evolution.

Introduction

The sex comb is an arrangement of thickened bristles, located at the distal region of the most proximal tarsal segment of the front legs in *Drosophila* males (Atallah *et al.*, 2009) and is derived from a transverse row that is rotated approximately 90° during pupal development (Figure 1). Male and female legs share similar patterns of bristles, but the most notable difference is the presence or absence of a sex comb. As a secondary sexual dimorphic characteristic, the sex comb displays enormous diversity in comb size and location in different species (Atallah *et al.,* 2009; Tanaka *et al.,* 2009). This makes the sex comb in *Drosophila* males a particularly good system to study the diverse developmental (Tanaka *et al.,* 2009; Atallah, 2008) and genetic mechanisms controlling morphogenesis and their rapid evolution compared to other bristle patterns in these flies (Barmina and Kopp, 2007; Ahuja and Singh, 2008; True, 2008; Randsholt and Santamaria, 2008)

Figure 1: Schematic for the location of landmark bristles on the first leg of a female and a male *Drosophila melanogaster* (*D. melanogaster*). (A) All transverse rows are aligned perpendicular to the long axes of the leg in female. **(B)** The sex comb is located almost perpendicular to the rest of the transverse rows in male. Blue dots indicate bristles on the transverse rows. Red dots indicate sex comb teeth. Brown dot indicates the central bristle. Green dot indicates the chemosensory bristle. Purple dots indicate longitudinal rows. Post stands for posterior region and Ant stands for anterior region of the leg. Proximal and distal region of tarsal segments are indicated.

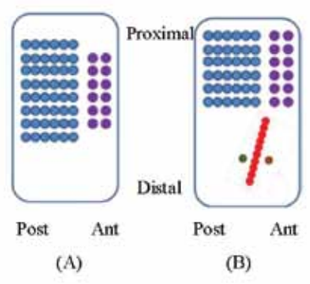

In order to address the issue of rapidly evolving sex comb morphologies, we identified and characterized available mutants of *D. melanogaster*, which possessed altered sex comb position, morphology and bristle type. Specifically, we attempted to find mutants that mimicked sex comb patterns of different species related to *D. melanogaster*. This approach allowed us to infer the minimal genetic changes required to reproduce the phenotypes found in other species. Eventually, we aim to indentify the cellular changes responsible for patterns found in both mutants and other species.

We found that single mutations could perturb the bristle morphology, producing phenotypes that occurred in different species, some of which were in the same phylogenetic subgroup as *D. melanogaster* and some in a phylogenetically distant subgroup. We interpret our findings to suggest that there exist common developmental potentials in all species in which males produce sex combs. These potentials can be perturbed by mutations producing the diversity of species morphologies currently found.

Materials and Methods

Fly stocks

The *bric à brac* (bab^{PR72}) line was generated by Godt *et al.* (1993). *dsx*, *dpp*, *scd*, and *Tsc* stocks were obtained from the Bloomington Drosophila Stock Center at Indiana University (Supplementary Table 1). Flies were selected for abnormal sex comb morphology both for breeding and data collection. In bab^{PR72}, flies that display intermediate phenotypes of sex comb morphology and number of sex comb teeth were selected. In *scd*, *dsx*, *dpp,* and *Tsc* mutants, flies with a high number of ectopic sex comb teeth were selected. We observed at least 15 flies in each mutant type. The specimens photographed here were repeated at least 7 times.

Collection and Crossing

Standard fly culture conditions were used (Atallah, 2008). Flies were kept in bottles on yeast medium at 25°C. The adult legs were dissected, digested and mounted following the protocol described by Atallah (2008). Images were taken using an Olympus light microscope (BX41M) with *Cool Snap* software (a detailed description of methods can be found in the supplementary information section).

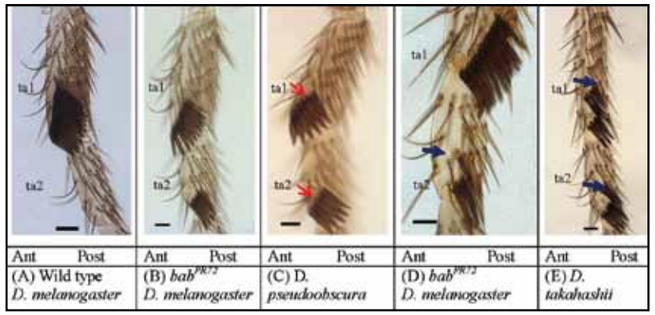

Figure 2: *D. melanogaster* mutants which mimic aspects of sex comb morphology and patterns in other drosophila species. *D. melanogaster* mutant bab^{PR72} mimics some aspects of sex comb morphology observed in other species such as *D. pseudoobscura* and *D. takahashii.* Each arrow indicates similar sex comb patterns and morphology. The images on **(C)** and **(E)** are modified from Atallah *et al.*, 2009. Each tarsal segment (ta) is labeled. Ant stands for anterior region. Post stands for posterior region. Scale bars: 20μm.

Results

Comparison of sex comb morphology among *D. melanogaster* mutants and other Drosophila species

In wild type *D. melanogaster*, the sex comb is observed only in the first tarsal segment. It is parallel to the long axis of the leg and each sex comb tooth is aligned vertically (Figure 2A). During development, the sex comb starts rotating from the posterior region to the anterior region. In the mutant bab^{PR72}, an ectopic sex comb is observed in the second tarsal segment, which is commonly observed in both *D. pseudoobscura* and *D. takahashii* (Figures 2B-E). The mutant bab^{PR72} also reproduces an atypical feature of *D. takahashii* sex combs—a transition between two different types of bristles in the same row (Figures 2D and E; blue arrows).

Comparison of degree of sex comb rotation among *D. melanogaster* mutants and *D. guanche*

The normal sex comb phenotype in *D. melanogaster* is a straight row of bristles almost parallel to the long axis of the leg (Figures 2A, 3A). The bab^{PR72} mutant mimics the degree of rotation observed in both *D. pseudoobscura* and *D. takahashii* (Figures 2B-D). As illustrated in figures 3B and 3C, mutants dsx^D and *Tsc* also have incomplete rotation. In these mutants the distal part of the sex comb has a different angle with respect to the proximal region. The disruption of the sex comb rotation angle is more severe in *Tsc* than in dsx^D, possibly due to extra sex comb teeth found in *Tsc* mutants. *D. guanche* (Figure 3D), contains a larger number of sex comb teeth than *D. melanogaster* wild type but displays incomplete rotation of the distal region, which is observed in *D. melanogaster* mutants dsx^D and *Tsc/CyO* (Figure 3B, 3C).

D. melanogaster mutants show sex comb teeth in atypical locations

Depending on the mutation, we observed ectopic sex comb teeth appearing where transverse rows (Figures 4A and C), longitudinal rows (Figure 4B), and chemosensory bristles (Figures 4B and C) were expected. In the second tarsal segment of sex comb distal (*scd*), a sex comb tooth is observed at the edges of the transverse row (Figure 4A; red arrow). In the first tarsal segment of decapentaplegic (*dpp*), a sex comb tooth (Figure 4B; white arrow)

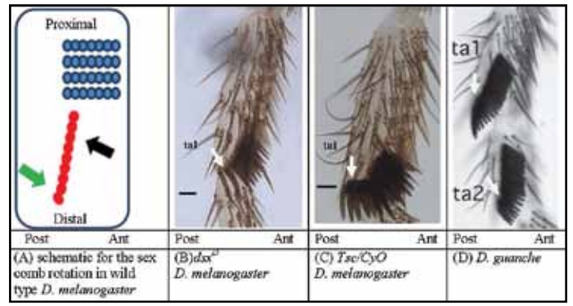

Figure 3: *D. melanogaster* mutants show altered sex comb rotation that resemble the phenotypes of related species *D. guanche*. *D. melanogaster* mutants mimic sex comb rotation observed in other species. Blue dots indicate bristles on transverse rows. Red dots indicate sex comb teeth. The green and black arrows indicate direction of sex comb rotation. White arrows indicate similar sex comb morphologies in *D. melanogaster* mutants and *D. guanche* due to a rotation abnormality in the dsx^D *D. melanogaster* mutant. The image in (D) is modified from Tanaka *et al.* (2009). Each tarsal segment (ta) is labeled. Post stands for posterior region. Ant stands for anterior region. Scale bars: 20μm.

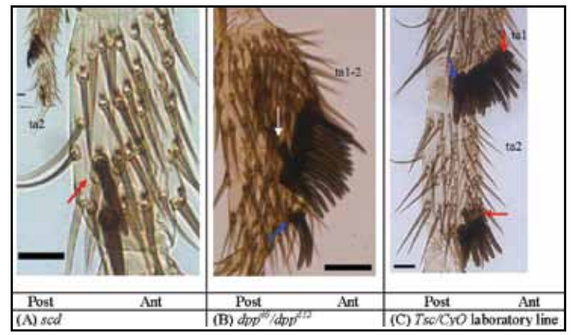

Figure 4: Sex comb teeth that are located in positions where landmark bristles are expected in *D. melanogaster* mutants. In *D. melanogaster* mutants, sex comb teeth are observed in atypical locations where other types of bristles are expected. Each arrow indicates ectopic sex comb teeth in a tarsal segment labeled as ta. Post stands for posterior region. Ant stands for anterior region. Scale bars: 20μm.

is observed where the chemosensory bristle is located in wild type *D. melanogaster*. This leg displays a fusion between the first and the second tarsal segments. As a result, two ectopic sex comb teeth are observed where longitudinal bristles are normally found in wild type (Figure 4B; blue arrow). Sex comb teeth in the *Tsc* mutant are observed where longitudinal (blue arrow) and transverse row bristles (red arrow) are expected in the first tarsal segment (Figure 4C). In the second tarsal segment, sex comb teeth are observed where bristles on the transverse rows are located in wild type (Figure 4C; red arrow).

Discussion

Phenotypic similarities between mutants and other species suggest a shared ground plan for sex comb development among drosophilids

By modifying the expressivity of *D. melanogaster* mutants, sex comb characteristics similar to those of other species are observed. We have shown that the variable bab^{PR72} mutant may show similar sex comb rotation, location, morphology and pattern of bristles to *D. pseudoobscura* and *D. takahashii*. Similarities between *D. melanogaster* mutant sex combs and those of other species have also been observed by other researchers. Malagon (unpublished) noticed that among bab^{PR72} mutants there were two patterns reminiscent of *D. affinis* and of *D. biarmipes*. Atallah *et al.* (2009) were also able to mimic the *D. biarmipes* phenotype by perturbing *Dachshund* expression. In addition, Randsholt and Santamaria (2008) used the *Montium-like* mutations (*MtlT5* and *Mtl10*) to generate phenotypes similar to those of the Montium group, having sex combs in the second tarsal segment. Phenotypic similarities between D. melanogaster mutants and other species suggest that there may be a basic "ground plan" in sex comb development in tarsal segments which may be modified in various ways in mutant phenotypes but are fixed in different species.

Correlation of sex comb tooth number with rotation phenotype suggests similar sex comb rotation mechanisms among species

The phenotypic similarities seen between mutant and wild type phenotypes may extend to common cellular and developmental mechanisms. In other words, we suggest that mutant perturbations in the rotation mechanism might mimic processes occurring in other species. According to Atallah *et al.*(2009) there are two stages of sex comb rotation: early proximal rotation and late distal rotation. *D. melanogaster* mutants dsx^D and *Tsc* are characterized by a disrupted second stage that displays an incomplete rotation (Figure 2). In addition, genetic perturbation in sex determination pathways such as dsx^D and *transformer-2* ($tra\text{-}2^{ts1}$) frequently show defects in the rotation of the distal region (Robinett *et al.*, 2010; Belote and Baker, 1982). The reduced degree of rotation in the *Tsc* mutant compared to dsx^D shows a correlation between the number of sex comb teeth and the degree of abnormal sex comb rotation. Increased number of sex comb teeth might account for the observed curvature of the sex comb in *D. guanche*. Malagon (unpublished) showed that the rotation of the distal region in *D. melanogaster* is due to a dynamic movement of cells in the same direction as the sex comb rotation. Detailed temporal and spatial monitoring of cellular processes would be required to determine if sex comb rotation in *D. guanche* employs the same mechanism.

Is any tarsal bristle a potential sex comb tooth?

In *D. melanogaster* mutants, sex comb teeth are observed in locations where landmark bristles are usually located in wild type flies. Jursnich and Burtis (1993) used transgenes that express the male doublesex isoform under the control of a heat-inducible promoter ($hs{:}dsx^M$) to show that any bristle can be transformed to a sex comb tooth. It is likely that bristles are pluripotent structures during early stages of development. Development of a sex comb in atypical locations provides evidence that any bristle can become a sex comb tooth when driven by the right perturbations to the system. Depending on the location, bristles can differentiate into chemosensory, longitudinal, or central bristles. If the bristle is located near a developing sex comb, it is more likely to transform into a sex comb tooth (Supplementary Figure 1). Mukherjee (1964) reported similar findings using only the mutant sexcombless, suggesting that this is not specific to the mutant, but instead a general property of the system. Currently, the evidence suggests that any tarsal bristle is a potential sex comb tooth.

Why is it so easy for mutants to mimic sex comb traits in different species?

Darwin (1859) was among the first to link morphological changes in evolution to hereditary changes affecting development. Our findings indicate that selected *D. melanogaster* mutants can mimic specific morphologies of other species, contingent on the genetics of the organism. This mimicry reflects changes in common developmental modules such as cell behaviours involved in rotation and the ability of bristles to be easily transformed from one type of bristle precursor to another. We have shown that mutations altering sex comb bristle types, rotation and location can produce phenotypes resembling those of other species.

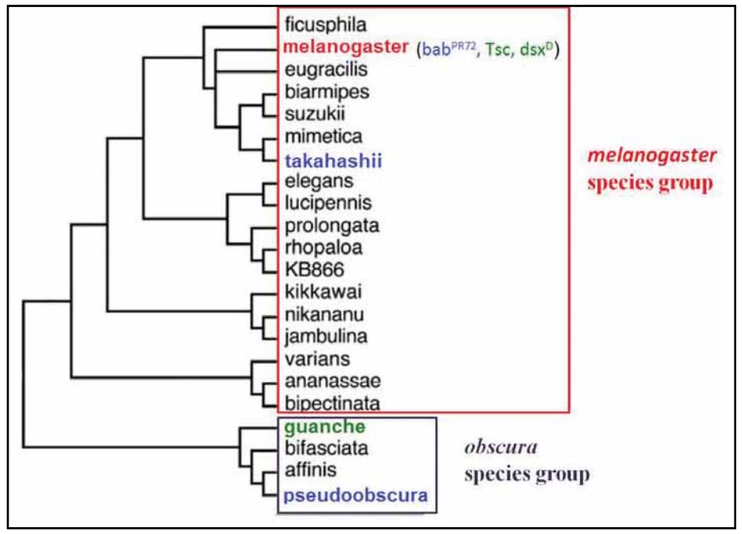

Figure 5: Phylogenetic distribution that describe the relationship between the *Drosophila* species. As colour indicated, bab^{PR72} showed similar sex comb phenotypes to *takahashii* and *pseudoobscura* (Figure 2) while *Tsc* and dsx^D showed similar phenotypes to *guanche* (Figure 3). The image is modified from Barmina and Kopp (2007).

Table S1: List of stocks used in this paper.

Name	Genotypes	Stock number*	Location
decapentaplegic (dpp)	dpp^{d6}/CyO dpp^{d12}/CyO	2062 2070	2 2
doublesex (dsx)	T(1;3)OR60/TM2/In(3R)C,dsx^DSb^{1}sprd^{1}e^{1}l(3)e^1	840	1;3
Triple sex comb (Tsc)	Tsc^1/CyO	2058	2
sex comb distal (scd)	$y^1scd^1ras^1v^1f^1$	5070	1

* Bloomington Stock Center

The reason that we stress a common "ground plan" basis for the mutant phenotypes we have observed is twofold. First of all is the findings of the Kopp lab (Tanaka *et al.*, 2009; Barmina and Kopp, 2007; True, 2008) which state that gain and loss of *scr* gene expression in the first leg as well as the cellular mechanisms underlying sex comb position were not conserved in any particular lineage. Second, the similarities between mutants and their mimicked species were not congruent with species relatedness. In the cladogram, we note that *D. takahashii* is distant from *D. melanogaster* while still remaining in the *melanogaster* subgroup *whereas D. guanche* and *D. pseudobscura* are in an entirely different subgroup, which is the *obscura* subgroup (Figure 5). We therefore feel justified in looking for an underlying developmental basis rather than a purely phylogenetic one.

In principle, sex comb phenotypes should be achievable without extensive genetic modification. Future work should compare developmental processes in *D. melanogaster* mutants and other species to determine if similar mechanisms are responsible for the observed phenotypic match in sex comb characteristics.

Acknowledgements

We thank Sheng Cheng and Abha Ahuja for helpful suggestions and technical assistance.

References

Ahuja, A. and Singh, R. S. (2008). Variation and evolution of male sex combs in Drosophila: Nature of selection response and theories of genetic variation for sexual traits. The Genetics Society of America. *179*, 503-509.
Atallah, J., Liu, N., Dennis P., Hon A., Godt D., Larsen, E. (2009). Cell dynamics and developmental bias in the ontogeny of a complex sexually dimorphic trait in *Drosophila melanogaster.* Evolution and Development. *11*, 191-204.
Atallah, J. (2007). The Development and Evolution of Complex Patterns: The Drosophila Comb As a Model System. Cell and System Biology. Toronto, University of Toronto. Ph.D.
Barmina, O., and Kopp, A. (2007). Sex-specific expression of a HOX gene associated with rapid morphological evolution. Developmental Biology. *311*, 277-286.
Belote, J. M., and Baker, B. S. (1982). Sex determination in Drosophila melanogaster: Analysis of transformer-2, a sex-transforming locus. Genetics. *79*, 1568-1572.
Darwin, C. (1859). On the origin of species. Cambridge, Harvard University Press.
Godt, D., Couderc, J., Cramton, S.E., and Laski, F.A. (1993). Pattern formation in the limbs of Drosophila: bric à brac is expressed in both a gradient and a wave-like pattern and is required for segmentation of the tarsus. Development. *119*, 799-812.
Jursnich, V. A., and Burtis, K.C. (1993*). A positive role in differentiation for the male doublesex protein of Drosophila.* Developmental Biology. *155*, 235-249.
Mukherjee, A. S. (1964). The effects of sexcombless on the forlegs of Drosophila melanogaster. The Genetic Society of America. *51*, 285-304.
Randsholt, N. B., and Santamaria, P. (2008). How Drosophila change their combs: the Hox gene sex combs reduced and sex comb variation among Sophophora species. Evolution and Development. *10*, 121-133.
Robinett, C. C., Vaughan, A, G., Knapp, J-M., and Baker, B.S. (2010). Sex and single cell. II. There is a time and place for sex. PLoS Biology. *8*, e1000365.
Tanaka, K., Barmina, O., and Kopp, A. (2009). Distinct developmental mechanisms underlie the evolutionary diversification of Drosophila sex combs. PNAS. *106*, 4764-4769.
True, J. R. (2008). Combing evolution. Evolution & Development. *10*, 400-402.

Supplementary Information:

Light Microscopy

Adult flies were collected using CO_2. The whole bodies of flies were collected into an eppendorf. Then, 75% ethanol was added until all flies were immersed, to preserve the sample. The ethanol was removed using a pipette, without touching any flies. 2N NaOH was then added until all flies were immersed. Then, the eppendorf was heated at 70°C for 40 minutes to digest any skeletal muscles which prevented a clear view of the sex combs. After the solution cooled, the 2N NaOH was removed using a pipette, without touching any flies. The sample was preserved in glycerol until mounting.

Each anesthetized fly was picked up with a paintbrush, and the first leg was dissected near the tibia using forceps. This allowed for easier manipulation during microscopy. The leg was placed in a drop of Hoyer's mounting medium on a slide and was oriented with the sex comb facing upwards. Hoyer's mounting medium contains chloral hydrate, used to fix the leg (Anderson, 1954). The coverslip was slowly placed in order to prevent any formation of bubbles.

Pictures were taken using the Olympus light microscope (BX41M) with Cool Snap software.

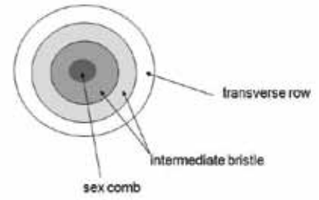

Figure S1: Schematic that shows a gradient around sex comb. It seems there is a gradient which controls sex comb development. Each circle is divided based on the gradient. At the center, the gradient is the highest. As moving away from the center, the gradient is decreased. This might lead to a change in morphology of bristles from sex comb teeth to intermediate bristles and bristles in the transverse row.

References (Supplementary Information):

Anderson, L.E. (1954). Hoyer's Solution as a rapid permanent mounting medium for bryophytes. The Bryologist. *57*, 242-244.

JULS RESEARCH

Validation of NASA Aura Satellite OMI and examination of the spatial distribution of air pollutants in GTA using Ogawa Passive Samplers

Yi Si (Lewis) Sun Liu

Department of Chemistry, Department of Laboratory Medicine and Pathobiology, University of Toronto

Abstract

Previous studies have shown that prolonged exposure to NO_2 (>30ppb) may contribute to respiratory disorders and premature mortality. To properly evaluate the links between pollution exposure and negative health outcomes, accurate measurements of pollutant concentrations on spatial scales relevant to human exposure are urgently required. Currently, two ground measuring devices located at Hendon/Young and Bay/Wellesley from the Ministry of Environment (ME) have been measuring such pollutants in North York and Downtown Toronto respectively. However, such measurements are not representative of personal exposure, since NO2 fields are often very heterogeneous and vary significantly within urban areas. One promising approach is remote sensing measurements of pollutants from space, for example the Ozone Monitoring Instrument (OMI) onboard NASA's AURA satellite. In this investigation, OMI will be compared to data collected using a network of Ogawa Passive Samplers (OPS). Satellite –ground spatial comparisons are complicated by a number of factors, the greatest of which are that OMI observations average [NO_2] over its field of view (340km²) and integrates the entire atmospheric column, while a ground-based instrument samples at a single point. Ground measurements were averaged within the OMI FOV to solve this problem. Comparison showed OMI overestimating by only 18% but as high as 45% for ME. Spatial distribution of the mapped air pollutants showed that the concentration was lower than potential levels of health threat. By providing a spatial comparison of measurements made by ME, OPS and OMI, this study hopes to pave the way for understanding and using satellite-based epidemiology.

Introduction

Previous studies have shown that prolonged exposure to high ambient [NO_2] (>30ppb) may contribute to respiratory disorders, premature mortality and lung cancer (D.P.Anderson et al., 1962; Jerrett et al., 2009; Novaes et al., 2007; Reece et al., 1984). Ergo it is essential to accurately measure the pollutant concentrations on spatial scales relevant to human exposure. Currently, two ground measuring device located at Hendon/Young and Bay/Wellesley from Ministry of Environment (ME) have been measuring such pollutants in North York and Downtown respectively. However, such measurements are not representative of personal exposure in GTA; since NO_2 fields are often very heterogeneous, varying significantly within urban areas. One promising approach is remote sensing measurements of pollutants from space, for example the Ozone Monitoring instrument (OMI) onboard NASA's AURA satellite.

The Ozone Monitoring Instrument (OMI) is a space-borne spectroradiometer that uses a two-dimensional charge coupled device (CCD) array detector to simultaneously measure the spectra of the Earth shine radiance at large number of viewing angles. Among

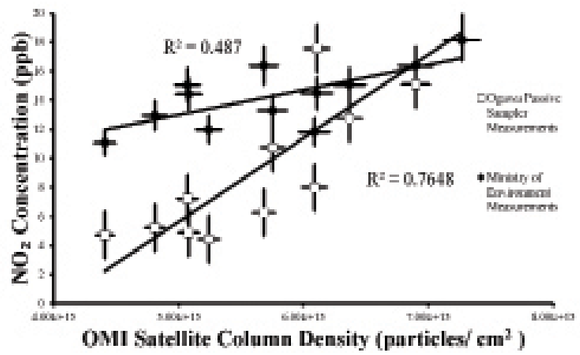

Figure 1: Comparison of the measurements made OMI (x axis) in column density, OPS in ppb (filled y-axis) and Hourly Active Sampler from Environmental Canada (unfilled y-axis) after using correction algorithm (cloud density >0.2). OMI over-measurement of NO2 is shown by the non-zero origin.

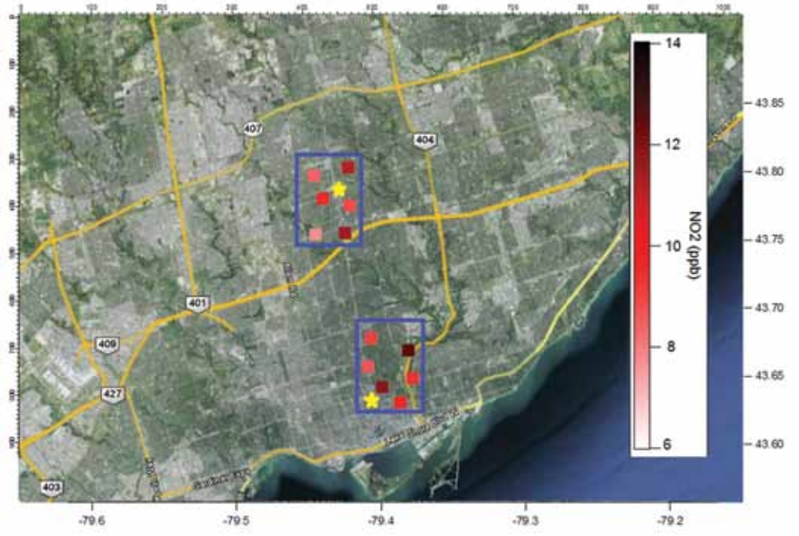

Figure 2: A map of the Downtown and North York target cells and the locations of the 12 passive sampling monitoring sites (squares) and the ME monitoring sites (stars). The squares are coloured by the concentration of NO2 observed at each site. Blue box represents the FOV of Aura OMI.

the broad spectral regions, ozone (O_3) and nitrogen dioxide (NO_2) can be identified and measured, both for the ongoing monitoring of the Earth's stratospheric ozone layer and for the monitoring of air quality in the troposphere (lowest ~10 km). In this investigation, Ogawa Passive Samplers will be deployed in Greater Toronto Area within the two OMI target grid cells and a comparison will be presented. Simultaneous measurements of NH_3, another atmospheric pollutant, could also be made with the passive sampler and are included in this report.

Methods and Materials

Site Deployment

Ogawa Passive Samplers (Ogawa, Pompano Beach, FL, USA) were used in sampling NO_2 and NH_3 at 12 locations across Toronto (6 Downtown and 6 in North York). Locations were chosen within the FOV of OMIand represent the industrial, traffic, commercial, residential, and rural regions of the city. The samplers were exposed at each location and were replaced monthly for a period of 6 months (March – August 2010). Each sampler contained two reactive pads impregnated with Triethanolamine and citric acid for simultaneous measurement of NO_2 and NH_3 respectively.

Extraction

After the appropriate sampling interval (20 – 30 days), samplers exposed to ambient air were collected; the reactive pads were taken out using clean forceps and then immersed into 8.0ml deionized water contained in clean plastic vials. The vials were then closed and shacked to extract the ions from the filters. The vials were then centrifuged for 20 minutes. The vials were then stored in a refrigerator at 4°C until analysis.

Ion Chromatography (IC) Analysis

Nitrite ions (from NO_2) and ammonium ions (from NH_3) were detected using ion chromatography (Dionex ICS 2000). In each case, 1.6 mL of sample was injected, using potassium hydroxide as the eluent for the anion system, and methane sulfonic acid for the cation system. Calibration graphs of integrated areas versus concentrations were constructed using standard solutions (refer to supplementary materials). Sampler extracts were measured under the same conditions.

Concentrations from the passive samplers (in units of moles per mL of extraction solution) were converted to atmospheric concentrations (in units of parts per billion (ppb) by volume) using a formula that took into account the rate of diffusion of the individual molecules to the surface of the reactive pad and the length of exposure (refer to supplementary materials).

Results

Averaging data for all of the sites over six months yielded concentrations of 1.71 ppb for ammonia and 6.03 ppb for nitrogen dioxide. Measurements of NO_2 were closer in comparison with data obtained from ME (7.9 ppb) than Jerrett's LUR interpolation (14.3ppb). Concentration levels were shown to be as much as 25% higher for both pollutants near major roads and highways which is consistent with the study done by Gilbert et al. (Gilbert et al., 2005); while concentrations obtained differ as much as 20% during temperature differences of 15 Celsius, which is also consistent with previous studies(Ray, 2001; Yanagisawa and Nishimura, 1982). Stronger correlation in Figure 3 was shown between NO_2 and NH_3 concentrations in North York (R =0.82) compared to Downtown (R =0.38). The variability of the measurements (quantified by the standard deviations) of ammonia and nitrogen dioxide was greater in Downtown (Ammonia: 1.10 ppb, Nitrogen Dioxide: 1.43 ppb) than North York (Ammonia: 0.6 ppb, Nitrogen Dioxide: 1.22 ppb), signifying more NO_2 and NH_3 emission sources in Downtown. One objective of the study is to examine the variability of spatial scales smaller than those that can be measured by the satellite, and the standard deviations represent information about the range of possible exposures within a single target grid cell.The data points in Figure 2 are coloured by the NO_2 atmospheric concentration observed at each site for the six months.

The measurements made using the passive samplers were averaged for each target grid cell for each month, and compared to two different data sets. One was the average monthly measurement obtained for the ME site in the grid cell, and the other was the average monthly measurement from OMI. In the case of the OMI data, the first step in the analysis was to reject any data with significant cloud cover (cloud fraction > 0.2), before averaging the remaining days. This was necessary because if most of the field of view was obscured by clouds, then the satellite could not accurately measure pollutants close to the surface(Boersma et al., 2008; Bucsela et al., 2005; Celarier et al., 2008). No correlation was shown between the measurements when raw OMI data was used, as shown in figure 3. Using Igor Pro Optimization programming, the correlation coefficient rose up to 0.89with OMI's maximum overestimation of 12%

when data with cloud fraction of less than 0.2 was considered.In Figure 1, the average [NO_2] measured by OMI for each month in each grid cell is compared to the passive samples (unfilled) and the ME ground-based instrument (filled). The coefficient of determination (R^2) is quite strong in both cases (R > 0.65).

Discussion

The significant increase in correlation between measurements when cloud fraction is considered shows the importance of its inclusion in correction algorithm. Cloud fraction defines the relative amount of cloud present during the day of the OMI sampling. High cloud fraction is present when there are significant amount of cloud cover and produces high uncertainly; lower cloud fraction produces lower uncertainly (Celarier et al., 2008). Considerations of cloud fraction must be carefully analyzed; taking higher cloud fraction values will give more data points, but will produce higher uncertainty and disturbances. Having too small values will yield a low number of data points for usage. Igor Pro Optimization programming was used to apply correction algorithm. Generally, about 75% of measured data remained with cloud fraction of less than 0.2.

Overestimation of NO_2 by OMI is likely due to the intrinsic difference in method sampling and the overestimation of tropospheric boundaries (Celarier et al., 2008). Higher measurements obtained by ME instrument compared with OPS measurements shown in figure 1is most likely due to sampling variation. As shown in Figure 2, both ME locations are close proximity to major roads (Hendon/Young and Bay/Wellesley) and cars are one of the main NO_2 emission sources (Gilbert et al., 2005). Despite the large OMI FOV (340 km2),strong correlation was still shown between OPS and OMI measurements; suggesting that the 12 OPS sampling locations were exceptionally well representative sites of the OMI FOV, and that normalization reduced the heterogeneous nature of the tropospheric NO_2 field within large FOV measurements

Concentrations obtained for nitrogen dioxide in GTA are shown to be lower than levels of threat (30ppb), even near highway areas as shown in Figure 2. This indicates GTA to be a relatively clean city, with no significant NO_2 pollution(Ray, 2001; Yanagisawa and Nishimura, 1982).Higher correlation shown in Figure 3 between NO_2 and NH_3 measurements in North York compared to Downtown suggests the possibility of a common emission source in North York. Lower correlation between the air pollutants in Downtown suggests multiple and different emission sources (Gilbert et al., 2005). High standard deviation shown between monthly measurements may be due to the close proximity of emission sources and also because of the high rate of photolysis of NO_2 in the presence of high temperature and UV, especially during the summer (July – August) compared to winter (December – February)(Yanagisawa and Nishimura, 1982). On the other hand, concentration of ammonia has been relatively low and the spatial distribution has been hard to assess. Concentration of ammonia was measured with a range of 1 – 2ppb in previous studies by the ME, which is consistent with the monthly averages obtained from the OPS.

Conclusion

This study demonstrates that that variation in location sampling of NO_2 and implementation of cloud fraction consideration can have significant impacts on the interpretation of OMI measurements. Although tropospheric NO2 field is heterogeneous and OMI FOV span as much as 340 km^2, careful and thoughtful deployment of ground based instruments can overcome this problem. By using OMI, spatial distribution of NO_2 was obtained and ground measurements by ME and OPS were assessed. Concentrations of NH_3 obtained were low and spatial distribution has been hard to assess. Measurements of NH_3 concentrations were consistent with previous measurements made by ME. Spatial distribution of NO_2 mapped showed that the concentration was lower than potential levels of health threat. By providing a primitive interpretation of ground-spatial measurements, this study hopes to pave the way for a more extensive study of satellite-based epidemiology in the future.

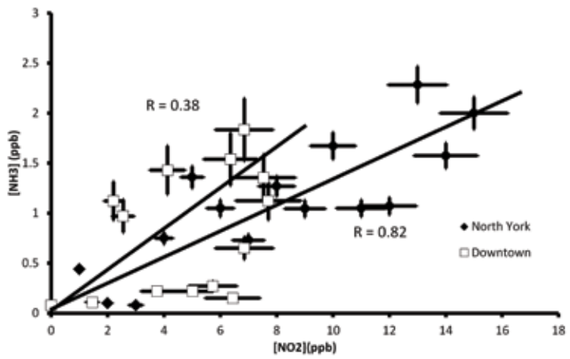

Figure 3: Comparison of concentration of NO2 and NH3 measured in North York and Downtown. Higher correlation was shown in North York compared to Downtown.

Acknowledgments

This study was funded by the Chemistry Department ROP299 program and the Atmospheric Lab. I would like to thank Professor Jennifer Murphy for supervising and giving me this opportunity to work in her lab. I would also like to thank Jack Zhang, Heeba Abdullah, Milos Markovic, Lori Yin, Avila De Sousa, Trevor VandenBoer, Alex Petroff, Jeff Geddes and the rest of the Atmospheric Chemistry group for their wonderful help, support and encouragement. In addition, I would like to thank NASA for providing our lab with the available OMI data and their technical support.

References

Boersma, K.F., Jacob, D.J., Eskes, H.J., Pinder, R.W., Wang, J., and A, R.J.v.d. (2008). Intercomparison of SCIAMACHY and OMI tropospheric NO 2 columns: Observing the diurnal evolution of chemistry and emissions from space. J Geophys Res 113.

Bucsela, E.J., Perring, A., Cohen, R.C., Boersma, K.F., Celarier, E.A., Gleason, J.F., Wenig, M., Bertram, T., Wooldrige, P., Dirksen, R., et al. (2005). Comparison of tropospheric NO2 from in situ aircraft measurements with near-real-time and standard product data from OMI. J Geophys Res.

Celarier, E.A., E. J. Brinksma, Gleason, J.F., Veefkind, J.P., Cede, A., Herman, J.R., Ionov, D., Goutail, F., Pommereau, J.-P., Lambert, J.-C., et al. (2008). Validation of Ozone Monitoring Instrument nitrogen dioxide columns. JOURNAL OF GEOPHYSICAL RESEARCH 113.

D.P.Anderson, C.W.Beard, and R.P.Hanson (1962). The Adverse Effects of Ammonia on Chickens Including Resistance to Infection with Newcastle Disease Virus. American Association of Avian Pathologists, 369 - 371.

Gilbert, N.L., Goldberg, M.S., Beckerman, B., Brook, J.R., and Jerrett, M. (2005). Assessing Spatial Variability of Ambient Nitrogen Dioxide in Montreal, Canada, with a Land-Use Regression Model. Air & Waste Management Association, 1059 - 1063.

Jerrett, M., Finkelstein, M.M., Brook, J.R., Arain, M.A., Kanaroglou, P., Stieb, D.M., Gilbert, N.L., Verma, D., Finkelstein, N., Chapman, K.R., et al. (2009). A Cohort Study of Traffic-Related Air Pollution and Mortality in Toronto, Ontario, Canada. Environmental Health Perspectives, 772- 777.

Novaes, P., Saldiva, P.H.d.N., Kara-José, N., and Macchione, M. (2007). Ambient Levels of Air Pollution Induce Goblet-Cell Hyperplasia. Environmental Health Perspectives, 1753-1756.

Ray, J.D. (2001). Spatial distribution of tropospheric ozone in national parks of California: interpretation of passive-sampler data. TheScientificWorld 1, 483-497.

Reece, F.N., Lott, B.D., and Deaton, J.W. (1984). Ammonia in the atmosphere during brooding affects performance of broiler chickens. Poultry Science, 486-488.

Yanagisawa, Y., and Nishimura, H. (1982). A badge-type personal sampler for measurement of personal exposure to NO2 and NO in ambient air. Environment International 8, 235-242.

JULS RESEARCH

The relationship between amino-terminal pro brain natriuretic peptide (NT-proBNP) and right ventricle systolic pressure in heart failure patients

Andrew M. Micieli*[1], Edson Nemi[2]

[1]Faculty of Arts and Science, University of Toronto, Toronto, ON Canada, andrew.micieli@utoronto.ca, *Corresponding author
[2]St. Michael's Hospital, University of Toronto, Toronto, ON Canada, nemie@smh.toronto.on.ca

Abstract

Background: Although the value of amino-terminal pro brain natriuretic peptide (NT-proBNP) measurement in differentiating between cardiac and non-cardiac causes of dyspnea is well established, the variation of these levels in patients with established heart failure and its correlation with non-invasively determined right ventricle systolic pressure (RVSP) is currently limited.

Methods: A retrospective chart review of 106 systolic heart failure patients referred to the St. Michael's Hospital heart failure clinic between October 2006 and August 2009.

Results: A correlation for the data revealed that NT-proBNP and RVSP were significantly correlated, r = 0.43, P<0.001.

Conclusions: Clinical usage of NT-proBNP as a marker of elevated RVSP in systolic heart failure patients may help physicians estimate changes in filling pressures over time without the need for repeated echocardiograms.

Introduction

Heart failure is a major public health concern in the Western world that continues to grow despite advances in therapeutic approaches (Haldeman et al., 1999). Effective initial and serial assessments of patients presenting with or without symptoms of heart failure are therefore needed to facilitate diagnostic and therapeutic decisions. The B-type natriuretic peptides have accordingly assumed an important role as an adjunct in assessing the prognosis of heart failure patients. Brain natriuretic peptide (BNP) is a vasodilatory, natriuretic factor that is released predominantly by cardiac myocytes to inhibit cardiac sympathetic traffic, renin angiotensin aldosterone activity and cardiac fibrosis within its half life of 22 minutes (Troughton and Richards, 2009). Translation of the BNP gene results in an initial product that must undergo further modification through the removal of a 26 amino acid (aa) peptide sequence and subsequent cleavages by proteolytic enzymes. The end stage products are BNP and NT-proBNP, a biologically active 32 aa molecule and a biologically inert 76 aa amino terminal portion, respectively (Martinez-Rumayor et al., 2008).

Although BNP and NT-proBNP are released from the same pre-protein, there are some key differences in the characteristics of these two factors. NT-proBNP has no biological activity and is cleared by the reticuloendothelial system and renal mechanisms rather than by endocytosis through the natiuretic peptide receptor C (Balion et al., 2006). Moreover, NT-proBNP is estimated to circulate with a longer half-life of 1 to 2 hours in comparison with BNP and has demonstrated less intra-patient variability (O'Hanlon et al., 2007). Mueller and colleagues showed that in detecting patients with asymptomatic left ventricle dysfunction, NT-proBNP had superior sensitivity to BNP (Mueller et al., 2004). Consequently, there may be important variability between BNP and NT-proBNP when trying to correlate their plasma values with cardiac filling pressures and patient outcomes.

Although the value of natriuretic peptide measurement in differentiating between cardiac and non-cardiac causes of dyspnea is well established (Januzzi et al., 2005; McCullough et al., 2002), the variation of these BNP and NT-proBNP levels in patients with established systolic heart failure and their correlation with non-invasively determined right ventricle systolic pressure (RVSP) has demonstrated inconsistent results. In 19 outpatients with chronic heart failure (left ventricle ejection fraction <40%), Braunschweig et al. found that single measurements of NT-proBNP were not significantly correlated with RVSP at both "24 h" daily living activities (r = 0.28) and "rest" (r = 0.31) (Braunschweig et al., 2006). However, within patient serial measurements showed significant positive correlations between NT-proBNP and RVSP (P=0.006). Using BNP rather than NT-proBNP, Nakao et al. collected plasma BNP levels on admission and in the chronic stage for 25 patients presenting with diastolic heart failure and 25 with systolic heart failure (Nakao et al., 2007). Specifically in the 25 patients with systolic heart failure they found a significant

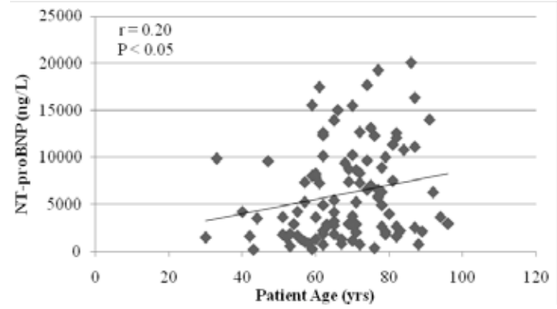

Figure 1: Significant relationship between NT-proBNP (amino-terminal pro brain natriuretic peptide) with Patent Age.

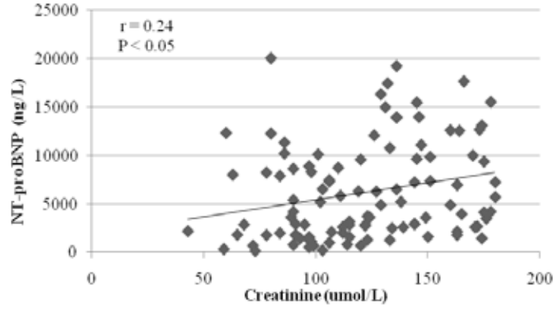

Figure 2: Significant relationship between NT-proBNP (amino-terminal pro brain natriuretic peptide) with blood Creatinine levels.

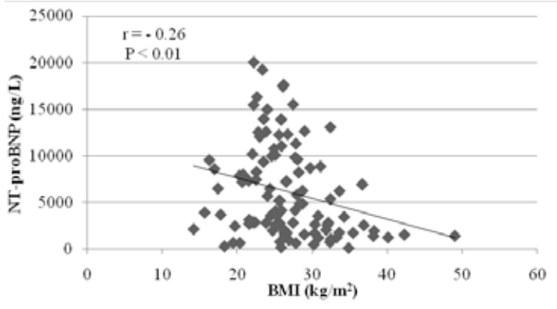

Figure 3: Significant relationship between NT-proBNP (amino-terminal pro brain natriuretic peptide) with BMI (body mass index).

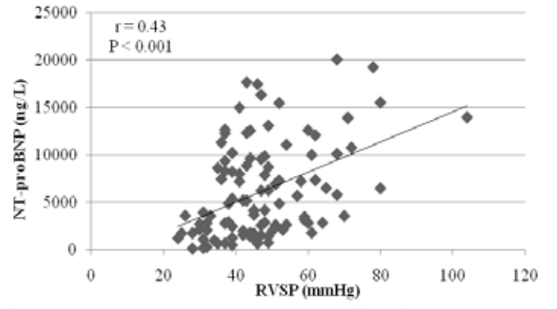

Figure 4: Significant relationship between NT-proBNP (amino-terminal pro brain natriuretic peptide) with RVSP (right ventricle systolic pressure).

correlation between BNP and estimated pulmonary artery systolic pressure (r = 0.63; P<0.01). Also using BNP, Troisi et al. used a population of 60 patients with chronic systolic heart failure (according to the European Society of Cardiology Guidelines for diagnosis and treatment of CHF) and stable clinical conditions to assess if right ventricle function could be related to BNP levels (Troisi et al., 2008). Univariate regression analysis showed a significant relationship between BNP and PAP (r = 0.42; P<0.05).

Given the increasing usage of NT-proBNP rather than BNP in hospital settings for the diagnosis and treatment of heart failure, the goal of this present study is to further investigate the relationship between NT-proBNP with echocardiogram parameters, specifically RVSP, to investigate whether a significant correlation exists between the two parameters. A number of patient variables including concomitant systemic diseases and lifestyle factors may influence the relationship between NT-proBNP and RVSP, further emphasizing the need for additional evidence and larger sample sizes. If a significant correlation exists then the information gathered will help determine the role of substituting NT-proBNP measurements for repeated echocardiography in systolic heart failure patients.

Methods

A retrospective chart review of consecutive patients referred to the St. Michael's Hospital heart failure clinic between October 2006 and August 2009 who were meeting the inclusion criteria outlined below were selected for the study. For inclusion patients must have: 1) a diagnosis of heart failure 2) documented measurements of NT-proBNP and right ventricle systolic pressure (RVSP) and 3) preserved renal function with a blood creatinine level <180umol/L. A diagnosis of clinical systolic heart failure was made by a St. Michael's Hospital Cardiologist, according to the Canadian Cardiovascular Society consensus conference recommendations on heart failure (Arnold et al., 2006). Transthoracic Doppler echocardiography was performed at St. Michael's Hospital and used as the primary diagnostic test to assess standard parameters such as left ventricle ejection fraction (LVEF), RVSP, left ventricle end diastolic diameter (LVEDD), left ventricle end systolic diameter (LVESD) and left atrium (LA) size. NT-proBNP samples were collected using the ECLIA (electrochemiluminescence) immunoassay (Prontera et al., 2009). In addition to the NT-proBNP and RVSP measurements, patient demographics, cardiovascular history, lab work, electrocardiography and echocardiography data were collected from the patient charts. The time period between NT-proBNP samples and echocardiography must have been obtained on the same day or within one week of each other.

Continuous variables are presented as mean ± standard deviation (SD), unless otherwise stated. Linear regression and Pearson correlation (r) analyses were performed using Microsoft Excel 2007 (Microsoft Corporation, Redmond, WA) to assess the relations between variables. In the comparison, P<0.05 defines a statistically significant difference.

Results

A total of 106 systolic heart failure patients met the inclusion criteria and were selected for the study. The mean (± SD) age was 68.64 (± 13.12 years); 79 were male and 27 were female. NT-proBNP values were significantly correlated with patient age (r = 0.20; P<0.05; Fig.1), creatinine levels (r = 0.24; P<0.05; Fig. 2), and body mass index (r = -0.26; P<0.01; Fig. 3). Patient clinical characteristics are presented in Table 1. Mean NT-proBNP (6165.64 ± 4939.83) and RVSP (47.26 ± 13.48) values were above the normal range(Felker et al., 2006; Marketing, 2009). A correlation for the data revealed that NT-proBNP and RVSP were significantly related,

r = 0.43, P<0.001. This information is summarized in Table 2 and the relationship between the two variables is illustrated in Figure 4.

Discussion

There is evidence to suggest that the prevalence of heart failure is increasing and projected to increase further over the next decade (Johansen et al., 2003; O'Connell, 2000). Rapid and accurate diagnosis of heart failure is essential in reducing mortality and increasing patient quality of life. For these reasons biomarkers, such as natriuretic peptides, are being incorporated into the clinical assessment, diagnosis, and management of systolic heart failure. The results of this study add further support to the clinical use of NT-proBNP as a marker of elevated RVSP in systolic heart failure patients, which may help physicians estimate changes in filling pressures over time without the need for repeated echocardiograms.

Table 1: Demographic and clinical data of heart failure outpatients.

Variable	Mean ± S.D.
n = 106	
Demographic:	
Age (yrs)	68.64 ± 13.12
Gender (M/F)	79/27
BMI (kg/m2)	26.85 ± 5.78
Systolic BP (mmHg)	119.82 ± 21.16
Diastolic BP (mmHg)	71.43 ± 13.30
Heart Rate (beats/min)	74.05 ± 18.46
LVEF (%)	26.31 ± 7.38
ICD (Y/N)	44/62
Cardiovascular History:	
Smoking (Y/N)	42/64
Hypertension (Y/N)	64/42
Diabetes Mellitus (Y/N)	32/74
Stroke (Y/N)	15/91
CAD (Y/N)	75/31
Sleep Apnea (Y/N)	17/89
Biochemical:	
NT-proBNP (ng/L)	6165.64 ± 4939.83
Blood Creatinine (umol/L)	121.83 ± 33.65
ECG:	
Atrial Fibrillation (Y/N)	50/56
QRS (msec)	138.92 ± 39.70
Echocardiogram:	
RVSP (mmHg)	47.26 ± 13.48
LVEDD (cm)	6.05 ± 0.91
LVESD (cm)	5.15 ± 1.01
LA size (cm)	4.91 ± 0.87

BMI: body mass index, CAD: coronary artery disease, ICD: implantable cardioverter-defibrillator, LA size: left atrium size, LVEDD: left ventricle end diastolic diameter, LVEF: left ventricle ejection fraction, LVESD: left ventricle end systolic diameter, NT-proBNP: amino-terminal pro brain natriuretic peptide, RVSP: right ventricle systolic pressure.

Ventricular NT-proBNP production is transcriptionally regulated by cardiac wall stretch, with an increased production resulting from pressure and volume overload (Rehman and Januzzi, 2008). This relationship between increased pressure, volume overload and NT-proBNP production should theoretically correspond to the severity of the patient's heart failure since the increased wall stretch and pressure is the result of reduced filling of blood in the left ventricle, thereby reducing ejection fraction and lowering cardiac output (Costello-Boerrigter et al., 2006). Mounting pressure backwards on the pulmonary artery system and the consequential increase in RVSP results in an effort to overcome this increased workload, reflecting the positive correlation found in this study. As pressure in pulmonary circulation increases, it triggers a direct expression of BNP especially by the right ventricle (Hasegawa et al., 1993; Hosoda et al., 1991; Nakanishi et al., 2001).

The variety of drug therapies used to treat heart failure such as angiotensin-converting enzyme inhibitors (ACEI), angiotensin-receptor blockers, and diuretics reduce levels of BNP leading to a better prognosis (Latini et al., 2002; Motwani et al., 1993; Tsutamoto et al., 2001). BNP levels are known to be strong predictors of the prognosis of heart failure patients (Anand et al., 2003; Maisel et al., 2004). If plasma levels are reduced after drug treatment because of improvement of left ventricle filling pressure, then the pressure in the right ventricle should be reduced as well. However, not all patients demonstrate a strong, predictable relationship between NT-proBNP and RVSP (Fig. 4), and selecting a subgroup of patients well below the regression line (i.e high RVSP and low NT-proBNP levels) may have important medical implications. Perhaps after drug treatment NT-proBNP levels reduce in these patients but RVSP stays the same as pre-treatment and/or increases over time. Screening for these patients and monitoring the progression of their disease may provide a basis for prospective studies to investigate. Perhaps these patients have a less promising prognosis and require extensive follow-up or more aggressive drug management. Clinical usage of this relationship between NT-proBNP and RVSP, such as identifying patients whose condition will evolve rapidly to irreversible pulmonary hypertension, which would preclude their referral for a heart transplant, may be used as an additional tool to indicate early referral for transplant. Further prospective studies may investigate the potential benefits and clinical applications of using the abovementioned relationship in order to identify patients whom during the course of treatment show signs of this reciprocal relationship between NT-proBNP and RVSP. If these are patients that will eventually evolve to irreversible pulmonary hypertension, then accurate and timely screening using natriuretic peptides, will allow us to carefully monitor and potentially intervene and delay this progression.

Table 2: Relationship between NT-proBNP and RVSP. NT-proBNP: amino-terminal pro brain natriuretic peptide, RVSP: right ventricle systolic pressure

	(x ± s.d)	Linear Regression	Pearson Correlation (r)	Coefficient of determination (r2)	P value
NT-proBNP	6165.64 ± 4939.83	y = 158.66x - 1333.30	0.43	0.187	p < 0.001
RVSP	47.26 ± 13.48				

Conclusion

NT-proBNP continues to emerge as an important biomarker for the detection of heart failure. In the present study NT-proBNP was found to significantly correlate with right ventricle systolic pressure in a population of heart failure patients.

References

Anand, I.S., Fisher, L.D., Chiang, Y.T., Latini, R., Masson, S., Maggioni, A.P., Glazer, R.D., Tognoni, G., and Cohn, J.N. (2003). Changes in brain natriuretic peptide and norepinephrine over time and mortality and morbidity in the Valsartan Heart Failure Trial (Val-HeFT). Circulation 107, 1278-1283.

Arnold, J.M., Liu, P., Demers, C., Dorian, P., Giannetti, N., Haddad, H., Heckman, G.A., Howlett, J.G., Ignaszewski, A., Johnstone, D.E., et al. (2006). Canadian Cardiovascular Society consensus conference recommendations on heart failure 2006: diagnosis and management. Can J Cardiol 22, 23-45.

Balion, C., Santaguida, P.L., Hill, S., Worster, A., McQueen, M., Oremus, M., McKelvie, R., Booker, L., Fagbemi, J., Reichert, S., et al. (2006). Testing for BNP and NT-proBNP in the diagnosis and prognosis of heart failure. Evid Rep Technol Assess (Full Rep), 1-147.

Braunschweig, F., Fahrleitner-Pammer, A., Mangiavacchi, M., Ghio, S., Fotuhi, P., Hoppe, U.C., and Linde, C. (2006). Correlation between serial measurements of N-terminal pro brain natriuretic peptide and ambulatory cardiac filling pressures in outpatients with chronic heart failure. Eur J Heart Fail 8, 797-803.

Costello-Boerrigter, L.C., Boerrigter, G., Redfield, M.M., Rodeheffer, R.J., Urban, L.H., Mahoney, D.W., Jacobsen, S.J., Heublein, D.M., and Burnett, J.C., Jr. (2006). Amino-terminal pro-B-type natriuretic peptide and B-type natriuretic peptide in the general community: determinants and detection of left ventricular dysfunction. J Am Coll Cardiol 47, 345-353.

Felker, G.M., Petersen, J.W., and Mark, D.B. (2006). Natriuretic peptides in the diagnosis and management of heart failure. CMAJ 175, 611-617.

Haldeman, G.A., Croft, J.B., Giles, W.H., and Rashidee, A. (1999). Hospitalization of patients with heart failure: National Hospital Discharge Survey, 1985 to 1995. Am Heart J 137, 352-360.

Hasegawa, K., Fujiwara, H., Doyama, K., Mukoyama, M., Nakao, K., Fujiwara, T., Imura, H., and Kawai, C. (1993). Ventricular expression of atrial and brain natriuretic peptides in dilated cardiomyopathy. An immunohistocytochemical study of the endomyocardial biopsy specimens using specific monoclonal antibodies. Am J Pathol 142, 107-116.

Hosoda, K., Nakao, K., Mukoyama, M., Saito, Y., Jougasaki, M., Shirakami, G., Suga, S., Ogawa, Y., Yasue, H., and Imura, H. (1991). Expression of brain natriuretic peptide gene in human heart. Production in the ventricle. Hypertension 17, 1152-1155.

Januzzi, J.L., Jr., Camargo, C.A., Anwaruddin, S., Baggish, A.L., Chen, A.A., Krauser, D.G., Tung, R., Cameron, R., Nagurney, J.T., Chae, C.U., et al. (2005). The N-terminal Pro-BNP investigation of dyspnea in the emergency department (PRIDE) study. Am J Cardiol 95, 948-954.

Johansen, H., Strauss, B., Arnold, J.M., Moe, G., and Liu, P. (2003). On the rise: The current and projected future burden of congestive heart failure hospitalization in Canada. Can J Cardiol 19, 430-435.

Latini, R., Masson, S., Anand, I., Judd, D., Maggioni, A.P., Chiang, Y.T., Bevilacqua, M., Salio, M., Cardano, P., Dunselman, P.H., et al. (2002). Effects of valsartan on circulating brain natriuretic peptide and norepinephrine in symptomatic chronic heart failure: the Valsartan Heart Failure Trial (Val-HeFT). Circulation 106, 2454-2458.

Maisel, A., Hollander, J.E., Guss, D., McCullough, P., Nowak, R., Green, G., Saltzberg, M., Ellison, S.R., Bhalla, M.A., Bhalla, V., et al. (2004). Primary results of the Rapid Emergency Department Heart Failure Outpatient Trial (REDHOT). A multicenter study of B-type natriuretic peptide levels, emergency department decision making, and outcomes in patients presenting with shortness of breath. J Am Coll Cardiol 44, 1328-1333.

Marketing, L.L.S.a. (2009). Normal Hemodynamic Parameters (Cambridge).

Martinez-Rumayor, A., Richards, A.M., Burnett, J.C., and Januzzi, J.L., Jr. (2008). Biology of the natriuretic peptides. Am J Cardiol 101, 3-8.

McCullough, P.A., Nowak, R.M., McCord, J., Hollander, J.E., Herrmann, H.C., Steg, P.G., Duc, P., Westheim, A., Omland, T., Knudsen, C.W., et al. (2002). B-type natriuretic peptide and clinical judgment in emergency diagnosis of heart failure: analysis from Breathing Not Properly (BNP) Multinational Study. Circulation 106, 416-422.

Motwani, J.G., McAlpine, H., Kennedy, N., and Struthers, A.D. (1993). Plasma brain natriuretic peptide as an indicator for angiotensin-converting-enzyme inhibition after myocardial infarction. Lancet 341, 1109-1113.

Mueller, T., Gegenhuber, A., Poelz, W., and Haltmayer, M. (2004). Head-to-head comparison of the diagnostic utility of BNP and NT-proBNP in symptomatic and asymptomatic structural heart disease. Clin Chim Acta 341, 41-48.

Nakanishi, K., Tajima, F., Itoh, H., Nakata, Y., Osada, H., Hama, N., Nakagawa, O., Nakao, K., Kawai, T., Takishima, K., et al. (2001). Changes in atrial natriuretic peptide and brain natriuretic peptide associated with hypobaric hypoxia-induced pulmonary hypertension in rats. Virchows Arch 439, 808-817.

Nakao, S., Goda, A., Yuba, M., Otsuka, M., Matsumoto, M., Yoshida, C., Ohyanagi, M., Naito, Y., Lee, M., Tsujino, T., et al. (2007). Characterization of left ventricular filling abnormalities and its relation to elevated plasma brain natriuretic peptide level in acute to chronic diastolic heart failure. Circ J 71, 1412-1417.

O'Connell, J.B. (2000). The economic burden of heart failure. Clin Cardiol 23, II16-10.

O'Hanlon, R., O'Shea, P., Ledwidge, M., O'Loughlin, C., Lange, S., Conlon, C., Phelan, D., Cunningham, S., and McDonald, K. (2007). The biologic variability of B-type natriuretic peptide and N-terminal pro-B-type natriuretic peptide in stable heart failure patients. J Card Fail 13, 50-55.

Prontera, C., Zucchelli, G.C., Vittorini, S., Storti, S., Emdin, M., and Clerico, A. (2009).

Comparison between analytical performances of polyclonal and monoclonal electrochemiluminescence immunoassays for NT-proBNP. Clin Chim Acta 400, 70-73.

Rehman, S.U., and Januzzi, J.L., Jr. (2008). Natriuretic peptide testing in clinical medicine. Cardiol Rev 16, 240-249.

Troisi, F., Greco, S., Brunetti, N.D., and Di Biase, M. (2008). Right heart dysfunction assessed with echography, B-type natriuretic peptide and cardiopulmonary test in patients with chronic heart failure. J Cardiovasc Med (Hagerstown) 9, 672-676.

Troughton, R.W., and Richards, A.M. (2009). B-type natriuretic peptides and echocardiographic measures of cardiac structure and function. JACC Cardiovasc Imaging 2, 216-225.

Tsutamoto, T., Wada, A., Maeda, K., Mabuchi, N., Hayashi, M., Tsutsui, T., Ohnishi, M., Sawaki, M., Fujii, M., Matsumoto, T., et al. (2001). Effect of spironolactone on plasma brain natriuretic peptide and left ventricular remodeling in patients with congestive heart failure. J Am Coll Cardiol 37, 1228-1233.

Immunology
UNIVERSITY OF TORONTO

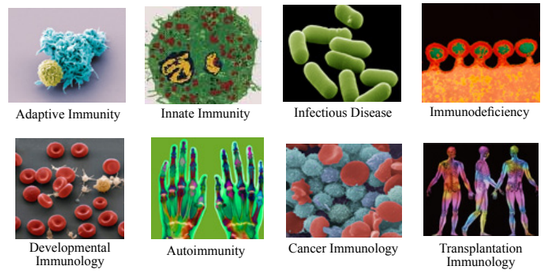

The Department of Immunology offers study programs in a wide range of immunological disciplines. These disciplines include molecular mechanisms of lymphocyte development and selection, T-cell and B-cell receptors, cell interactions, growth factor receptors, cytokine networks, antigen processing and presentation, signal transduction in lymphocytes, V(D)J recombination, anergy, apoptosis, transgenic and knock-out models, immuno-targeting and vaccine design, autoimmunity, AIDS, diabetes, and transplantation.

UNDERGRADUATE PROGRAM

The Department of Immunology in collaboration with Trinity College co-ordinates a specialist and a major program in Immunology.
Apply via the Faculty's Subject POST website.
http://www.artsci.utoronto.ca/current/undergraduate/subject-post-enrolment

Immunology Specialist Program
The emphasis of the specialist program is to provide students with a sound theoretical understanding of the cellular and molecular basis of non-self recognition, together with sufficient laboratory experience to enable the students to consider embarking on a career in the discipline.

Immunology Major Program
The major program offers students fundamental training in immunology and gives the student the opportunity to combine immunology with another program in Life Sciences, Basic Sciences, or within the Arts.

GRADUATE PROGRAM

The department offers study programs towards the Masters of Science and Doctor of Philosophy degrees in a wide range of immunological disciplines.

M.Sc.
The purpose of the M.Sc. degree is to provide advanced training in an area of specialization, with a particular emphasis on the acquisition of experience in the strategies and experimental methods of modern, original, scientific research.

Ph.D.
The Ph.D. degree is an advanced research degree intended to reflect a level of training consistent with the ability of the candidate to function as an independent research scientist. This involves successful completion of course work reflecting a knowledge of modern Immunology, as well as a demonstrated ability to carry out research of publishable quality.

For more detailed description of our programmes offered, please visit our website:
www.immunology.utoronto.ca

JULS RESEARCH

Selenium glycoside as a delivery vehicle for selenium supplements

Harun Mustafa[1], Sinisa Vukovic[2] and Imre G. Csizmadia[1,2]

[1]Department of Chemistry, University of Toronto, 80 St. George St, Toronto, ON, Canada M5S 3H6

Abstract

The glycoside hydrolysis reactions of $-OCH_3$, $-SCH_3$, and $-SeCH_3$ groups were compared in order to demonstrate the viability of selenium glycoside as a delivery method for organic selenium. The hydrolysis reaction has a multi-step, acid catalyzed mechanism which is modelled by the DFT B3LYP/6-31+G(d) method. The rate-determining step, protonation of the chalcogen, favours the selenium analog over oxygen, therefore eliminating the possibility of disturbing natural glycosides. At the same time, the potential energy surface confirms the validity of the hypothesis.

Introduction

Selenium (Se) is an important trace element for human metabolic function (Bellinger et al., 2009). Owing to its reactivity, the element cannot be stored in large quantities in the human body (Bellinger et al., 2009); with a recommended daily dosage of 55µg and an upper limit of 400µg (MacFarquhar et al., 2010). Insufficient Se intake can lead to disorders in the muscular, cardiovascular, inflammatory, immune, neurological, and endocrine systems. Possible ailments include Keshan disease (Papp et al., 2007), Kashin-Beck disease (Moreno-Reyes et al., 2003), Myxedematous endemic cretinism (Vanderpas, et al. 1990), and Myotonic dystrophy (Bellinger et al., 2009).

Se compounds are usually ingested through diet, in particular from plant sources, and are dependent on the selenium content of the soil in which the food was produced (Papp et al., 2007). Areas known to have low soil selenium content are usually the subject of tests relating to selenium-deficiency related illness (Moreno-Reyes et al., 2003; Papp et al., 2007; Vanderpas, et al. 1990). The vastness of Se-deficiency related disorders alone necessitates the production of efficient Se dietary supplements.

Selenium is incorporated into selenoproteins through the 21st amino acid, selenocysteine (Sec) (Small-Howard and Berry, 2005). Sec is the selenium analogue of cysteine with a selenium atom in the place of sulphur (Bellinger et al., 2009). In humans, there are 25 known selenoproteins. These are GPx 1, 2, 3, 4, and 6; TR 1, 2, and 3; Selenoproteins H, I, K, M, N, O, P, R, S, T, V, and W; 15kDa, SPS2, and DI 1, 2, and 3 (Kryukov et al., 2003). Selenoproteins are important for their main use as oxidoreductases for preventing and repairing cellular damage, and regulating protein redox state (Lobanov et al., 2009). It is coded in RNA by the UGA codon, which normally acts as one of the stop codons (Low and Berry, 1996). The Sec insertion sequence (SECIS), an element in the 3'-untranslated region (UTR) of selenoprotein mRNA, is required to properly encode the acid (Berry et al., 1993).

In order to ensure the body's rapid and proper acceptance of selenium supplements, it would be preferable to administer it as a bio-molecule, as opposed to salt supplements such as sodium selenite (Musik et al., 2009). An example of such a molecule is a glycoside, where the molecule may be synthesized with the hydroxyl on the 1' carbon replaced with a selenium compound. Upon digestion, it would dissociate to produce an organoselenium compound and glucose.

In this study, we used computational methods to test the validity of selenium glycoside hydrolysis as a possible mechanism for the delivery of Se into the body. A true complex designed to accomplish this would be selenium attached to two, three or four glucose molecules. In order to simplify this reaction with multiple substituents and conformations while still maintaining accuracy, we employed only one glucose linked to methyl selenium. The decomposition of the first three methyl chalcogen glycosides, $-OCH_3$, $-SCH_3$ and $-SeCH_3$, into glucose and their respective chalcogen methanes (CH_3XH) was tested to determine their relative reactivities.

Figure 1: Three glycosides of interest. The moieties are chalcogen methyls, with the chalcogens being (from left to right) oxygen, sulphur, and selenium.

The mechanism of glycoside hydrolysis is a four-step process with the first step as the rate-determining step and the following three steps identical for all three analogs (Figure 1). Computations were also done on various off-pathway reactions for either the initial protonation of the ring oxygen, one of the hydroxyl groups and evaluating the free energy change associated with such protonation events (Figure 2). This was done to demonstrate how favourable protonation of each moiety was relative to the desired event.

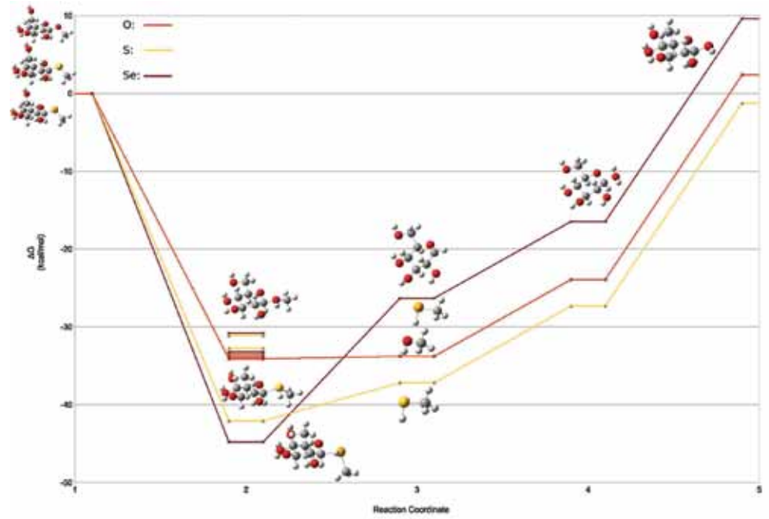

Figure 2: Energies (ΔG) of the three reaction mechanisms over the entire reaction. In step 2, additional bars for the energies of the off-pathway protonations are shown. Shown around each step are 3D renderings of their respective molecules. In step 3, a single rendering of the remaining ring is shown on top, with renderings of the mechanism-specific moieties shown beside their respective paths.

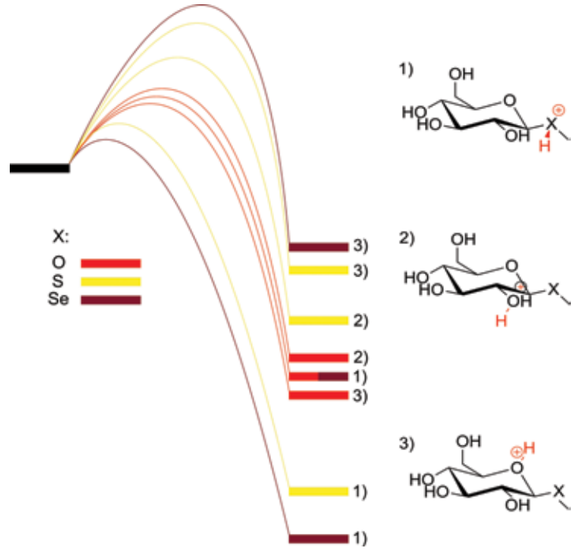

Figure 3: Initial protonation energies (ΔG) of the three mechanisms (including off-pathway protonations). The numbers to the right of the energy bars indicate which atom has been protonated, with corresponding structures drawn on the right.

Methods and Materials

Models were prepared and visually inspected using GaussView 5.0 (Dennington II et al, 2008) for each step in the reactions. Each model was then structurally optimized and thermochemically analyzed through computational methods. Computations were performed using the Gaussian03 A.2 (G03) software package (Frisch et al., 2003). Structural optimization and thermochemical analysis was performed by DFT methods (Hohenberg and Kohn, 1964), using the Becke, three parameter, Lee, Yang, and Parr (B3LYP) (Becke, 1993; Lee et al., 1988; Miehlich et al. 1989) method at the 6-31+G(d) level (Hehre et al, 1972; Hariharan and Pople, 1972). Heats and entropies for each model were given in Hartrees and calories per mole, respectively. This data was then used to calculate the changes in free energy with respect to the initial reactants in each mechanism.

Results

The rate-determining step of glycoside hydrolysis was the first step, i.e. protonation of the glycoside heteroatom. The protonation can happen at five different places on a glycoside (one at each chalcogen). In our tests, we approximated the protonation of the three hydroxyl groups by protonating the middle 2' hydroxyl. For oxygen, all of the protonation sites were very close in energy (-35.45 to -33.26 kcal/mol), not giving a preference to any of the oxygen atoms. However, S and Se were preferred spots for protonation in either of the other two analogs (Figure 3), indicating that off-pathway reactions were indeed less favoured compared to that of the desired and operative step.

The first step was exothermic in all analogs. Thermodynamically, protonation of the glycosyl moiety favoured Se by 10.92 kcal/mol with respect to O, and 2.73 kcal/mol with respect to S (Table 1). By Hammond's postulate, this means that the transition states for hydrolysis are also lower than transition states for oxygen - all types of transitions states for O, S and Se are early transition states resembling the glycoside rather than the protonated glycoside (i.e. limited degree of proton transfer in transition state).

Once the protonated methyl chalcogen was released from the glycoside, the three subsequent steps were endothermic and identical for the three analogs. Therefore, the mechanistic differences cannot result from these three steps. However, energetic differences in creating $H-OCH_3$, $H-SCH_3$ and $H-SeCH_3$ were evident, being the most endothermic for Se and least for O.

Overall, the reaction involving the sulphur was the most favourable, being exothermic. The oxygen and selenium reactions exhibited overall increases in free energy, with the selenium analog being the most endothermic.

Step 1: G-XMe + H_3O^+ → G-XHMe$^+$ + H_2O
→ GOH_2^+-XMe + H_2O
→ GOH$^+$-XMe + H_2O
Step 2: G-XHMe$^+$ → GdOH$^+$ + HXMe
Step 3: GdOH$^+$ + H_2O → G-OH_2^+
Step 4: G-OH_2^+ + H_2O → G + H_3O^+

Overall: G-XMe + H_2O → G + HXMe

	ΔG (kcal/m ol)		
Step	O	S	Se
1a	-33.87	-42.06	-44.79
b	-33.26	-32.73	-33.23
c	-35.45	-31.16	-30.79
2	0.31	4.89	18.48
	All		
3	9.86		
4	26.08		
	O	S	Se
Overall	2.38	-1.23	9.63

Table 1: Changes in Gibbs free energy (ΔG) for each step in the proposed mechanisms. The nomenclature emphazises the modifications to the molecules with respect to a glucose molecule (represented by the symbol G). The first steps represent the energies of the three protonations tested (chalcogen, OH, and ring O). GdOH+ represents glucose with the 1' carbon dehydroxylated whereas G-OH2+ represents the glucose with the 1' hydroxyl protonated.

Discussion

The overall results showed opposing trends for oxygen and selenium analogs while sulphur remained between the two, with the oxygen analog having little variance in protonation energies and the selenium analog having a strong preference for moiety protonation.

The protonation of natural methyl glycoside can either lead to the opening of the glucose ring or to the release of a hydroxide. This is an important feature, and interfering with both pathways by introducing an artificial glycoside (such as the Se analog) would lead to serious side effects. Fortunately, the Se glycoside prefers the rate determining step to be exclusively the protonation of selenium, therefore eliminating the chance of the glucose ring opening and entering the cycles of a natural glycoside. Moreover, an overwhelming advantage in stabilization of protonated selenium over the oxygen analog indicates that the rate of overall hydrolysis is much faster (lower transition states for Se analog). This is even more evidence that selenium glucoside should not interfere with the cycles of natural glycoside hydrolysis.

Thermodynamically, the overall reaction favoured natural glycoside and disfavoured the selenium analogue by 9.63 kcal/mol. If this reaction was in equilibrium, one could expect the Se analog not to be able to hydrolyze as well as a natural glycoside. However, due to metabolic processing of the intermediates, the reaction is not in equilibrium and thus, not reversible. Therefore, glycoside hydrolysis has a kinetic product that drives the reaction (one with a lower transition state), not the thermodynamic product (overall more stable). Once H–$SeCH_3$ and glucose are formed, one cannot expect them to recombine because that would require protonation of glucose as the initial step. We have already demonstrated that ring opening and protonation of other hydroxyl groups are valid options, so even statistically H–$SeCH_3$ would not recombine with glucose.

These results imply that when ingested, the selenium glycoside will be readily hydrolysed causing the selenium to be released, as desired. This lends credibility to the hypothesis that a glycoside can act as a viable organic selenium delivery method. The remaining by-product can then processed through the body's normal metabolic processes. This could also lead to the possibility of directly delivering selenocysteine through a glycoside. Further theoretical study would focus on analyzing the hydrolysis of selenocysteine in a glycoside to verify analogy to our simplified mechanism.

Conclusion

This data indicates that a selenium glycoside could be used as an effective organic delivery molecule for dietary selenium. Of the mechanisms tested, the selenium glycoside hydrolysis demonstrated the fastest kinetics while still being thermodynamically favourable until the release of the moiety.

If glycoside complexes were to be synthesized with selenocysteine instead of the –$SeCH_3$ group, this method could be used for direct ingestion, thereby offering a quick method that bypasses the body's synthesis mechanism. Further study is required to test the validity of our results in regards to a Sec-incorporated glycoside, and to verify our results both in vitro and in vivo. Positive results from such studies may lead to the development of new dietary selenium supplements that can more effectively be absorbed by the body. These supplements could then be administered to populations with selenium-deficient diets.

Acknowledgments

We would like to thank the Research Opportunity Program at the University of Toronto for allowing the opportunity to conduct research. We are grateful to the assistance offered by the alumni students of the CHM299 course, in particular to Natalie Galant for proofreading the manuscript. We would like to thank GIOCOMMS for offering their computational and teaching resources throughout the year.

References

Becke, A. D. (1993). Density-functional thermochemistry. III. The role of exact exchange. J. Chem. Phys. 98, 5648-5652.
Bellinger, F. P., Raman, A. V., Reeves, M. A., et al. (2009). Regulation and function of selenoproteins in human disease, Biochem. J. 422, 11-22.
Berry, M. J., Banu, L., Harney, J. W., and Larsen, P. R. (1993). Functional characterization of the eukaryotic SECIS elements which direct selenocysteine insertion at UGA codons. EMBO J. 12, 3315–3322.
Dennington II, R., Keith, T. A., Millam, J. (2008). GaussView (Version 5.0) (Shawnee Mission, Kansas: Semichem Inc.).
Frisch, M. J., Trucks, G. W., Schlegel, H. B., Scuseria, G. E., Robb, M. A., et al. (2003). Gaussian 03, Revision A.2. (Pittsburgh: Pennsylvania: Gaussian Inc.).
Hariharan, P. C., and Pople, J. A. (1972). The influence of polarization functions on molecular orbital hydrogenation energies. Theoret. Chimica Acta 28, 213-222.
Hehre, W. J., Ditchfield, R., and Pople, J. A. (1972). Self-Consistent Molecular Orbital Methods. XII. Further Extensions of Gaussian-Type Basis Sets for Use in Molecular Orbital Studies of Organic Molecules. J. Chem. Phys. 56, 2257-2261.
Hohenberg, P., Kohn, W. (1964). Inhomogeneous Electron Gas. Phys. Rev. 136, B864-B871.
Kohn, W., Sham, L. J. (1965). Self-Consistent Equations Including Exchange and Correlation Effects. Phys. Rev. 140, A1133-A1138.
Kryukov, G.V., Castellano, S., Novoselov, S.V., Lobanov, A.V., Zehtab, O., Guigo, R., and Gladyshev, V.N. (2003). Characterization of mammalian selenoproteomes, Science. 300, 1439–1443.
Lee, C., Yang, W., and Parr, R. G. (1988). Development of the Colle-Salvetti correlation-energy formula into a functional of the electron density. Phys. Rev. B. 37, 785-789.
Lobanov, A. V., Hatfield, D. L., and Gladyshev, V. N. (2009). Eukaryotic selenoproteins and selenoproteomes. Biochimica et Biophysica Acta. 1790, 1424-1428.
Low, S. C. and Berry, M. J. (1996). Knowing when not to stop: selenocysteine incorporation in eukaryotes. Trends Biochem. Sci. 21, 203–208.
MacFarquhar, J. K., Broussard, D. L., Melstrom, P., Hutchinson, R., Wolkin, A., et al. (2010). Acute Selenium Toxicity Associated With a Dietary Supplement. Arch Intern Med. 170, 256-261.
Miehlich, B., Savin, A., Stoll, H., Preuss, H. (1989). Results obtained with the correlation-energy density functionals of Becke and Lee, Yang and Parr. Chem. Phys. Lett. 157, 200-206.
Moreno-Reyes, R., Mathieu, F., Boelaert, M., Begaux, F., Suetens, C., Rivera, M. T., Neve, J., Perlmutter, N., and Vanderpas, J. (2003). Selenium and iodine supplementation of rural Tibetan children affected by Kashin–Beck osteoarthropathy. Am. J. Clin. Nutr. 78, 137– 144.
Musik, I., Hordyjewska, A., Boguszewska-Czubara, A., et al. (2009). Possible new organoselenium supplement evaluation of its influence on the kidneys in comparison with inorganic sodium selenite. Pharmacological Reports. 61, 885-891.
Papp, L. V., Lu, J., Holmgren, A. and Khanna, K. K. (2007). From selenium to selenoproteins: synthesis, identity, and their role in human health. Antioxid. Redox Signaling 9, 775–806.
Small-Howard, A. L. and Berry, M. J. (2005). Unique features of selenocysteine incorporation function within the context of general eukaryotic translational processes. Biochem. Soc. Trans. 33, 1493–1497.
Vanderpas, J. B., Contempre, B., Duale, N. L., Goossens, W., Bebe, N., et al. (1990). Iodine and selenium deficiency associated with cretinism in northern Zaire. Am. J. Clin. Nutr. 52, 1087–1093.

Department of Chemistry and Chemical Biology, McMaster University
BIOMOLECULES

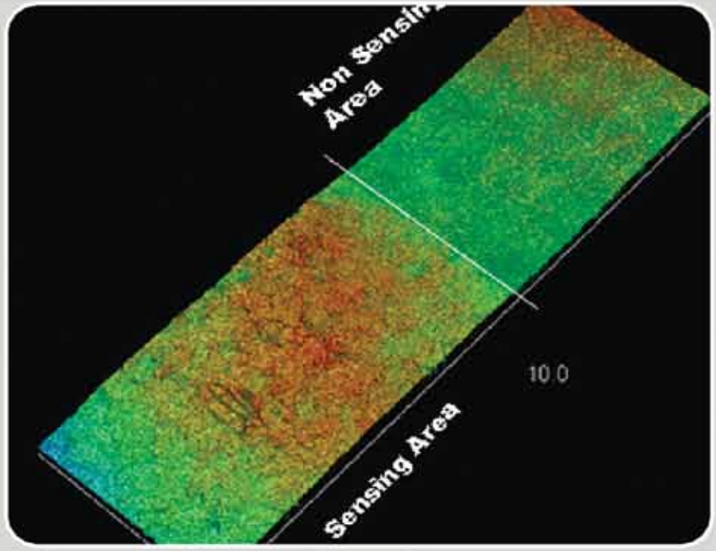

Bio-Active Paper for Cheap, Colorimetric Detection of Pathogens
The group of John Brennan, in the Department of Chemistry and Chemical Biology, recently invented a process to produce novel paper-based solid-phase biosensors that utilize piezoelectric inkjet printing of biocompatible, enzyme-doped, sol-gel-based inks to create colorimetric sensor strips. Acetylcholinesterase inhibitors, including paraoxon and aflatoxin B1, were detected successfully using this sensor, with toxin concentrations determinable by eye, without any expensive equipment.

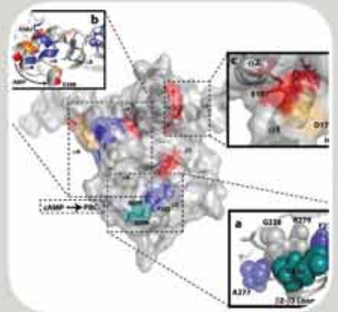

Melacini Research Group
Investigates biomolecules by NMR to determine structure, dynamics, and iteractions. Specific areas of research revolve around allosteric control of signaling pathways and amyloid fibril formation.

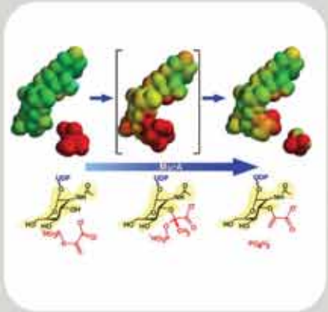

Berti Research Group
Investigates enzymatic transition states, specifically focusing on the enzymes that nature uses for DNA repair, and in microbial processes that are critical to bacterial survival, and therefore serve as excellent antimicrobial targets.

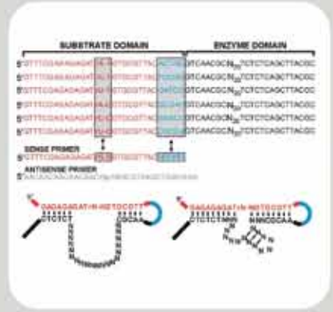

Li Research Group
Examines unusual functions of artificial single-stranded DNA or RNA molecules capable of catalytic or highly specific binding functions, generated through in-vitro selection.

Interested in learning more?? Visit www.chemistry.mcmaster.ca

McMaster University
World-class research... state-of-the-art facilities...
supportive and caring atmosphere...
Chemistry Graduate Studies at McMaster University
is it right for you?

To apply: visit www.chemistry.mcmaster.ca and follow the links to Graduate Studies

JULS RESEARCH

LED-activated Pheophorbide-a Induces Cellular Destruction of Ovarian Cancer Cells

Eric Chuck Hey Pun[a], Ling Liu[c], Chuan Shan Xu[c], Dun Yuan Zhou[b], Albert Wing Nang Leung[c]

[a]Department of Immunology, University of Toronto, Toronto, ON, Canada, [b]Department of Physiology, University of Toronto, Toronto, ON, Canada, [c]School of Chinese Medicine, Chinese University of Hong Kong

Abstract

Photodynamic therapy (PDT) has recently emerged as a novel therapeutic modality for treatment of cancer. Pheophorbide a (Pa), a Chinese herbal medicine derived from *Scutellaria Barbata*, is a photosensitizer that inhibits proliferation in a number of cancer cell lines when used in conjunction with PDT (Pa-PDT). In this study, we investigated the mechanism of action of Light Emitting Diode (LED)-activated Pa in the ovarian cancer cell line HO-8910. The anti-proliferative effects were investigated by both 3-(4,5-Dimethylthiazol-2-yl)-2,5-diphenyltetrazolium bromide (MTT) and sulforhodamine B (SRB) microplate assays. The photocytotoxicity (%) as measured by MTT assay showed a significant 90.1% increase and it also indicated the absence of dark cytotoxicity of Pa in HO-8910 cancer cells. Drug-dose dependent cytotoxicity was found in the cells at the dose of 0.125-0.5 μM. Time dependent cytotoxicity, however, was not found by varying the time lengths from 10-100 s. Cell cycle analysis by propidium iodide (PI) staining indicated the appearance of sub-G1 peak in the LED-activated Pa treatment, suggesting a loss of DNA content or DNA fragmentation. Additionally, Pa treatment induced depolarization of mitochondrial membrane potential (ΔΨm), which is a hallmark of apoptosis. Taken together, these data suggest that the anti-proliferative effect by LED-activated Pa treatment is mediated by induction of apoptosis following DNA damage.

Introduction

Ovarian cancer is a leading cause of death among the many gyneacological malignancies. The 5-year survival rate for patients in the advanced stages of disease rapidly declines to <40% and a majority of patients are resistant to treatment and develop recurrence (Fung-Kee-Fung et al., 2007; Jemal et al., 2009). Current management of advanced epithelial ovarian cancer involves cytoreductive surgery followed by combination chemotherapy. Although this approach has been regarded as an effective treatment, one of the substantial problems is the occurrence of chemo-resistance. Consequently, there is a need to develop novel therapies that overcome these challenges.

Photodynamic therapy (PDT) is an alternative therapeutic approach for cancer treatment. It requires the presence of both a photosensitizer (PS) and light of an appropriate wavelength, which are non-cytotoxic individually. Following the activation of the PS by light irradiation, reactive oxygen species (ROS) including singlet oxygen, superoxide anion and hydroxyl radical are generated. These are transient species, which are thought to induce cellular apoptosis through damage to cellular components such as lipids, proteins and DNA (Pervaiz, 2001). Currently, most patients who suffer from ovarian cancer are treated with chemotherapy. Radiation therapy is often employed to treat patients who respond well to initial treatment. However these patients remain at high risk of tumor recurrence, PDT may be one therapeutic option that overcomes these challenges.

Scutellaria barbata (SB) is a traditional Chinese medicine known as Ban Zhi Lian and is used generally as antipyretics, relieving toxic effects and reducing sores and abscesses (Dharmananda, 2004). Although this herb has been widely used because of its anti-tumor, anti-inflammatory and diuretic properties (Qian, 1987), the mechanisms underlying its anti-tumor capacity have not been thoroughly investigated. In this study, we investigated pheophorbide-a (Pa), an active anti-tumor compound in *S. barbata* (Chan et al., 2006). Pa is photosensitive and has been reported to inhibit proliferation of a number of cancers including: Jurkat leukemia, pigmented melanoma, pancreatic carcinoma and colonic cancer in the presence of light of an appropriate wavelength (Hajri et al., 1999; Hajri et al., 2002; Lee et al., 2004; Lim et al., 2004; Moore et al., 1997).

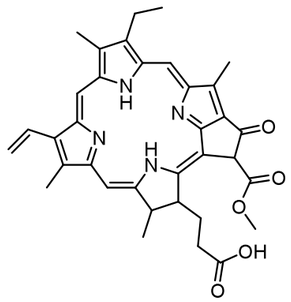

Figure 1: Chemical structure of Pa.

Studies have shown that other photosensitizers, such as hypocrellin B and MPPa, can be activated by an LED light source to kill ovarian cancer cells and nasopharyngeal carcinoma cells (Bai et al., 2010; Tan et al., 2009 a, b). The selection of a photosensitizer is paramount to the success of PDT and it should possess, optimally, the following characteristics: the ability to absorb in the red spectrum (600-800 nm) to elicit photoactivation within deeper issues, minimal dark toxicity, selective uptake by malignant cells and the ability to generate singlet oxygen species.

The aim of this study was to determine the mechanism by which LED-activated Pa inhibits proliferation of ovarian cancer cells *in vitro.*

2.) Materials and methods

2.1.) Photosensitizer

Pheophorbide a ($C_{35}H_{36}N_4O_5$), derived from Chinese medicine *Scutellaria Barbata*, was purchased from Frontier Scientific Inc. (Utah, USA) and did not undergo further purification. A stock solution (50 mM) was made in dimethyl sulphoxide (DMSO) and stored in the dark at -20°C.

2.2) Cell culture

Ovarian cancer cell line HO-8910 cells were investigated in this study. They were presented by Junyan Xiang from the Institute of Ultrasound and Medicine Engineering, Chongqing Medical University, Chongqing. The cells were grown in Dulbecco's modified Eagle Medium (DMEM) supplemented with 10% fetal bovine serum (FBS) and antibiotics (50 μg/mL penicillin and 50 μg/mL streptomycin; Gibco). The cells were incubated at 37 °C in a humidified atmosphere of air/CO_2 (95%/5%).

2.3) Activation of photosensitizer

HO-8910 cells were incubated with Pa for four hours before light irradiation. The cells were then irradiated by a red light from a light-emitting diode (LED) system with the wavelength of 630 nm and energy density of 1.5 J/cm^2 under different time lengths.

2.4) SRB assay

The experiments were conducted in a 96-well format and the assay was performed according to the method described by Skehan et al (Skehan et al., 1990). Briefly, the ovarian cancer cells (1×10^4 cells/well) were incubated in a 96-well microplate and were then allowed to grow overnight. Pa (0.5 μM) was added to the cells in the dark and incubated for four hours. The cells were then fixed by the addition of 25 μL of cold 50% trichloroacetic acid (TCA). After incubation for one hour at 4°C, the plate was washed five times with tap water to remove TCA, medium and dead cells. The plate was then dried in air. Subsequently, 50 μL of 0.4% SRB dissolved in 1% acetic acid was added into each well and allowed to stand for 30 min. The plate was subsequently washed four times with 1% acetic acid and then dried in air again, and 150 μL of 10 mM aqueous Tris-Base [tris(hydroxylmethyl)aminomethane] was added to solubilize the cell-bound dye. The plate was then shaken on a gyratory shaker for 10 min. followed by the reading of optical density (OD) at 570 nm in a microplate spectrophotometer (BioTek, Gene Company limited. US).

The percentage of cytotoxicity was calculated using the following equation:

$$Cytotoxicity(\%) = \frac{(OD_{control} - OD_{treated})}{OD_{control}} \times 100$$

2.5.) MTT assay

MTT assay is used in this study to quantify cytotoxicity of Pa and to confirm the results obtained by SRB assay. Pa was added to the cultured cells in the 96-well plate and was incubated in the dark for four hours. MTT was then added to the wells at a final concentration of 0.5 mg/mL and incubated at 37 °C for four hours. The medium was subsequently removed from the wells and 100 μL of DMSO was added into each well. The plate was shaken for 10 min on a gyratory shaker and the OD of the dissolved formazan dye was recorded at 570 nm using a microplate spectrophotometer (BioTek, Gene Company limited. US). The percentage cytotoxicity was calculated using the same equation used in the SRB assay.

2.6.) Estimation of the changes of mitochondrial membrane potential (ΔΨm)

The cationic dye JC-1 (5,5',6,6'-tetrachloro-1,1',3,3' tetraethylbenzimidazolylcarbocyanine iodide) was used to evaluate the depolarization of MMP. 3×10^5 cells were seeded in 6-well plate and incubated for 24 hours. 0.5 μL Pa was then added in the dark and the cells were incubated for another four hours. The cells were then washed to remove unbound drug and then exposed to red light emitted from a light emitting diode (LED) source. Three hours after the treatment, trypsonized, pooled together and washed with PBS. 10 μL of JC-1 was added to the cells suspended in PBS in the dark and incubated for 15 min at 37 °C. Following incubation, the cells were washed with PBS again and were subject to flow cytometric analysis using a FACSort flow cytometer (Cytomics FC500, Beckman Coulter, Fullerton, CA, USA) in which the Cell Quest programme was used.

2.7) Cell cycle analysis by propidium iodide (PI) staining

Approximately 3×10^5 cells were seeded on 6-well plates for 48 hours. 0.5 μL of Pa was added to the wells and the cells were further incubated for four hours. The cells were then washed to remove unbound drugs and then exposed to red light emitted from a LED light source. Six hours after the treatment, trypsonization was performed to harvest the adherent cells and they were pooled together along with the floating cells. The cells were then fixed in 70% ethanol at 4 °C overnight, and were then re-suspended in 200 μL PI solution (2 mg/mL) with RNAase and incubated in the dark at 37 °C for 30 min. A FACSort flow cytometer (Cytomics FC500, Beckman Coulter, Fullerton, CA, USA) was used to carry out DNA content analysis in which the CellQuest programme was used to analyze the results.

2.8.) Light microscopy observation

A phase-contrast light microscope was used to observe morphological features of the ovarian cancer cells immediately after SRB assay. Figure 3 shows the cell morphological features stained by SRB.

Results

LED-activated Pa inhibits proliferation of ovarian cancer cells

The photocytotoxic effects of Pa on HO-8910 cells were determined 24 hours after LED light irradiation. The cells were under different treatments, namely, cells only, cells treated with Pa only, cells exposed to LED light (1.5 J/cm^2) only and cells treated with both LED-light and Pa. Figure 2 shows the photocytotoxic effects of Pa on HO-8910 cells as assessed by SRB assay. The results indicate that combined treatment of both Pa and LED light is necessary to elicit a significant photocytotoxic effect, while individually neither Pa nor LED light irradiation has photocytotoxic effect. The MTT

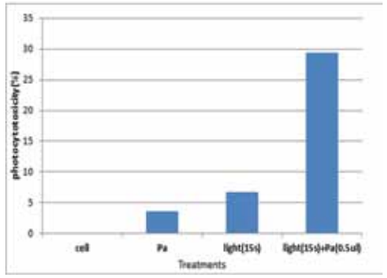

Figure 2: Photocytotoxicity (%) of HO-8910 cells measured under different treatments assessed by SRB assay.

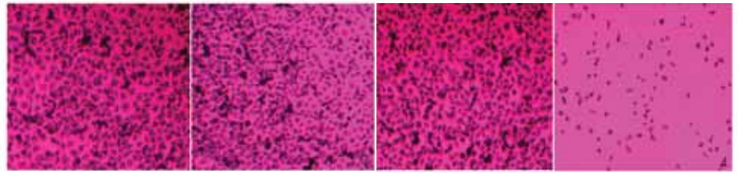

Figure 3: Photo-destruction of Pa in HO-8910 cells after SRB assay by an inverted microscope (×20). HO-8910 cells were under different treatments. **(a)** cell only **(b)** light irradiation only **(c)** Pa only **(d)** PDT with Pa.

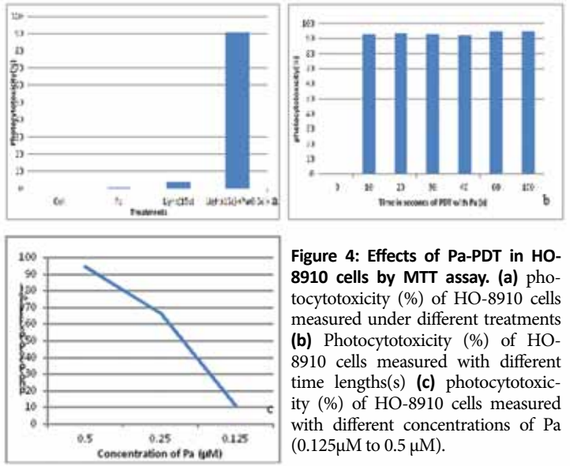

Figure 4: Effects of Pa-PDT in HO-8910 cells by MTT assay. (a) photocytotoxicity (%) of HO-8910 cells measured under different treatments **(b)** Photocytotoxicity (%) of HO-8910 cells measured with different time lengths(s) **(c)** photocytotoxicity (%) of HO-8910 cells measured with different concentrations of Pa (0.125μM to 0.5 μM).

assay reiterates the necessity of both light and Pa to inhibit proliferation (Figure 4). Figure 5 shows the result of MTT assay with various time lengths of PDT with Pa on the cells. No significant difference of photocytotoxicities of Pa in cells was observed for different Pa-PDT exposure periods ranging from 10 s to 100 s, with the highest and lowest photocytotoxicities being 93% and 95% respectively (Figure 4b). In addition, it showed a drug-dose dependent photocytotoxicity in the cells (Figure 4c), with the photocytotoxicities of 0.5 μM, 0.25μM and 0.125 μM concentrations associated with 94, 66.5 and 11.6 percentrage photocytotoxicities respectively.

LED-activated pheophorbide-a induces cell cycle arrest

Figure 5 shows the flow cytometric measurement of PI-stained DNA. The combined treatment of both Pa and LED irradiation resulted in the appearance of the sub-G1 phase, indicating that Led-activated Pa treatment induced apoptosis However, Pa or LED irradiation could not individually induce the sub-G1 phase.

Collapse of the mitochondrial membrane potential (ΔΨm) of ovarian cancer cells

JC-1 staining was used to measure the mitochondrial membrane potential (ΔΨm) of HO-8910 cells. The cells were sensitized by Pa and then irradiated by a LED light at light dose of 1.5 J/cm^2 Figure 6d shows the combined treatment of both Pa and LED irradiation on the cells three hours after LED activation of Pa, which triggered mitochondrial membrane depolarization (ΔΨm). A significant number of cells (55.1%) treated with both Pa and LED light showed a collapse in ΔΨm. Again, either Pa alone (Figure 6b) or light irradiation alone (Figure 6c) could not induce the loss of ΔΨm.

Discussion

PDT, a minimally invasive procedure that combines a light source and a photosensitizer, is currently used to treat a range of malignancies including lung cancer, head and neck cancer, and prostate cancer (Harrod-Kim, 2006). Its successful application depends crucially on the properties of the photosensitizer, such as efficient uptake by the cells, minimal dark toxicity and the ability to generate singlet oxygen species. Over the years, a number of photosensitizers have been proposed, with Photofrin being one of the most widely used in the clinic (Kaye et al., 1988). Photofrin, however, has a less than ideal absorption wavelength of approximately 630 nm (Rapozzi et al., 2009). Light at longer wavelengths (>650 nm) is desirable because it can penetrate deep-seated or larger tumors. Therefore, this prompts the search for second-generation photosensitizers. Pa has emerged as an ideal candidate for investigation because it has a higher absorption wavelength between 650-700 nm, which falls in the range of tissue-penetrating wavelength and it is selectively accumulated in tumor cells and incorporated into their nuclei, mitochondria and lysosomes (Tanielian et al., 2001). It was recently shown to be effective in combating liver cancer cells, (Chan et al., 2006; Ma et al., 2006; Tang et al., 2006) suggesting that it might be an efficient second-generation photosensitizer. The aim of this study was to determine the effects of LED-activated Pa on ovarian cancer cells and elucidate the molecular mechanism underlying its photocytotoxic effects.

Our results showed a significant reduction in the number of cells treated with both Pa and irradiation (Figure 3), which confirmed the photocytotoxicity values calculated. A significant time-dependent photocytotoxicity however, was not found in this study when varying the time of exposure from 10 s to 100 s (Figure 4b). It could possibly be due to either the fact that the photocytotoxicity reached a plateau at 10 s or a longer time period (in hours) is required before a noticeable difference in photocytotoxicity is observed. The exact mechanism for this remains to be investigated in future studies.

Mitochondria play a pivotal role in regulating cell death and longevity (Hajnoczky and Hoek, 2007). The maintenance of the mitochondrial membrane potential (ΔΨm) is essential for ATP synthesis and oxidative phosphorylation (Gottlieb, 2001). The depolarization of ΔΨm in HO-8910 cells was investigated by flow cyto-

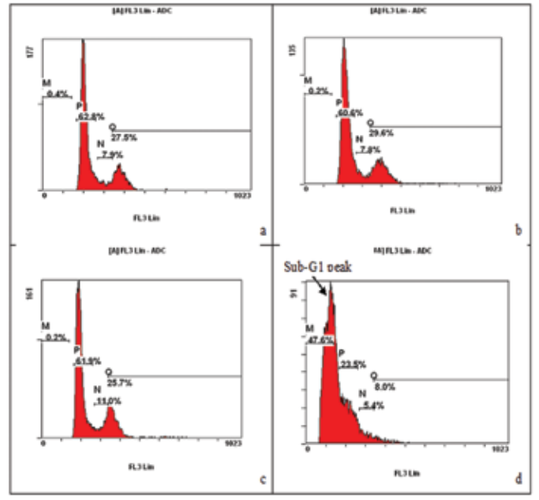

Figure 5: Flow cytometric analysis of cell cycle distribution with propium iodide (PI) staining. (a) Cell only **(b)** Pa (0.5μM) only **(c)** Light irradiation (15s) only **(d)** PDT with Pa. Note the appearance of the sub-G1 phase upon the combined treatment of both Pa and LED light.

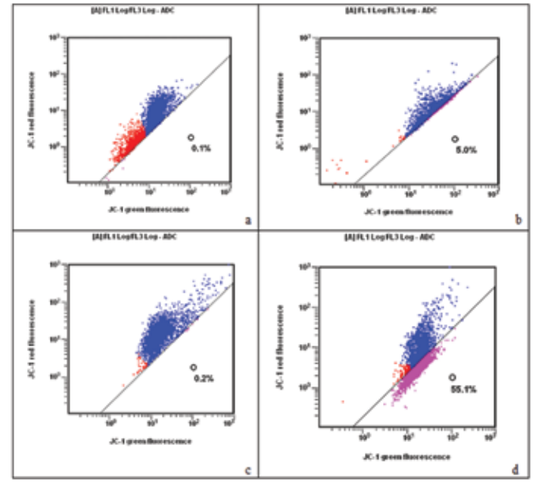

Figure 6: Flow cytometric analysis of mitochondrial membrane potential (Δψm) with JC-1 staining. The MMP of the cells were monitored 3 hours after treatment, where the collected cells were then stained with JC-1 for 30 min and the red and green fluorescence of JC-1 were acquired. **(a)** Cell only **(b)** Pa (0.5μl) only **(c)** Light irradiation (15s) only **(d)** PDT with Pa.

metric analysis with JC-1 staining. JC-1 is a cationic dye that signals the loss of the ΔΨm, a hallmark of apoptosis. The ΔΨm of HO-8910 cells indicated that a significant number of cells (55.1%) showed depolarized ΔΨm when exposed to both light irradiation and Pa (figure 6d). In contrast, only 5.0% and 0.2% of cells were depolarized when cells were treated with either Pa or light irradiation (Figures 6b and 6c) respectively. The decrease in ΔΨm increases the probability that permeability transition pores (PTP), found on mitochondrial membranes, will open. When PTPs open, K^+, Mg^{2+}, Ca^{2+} ions and water enter the mitochondria, causing the mitochondrial matrix to swell. Consequently, the outer membrane ruptures, resulting in the leakage of cytochrome *c* and other apoptosis-inducing factors into the cytoplasm (Kroemer, 1997).Propidium iodide (PI) staining was also used to assess apoptosis and based on the principle that apoptotic cells display fragmented DNA and consequently, loss of nuclear DNA content. When apoptotic cells are stained with PI, a sub-G1 peak, which indicates the occurrence of apoptosis, can be readily observed and distinguished from the normal peak of cells in the red fluorescence channels. A sub-G1 peak was observed in a significant percentage of cells (47.6%) treated by both Pa (0.5μM) and light irradiation (1.5J/cm^2) for 10 s (Figure 5d), while cells treated by either Pa or light irradiation alone indicated a low 0.2% sub-G1 peak.

It should be noted however, that the findings of this paper are preliminary and more rigorous investigations are needed to prove the occurrence of apoptosis. For example, DNA fragmentation by PI staining is not a universal finding in apoptotic cells, since necrotic cells can also display a certain degree of DNA degradation. In addition, the sub-G1 peak can represent, apart from apoptosis, nuclear fragments, micronuclei and clumps of chromosomes as well. Therefore, other experiments such as morphological observation of apoptotic cells, a DNA ladder in agarose gel or TDT (terminal deoxynucleotidyl transferase) assay for the specific demonstration of DNA breaks should be employed to confirm the results in this study.

In the view of Traditional Chinese Medicine (TCM), promoting apoptosis is only one component in cancer therapy. Inhibiting angiogenesis, overcoming multi-drug resistance (MDR) and boosting immune system function are also indispensible in the treatment of cancer. Therefore, a successful therapeutic paradigm must incorporate all of these components, in addition to treatments that induce apoptosis in cancer cells. In conclusion, Pa-PDT in conjunction with conventional chemotherapy is a potentially promising therapeutic intervention in the treatment of ovarian cancer. Future investigations involving the feasibility and applicability of Pa-PDT will undoubtedly be worthwhile and beneficial to the medical and scientific community.

References:

Bai, D.Q., Yow, C.M.N., Tan, Y., Chu, E.S.M., and Xu, C.S. (2010). Photodynamic action of LED-activated nanoscale photosensitizer in nasopharyngeal carcinoma cells. Laser phys *20*, 544-550.

Chan, J.Y.W., Tang, P.M.K., Hon, P.M., Au, S.W.N., Tsui, S.K.W., Waye, M.M.Y., Kong, S.K.W., and Fung, K.P. (2006). Pheophorbide a, a Major Antitumor Component Purified from Scutellaria barbata, Induces Apoptosis in Human Hepatocellular Carcinoma Cells. Planta Medica *72*, 28-33.

Fung-Kee-Fung, M., Oliver, T., Elit, L., Oza, A., Hirte, H.W., and Bryson, P. (2007). Optimal chemotherapy treatment for women with recurrent ovarian cancer. Curr Oncol *14*, 195-208.

Gottlieb, R.A. (2001). Mitochondria and apoptosis. Biol Signals Recept *10*, 147-161.

Hajnoczky, G., and Hoek, J.B. (2007). Cell signaling. Mitochondrial longevity pathways. Science *315*, 607-609.

Hajri, A., Coffy, S., Vallat, F., Evrard, S., Marescaux, J., and Aprahamian, M. (1999). Human pancreatic carcinoma cells are sensitive to photodynamic therapy in vitro and in vivo. Br J Surg *86*, 899-906.

Hajri, A., Wack, S., Meyer, C., Smith, M.K., Leberquier, C., Kedinger, M., and Aprahamian, M. (2002). In vitro and in vivo efficacy of photofrin and pheophorbide a, a bacteriochlorin, in photodynamic therapy of colonic cancer cells. Photochem Photobiol *75*, 140-148.

Harrod-Kim, P. (2006). Tumor ablation with photodynamic therapy: introduction to mechanism and clinical applications. J Vasc Interv Radiol *17*, 1441-1448.

Jemal, A., Siegel, R., Ward, E., Hao, Y., Xu, J., and Thun, M.J. (2009). Cancer statistics, 2009. CA Cancer J Clin *59*, 225-249.

Kaye, A.H., Morstyn, G., and Apuzzo, M.L. (1988). Photoradiation therapy and its potential in the management of neurological tumors. J Neurosurg *69*, 1-14.

Kroemer, G. (1997). Mitochondrial implication in apoptosis. Towards an endosymbiont hypothesis of apoptosis evolution. Cell Death Differ *4*, 443-456.

Lee, W.Y., Lim, D.S., Ko, S.H., Park, Y.J., Ryu, K.S., Ahn, M.Y., Kim, Y.R., Lee, D.W., and Cho, C.W. (2004). Photoactivation of pheophorbide a induces a mitochondrial-mediated apoptosis in Jurkat leukaemia cells. J Photochem Photobiol B *75*, 119-126.

Lim, D.S., Ko, S.H., and Lee, W.Y. (2004). Silkworm-pheophorbide alpha mediated photodynamic therapy against B16F10 pigmented melanoma. J Photochem Photobiol B *74*, 1-6.

Ma, J., Chen, M., Dai, Y., and Qiao, L. (2006). Enhancing the Efficacy of Photodynamic Therapy by a Chinese Herbal Medicine for Hepatocellular Carcinoma. Cancer Biology and Therapy *5*, 1117-1119.

Moore, J.V., West, C.M., and Whitehurst, C. (1997). The biology of photodynamic therapy. Phys Med Biol *42*, 913-935.

Pervaiz, S. (2001). Reactive oxygen-dependent production of novel photochemotherapeutic agents. FASEB J *15*, 612-617.

Qian, B. (1987). Clinical-Effects of Anticancer Chinese Medicine.

Rapozzi, V., Miculan, M., and Xodo, L.E. (2009). Evidence that photoactivated pheophorbide a causes in human cancer cells a photodynamic effect involving lipid peroxidation. Cancer Biol Ther *8*, 1318-1327.

Skehan, P., Storeng, R., Scudiero, D., Monks, A., McMahon, J., Vistica, D., Warren, J.T., Bokesch, H., Kenney, S., and Boyd, M.R. (1990). New colorimetric cytotoxicity assay for anticancer-drug screening. J Natl Cancer Inst *82*, 1107-1112.

Tan, Y., Xu, C.S., Xia, X.S., Yu, H.P., Bai, D.Q., He, Y., Xu, J., Wang, P., Wang, X.N., and Leung, A.W.N. (2009a). Photodynamic action of LED-activated pyropheophorbide-a methyl ester in cisplatin-resistant human ovarian carcinoma cells. Laser phys *6*, 321-327.

Tan, Y., Xu, C.S., Xia, X.S., Yu, H.P., Bai, D.Q., He, Y., Xu, J., Wang, P., Wang, X.N., and Leung, A.W.N. (2009b). Preliminary studies on LED-activated pyropheophorbide-a methyl ester killing cisplatin-resistant ovarian carcinoma cells. Laser phys *19*, 1045-1049.

Tang, P.M.K., Chan, J.Y.W., Au, S.W.N., Kong, S.K., Tsui, S.K.W., Waye, M.M.Y., Mak, T.C.W., Fong, W.P., and Fung, K.P. (2006). Pheophorbide a, an active compound isolated from Scutellaria barbata, possesses photodynamic activities by inducing apoptosis in human hepatocellular carcinoma. Cancer Biology and Therapy *5*, 1111-1116.

Tanielian, C., Kobayashi, M., and Wolff, C. (2001). Mechanism of photodynamic activity of pheophorbides. J Biomed Opt *6*, 252-256.

JULS RESEARCH

Attentional and learning mechanisms of suppressing behaviourally-irrelevant information in rats

Clara W. Y. Siu, Eve De Rosa

Department of Psychology, University of Toronto, 100 St. George Street, Toronto, ON Canada M5S 3G3

Abstract

Selective attention is the ability to focus on behaviourally-relevant information while suppressing behaviourally-irrelevant information. It has been demonstrated in humans that attention to previously-irrelevant information becomes impaired through both inhibitory attentional processes and learning; this phenomenon is termed 'learning-to-ignore'. When such attentional suppression to an ignored stimulus occurs across different learning contexts, generalization occurs, resulting in a sustained impairment in subsequently attending to the previously-ignored stimulus. In the present study, acquisition of attentional suppression was translated from the human paradigm to one for rats, to assess whether this inhibitory attentional process in humans is also present in these rodents. If so, then future studies will examine the neural underpinnings for this ability. Twenty Long-Evans rats were trained to associate one of two visual cues simultaneously presented on monitors in touchscreen-equipped operant chambers, such that one cue was ignored or unattended over numerous trials. There were three learning phases: two priming phases and then a test or probe phase. Four experimental conditions were used to assess either stimulus or response inhibition: Learning to Ignore – one context (LI1) and Learning to Ignore – two contexts (LI2) examined the inhibition of an ignored stimulus, while Response Reversal (RR) and Proactive Interference (PI) assessed the inhibition of a prepotent response. The study found that it was significantly more difficult to surmount the suppression of a previously-ignored stimulus (LI1 and LI2) than to surmount a prepotent response (PI). However, in rats, it was also found to be most difficult to successfully surmount both an ignored stimulus and prepotent response (RR). This was a condition that was not included in the previous human work. Therefore, the current study provides evidence that rats utilize similar attentional and learning mechanisms as humans in the learning-to-ignore phenomenon.

Introduction

We are constantly confronted with more information than we can process at any given point in time, but our attention is limited to only specific aspects of the surrounding. This is possible because we can selectively attend to those stimuli that are important to the task at hand, while ignoring distracting stimuli that are behaviourally-irrelevant. Classically, the 'biased competition' model of attention (Desimone and Duncan, 1995) proposed that selective attention works to resolve this competition by enhancing the processing of behaviourally-relevant stimuli and suppressing the processing of behaviourally-irrelevant stimuli. Since that time, it has been shown that attentional resources are allocated to those target stimuli that are behaviourally-relevant to the task, and that distractor stimuli that are behaviourally-irrelevant to the task are suppressed (Cave and Bichot, 1999; Dubois et al., 2009; Lamers et al., 2010).

In the aged human population, deficits in selective attention are evidence as one form of cognitive decline (Connelly et al., 1991; Craik and Salthouse, 2000; Schmitz et al., 2010). In older adults, performance on tests in laboratory settings revealed a reduction in their working memory capacity and processing speed when distracting stimuli were present, as compared to that of the younger adults (Gazzaley et al., 2005; Lustig et al., 2006). In addition, tests involving visual targets and distractors revealed that better performance was found in remembering the ignored distractors in the older population relative to younger adults (Machado et al., 2009; Rowe et al., 2006; Schmitz et al., 2010). Accordingly, these studies evidenced that attention to the behaviourally-relevant information was diminished with normal aging, due to the fact that more attentional resources were allocated to what was behaviourally-irrelevant. Hence, this failure to ignore the behaviourally-irrelevant distractors is attributed to impairment in attentional inhibition.

Attentional inhibition involves suppressing behaviourally-irrelevant information or a distractor, such as tuning out the ring tone for your roommate's cell phone so that you do not orient every time their phone rings (Cave and Bichot, 1999). If the same distractor was presented over many trials, and generalized over different contexts, then this distractor stimulus would eventually become suppressed (Dixon et al., 2009). As a result, if this ring tone subsequently became important, then attending to this previously-ignored stimulus would be significantly impaired

(Dixon et al., 2009). In essence, this means that multiple exposures to the behaviourally-irrelevant stimulus involve a learning process that gradually accumulates inhibition. This phenomenon, known as learning-to-ignore, is essential in that it allows the formation of expectations in the environment (Dixon et al., 2009). Low performance on selective attention in older adults compared to young adults might, therefore, be rooted in an impairment in attentional inhibition (Schmitz et al., 2010).

The learning-to-ignore phenomenon was demonstrated by Dixon et al. (2009) in humans, but what is unknown is whether this phenomenon can also occur in nonhuman animals such as rats. Selective attention impairment in normally aging older adults could be the result of various physiological changes, such as a decline in the function of the neurochemical acetylcholine (Schmitz et al., 2010); but since invasive procedures cannot be performed in humans, nonhuman animal studies might be able to provide the physiological mechanism for this effect. Hence, it would be beneficial to determine whether the mechanisms supporting human selective attention can be observed in rats.

In the present study, the human paradigm for learning-to-ignore was translated to one for rats, to test whether the process of attentional suppression is also present in these rodents. If attention to behaviourally-irrelevant stimuli can be suppressed with experience in rats, then when required to attend to the previously-irrelevant stimuli, it is hypothesized that rats will show an impairment on this task, comparable to humans (Dixon et al., 2009).

The experiment was conducted in three learning phases, which comprised of two priming phases and a test or probe phase. Four experimental conditions were used to assess stimulus inhibition of an ignored stimulus, as well as behavioural inhibition of a prepotent response to a target stimulus. This was a within-subjects design, so the four conditions were performed within four rotations and counterbalanced appropriately such that each rat participated in each condition. In the probe phase for all four conditions, the rats responded to the exact same stimuli so that any behavioural differences could be attributed to the priming phases that preceded the probe phase (Figure 1).

Learning to Ignore – one context (LI1) and Learning to Ignore – two contexts (LI2) were the stimulus inhibition measures, while Response Reversal (RR) and Proactive Interference (PI) were included as the response inhibition measure. RR was included because it is the classic test of behavioural inhibition. Rats were trained through operant conditioning to associate reward with a correct response to the target stimulus, while the irrelevant distractor stimulus was presumably suppressed. It was hypothesized that the greatest performance impairment will occur in LI1 and LI2 relative to in PI, because human data have revealed that LI induces a persistent behavioural decrement relative to the transient one when experiencing PI (De Rosa et al., 2004; Dixon et al., 2009) Moreover, it is anticipated that performance in RR will have the greatest decrement; this is because RR, unlike the other conditions that required either stimulus inhibition or response inhibition, required both forms of inhibition (Figure 1).

Response reversal (RR)

Prime 1		Prime 2		Probe	
D+	B-	D+	B-	B+	D-

Proactive Interference (PI)

Prime 1		Prime 2		Probe	
D+	A-	D+	A-	B+	D-

Learning to Ignore – one context (LI-1)

Prime 1		Prime 2		Probe	
A+	B-	A+	B-	B+	D-

Learning to Ignore – two contexts (LI-2)

Prime 1		Prime 2		Probe	
A+	B-	C+	B-	B+	D-

Figure 1: The four experimental conditions. Each condition was divided into three phases: Prime 1, Prime 2, and Probe. Target (+) and distractor (-) stimuli appeared simultaneously on touchscreens in operant chambers. Both stimuli differ across each condition for the Prime phases, but the same target and distractor stimulus were used for all four conditions during the Probe phase. RR and PI assessed the inhibition of a pre-potent response, and LI1 and LI2 assessed the inhibition of an ignored stimulus. Moreover, PI, LI1, and LI2 use a novel stimulus during the Probe sessions.

Figure 2: Photograph of the operant chamber used for training and testing. Upon correct response to the target stimulus on the touchscreen at the front of the chamber, the circular white light at the rear lit up as a cue for a water reward being available at the water-well. Movement-detecting infrared (IR) beams were situated in the middle and back of the chamber to detect the location of the rat. Each chamber was also equipped with a speaker for emitting warning tones for subsequent stimuli presentation.

Materials and Methds

Participants

Twenty experimentally-naïve male Long-Evans rats, weighing between 450-530 g, were trained and tested at 6 weeks of age (Charles River, Montreal, Quebec). Rats were raised on a reversed 12 hour light – 12 hour dark cycle (i.e., lights off at 8am, lights on 8pm), and were housed independently in 45 cm long x 25 cm wide plastic tub cages. All rats were water restricted to 25-30 min daily access to water and also received water as a reward for correct responding during training. Training or testing occurred in the dark phase of the light cycle because rats are nocturnal. This study was approved by the University of Toronto's Institutional Animal Care Committee.

In between each rotation, rats were given a two-week break, in which they had *ad libitum* access to water and food. During this two week period, they were handled for fifteen minutes each day for seven days, and were then deprived of water for the twenty-four hours before the first session of training.

Apparatus

Four operant chambers measuring 41.2 cm x 41.2 cm x 29.2 cm (l x w x h), equipped with touchscreen monitors measuring 24.7 cm wide x 18.5 cm high, were used for training and testing (MED Associates Inc; ELO).

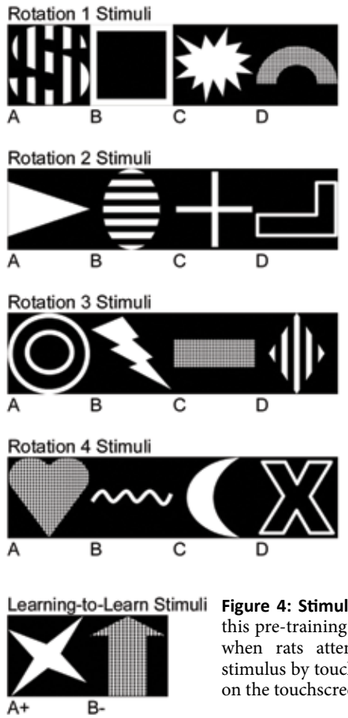

Figure 3: Stimuli used in the four rotations. For each rotation, rats were trained to touch the corresponding target stimulus on the touchscreen (Figure 1) in order to receive the water reward. Target stimuli appeared on each side of the screen for equal number of times, at random, to ensure a counterbalancing effect.

Figure 4: Stimuli for Learning-to-Learn. In this pre-training phase, water was rewarded when rats attended to the task-relevant stimulus by touching the target stimulus (+) on the touchscreen.

Clear Plexiglas was used for the chamber ceiling and the right and left chamber walls. The right chamber wall was hinged to allow for entry into the chamber. Stainless steel was used for the front and rear walls (Figure 2).

For each operant chamber, the touchscreen was positioned in the centre of the front wall of the chamber, with 7.9 cm of space on either side and inset 1.6 cm from the front wall of the chamber. A rectangular water-well, measuring 5 cm x 5 cm x 5 cm, was positioned at the lower centre of the rear wall. A correct response, i.e., touch their nose to the appropriate stimulus, by each rat was followed by a lit circular white light at 2.2 cm above the water-well to signal for the presence of water. The rat would then break the infrared (IR) beam across the water well with its nose, and 0.05 ml of water was dispensed into the water-well by an infusion pump equipped with a 25 ml syringe filled with water.

The floor of the chamber was lined with steel rods 5 mm in diameter, running from left to right along the floor spacing 1.1 cm apart. At 4 cm above the floor, two pairs of IR beams were positioned across the side walls. The back IR beam was located 5.5 cm from the rear wall, and the middle IR beam was located at the midline between the rear and the front wall. Both pairs of IR beams were used to detect movement for the purpose of locating the rat in the chamber. Underneath the floor with the steel rods was a removable shallow container for emptying waste products.

Each chamber was further equipped with a webcam, as well as a speaker through which warning tones were emitted to indicate stimuli presentation. This system was enclosed in a wooden sound- and light-attenuating enclosure, measuring 74 cm x 60.5 cm x 60 cm. The enclosure was equipped with a fan for providing ventilation and white noise so that the rats would not be startled by noises outside of the chamber.

Two computers were placed on top of each wooden enclosure: one for stimuli presentation and detection of responses on the touchscreen, and the other for video recording via the webcam. Two more computers were placed outside of the testing room: one was used for the operant chamber control and data recording via a control interface (MED Associates Inc.), and the other for video recording control.

Visual Stimuli

Stimuli of specific shapes and designs were used (Figure 3). A target stimulus and distractor stimulus corresponding to the rotation and condition was presented simultaneously on the touchscreen for each trial (Figure 1). Stimuli were black and white, and were displayed on a black background. Each stimulus measured 5 X 5 cm and were chosen to be discriminable by the rats.

Pre-training Procedures

Prior to water restriction, each rat was exposed to the inside of an operant chamber for 15 minutes per day for 2 days. Then twenty-four hours after water restriction, the rats began the first pre-training phase, Variable-Light-Water, where they were trained to associate the light cue above the water-well with the opportunity to retrieve water. This phase was conducted in 30-minute sessions per day until the latency between light cue and drinking behaviour decreased to an average of less than two seconds.

Each day of Touch-Light-Water, the second pre-training phase, was conducted in 72-trial sessions, or 40-minute sessions if the rat could not complete all 72 trials within 40 minutes. Water-light activation was triggered when rats touched the touchscreen with their nose or front paws, and latency was measured by the time between the offset of light-water response and touching the touchscreen. Completion of this phase was indicated by an average latency of less than ten seconds.

Single-Stimulus, the third pre-training phase, was marked by the addition of a white square stimulus to the Touch-Light-Water phase. Each trial was initiated by the presentation of a two-second tone, which was followed, after a one-second delay, by a white-square stimulus appearing at the centre of the touchscreen. Light-water activation was triggered only when rats touched the image of the stimulus on the touchscreen.

Moving-Stimulus, the fourth pre-training phase, was conducted in 80-trial sessions each day. Every rat had to complete all 80 trials every day. This phase was identical to the Single-Stimulus phase, with the exception that the stimulus was presented on either the bottom left or right side of the touchsceen, rather than in the centre. Completion of this phase was marked by an average of less than ten seconds of touching the stimulus after stimulus onset.

Finally, in Learning-to-Learn, the last pre-training phase, two novel stimuli were presented simultaneously: one was the target or correct stimulus and the other was the distractor or incorrect response (Figure 4). Through trial and error, rats learned to associate only the predefined target stimulus with reward. This phase was also conducted in 80-trial sessions. This phase continued until all of the rats achieved two sessions during which a criterion level of performance was met. Criterion was defined as 18/20 correct responses anywhere within the 80-trial session.

Experimental Conditions

Four experimental conditions were used, and each was conducted in three learning phases. The two priming phases (Prime 1 and Prime 2) each consisted of ten 80-trial sessions, and were followed by a test or probe phase (Probe) that consisted of twenty 80-trial sessions. The four conditions were RR, PI, LI1, and LI2 (Figure 1; and Figure 3 for the corresponding stimuli).

Similar to Learning-to-Learn, the target and distractor stimuli were presented simultaneously on the left and right side of the screen, such that the occurrence of both stimuli on each side was counterbalanced, with the target stimulus appearing on the same side of the screen in no more than three consecutive trials. As in the pre-training phases, initiation of each trial began with the presentation of a two-second tone. Presentation of the stimuli occurred after a one-second delay, and light-water activation was triggered only when rats touched the image of the target stimulus on the touchscreen with their nose or front paws.

Statistical Analysis

SPSS Statistics 17.0 was used to conduct statistical analysis. The mean accuracy score was used to assess performance based on an □-level of 0.05. Paired-samples t-test and mixed-model repeated measures analysis of variance (ANOVA), with simple contrast, were used in the analyses.

Results

Performance

The mean accuracy scores for all twenty rats in Prime 1, Prime 2, and Probe for all four conditions are shown in Figure 5. A paired-samples t-test was conducted to reveal a significant difference between the last session of Prime 1 (Session #10) of LI2 and the first session of Prime 2 Session (Session #11) of LI2 [$t(19) = 2.25$, $p < .05$]. Separate mixed-model repeated measures ANOVA were conducted for Prime 1, Prime 2, and Probe data. Accuracy was collected under four different rotations in this within-subjects design. Hence each rat was grouped into one of four sequences of testing: LI1, LI2, PI, RR (Sequence 1), RR, PI, LI2, LI1 (Sequence 2), PI, LI1, RR, LI2 (Sequence 3), and LI2, RR, LI1, PI (Sequence 4). No significant differences were found between the rotations for all of the proceeding analyses.

Overall Prime 1, Prime 2, and Probe Performance

Significant main effects were found by repeated ANOVA between each session and condition in Prime 1 [$F(3.59, 57.49) = 80.17$, $p < .001$; $F(3, 48) = 15.41$, $p < .001$], Prime 2 [$F(9, 144) = 15.22$, $p < .001$; $F(3, 48) = 17.28$, $p < .001$], and Probe [$F(2.87, 45.84) = 134.00$, $p < .001$; $F(3, 48) = 28.67$, $p < .001$]. Significant differences revealed the process of learning throughout the phases.

End of Prime Sessions (Session #20)

A significant difference was found between the four conditions by repeated ANOVA [$F(3, 48) = 4.37$, $p < .01$]. Further analyses were performed via simple contrast, which revealed significant differences between LI1 and RR ($p = .003$), LI1 and PI ($p = .028$), and LI1 and LI2 ($p = .008$). These indicated that the conditions have not all attained the same level of performance by the end of the Prime Sessions or before Probe Sessions.

Beginning of Probe Sessions (Session #21)

As expected, a significant difference between conditions was found by repeated ANOVA [$F(1.93, 30.92) = 7.44$, $p < .01$]. Although all rats were attending to the same set of stimuli during each rotation, performance was expected to differ as a result of either inhibition of an ignored stimulus (LI1, LI2, RR) or inhibition of a prepotent response (PI, RR). Specific analyses by simple contrast revealed differences between PI and LI2 ($p = .000$), and RR and PI ($p = .000$), confirming the hypothesis that inhibiting the suppression of a previously-ignored stimulus was more difficult than suppressing the response to a prepotent stimulus.

End of Probe Sessions (Session #40)

By the end of the Probe phase, a significant difference remained between the conditions [$F(1.95, 31.22) = 5.14$, $p < .05$]. The same differences as the beginning of Probe were revealed by simple contrast, between PI and LI-2 ($p = .006$), and RR and PI ($p = .000$), as well as between and LI-2 ($p = .030$). Consistent differences between the conditions persisted through all 20 sessions.

Discussion

As expected, the greatest impairment was observed during the first session where the contingencies were reversed for one stimulus in the probe phase. When performance based on the mean average scores was compared across all four conditions, better performance was observed in PI than in LI1 and LI2, and the lowest performance score was found in RR (Figure 5). PI represented inhibition of a prepotent response, and LI1 and LI2 represented attentional inhibition of a behaviourally-irrelevant stimulus. Indeed, better performance in PI revealed that the impairment in LI1 and

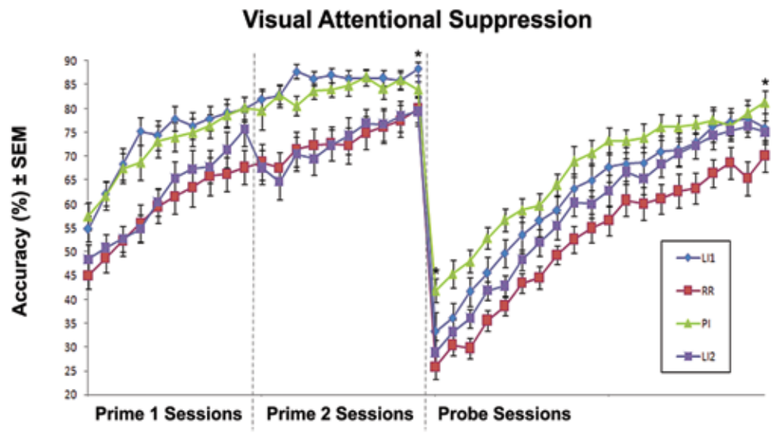

Figure 5: Progress of rats during Prime 1, Prime 2, and Probe phases. Ten sessions for Prime 1 were followed by ten sessions of Prime 2, which were then followed by twenty sessions of Probe. Means with ± standard error were plotted for Proactive Interference (PI), Learning to Ignore – one context (LI1), Learning to Ignore – two contexts (LI2), and Response Reversal (RR). No significant differences were found between the rotations required for the within-subjects design, so the data were collapsed into the four conditions. Learning was observed in each of Prime 1, Prime 2, and Probe, as significant main effects of Session were found for all three phases. Performance in PI was also significantly better than performance in LI1 and LI2 in the first Probe Session (Session #21). At the same time, significant impairment in performance was found in RR in the first Probe session. The differences between the conditions persisted until the end of Probe (Session #40).

LI2 was accounted for by the attentional suppression mechanism. Therefore, this lead to the finding that the learning-to-ignore phenomenon first demonstrated in humans (Dixon et al., 2009) was also present in rats.

RR is the classic measure of cognitive inhibition. We included it in this study to show that it represents both inhibition of a prepotent response and attentional inhibition of a behaviourally-irrelevant stimulus. This is because, unlike the other three conditions where one new stimulus was presented in the probe phase, the exact same stimuli were presented in the probe phase of the RR condition. And as hypothesized, the greatest impairment was observed in the RR probe condition (Figure 5). In PI, LI1, and LI2, rats could learn to associate the novel stimulus in the probe phase with the correct or incorrect response; whereas in RR, rats must relearn this association for both the target and distractor stimuli, in order to inhibit both the ignored stimulus and the prepotent response.

By the last probe session (Session #40), significant differences between the PI and LI2 conditions persisted, indicating that the effect of attentional suppression might have been sustained, as attending to the previously-irrelevant stimuli was still relatively more difficult than suppressing a prepotent response even after a learning period. This result further reinforced the finding that rats utilize a similar attentional suppression mechanism as humans.

The successful translation of the human paradigm of learning-to-ignore to one for rats will provide an opportunity for studying the physiological mechanism underlying this behavioural phenomenon. As a result, it is possible to use rat models to study the neurochemical aspect of inhibition impairment in aging, via techniques like lesion studies, genetic manipulation, or administration of drugs through cannula infusion.

Previous studies have found that neuromodulation of attention was related to the influence of the neurochemical acetylcholine. For example, Broussard and colleagues (2009) found that removing cholinergic input from the basal forebrain during the presentation of a visual cue resulted in a diminished activation of posterior parietal cortex (PPC) neurons. At the same time, this removal also resulted in the activation of some PPC neurons when the cue was directed to the distractor. These findings suggest that cholinergic projections to the neocortex might play a role in the learning-to-ignore phenomenon.

Moreover, functional magnetic resonance imaging (fMRI) study on humans have demonstrated intact selective attention in young adults and impairment in older adults (Gazzaley et al., 2005; Schmitz et al., 2010). Schmitz and colleagues (2010) have found that when looking at repeating faces targets and places distractors, young adults demonstrated neural adaptation in the cortical region that processes face stimuli, the fusiform face area (FFA), and no adaptation in the place region, parahippocampal place area (PPA). In contrast, older adults showed weaker adaptation in the FFA, and paradoxically showed large adaptation in the PPA for the unattended places. Thus, adaptation in PPA indicated selective attention deficits in the aged population. Neurochemical approaches can now be used in rat models to examine the deficit in selective attention in older adults.

Conclusion

Through the successful translation of the human paradigm of learning-to-ignore to one for rats, it was demonstrated that rats may exhibit similar attentional inhibition mechanism as humans for attending to behaviourally-relevant information, while ignoring behaviourally-irrelevant information in their environments. This finding has implications for studies of cognitive decline in the aged population, because testing with rat models could provide insight into the neurochemical mechanisms of the behaviour. Studies have found an association between activity in the neocortex and the role of acetylcholine with attentional regulation (Broussard et al., 2009; De Rosa et al., 2004) Hence, future studies will test whether selective attention, through suppression of behaviourally-irrelevant information, could be influenced by the activity of acetylcholine in the neocortex.

Acknowledgements

The author would like to thank Dr. Eve De Rosa for her invaluable help and guidance throughout this work. In addition, the author would like to thank Dr. Leigh Botly and Vladimir Ljubojevic for their invaluable guidance in animal welfare and statistics, as well as and Hilary Bond, Graham Chamberlain, Valya Sergeeva, Seba Tumer, Gennie Wang, and Fida Zaman for working as a team to collect the data. This work was supported by Dr. Eve De Rosa's grant from the Natural Sciences and Engineering Council of Canada (NSERC).

References

Broussard, J.I., Karelina, K., Sarter, M., and Givens, B. (2009). Cholinergic optimization of cue-evoked parietal activity during challenged attentional performance. European Journal of Neuroscience *29*, 1711-1722.

Cave, K.R., and Bichot, N.P. (1999). Visuospatial attention: Beyond a spotlight model. Psychonomic Bulletin & Review *6*, 204-223.

Connelly, S.L., Hasher, L., and Zacks, R. (1991). Age and reading: The impact of distraction. Psychology and Aging *6*, 533-541.

Craik, F.I.M., and Salthouse, T.A. (2000). The handbook of aging and cognition - 2nd ed. (Mahwah, NJ, Lawrence Erlbaum Associates, Inc.).

De Rosa, E., Desmond, J.E., Anderson, A.K., Pfefferbaum, A., and Sullivan, E.V. (2004). The human basal forebrain integrates the old and the new. Neuron *41*, 825-837.

Desimone, R., and Duncan, J. (1995). Neural mechanisms of selective visual attention. Annual Review of Neuroscience *18*, 193-222.

Dixon, M.L., Ruppel, J., Pratt, J., and De Rosa, E. (2009). Learning to ignore: Acquisition of sustained attentional suppression. Psychonomic Bulletin & Review *16*, 418-423.

Dubois, J., Hamker, F.H., and VanRullen, R. (2009). Attentional selection of noncontiguous locations: The spotlight is only transiently "split". Journal of Vision *9*, 1-11.

Gazzaley, A., Cooney, J.W., Rissman, J., and D'Esposito, M. (2005). Top-down suppression deficit underlies working memory impairment in normal aging. Nature Neuroscience *8*, 1298-1300.

Lamers, M.J.M., Roelofs, A., and Rabeling-Keus, I.M. (2010). Selective attention and response set in the Stroop task. Memory & Cognition *38*, 893-904.

Lustig, C., Hasher, L., and Tonev, S.T. (2006). Distraction as a determinant of processing speed. Psychonomic Bulletin & Review *13*, 619-625.

Machado, L., Devine, A., and Wyatt, N. (2009). Distractibility with advancing age and Parkinson's disease. Neuropsychologia *47*, 1756-1764.

Rowe, G., Valderrama, S., Hasher, L., and Lenartowicz, A. (2006). Attentional Disregulation: A Benefit for Implicit Memory. Psychology and Aging *21*, 826-830.

Schmitz, T.W., Cheng, F.H.T., and De Rosa, E. (2010). Failing to ignore: Paradoxical neural effects of perceptual load on early attentional selection in normal aging. The Journal of Neuroscience *30*, 14750-14758.

Consider Graduate Studies in the Department of Molecular Genetics at the University of Toronto

Why Choose Our Department for Graduate Studies?

Cutting Edge Science: Our Department is a world-reknowned global leader in Molecular Genetics research.

Choice: Our Department has well over 80 different labs that you can choose from to pursue your Graduate work.

A Perfect Fit: We provide you with the unique opportunity of rotating through at least 3 labs before choosing a permanent lab. Unlike other departments, our (non-visa) students are not required to have confirmed a supervisor or even rotations upon joining our Department. Instead, students sample research projects & environments before choosing their thesis topic. Our rotation system facilitates the perfect match between you and your future lab!

About Molecular Genetics

While the discipline of genetics has its origins in the pioneering work of Mendel over a century ago, the modern revolution in genetics began with the cloning & sequencing of individual genes. Genetic engineering has had a phenomenal impact on all aspects of biological & medical sciences, and indeed every day life. With state of the art training in molecular genetics, our graduate students & post-doctoral fellows continue to be an integral part of the molecular revolution.

What Does Your Future Hold?

Technological advances in genetics have vastly broadened the career opportunities for our Graduates, who are in high demand in academic departments, research institutes, and biotech industries throughout the world. With a Molecular Genetics degree in hand, your future is limited only by your imagination!

Our Areas of Research

- Functional Genomics, Proteomics & Bioinformatics
- Cell Biology & Signal Transduction
- Molecular Microbiology & Virology
- Molecular Medicine & Human Genetics
- Molecular Biology & Biochemistry
- Model Organism Genetics
- Genetics of Development
- Structural Biology

To learn more about our Faculty members, their research interests and how to become a Graduate Student in our Department, visit: http://www.moleculargenetics.utoronto.ca

JULS RESEARCH

Investigation of the Anti-Proliferative Effect and the Underlying Mechanism of the Crude Extract of *Celastrus Orbiculatus* on Human HaCaT Keratinocytes

Dun Yuan Zhou[a], Lin Li Zhou[b], Ling Liu[b], Eric Chuck Hey Pun[a] and Zhi-Xiu Lin[b].

[a] University of Toronto, Toronto, ON Canada
[b] School of Chinese Medicine, The Chinese University of Hong Kong, Shatin, Hong Kong, China

Abstract

Traditional Chinese Medicine (TCM) has a long history in treating a variety of skin diseases, including psoriasis. In this present study, the anti-proliferative effect of the crude extract of Celastrus orbiculatus (also known as Nan She Teng, or NST) and its underlying mechanism were investigated. Sulforhodamine B (SRB) and 3-(4,5-Dimethylthiazol-2-yl)-2,5-diphenyltetrazolium bromide (MTT) assays were employed and confirmed a half maximal inhibitory concentration (IC50) value of 29.4μg/mL for NST on HaCaT cells treated for 48h. In addition, cellular morphology was examined with Hoechst 33342 stain, which detected chromosomal condensation with changes in cell membrane shape. Cell cycle analysis by propidium iodide (PI) staining displayed substantial sub-G1 peaks(49.4%) at 45μg/mL(1.5×IC50) of NST compared to less than 11% in the control. Moreover, flow cytometric analysis by Annexin-V PI staining revealed dose-dependent apoptosis due to NST application – 60.1% in the 45μg/mL while only 6.0% in the control. Similarly, flow cytometry with JC-1 staining yielded 6.7% of cells in the control with a low mitochondrial membrane potential (MMP/ΔΨm), whereas cells treated with 30μg/mL (IC50) presented 57.2% low MMP. In conclusion, our experimental data validate the anti-proliferative effect of the crude extract of NST, and the observed inhibition on cell growth was attributed to the induction of apoptosis.

Introduction

Psoriasis is a chronic immune-mediated skin disorder, for which there is currently no cure. Worldwide, 2-4% of the population is inflicted with psoriasis; hence, it can cause considerable physical, psychological and social impacts in patients (de Arruda and De Moraes, 2001). Even though there are established therapeutic treatments, namely – vitamin D topical therapy, phototherapy, and systemic therapy, all of them have problems: low efficacy, drug intolerance, drug resistance and concomitant adverse effects, all of which spur substantial interest in the field of psoriasis for further drug exploration and development.

In psoriasis, hyperproliferation and abnormal differentiation of keratinocytes are the two most characteristic features (Rashmi et al., 2009; Kastelan et al., 2009). The spontaneously transformed and immortalized human keratinocyte cell line has been used as a prominent *in vitro* model for studies on psoriasis pathology and evaluation of anti-psoriatic drugs (George et al., 2010; Zeeli et al., 2010).

Now, greater numbers of patients with chronic psoriasis are turning to Traditional Chinese Medicine (TCM) as an alternative or complementary form of medicine for treatments with higher efficacy or reduced adverse effects (Ben-Arye et al., 2003). In China, TCM has been widely applied for centuries in treating psoriasis, and is perceived as effective, affordable and with few long-term side-effects (Koo and Arain, 1998). TCM classifies psoriasis into three key syndromes –'blood heat', 'blood dryness' and 'blood stasis', all of which contribute to symptoms like yellow coating on the tongue, hot temperature aversion, rapid pulse, rough and scaly skin, etc. Also, blood stasis and blood heat are understood in biomedical terms to be haematological disorders such as haemorrhage, congestion, local ischemia and tissue changes. Various plants are medicinally employed to combat psoriatic conditions and reinstate balance in the patient (Tse, 2003).

Celastrus orbiculatus, commonly known as Oriental Bittersweet, or Nan She Teng in Chinese (NST), is a woody, perennial vine found over much of China, Japan, and the Korean peninsula. With a widespread presence in China, NST has a long history of use as a folk drug in rheumatoid arthritis and bacterial infection (Zhu et al., 2008). From the TCM perspective and knowledge, 15 species of NST have functions of expelling wind-dampness, promoting Qi (the TCM term representing energy flow) and blood circulation, and removing blood stasis and toxins. This plant genus has given rise to at least 60 isolated compounds, with the most common being sesquiterpenoids, triterpenes, flavonoids, and alkaloids, thus establishing *C. Orbiculatus* as a potent herbal material that acts as an antifeedant, antitumour, antivirus, antioxidant, multidrug resistance reversing factor, capable of cytotoxic effects (Feng et al., 2007).

Hyperproliferative epidermal cells found in psoriatic lesions exhibit a decreased level of apoptosis in comparison to normal skin cells (Tse et al., 2008). Undoubtedly, apoptosis maintains tissue homeostasis in all organ systems including the skin. Various dermatological diseases, such as lupus erythematosus, lichen planus and psoriasis are characterized by modified apoptosis rates in the epidermal layer (Teraki and Shiohara, 1999). Therefore, anti-psoriatic drugs are intended to reestablish the homeostatic conditions in diseased keratinocytes by restraining hyperproliferation and abnormal differentiation (Pol et al., 2003). Candidate cytotoxic compounds and materials can cause different outcomes in a cell, such as necrosis and apoptosis (Reed, 2000).

Our study examined the anti-proliferative properties of the crude extract of NST, and investigated its underlying mechanism of growth inhibition on cultured human HaCaT keratinocytes.

Materials and Methods

Chemicals and Medicinal Materials

All chemicals and reagents used were obtained from Sigma Chemical Company (Sigma–Aldrich Co. Ltd., USA) unless stated otherwise. The herb, NST, was purchased from Hung Kei Herbal Company, Hong Kong. The extract was made using 80% aqueous ethanol, and sterilized by filtration.

General Cell Culture

The HaCaT cell line (provided by the China Centre for Type Culture Collection, Wuhan, China), was grown in flasks (Corning, NY, USA) and maintained in Dulbecco's modified Eagle's medium (DMEM), 10% fetal bovine serum (FBS) and 1% penicillin/streptomycin (Invitrogen Corporation, CA, USA) at 37˚C in a humidified atmosphere containing 5% CO_2.

Proliferation Assay – SRB and MTT

HaCaT cells were cultured in a 96-well plate one day prior to the experiment, at 10^4 cells per well, with 150μL of DMEM. Each replicate contained one control well, and nine other wells treated with serial diluting drug concentrations, from the highest 125μg/mL to the lowest 0.49μg/mL. In each plate, there were six replicates. The cells were incubated for 24, 48, and 72h, after which the proliferation rates of HaCaT under the influence of NST crude extract were measured by an SRB or an MTT assay using a plate reader. These assays were employed to determine the IC50 for the NST crude extract after one of the three planned incubation periods (24, 48, 72h) on the HaCaT cell line.

IC50 is a quantitative measure of a compound's potency in inhibiting biological or biochemical functions. It denotes how much of a particular drug or inhibitor is required to suppress a given biological process by half. It is commonly used as a measure of antagonist drug potency in pharmacological research.

Sulforhodamine B (SRB) is a colorimetric end-point microplate assay which quantifies viable cells by staining their cellular protein content (Lin et al., 1999).We performed SRB assays using the method described by Skehan et al.(Skehan et al, 1990).

An MTT assay was applied concurrently as explained in Tse *et al.* (2006) to confirm the results obtained by SRB assays. MTT is a tetrazolium salt that can be cleaved by active mitochondria of viable cells to form a dark blue formazan product, which can be measured colorimetrically. In both SRB and MTT assays, the plate was read at optical density = 540nm in a microplate spectrophotometer (BMG Labtechnologies, Fluostar Optima).

Cell Cycle Analysis with PI Staining

Propidium iodide (PI), a fluorogenic compound, binds stiochiometrically to nucleic acids and sends off fluorescent emission proportional to the DNA content of a cell (Riccardi and Nicoletti, 2006). After 48h of NST treatment at 15μg/mL, 30μg/mL, and 45μg/mL, cells were trypsinized and fixed in 70% ethanol at 4˚C overnight, followed by re-suspension in 10μL PI solution (2 mg/mL) with 50μL RNAase (10 mg/mL) and incubation in the dark at 37˚C for 30 min. Cells were then subjected to DNA content analysis using a FACSort flow cytometer (Becton-Dickinson)

Quantitative Analysis of Apoptotic Cells by Annexin-V PI Staining

Annexin-V PI labeling enables detection of apoptotic cells by externalization of phosphatidylserine (Li et al., 2010). After 48h of NST treatment at 15μg/mL, 30μg/mL, and 45μg/mL, the cells were trypsinized, pooled together, and stained concomitantly with Annexin-V and PI. The Annexin-V contains fused green fluorescent protein (GFP) to its N-terminus (Ernst et al., 1998) and Annexin-V staining detects apoptosis in the early stage based on cell membrane alterations (Dong et al., 2005). The stained cells were subsequently analyzed by flow cytometry (Becton-Dickinson).

Fluorescent Staining of HaCaT Cells for Morphological Evaluation

After 48h with NST treatment at 15μg/mL, 30μg/mL, and45μg/mLin a 6-well plate, the cells were washed twice with PBS, treated with 70% ice-cold ethanol for 15min. Following one more wash with PBS, 500μl of 20μg/mLHoechst 33342 was added to each well to stain the cells for 15 min at room temperature in the dark. Subsequently, an inverted fluorescent microscope (Olympus, Tokyo, Japan) was used to observe morphological changes (mainly DNA conformation) of the NST-treated cells.

Flow Cytometric Analysis with JC-1 Staining

JC-1 is a hydrophobic fluorescent cation that is incorporated into the mitochondrial membrane where it forms aggregates due to changes in the mitochondrial membrane potential (Salvioli et al., 1997). After 48h, the NST crude extract treatment at 15μg/mL, 30μg/mL, and 45μg/mLin a 6-well plate, the cells were washed twice with Phosphate buffered saline PBS to wash away the medium, especially FBS, followed by the addition of 10μL of JC-1. The plate was incubated at 37˚C for 15min, after which cells were submitted to flow cytometry.

Results

Determining the IC50 of the NST Crude Extract

The use of anti-proliferation assays, SRB and MTT, aimed to determine the IC50 value of the crude extract of NST, which was to be used in downstream experiments. Data shown in Table 1 indicate that the anti-proliferative effect of the crude extract was the most potent at the 48h mark. The 24h treatment condition required a much higher drug concentration – 68.2μg/mL (MTT), 73.6μg/mL (SRB) more than doubling the IC50 values in the 48h treatment – to exert the same anti-proliferative action on HaCaT cells. In addition, the 72h treatment condition as well showed slightly higher IC50 values compared to the 48h treatment. These results demonstrated considerable growth inhibitory effects of the crude

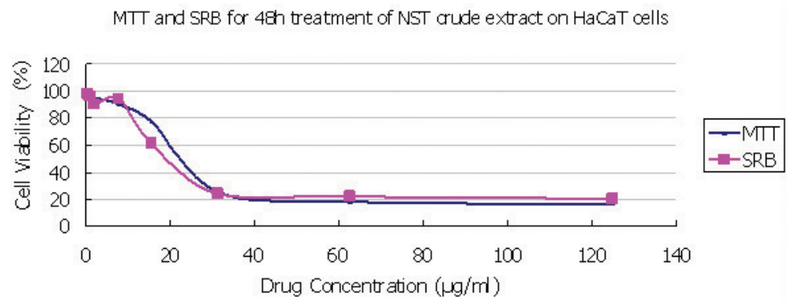

Figure 1: Cell viability curve of HaCaT cells treated with serial diluting concentrations of the NST crude extract for 48h. Regardless of the proliferation assay used, the viability curve remains largely in the same shape. SRB and MTT were able to confirm each other's result.

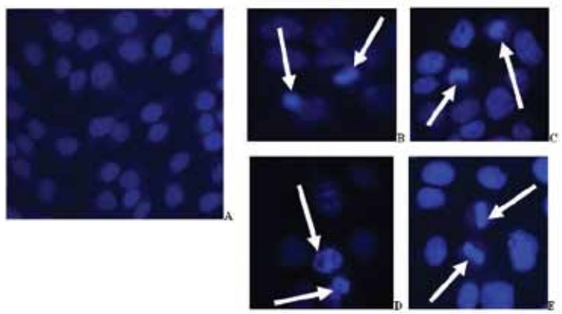

Figure 2: Effect of NST crude extract on HaCaT cellular morphology as examined by phase contrast microscopy after staining with Hoechst 33342. A) Normal HaCaT cells with no treatment used as control. **B, C)** HaCaT cells treated with NST crude extract at 30µg/ml for 48h. **D, E)** HaCaT cells treated with NST crude extract at 45µg/ml for 48h. Arrows are directed at cells that show chromatin condensation and/or fragmentation. Pictures displayed here in B, C, D, and E are enlarged three times to the original size, and the Control picture used in A is at the original size without any changes in scale.

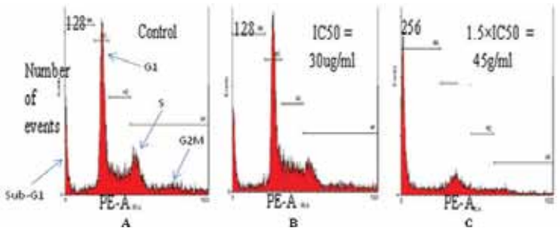

Figure 3. Summary of flow cytometric data with PI staining on NST treated HaCaT cells. **A)** Medium control. **B)** Cells treated with IC50 for 48H. **C)** Cells treated with 1.5IC50 for 48h. Peaks found in PI flow cytometry represent the corresponding amounts of cells in different states of cell cycle. Here, major differences are observed int eh sub-G1 peaks in A, B and C which are indicative of cell cycle arrest.

extract of NST on HaCaT keratinocytes, and suggested that 48h treatments to be the most effective. All following experiments' incubation time with NST was set to be 48h, and the 48h IC50 value was to be used at the approximation of 30µg/mL (Figure 1). This section had a sample size of four. With an established IC50, the potency of NST was confirmed and granted further investigation of its mechanism.

Induction of Change in Cellular Morphology Due to Treatment of NST Crude Extract by Hoechst Staining

Hoechst 33342 staining was employed to image the cellular morphological changes in cells treated with NST for 48h. After Hoechst 33342 staining, normal cell bodies show a pale blue colour under fluorescent microscopy, and the nuclei are much more conspicuous in a darker blue colour. This was observed in the control (Figure 2A). In the two treated conditions shown on the right (Figure 2 B, C, D, and E) the cells exhibited a rough cellular outline, and more importantly, their DNA chromatin appeared brighter and more concentrated. This experiment was repeated once. These images were an effective indicator suggesting that the NST crude extract could have induced apoptosis in the HaCaT cell line.

3.3 Flow cytometric analysis of HaCaT cells by PI flow cytometry

PI flow cytometry aimed to determine the amount of live cells remaining through the stoichiometric detection of DNA bound by PI, using fluorescence techniques. The flow cytometric data on PI-stained HaCaT cells are shown in Figure 3. As shown in Figure 3 and Table 2, the NST crude extract induced a substantial peak (49.4%) at the sub-G1 phase when 45µg/mL NST was applied, as compared to 13.3% at 30µg/mL, and 10.9% in the control. According to Table 2, this heightened increase in the number of cells detected in the 45µg/mL group was partially attributed to the decrease in the percentage of viable cells, represented by the G1 phase – with 35.9% in Control, and only 22.0% in 45µg/mL. Besides, the G1, S and G2M peaks of the 45µg/mL treatment are all sizeably lower than those of the control. This experiment was repeated twice. Flow cytometry by PI was the first piece of evidence towards revealing the mechanism of the crude extract of NST.

3.4 Flow cytometric analysis of HaCaT cells by Annexin V –PI (AV-PI) staining

Flow cytometry by AV-PI was used to detect apoptosis at an early stage through the detection of externalization of phosphatidylserine due to cell membrane alterations. As shown in Figure 4, the crude extract of NST exhibited its anti-proliferative effect and induced apoptosis in a dose-dependent manner. The NST crude extract considerably increased the percentage of apoptotic cells to 60.1% in 45µg/mL compared to 6.0% in the control. In Figure 4 A, cells in the control group were divided into three distinct categories – viable, apoptotic and necrotic. Using these categories, a momentous shift of cells from the viable to the apoptotic quadrant can be observed as the drug concentration is increased from 30 to 45µg/mL (Figure 4 B, C). This experiment was repeated three times.

3.5 Flow cytometric analysis of HaCaT cells by JC-1staining

JC-1 staining flow cytometry aimed to identify apoptosis by detecting JC-1 aggregates due to changes in cell MMP and confirm the results obtained in sections 3.3 and 3.4. The JC-1 analysis displayed a much higher percentage of cells with low MMP at 30µg/mL(57.2%) compared to only 6.7% in the control (Figure 5 A, B). This shows a strong likelihood of apoptosis among those cells. This experiment was performed once.

Discussion

Psoriasis is widely acknowledged as an immune-mediated inflammatory skin disorder. In treating this chronic disease, much of the field's focus has been on attempting to re-establish the homeostatic balance in the cell through suppressing hyperproliferation and abnormal differentiation of keratinocytes. Interestingly, in contrast to cancers that are accompanied by unrestricted cell growth, psoriatic skins have a reduced rate of apoptosis that causes the formation of a plaque (Chaturvedi et al., 2004).

For centuries, plant extracts and natural compounds purified from plants have been used for the treatment of a variety of inflammation-related diseases. In TCM, complex mixtures of herbs and herbal extracts are prescribed for the treatment of many diseases such as cancer and psoriasis. According to our data, it can be deduced that *C. orbiculatus* has potential anti-proliferative and apoptogenic effects. In fact, NST extracts have been proven to have inhibitory effects on the activation of the nuclear factor kappa-B (NF-kB) (Jin et al., 2002). The transcription factor NF-kB is essential for cellular processes including inflammation, immunity, cell proliferation and apoptosis; and many inflammatory diseases (including cancer, psoriasis, diabetes, asthma, osteoporosis, etc.) can be attributed to NF-kB activation (Baldwin, 2001). Specifically, NF-kB regulates the transcription of various inflammatory cytokines, cell adhesion molecules, growth factor receptors, etc. (Baeuerle and Henkel, 1994). Recently, NF-kB was proven to be largely over-expressed in psoriatic skin in comparison to normal skin (Abdou and Hanout, 2008). As the activation of NF-kB is involved in the expression of downstream genes that code for cytokines, adhesion molecules and inflammatory enzymes, drugs that target NF-kB may very well be effective against inflammatory diseases, including

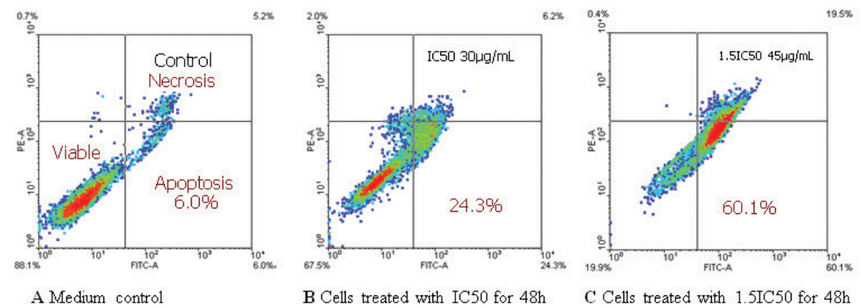

Figure 4. Flow cytometric analysis of HaCaT cell distribution using AV-PI staining. Percentage of cells for each quadrant is located in the corresponding corner. Note the intense shift into the apoptotic region observed in C as indicated by the red color, this is a piece of powerful evidence that suggests the crude extract of NST induces apoptosis in cells.

Table 1: Effect of anti-proliferation of NST crude extract by MTT and SRB assays. Three trials were performed and averaged to generate the data listed. Data were treated using software provided by Nagoya City University.

	IC50 (µg/ml)		
Assay type	24 h	48h	72h
MTT	68.2	29.4	38.8
SRB	73.6	28.8	41.9

Table 2: Summary of PI flow cytometric data on NST treated HaCaT cells, listed by phase of cycle.

	Control	IC50=30µg/ml	1.5*IC50=45µg/ml
Sub-G1	10.87%	13.29%	49.45%
G1	35.87	40.20	22.02
S	16.16	18.87	6.81
G2M	37.31	28.87	21.86

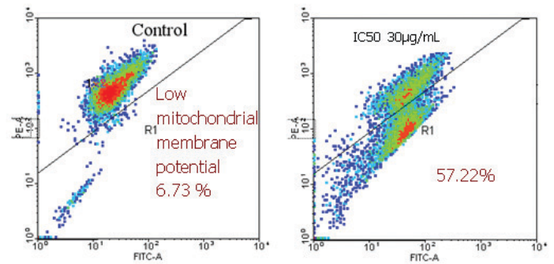

Figure 5: Flow cytometric analysis by JC-1 staining. A significant shift was detected in the treatment of 30µg/mL as 57.2% of cells exhibited low mitochondrial membrane potential.

hence easily detected by Annexin-V PI staining. More importantly, there is a loss of electrochemical gradient across the mitochondrial membrane, while vesicles simultaneously form and cytochrome c leaks into the cytoplasm through pores (Duval et al., 2008), as detected by JC-1.

Since no single assay could unequivocally establish the presence of apoptosis due to the application of NST crude extract, several assays and a dye were used. Hoechst 33342 staining was able to show nuclei condensation, the first line of evidence proving that apoptosis indeed took place by the induction of NST extracts. Cell cycle analysis then displayed a critical increase induced by NST in the sub-G1 peak (**Figure 3**), while the viable population of cells sharply decreased. With each peak representing the amount of cells in each corresponding stage of cell cycle, usually a large sub-G1 peak is indicative of cell cycle arrest. However, having a major sub-G1 peak in a cell cycle analysis cannot rule out possibilities other than apoptosis because sub-G1 can also represent nuclear fragments, clumps of chromosomes, altered chromatin structure, etc (Riccardi and Nicoletti, 2006). Nonetheless, Annexin-V PI exhibited a strong correlation between the percentage of apoptotic cells and the concentration of NST applied, indicating that NST is dose-dependent (Figure 4). In addition, JC-1 also showed a major increase in the number of cells that lost their MMP after NST treatment (Figure 5).

Moreover, JC-1 flow cytometry could provide more specific information on the particular pathway of apoptosis (mitochondrial

or extrinsic) due to its own detection mechanism. JC-1 ratio of green to red (non-apoptotic to apoptotic) fluorescence is dependent only on MMP and not any other factors (Green and Reed, 1998). The formation of JC1-aggregates in healthy cells causes a change in fluorescence of JC-1 and distinguishes apoptotic cells (only monomeric JC-1) from the rest (Green and Reed, 1998). JC-1 can only detect apoptosis through the mitochondrial pathway, which could be the only approach in NST induced apoptosis; the death receptor extrinsic pathway also found in apoptosis may not be initiated by NST.

Further experiments are needed to determine the specific pathway. Protein analysis could be used to qualitatively determine the expression level of cytochrome c, caspase 3, and/or a potential death receptor to provide us with more insight (Tse et al., 2008). If only cytochrome c and caspase 3 are detected, then it can corroborate that the NST crude extract causes apoptosis only through the mitochondrial-dependent pathway, not the external pathway of apoptosis.

As part of our effort to develop anti-psoriatic treatment from TCM remedies, the successful identification of the crude extract of NST as a potent anti-proliferative and apoptogenic inducer helps explain the continued use of this Chinese folk medicine, making it a hopeful candidate for further investigation and development for psoriasis treatment. This project was the first attempt to scientifically determine the mechanism underlying the effect of crude NST extract *in vitro* in HaCaT cells. More sophisticated experiments need be employed for characterizing a more detailed mechanism and must be carried out *in vivo* in relevant animal models before we can undeniably claim that crude extract of NST is suitable for use in psoriasis treatment.

Acknowledgement

This study was supported by the summer exchange program between the Chinese University of Hong Kong and the University of Toronto.

References

Abdou, A.G., and Hanout, H.M. *Evaluation of survivin and NF-kappaB in psoriasis, an immunohistochemical study*. Journal of *Cutaneous Pathology*, 2008. ***35***, 445-451.

Baeuerle, P.A., and Henkel, T. *Function and activation of NF-kappa B in the immune system*. *Annual* Review of Immunology, 1994. ***12***, 141-179.

Baldwin, A.S., Jr. *Series introduction: the transcription factor NF-kappaB and human disease*. The Journal of Clinical Investigation, 2001. ***107***, 3-6.

Ben-Arye, E., Ziv, M., Frenkel, M., Lavi, I., and Rosenman, D. *Complementary medicine and psoriasis: linking the patient's outlook with evidence-based medicine*. Dermatology, 2003. ***207***, 302-307.

Callahan, M.K., Williamson, P., and Schlegel, R.A. *Surface expression of phosphatidylserine on macrophages is required for phagocytosis of apoptotic thymocytes*. *Cell Death* & Differentiation, 2000. ***7***, 645-653.

Chaturvedi, V., Qin, J.Z., Stennett, L., Choubey, D., and Nickoloff, B.J. *Resistance to UV-induced apoptosis in human keratinocytes during accelerated senescence is associated with functional inactivation of p53*. *Journal of* Cellular *Physiology*, 2004. ***198***, 100-109.

Cossarizza, A., Baccarani-Contri, M., Kalashnikova, G., and Franceschi, C. *A new method for the cytofluorimetric analysis of mitochondrial membrane potential using the J-aggregate forming lipophilic cation 5,5′,6,6′-tetrachloro-1,1′,3,3′-tetraethylbenzimidazolcarbocyanine iodide (JC-1)*. Biochemical and Biophysical Research Communications, 1993. ***197***, 40-45.

De Arruda, L.H., and De Moraes, A.P. *The impact of psoriasis on quality of life*. *British Journal* of *Dermatology*, 2001. *Suppl 144,* ***58***, 33-36.

Dong, C., Li, Q., Lyu, S.C., Krensky, A.M., and Clayberger, C. *A novel apoptosis pathwayactivated by the carboxyl terminus of p21*. Blood, 2005. ***105***, 1187-1194.

Duval, R.E., Harmand, P.O., Jayat-Vignoles, C., Cook-Moreau, J., Pinon, A., Delage, C., and Simon, A. *Differential involvement of mitochondria during ursolic acid-induced apoptotic process in HaCaT and M4Beu cells*. *Oncology* Reports, 2008. ***19***, 145-149.

Ernst, J.D., Yang, L., Rosales, J.L., and Broaddus, V.C. *Preparation and characterization of an endogenously fluorescent annexin for detection of apoptotic cells*. Analytical Biochemistry, 1998. ***260***, 18-23.

Feng, W.S., Hao, Z.Y., and Zheng, X.K. *Chemical Constituents of Genus Celastrus.* Chinese Journal of New Drugs, 2007. ***42***, 16.

George, S.E., Anderson, R.J., Cunningham, A., Donaldson, M., and Groundwater, P.W. *Evaluation of a range of anti-proliferative assays for the preclinical screening of anti-psoriatic drugs: a comparison of colorimetric and fluorimetric assays with the thymidine incorporation assay*. *Assay* and *Drug Development Technologies*, 2010. ***8***, 389-400.

Green, D.R., and Reed, J.C. *Mitochondria and apoptosis*. Science, 1998 ***281***, 1309-1312.

Hengartner, M.O. *Apoptosis and the shape of death*. Developmental Genetics, 1997. ***21***, 245-248.

Jin, H.Z., Hwang, B.Y., Kim, H.S., Lee, J.H., Kim, Y.H., and Lee, J.J. *Anti-inflammatory constituents of Celastrus orbiculatus inhibit the NF-kappaB activation and NO production*. *Journal* of Natural Products, 2002. ***65***, 89-91.

Kastelan, M., Prpic-Massari, L., and Brajac, I. *Apoptosis in psoriasis*. *Acta Dermatovenerologica Croatica*, 2009. ***17***, 182-186.

Koo, J., and Arain, S. *Traditional Chinese medicine for the treatment ofdermatologic disorders*. Archives of *Dermatology*, 1998. ***134***, 1388-1393.

Li, Q., Kobayashi, M., and Kawada, T. *Ziram induces apoptosis and necrosis in human immune cells*. Archives of *Toxicology*, 2010.

Lin, Z.X., Hoult, J.R., and Raman, A. *Sulphorhodamine B assay for measuring proliferation of a pigmented melanocyte cell line and its application to the evaluation of crude drugs used in the treatment of vitiligo*. Journal of *Ethnopharmacology*, 1999. ***66***, 141-150.

Pol, A., Bergers, M., and Schalkwijk, J. *Comparison of antiproliferative effects of experimental and established antipsoriatic drugs on human keratinocytes, using a simple 96-well-plate assay*. *In Vitro Cellular* & Developmental *Biology - Animal*, 2003. ***39***, 36-42.

Rashmi, R., Rao, K.S., and Basavaraj, K.H. *A comprehensive review of biomarkers in psoriasis*. *Clinical* and Experimental *Dermatology*, 2009. ***34***, 658-663.

Reed, C.J. *Apoptosis and cancer: strategies for integrating programmed cell death*. Seminars in *Hematology*, 2000. ***37***, 9-16.

Riccardi, C., and Nicoletti, I. *Analysis of apoptosis by propidium iodide staining and flow cytometry*. Nature Protocols, 2006. ***1***, 1458-1461.

Salvioli, S., Ardizzoni, A., Franceschi, C., and Cossarizza, A. *JC-1, but not DiOC6(3) or rhodamine 123, is a reliable fluorescent probe to assess delta psi changes in intact cells: implications for studies on mitochondrial functionality during apoptosis*. *FEBS Letters*, 1997. ***411***, 77-82.

Skehan, P., Storeng, R., Scudiero, D., Monks, A., McMahon, J., Vistica, D., Warren, J.T., Bokesch, H., Kenney, S., and Boyd, M.R. *New colorimetric cytotoxicity assay for anticancer-drug screening*. Journal of *National Cancer Institute*, 1990. ***82***, 1107-1112.

Teraki, Y., and Shiohara, T. *Apoptosis and the skin*. *European* Journal of Dermatology, 1999. ***9***, 413-425; quiz 426.

Tse, T.W. *Use of common Chinese herbs in the treatment of psoriasis*. *Clinical* and Experimental *Dermatology*, 2003. ***28***, 469-475.

Tse, W.P.,Che, C.T., Liu, K., and Lin, Z.X. Evaluation of the anti-proliferative properties of selected psoriasis-treating Chinese medicines on cultured HaCaT cells. Journal of Ethnopharmacology, 2006. ***108***, 133-141.

Tse, W.P., Cheng, C.H., Che, C.T., and Lin, Z.X. *Arsenic trioxide, arsenic pentoxide, and arsenic iodide inhibit human keratinocyte proliferation through the induction of apoptosis*. Journal of Pharmacology and Experimental Therapeutics, 2008. ***326***, 388-394.

Yamamoto, Y., and Gaynor, R.B. *Role of the NF-kappaB pathway in the pathogenesis of human disease states*. *Current Molecular Medicine*, 2001. ***1***, 287-296.

Zeeli, T., Langberg, M., Rotem, C., David, M., Koren, R., and Ravid, A. *Vitamin D inhibits captopril-induced cell detachment and apoptosis in keratinocytes*. *British Journal* of *Dermatology*, 2010. ***164***, 62-7

Zhu, Y., Miao, Z., Ding, J.,and Zhao, W. Cytotoxic dihydroagarofuranoid sesquiterpenes from the seeds of Celastrus orbiculatus. Journal of Natural Products, 2008. 71, 1005-1010.

Biochemistry

Graduate Studies at the University of Toronto

The Department of Biochemistry offers M.Sc. and Ph.D. degrees with cutting-edge research opportunities in the areas of structural, molecular, and cellular biology.

Biomolecular Structure & Function
Protein Folding
Proteomics and Bioinformatics
Membranes and Transport

Molecular and Cell Biology
Gene Expression and Development
Signal Transduction and Regulation
Molecular Medicine

The Department of Biochemistry at the University of Toronto is a modern, research-intensive enterprise within the Faculty of Medicine. Founded in 1907-08, we are the second-oldest Department of Biochemistry in the world. The Department boasts a large faculty conducting research at the downtown campus of the University of Toronto in the Medical Sciences, McMurrich, and Donnelly CCBR buildings, as well as the University of Toronto Scarborough campus. Research facilities are also located at MaRS, the Leslie Dan Pharmacy Building, the Banting and Best Department of Medical Research, the Hospital for Sick Children, Princess Margaret, and Mt. Sinai Hospitals. The laboratories in these facilities feature state of the art X-ray crystallography and NMR equipment, confocal and electron microscopes, high-throughput instrumentation, mass spectrometers, and other modern biophysical apparatus. Over the past five years, more than one thousand research articles have been published by members of the Department of Biochemistry.

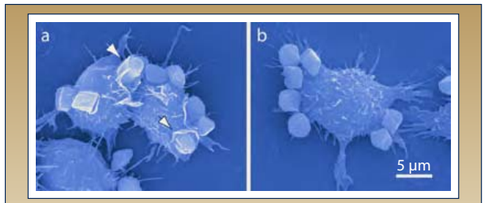

Macrophage cells extend lamellapodia (arrows) around opsonized red blood cells during phagocytosis (a). Inhibition of the coronin1 protein blocks lamellapodia formation but not binding (b). Yan M, Collins RF, Grinstein S, Trimble WS. (2005). *Mol Biol Cell*. **16**(7):3077-87.

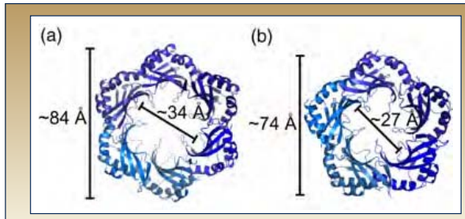

Crystal structure of the mutant gpU D75A tail terminator protein hexamer from bacteriophage λ (a) and wild-type gpU pentamer (b). Pell LG, Liu A, Edmonds L, Donaldson LW, Howell PL, Davidson AR. (2009) *J Mol Biol*. **389**(5):938-51.

Financial Support:

All graduate students are guaranteed an annual stipend of $24,500/year for M.Sc. candidates and $25,500/year for Ph.D. candidates. Outstanding students with external funding receive a $3,000 bonus. Opportunities for teaching assistantships are also available within the Department, providing additional funding.

Special events include:

Departmental Open House
Connell Lectures
Sports Teams -- Softball and Volleyball
Schachter Lectures
Golf Day and Ski Day
New Student Welcome

BGSU

The Biochemistry Graduate Student Union (BGSU) acts as a liaison between studnets and the Department of Biochemistry, improving the overall student experience while organizing academic and social events.

http://www.biochemistry.utoronto.ca

JULS INTERVIEWS

Dr. Nicholas White

Dr. Nicholas J. White completed medical school at the University of London and currently holds faculty appointments at the University of Oxford and Mahidol University in Bangkok, Thailand. He is a Professor of Tropical Medicine with a particular research interest in malaria. He has published hundreds of peer-reviewed articles and is actively involved in global health, serving in both the Wellcome Trust and the World Health Organization.

Interview conducted by: Jong Park and Nancy Song

J: What led you to pursue the study of tropical diseases?

N: I think the fact that I grew up in many different countries was influential. I grew up in Malta, in Singapore, in Cyprus as well as in the UK. Then as a medical student, I really wanted to go to Asia. The day I qualified, literally the day I qualified, I got on an Iraqi airline's jet via Bangkok/Baghdad and went to work in Nepal, strongly against the advice of the Dean of the medical school. That was fascinating, difficult, I was on my own, and I realized that I wasn't very much use clinically. Although I was the only one there so I was probably better than nothing. Made me sort of realize that I needed to get properly trained. And then luck was an important contributor because it just so happened that I went to work at Oxford where my boss, Sir David Weatherall, was very interested in thalassemias, and had a very strong emotional as well as intellectual association with tropical diseases. And so the opportunity arose to come and work in Thailand. Which I took, not really having great plans as to what would happen next. I never have had any clear plans as to what was to happen next.

J: So when you went to Thailand, you decided to stay there…

N: No, I never decided to stay there, I just decided never to come back.

J: Do you like it there?

N: Obviously yes! I do like it there, I like Thai people. You're always a foreigner no matter how well you speak the language or a part of the institution, you're always a foreigner and it's quite interesting to be a foreigner. I mean, it's interesting for you, you're Asian but you're actually in a multi-cultural society, and I don't suspect you 'feel' anything. You don't feel particularly different do you?

J: Not generally.

N: No, because there are so many other people of your origin here. But it helps you feel what it's like being a minority group in a country where the majority mainly like you but some don't. Thailand's a very welcoming country, but I'm a foreigner and it's not always been easy, but in our particular field of tropical medicine and international health, the future is multinational, multicultural. I like the fact that there is a whole heap of nationalities in our research group in Thailand, but we're actually part of a Thai institution and a Thai university.

J: You have lived in a foreign country and have travelled extensively. Do you think you've gained some socioeconomic awareness that has influenced your work?

N: Yes, you can't really live in another country and be part of its system and apparatus without having a lot of empathy and understanding, a gradual understanding for the culture. I mean, I happen to love people in Southeast Asia. I happen to think they're very interesting, but they're very different. Particularly in the West, we underestimate the complexity of Asian cultures. We think that a bland façade hides nothing, but it hides everything, and it takes some time to learn that. It takes time to learn some tonal languages, time to gradually understand and appreciate things. I've been there for more than half my life now. I guess I'm more of a foreigner in my own country of birth, Britain, than I am in Thailand.

J: Do you visit Britain often?

N: Yes, I do. I spend about two months every year working in the wards as an attending physician in Oxford, just doing internal, general medicine, which I really like. It's very different from what I normally do. The diseases are very different, everything's different. I like that, I enjoy that. But I consider my home to be Thailand.

J: You've advocated the use of ACTs to treat malaria and it has been going on for a while. You've mentioned in your talk that there's recently been an emergence of resistance to artemisinins in western Cambodia. How do you think the strategy should be set up to target this problem?

> *"I was the only one there so I was probably better than nothing. Made me sort of realize that I needed to get properly trained."*

N: That's a good question. I do not feel we're doing enough, putting it bluntly. And I think we could deal with this problem. We could get rid of it. But I'm not sure if we will because we just don't have the appetite for radical actions. It's a very slow process to build up sufficient impetus politically, socially, to do something… tough. You remember that you and I were worried about bird flu a few years ago, sweeping across the world and killing maybe a third of the world population or something horrendous. But then we've sort of forgotten that a bit even though the risks haven't changed. And every so often we become particularly concerned about you know, bio terrorism, there's a threat for this or whatever. When the problem is a long way away, we just don't feel it in the same way. It really depends on what it is. If it isn't going to affect you, your parents or your children, then you are able to dissociate from it. Artemisinin resistance is a problem that could sweep across the world. I hope it doesn't, and kill millions of children. Now if you're Canadian and if I was to say to you, "well tomorrow we're going to kill every child in Canada", there would be quite some response to that. Well those are the sort of numbers that this could kill. So I think, I feel, our response to it is inappropriately muted, and therefore unsatisfactory. Now it may well be that this doesn't mature into something awful, I really hope so. But, if it did, we could have prevented it. Now, if you could have prevented killing every child in Canada…wow. Putting that rather dramatic perspective into it, which I don't think is an illegitimate one, I think it fits perfectlyI mean these are kids in Africa who will die. Are we really doing everything we possibly can? We're not. So I'm unhappy about that.

J: So what do you think we could do to possibly increase more awareness or the sense of urgency, especially given in the past, how developing a resistance to other drugs has really determined the whole fight against malaria?

N: Well I guess the first thing to do is to get the whole world aware of it. At the moment, it's being dealt with at a local or regional basis. And quite honestly, why should Cambodia or Thailand do painful things locally to save everybody else? Where's the incentive? So I think you need to get the South American, African and Indian people who are representing their children saying, "Look, you could actually really damage us", you know a bit like a radioactivity leak or oil leak or something. That leak in the gulf caught people's attention when the oil started to lap on the shores of the United States. Well, things happened. I think we just need to get it at that level. It has to be at a very high level politically. Now, high level politicians are, for some unknown reason, willing at the moment to be interested in malaria and to talk about it. We've got the Melinda and Bill Gates Foundation pledging their entire 40-50 years of monies towards elimination. Well, this will screw it up. There's no doubt if artemisinin resistance spreads across the world, it would screw it up. So, there needs to be a really high level engagement. It needs to be at a country leader level, the Minister of Health and then down to those who would actually have to do the dirty business. But it's not fair to ask a local malaria control manager to ask the prime minister to get the army out, the students out, do things like that, which is unusual. I mean, that's a big political risk for an individual. You know, give lots of drugs to people who aren't ill, and have some side effects, that's nasty business. But sometimes you have to do nasty things. I think the cancer analogy is a good one. If you're going to cut out a cancer, then that's a big thing and you have to know, is it worth it? Is it the right thing to do? Well, you know as well as I do that some of these cancers, you can cut them out, but it's tough and you may have to do a lot of nasty chemotherapy, and you think "well, am I doing the right thing here?" and if it's spread to the lung or liver you don't do that do you? You know that right? So, that's the same.

J: Considering the issue of eradication, you present the really interesting idea of doing a mass treatment to effectively wipe out malaria.

N: In that particular area. The idea here is an interesting one. You're not trying to eliminate malaria forever. You're just trying to get rid of all the resistant parasites. It might come back. You don't have to sustain it. You just have to get rid of it once.

> *"You can't really live in another country and be part of its system and apparatus without having a lot of empathy and understanding, a gradual understanding for the culture."*

J: You've travelled extensively and you've worked for many years. A lot of your ground breaking research has been widely acknowledged and acclaimed, what does this award, the Canada Gairdner Global Health Award mean to you?

N: Well, quite a lot actually. It's nice to be recognized. You know you do stuff because you think it's the right thing to do, but you also have the selfish aspect of hoping that what you're producing is good, and this is a very prestigious and highly respected award so it's sort of the thing that my mum would be happy about. I don't mean that facetiously, I really do. I'm very grateful for it. It also recognizes everybody that did the work because it wasn't just me, at all. I'm just a bit of it. And I like the fact that this is Canadian because I consider Canada as one of the really good countries in international health. Canada is very concerned about world issues. They tend to make sensible decisions about international affairs.

And I really like the multi-cultural aspects of Canada. So it's nice that it comes from here in a sense. I think that it's an honour. Because it's also the Canada Gairdner Foundation, so the Canadian government and all of Canada are somehow reflected in this prize. And for purely selfish reasons, it's really nice to come and meet people like you, go to nice places and drink some nice beer and have some interesting conversations, which is not what I normally do (but I do drink quite a lot of beer). You know it's just different. It's a prize, it really is a prize.

JULS INTERVIEWS

Dr. Peter J. Ratcliffe

Dr. Peter J. Ratcliffe completed his medical degree in 1978 at Cambridge University and St. Bartholomew's Hospital in London. He is currently the Head of the Department of Clinical Medicine at Oxford University. Dr. Ratcliffe's original research interests focused on the physiology of renal oxygenation and its implications for renal injury in shock. As his research interests evolved, he founded his laboratory in 1989 at Oxford in order to study the detection and signaling mechanisms used by cells in response to hypoxia, or low oxygen levels. Dr. Ratcliffe's laboratory determined that all animals share a fundamental oxygen sensing pathway and defined the oxygen sensing and signalling pathways which link oxygen availability with hypoxia inducible factor (HIF), an essential transcription factor. Hypoxia is an important element in a variety of human diseases including cancer, heart disease, and stroke. Dr. Ratcliffe endeavors to elucidate ways in which oxygen sensing pathways may be manipulated for the treatment of various human diseases.

Interview conducted by: Ana Komparic and Tina Binesh Marvasti

TB: You seem to have had an interest in the field of oxygen sensing pathways since you were a medical student in 1978 examining the physiology of renal oxygenation and its implications for renal injury. What first made you interested in studying the mechanisms of oxygen regulation?

PJR: I trained as a kidney specialist and my first research ambition was to try to understand why the kidney is susceptible to injury in shock. If you have low blood pressure and low circulation, the kidney is often injured, and that was my initial attempt was to work out why that might be. The kidney has very unusual circulation and I believed, along with others, that it might be an aspect of that circulation that made it susceptible in that way. We never solved that problem, but it did give me an interest in kidney circulation, which led to an interest in why it was that the kidney was the organ responsible for oxygen-regulated EPO production. I thought I would be able to puzzle out some interesting aspect of the kidney circulation that underlay that. As you've heard, in fact, we didn't solve that problem either, but we did come by the evidence that this was a general sensing system for oxygen in all animal cells. That changed our entire research direction and I guess that's why I'm here today.

AK: Would you characterize this change in interests as somewhat of an anomaly in the research community, or do you think such changes in research direction happen rather often?

PJR: I think it happens all the time. If I have any advice for young people embarking on a scientific career, it is that you should pick a problem that you think is soluble. Do not worry at the outset whether it is perceived to be an important problem or not. The importance will generally become clear after the solution and that's what happened in this case. That is by no means an anomaly; it is almost the norm in science.

> *"It's far easier to collaborate than to learn everything from scratch."*

TB: You have received many prestigious awards for your outstanding research on development of new treatments for cancer and heart disease. What do you see as the greatest challenge that is ahead for you? What do you see the future of research in these fields to be like?

PJR: A really great challenge now is can we make a drug or can the research community make a drug that would adapt this signaling system to promote repair or to improve the outcome of the many, many human diseases characterized by hypoxia? That, as I said in the lecture, remains a challenge because of the massive number of processes that are regulated. How to achieve the specific, safe upregulation of the system in precisely the way that will be medically useful is going to be an interesting challenge for the future. We're also interested in moving further through biology to try to understand whether this type of signaling has other roles in biology that are connected.

AK: Having both a medical and research background and being both an active clinician and researcher, what skills have you gained from being immersed in both communities, and how has your work benefited from this relationship?

PJR: In some ways they are quite different, although in some ways they are quite similar, both medicine and laboratory practice. Each of them is trying to work out from often limited evidence, what is going on, what is the patient's diagnosis, what is the biological system that we're studying. I do draw one important distinction, which is interesting. In the clinic, if we don't know what to do with a patient, a great rule is don't do anything— wait and see. That's often a successful way of conducting clinical practices. In the lab it's absolutely fatal. In the lab if you don't know what to do, you must do something. You must do an experiment. That's because of course, in a clinic the experiment is evolving before your eyes, whereas in the lab nothing will happen unless you make it happen. So, there are interfaces, but also some striking differences.

TB: As a medical practitioner and a research scientist, what advice would you have for undergraduate students willing to undertake a career in medicine or research, or both? What personal qualities should they develop?

PJR: Confidence, persistence. I cannot really tell you why I got into research, I can't tell you why I persisted, but I find that it's addictive. The high of occasional positive results is really reinforcing. However, as I indicated in the talk, many, many things are not positive. This is because of the complexity of biology. You have to be robust; you have to have the confidence to address and to keep on addressing. There are many, many reasons why research is not done, which you have to consider. People don't do it because they don't think it's important, because they don't think it'll be soluble, because they predict some other group will do it before them, that it doesn't matter. All of these are illegitimate reasons if you are going to succeed, so you have to have the confidence to go through that and do it, even if you think it is going to be difficult, or impossible, or unimportant, or done by others. Essentially, I think one of the qualities is confidence. I don't think it's necessary to be extraordinarily intelligent in biology, neither necessary nor sufficient, for many of the concepts are quite simple.

> *"In the clinic, if we don't know what to do with a patient, a great rule is don't do anything—wait and see. That's often a successful way of conducting clinical practices. In the lab it's absolutely fatal."*

AK: As the 2010 Canadian Gairdner International Award Recipient, how would you characterize the role that the international research community has played in your research and career, and what value do you ascribe to international research collaborations?

PJR: Great value. We've enjoyed terrific collaborations in all sorts of things. In part, that's because that the journey that I've shown you has involved a great many different techniques, as you may have seen. It's far easier to collaborate than to learn everything from scratch. So international collaboration, as you saw with the *C. elegans* worm community, being able to post those worms to me or to do the analysis across the globe is terrific.

From molecules to medicine and beyond...
Graduate Studies Program in Chemical Biology
Multidisciplinary research in a highly collaborative environment
- Chemical genomics
- Biomolecular interactions
- Small molecule synthesis and screening
- Biomolecular structure, dynamics and function

McMaster University
chembio.mcmaster.ca

JULS INTERVIEWS

Dr. Gregg L. Semenza

Dr. Gregg L. Semenza received his M.D. and Ph.D. degrees at the University of Pennsylvania. He did his residency in paediatrics at Duke University and then a postdoctoral fellowship in medical genetics at Johns Hopkins. He has stayed on as a faculty member at Hopkins since 1990, focusing his research on the cellular and genetic processes of oxygen regulation. In addition to being the C. Michael Armstrong Professor of Paediatrics at Hopkins, he is a member of the McKusick-Nathans Institute of Genetic Medicine and the director of the vascular program at the Johns Hopkins Institute for Cell Engineering.

Interview conducted by: Richard Cheng and Siyang Li

J: You were a recipient of the 2010 Canada Gairdner International award. Tell us about your path to becoming a scientist. What were your primary motivations and how did your education and mentors shape your career path?

S: Like many people, I was inspired by a biology teacher in high school: her name was Rose Nelson. She really inspired my interest in biology. She also had a PhD, so she was trained in research. She was able to show us how exciting research was and the discovery of new scientific knowledge. As a result of that experience in high school, my first interest was in biology when I went to college, and I was particularly interested in genetics. I did research in a genetics laboratory and I became more interested in medical research. As a result of that, I wanted to do both research and see patients. In order to do that I went to University of Pennsylvania for an MD and PhD.

> *"Like many people, I was inspired by a biology teacher in high school."*

J: How was that experience?

S: As I did my research, I started over twice. I was very fortunate to be able to do that. I was interested in doing genetics research and decided to do my medical training in paediatrics, so I went to Duke University. And then finally, went to Johns Hopkins for my specialization in medical genetics. I started working on my research project there, and I've been there ever since. I've stayed there for 26 years, I was very fortunate to have mentors who helped me set up my research project, helped me get grants to fund the project, and helped me to get my scientific papers published.

J: You said that you wanted to do research and see patients at the same time. Are you still a clinician, or are you mostly doing research now?

S: For about 20 years, I was a medical genetics MD, which means that I saw patients in clinics every week, and one month in every year, I was in charge of the whole genetics service in the hospital. Until about 7 years ago when I stopped. And at that time, I started a new program at the Johns Hopkins Institute for Cell Engineering, focusing on stimulating blood vessel formation as I mentioned in my lecture. And at that time, I stopped seeing patients and just really focused on research, teaching graduate students and other activities, like being the editor for a journal.

J: Speaking of that, you are the editor in chief for the Journal of Molecular Medicine. You clearly influence research dissemination to the general public and the scientific community. What are some of the challenges and how do you handle them?

S: Of course we want to get high quality papers in the journal. One of the ways that I try to influence that is by recruiting people who are very good to serve on the editorial board along with me. And we try to publish papers that will review an important area in science. For example, we will get someone who is an expert in those fields to write a review article, and that will attract people to the journal, which will raise interest in the journal. And people will see that there's good work being published by this journal, it will attract their work, and it becomes a mutually reinforcing thing. So that is a goal, it takes a while to build a reputation. It's a gradual process. However, this journal has a very long history, it's a journal started in Germany, and published a lot of very classical research. For example, research by someone like Robert Koch, who was one of the original discoverers of bacteria and infection. So, we had very classic papers and it has been reborn as a journal on molecular medicine. It is still kind of European focused, but now we're trying to make it more international.

J: For how long have you been the editor in chief?

S: It's been 4 or 5 years now.

J: How did you feel when you were awarded the Gairdner award and were you surprised?

S: It was a very pleasant surprise. I remember we were awarded in January and the announcement wasn't until April. So, we had to keep it a secret for a very long time. And of course, I wanted to tell people, but we were sworn to secrecy.

J: JULS has a large reader base consisting of mostly undergraduates. What would you say to students aspiring to become future scientists?

S: I would tell them that it's a really wonderful field, because you have an incredible amount of freedom and independence to follow all of your ideas and be creative. And there aren't many jobs like that, where you would get those opportunities. It's a very fantastic career because of that, and most of us feel very fortunate to get paid to do this because it's something that we enjoy doing so much. Many people have jobs to support their families, and it may not be the most enjoyable job for them, but most people who are in science usually have to be forced to retire!

> *"Many people have jobs to support their families, and it may not be the most enjoyable job for them, but most people who are in science usually have to be forced to retire!"*

University of Toronto's
Gerstein Science Information Centre
THE LARGEST ACADEMIC SCIENCE & HEALTH SCIENCE LIBRARY IN CANADA

Provides
quiet and group study space | research assistance | computers and photocopiers for students
helpful library staff | over **one million** items in our collection

Visit us at http://www.library.utoronto.ca/gerstein.
Or come in and see us at 7–9 King's College Circle!

UNIVERSITY OF TORONTO
LIBRARIES

Microfluidics and the Future of Drug Research

Kelvin Chen

Department of Chemistry, University of Toronto, 80 St. George Street, Toronto, Canada M5S 3H6

Abstract

Drug development is a resource-intensive enterprise. It boasts a very unappealing attrition rate, where 9 in 10 drugs entering clinical trials are rejected. This is often a result of lacking enough knowledge about the drug's efficacy and toxicity in humans, which can currently only be observed through clinical trials. This poses a problem for the primary healthcare and pharmaceutical industry because the full characterization of the drug's pharmacokinetic and pharmacodynamic properties is unknown until a large amount time and research funds have already been spent on developing the drug. Using what are largely static multi-well plate assays, current in vitro studies clearly do not possess the sophistication required to help scientists fully understand the complex interactions and behaviours of certain drugs in the body. Hence, more than ever, there is a growing demand for an alternative to current strategies for drug testing.

Enter the rapidly burgeoning field of microfluidics. Microfluidics, in a nutshell, is simply the manipulation of fluids inside closed channels whose dimensions are on the order of tens of microns, which coincides with the approximate dimensions of blood capillaries. At such a small scale, microfluidic systems possess the unique ability to mimic the interior geometric architecture of, and any existing fluid dynamics within, the human body's circulatory system. By artificially reconstructing the target tissue or organ using a small microfluidic device, scientists are able to reliably study the pharmacokinetics and pharmacodynamics of a drug as the solution flows through these capillary-like channels and interacts with various human cells or tissues. Although still at its infancy, the incipient field of microfluidics promises to revolutionize the very foundations of drug research in the years to come.

Introduction

The Problem

As the current state of affairs stands, drug development is a costly and time-demanding process. Due to the sheer complexity of discovering and developing viable drugs, it suffers from a remarkably high attrition rate where only 1 in 10 drugs entering clinical trials are approved due to unforeseen lack of efficacy and/or toxicity (Sung et al., 2010). The bulk of the costs in creating a new drug from scratch occurs in the latter stages of the developmental process as it enters clinical trials (Sung et al., 2010). Evidently, the ability to screen for any potential pharmacological deficits early in the process will save a great deal of resources. In many cases, finer details concerning the drug's delivery mechanics and issues concerning its efficacy are only gauged through the experimental outcomes of these clinical trials. This poses a problem for many pharmaceutical companies because the full characterization of the drug's pharmacokinetic and pharmacodynamic properties are unknown until a substantial amount of resources have been spent on developing the drug; from initial synthesis to preclinical testing with animals — a process that requires as long as three years (Dickson and Gagnon, 2004). Therefore, it is clear that current in vitro studies need to be improved. As such, there is an increasing interest in developing sophisticated models that can provide more in-depth information concerning the drug's behaviour in the human body, but without actually needing one.

At the pre-clinical stage of development, the drug candidate undergoes a series of in vitro tests culminating with in vivo animal studies to assess the compound's toxic and pharmacological effects (Dickson and Gagnon, 2004). The conventional platform for in vitro analysis implements the use of standardized multi-well plate assays where the trend has thus far been to merely increase the density of wells present on a plate in order to achieve higher efficiency (Sundberg, 2000)., the cell cultures and drug cocktails are still placed in largely static conditions and left over a period of time before they are analyzed. These and other similar methods do not account for the myriad of variables that are present in the internal system of the body, which are otherwise completely absent in this in vitro environment. These conventional approaches lack the ability to model multi-organ interactions, fail to reproduce the pharmacokinetics of the drugs and, thus, fail to grasp the overall pharmacological effects of the drugs (Lin and Lu, 1997).

The Solution

This is where microfluidics enters the picture. As the name suggests, microfluidics is the study of the behaviours and interactions of fluids in a microscopic environment enclosed within small

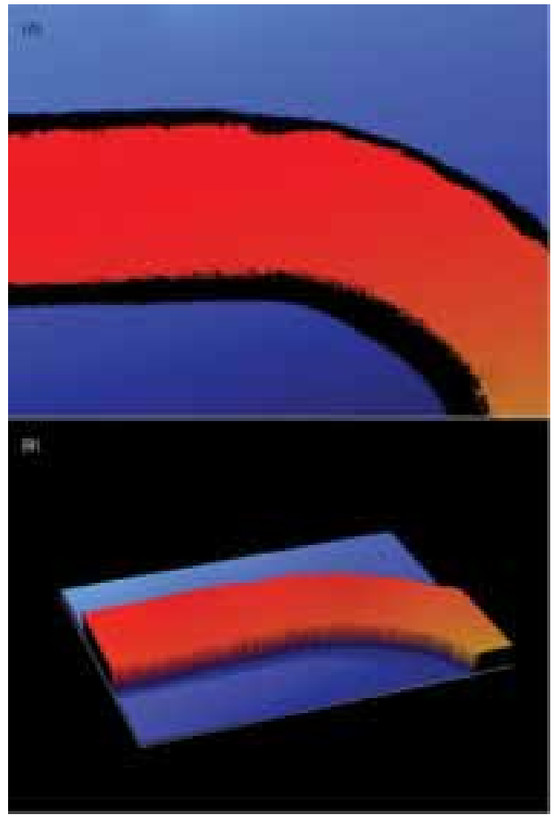

Figure 1: (A) Orthographic projection of micro-channels. (B) Oblique projection of micro-channels. Images were taken using optical profilometry. Based on visual inspection, there are two clearly defined levels on the chip with the red surface protruding outwards. This is the stamp used to etch in the micro-channels on the substrate.

"micro"-channels, which are on the order of tens of microns wide. These channels are etched onto a substrate and sealed off at the base to become what is known as a microfluidic device. (See Figure 1) The fluid inside may be pressure-driven using an external pump or driven through other means such as gravity-induced flow (Sung et al., 2010). The network of channels on the device allows many different chemical solutions to flow through, mix and react at specific junctures along its path. (See Figure 2) What is essentially the miniaturization of numerous, otherwise, test-tube experiments, the microfluidic device is frequently referred to as a lab-on-a-chip. These chips are especially useful because they require only very small quantities of the active reagents to carry out many separate reactions simultaneously that are necessary for high-speed, high-throughput experimentation (Whitesides, 2006). Microfluidic systems enable precision control of all operating variables (e.g. flow rate and solute concentration) involved in the experiment. This high level of control stems from the relative ease of manipulating various physical processes when the scale tends to the miniscule (deMello, 2006). In a closed system, the problems associated with evaporation and reagent exposure to the air is reduced significantly (Yeo et al., 2011). Moreover, at such a small scale, fluids flowing through such confined spaces exhibit laminar flow due to low convective mixing. This allows an additional degree of control as to where solutes in the flowing continuous phase are located (Khademhosseini et al., 2005). Finally, a variety of analytical instruments can be integrated to interface with the chip at any point; permitting high-resolution, sensitive and precise measurements to be taken in situ.

Microfluidic technology has become the prime candidate for conducting the next generation of pre-clinical drug trials for three very important reasons. Firstly, the dimensions of the micro-channels are in the range of the dimensions of blood capillaries—both of which are on the order of tens to hundreds of microns. Using this as the foundation, scientists have continued to hone the fabrication of these channels to better resemble blood capillaries. Secondly, the versatility of the substrate of the chip allows for the integration of cell cultures into its interior. These cultures act effectively as localized tissue, with which the capillary-like micro-channels will interact in a manner that closely resembles similar interactions in the human body. Finally, and perhaps most importantly, no value would be derived from these microfluidic experiments if scientists could not take accurate measurements in real-time and in situ—a feat that is both limited and challenging in a test-tube. What will follow is a discussion about each of these three aspects in terms of what current microfluidic devices can do and notable advancements that have been made toward fabricating the most life-like biomimetic microfluidic chip.

Biomimetic Capillaries

The Substrate

The pioneers of microfluidics began by using glass and silicon to form the substrate of the device to which the channels are etched upon (Whitesides, 2006). A transition to silicone-based polymers like polydimethylsiloxane (PDMS), thermoplastics like polycarbonate (PC) and cyclic olefin copolymer (COC) — The shift to using polymer substrates was widespread. The ubiquitous use of certain thermoplastics even led one group to develop a quick and cost-effective method of fabricating thermoplastic microfluidic chips using photolithography and hot embossing (Greener et al., 2010). Today, a wide range of materials are still being put to the test in search for ones that would prove to be most durable, chemically inert and possessing similar

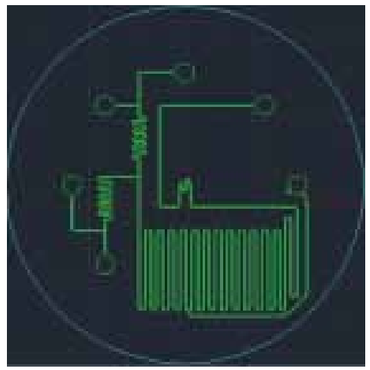

Figure 2: An image of a typical microfluidic chip. The intricate channel network is laid out in green. Fluids enter and exit the chip through inlets and outlets represented in the image as circles. The fluids mix at orthogonal intersections. The winding segments are used to agitate the solution as it flows through the channel to allow a more thorough mix. The serpentine loop in the center of the chip will interface with an analytical instrument for data collection.

physical properties to the endothelium of blood vessels. It is not surprising then, that hydrogels are very widely used in this regard. Hydrogels are highly water-absorbent polymers. This quality allows it to mimic the physiochemical properties of the extracellular matrix surrounding the body's blood vessels (Hoare and Kohane, 2008). Using a hydrogel substrate allows the observation of any ion exchanges that may occur as a result of competing hydrostatic and osmotic pressures as the fluid flows through the micro-channels, much like blood would interact with the interstitial fluid as it flows through the body. In addition, some more exotic materials have also been used as a substrate, namely cotton, which relies on capillary wicking to transport liquid (Li et al., 2010). There has also been increasing interest in fabricating three-dimensional devices where the fluid is free to flow down under the force of gravity, instead of the usual planar surface, to simulate effects such as blood-tissue-blood diffusion of certain chemical species (Mosadegh et al., 2010). On another note, one exciting, recent development concerns a "self-healing" synthetic vascular polymer. Researchers from the University of Illinois described what is a special epoxy matrix that lined the channel interior that was capable of reflowing, via capillary action, into a fracture that was made by a compressive force. This process is akin to the clotting response exhibited by a natural vessel in the event of a bone injury nearby (Hamilton et al., 2010).

The Channel

With the increasing complexity of microfluidic experiments, comes the necessity of more components operating synchronously with the rest of the system. Some of these components allow the experimenter to release a chemical species using a built-in valve. Droplets of a drug, for example, may be produced on demand with, to name a few, the use of electromagnetic switch, RF irradiation or via an electro-thermally induced structural failure actuator (ETISFA) that triggers a release of the drug by disrupting the membrane valve (Churski et al., 2010; Elman et al., 2010; Li et al., 2010). Yet another team developed a nanofluidic channel that would work in conjunction with the microfluidic device that was capable of modulating the zero-order release of therapeutic agents in a clinically-sufficient amount (Fine et al., 2010). The blood capillaries also consist of pores to allow exchange of ions and molecules across the membrane. Researchers have also developed novel ways of synthetically constructing and controlling pores for the channels. One example involved the use of an electric current to activate a magnetic field, which in turn translocated a series of microelectromagnetic particles to either block or open a micropore embedded onto a boundary layer (Basore et al., 2010). Instead of a ligand-gated transporter, another team created an ion-selective membrane instead, which consists of highly charged sulfonate groups and a number of transmembrane pores (Liu et al., 2010).

Modelling the Human Body

The Cultures

One of the main advantages of using microfluidic systems for the study of drug mechanics is not only that the fluids flow in a dynamic environment, but also the ability to model multi-compartmentalization. A drug injected into an artery will begin at a very high concentration at the injection point. However, the concentration of the drug decreases precipitously as the vessels branch apart successively. Continuously monitoring the concentration level of a drug at the target site will allow the determination of the necessary dosage at the beginning. Invariably, different pharmacokinetic and pharmacodynamic effects are present depending on the local concentration of the drug. Aside from the continuous branching off of blood vessels, the presence of cells also play a role in regulating the concentration of a specific solute. Much effort has been spent on creating what are known as "organ"-on-a-chip to monitor whether or not the drug is effective at the target cells in the organ and to measure the effects of metabolic break down that occurs as a result of enzymatic interactions with enzymes secreted by various organs in the body. Because of the plethora of agents interacting with each other, including drug-drug interactions, a full characterization of a drug is only remotely possible if the holistic microfluidic system can closely resemble the internal physiological construct of the human body complete with any relevant tissues.

Tissue engineering is therefore integral to this endeavour. Having access to a wide variety of implantable tissue is paramount in assaying for any potential negative properties (e.g. toxicity) that may arise in future in vivo studies. This has spurred many scientists to engineer microfluidic models embedded with microscale tissues cultures of major organs such as the liver, kidney and even the brain (Khetani and Bhatia, 2008; Jang and Suh, 2010; Park et al., 2006). For example, in studying the progression of malignant neoplasms, a reliable in vitro model is therefore one that can show tumour cells metastasizing as they naturally would in the body. Only when this is achieved can the basis of a good antimetastatic drug be rendered from the results (Griffith and Naughton, 2002). One of the fundamental aspects of cancer is its dynamic nature, made up of countless chemical signalling responses that make up the profile of a malignant cell (Wlodkowic and Cooper, 2010). For these experiments, a dynamic environment produced by microfluidics is essential.

The Harvest

Many studies have already been relying on microfluidics as the platform for their experiments. Using microfluidics, scientists have been able to perform high-throughput screening for viable formulations of protein drugs, investigating drug-protein interactions in anticancer drug testing and evaluating antibiotic efficacy using a microfluidic device coated with a bacterial biofilm (Capelle and Arvinte, 2009; Lombardi and Dittrich, 2010; Yu et al., 2010; Kim et al., 2010). A couple of groups have also focused on creating a three-dimensional lung-on-a-chip geared towards studying pulmonary inflammatory responses as well as to test the toxicity of an anticancer drug jointly with a mathematical model (Huh et al., 2010; Sung et al., 2010).

In situ Drug Monitoring

The efficacy of a drug is ultimately determined during clinical trials. Prior to this crucial step, the next best surrogate measure of efficacy appears to be the monitoring of the concentration of the drug localized around a specific area in the culture. Observing the tissue's reaction in comparison with the local concentration allows scientists to draw key conclusions, such as how much of the initial dosage remained after a duration, and how much of that was actually necessary to illicit the desired reaction in the tissue. In many incidences, there is a rather fine line between efficacy and toxicity.

To enhance drug monitoring beyond merely measuring the final drug concentration of the tissue culture, an in situ monitoring method is currently in development that is capable of real-time monitoring of drug concentrations inside microfluidic channels with pinpoint precision. By measuring drug concentrations in such a way, we are able to characterize a particular drug's release kinetics, and based on the data collected predict the pharmacokinetics and pharmacodynamics of the drug. The drug's infrared spectrum is taken using a technique called Attenuated Total Reflection Fourier Transform Infrared Spectroscopy (ATR-FTIR). The ATR-FTIR spectrometer is a well-entrenched analytical instrument that collects spectral data over a wide range of wavelengths across the infrared region. The utility of the spectrometer is in its ability to measure how well specific chemical or biological species are able to absorb or transmit light at each wavelength. The intensity of the signal will give an indication of the concentration of the drug at the point where the microfluidic chip was probed using the spectrometer. Using a protocol developed by one research group, it is possible to interface the instrument with a microfluidic chip in such a way as to allow in situ characterization of the local concentration of reactants or products at specific locations on the chip, or at specific times within the duration of the experiment (Greener et al., 2010). Although this technique is still in its infancy, results garnered from it are promising and some more research will be required before it can be fully implemented for data collection.

Conclusion

The Future

In the very near future, if not already, microfluidics will be at the forefront of drug research. Its commercial and industrial applications are limitless. Where it will go next, how it will get there and whether or not there is still some unrealized potential yet to be discovered is anybody's guess. The utility of this technology is abundant because it has broad implications for almost every aspect of scientific research. It promises to revolutionize not just chemistry and biology, but also territories of physics and engineering. Indeed, only with the convergence of the far-reaching corners of science can we fully exploit the vast potential of microfluidics.

Acknowledgments

I would like to express my gratitude to Dr. Jesse Greener and Professor Eugenia Kumacheva for the research opportunity at the University of Toronto and their enduring commitment to inspiring the next generation of scientists.

References

Basore, J.R., Lavrik, N.V., Baker, L.A. (2010). Single-pore membranes gated by microelectromagnetic traps. Advanced Materials 22, 2759-2763.
Capelle, M.A.H., Arvinte, T. (2009). High-throughput formulation screening of therapeutic proteins. Drug Discovery Today: Technologies 5, e71-e79.
Churski, K., Korczyk, P., Garstecki, P. (2010). High-throughput automated droplet microfluidic system for screening of reaction conditions. Lab on a Chip 10, 816-818.
DeMello, A.J. (2006). Control and detection of chemical reactions in microfluidic systems. Nature 442, 394-402.
Dickson, M., Gagnon, J.P. (2006). Key factors in the rising cost of new drug discovery and development. Nature Reviews 3, 417-429.
Elman, N.M., Masi, B.C., Cima, M.J., Langer, R. (2010). Electro-thermally induced structural failure actuator (ETISFA) for implantable controlled drug delivery devices based on Micro-Electro- Mechanical-Systems. Lab on a Chip 10, 2796-2804.
Fine, D., Grattoni, A., Hosali, S., Ziemys, A., De Rosa, E., Gill, J., Medema, R., Hudson, L., Kojic, M., Brousseau III, L., Goodall, R., Ferrari, M., Liu, X. (2010). A robust nanofluidic membrane with tunable zero-order release for implantable dose specific drug delivery. Lab on a Chip 10, 3074-3083.
Greener, J., Abbasi, B., Kumacheva, E. (2010). Attenuated total reflection Fourier transform infrared spectroscopy for on-chip monitoring of solute concentrations. Lab on a Chip 10, 1561-1566.
Greener, J., Li, W., Ren, J., Voicu, D., Pakharenko, V., Tang, T., Kumacheva, E. (2010). Rapid, cost-efficient fabrication of microfluidic reactors in thermoplastic polymers by combining photolithography and hot embossing. Lab on a Chip 10, 522-524.
Griffith, L.G., Naughton, G. (2010). Tissue engineering--Current challenges and expanding opportunities. Science 295, 1009-1016.
Hamilton, A.R., Sottos, N.R., White, S.R. (2010). Self-healing of internal damage in synthetic vascular materials. Advanced Materials 20, 1-5.
Hoare, T.R., Kohane, D.S. (2008). Hydrogels in drug delivery: Progress and challenges. Polymer 49, 1993-2007.
Huh, D., Matthews, B.D., Mammoto, A., Montoya-Zavala, M., Hsin, H.Y., Ingber, D.E. (2010). Reconstituting organ-level lung functions on a chip. Science 328, 1662-1668.
Jang, K., Suh, K. (2010). A multi-layer microfluidic device for efficient culture and analysis of renal tubular cells. Lab on a Chip 10, 34-42.
Khademhosseini, A., Langer, R., Borenstein, J., Vacanti, J.P. (2005). Microscale technologies for tissue engineering and biology. Proceedings of the National Academy of Sciences 103, 2480-2487.
Khetani, S.R., Bhatia, S.N. (2008). Microscale culture of human liver cells for drug development. Nature Biotechnology 26, 120-126.
Kim, K.P., Kim, Y., Choi, C., Kim, H., Lee, S., Chang, W., Lee, C. (2010). In situ monitoring of antibiotic susceptibility of bacterial biofilms in a microfluidic device. Lab on a Chip.
Li, P., Givrad, T.K., Sheybani, R., Holschneider, D.P., Maarek, J.I., Meng, E. (2010). A low power, on demand electrothermal valve for wireless drug delivery applications. Lab on a Chip 10, 101-110.
Li, X., Tian, J., Shen, W. (2010). Thread as a versatile material for low-cost microfluidic diagnostics. Applied Materials & Interfaces 2, 1-6.
Lin, J.H., Lu, A.Y.H. (1997). Role of pharmacokinetics and metabolism in drug discovery and development. Pharmacological Reviews 49, 403-449.
Liu, V., Song, Y., Han, J. (2010). Capillary-valve-based fabrication of ion-selective membrane junction for electrokinetic sample preconcentration in PDMS chip. Lab on a Chip 10, 1485-1490.
Lombardi, D., Dittrich, P.S. (2010). Droplet microfluidics with magnetic beads: a new tool to investigate drug–protein interactions. Analytical and Bioanalytical Chemistry.
Mosadegh, B., Agarwal, M., Torisawa, Y., Takayama, S. (2010). Simultaneous fabrication of PDMS through-holes for three-dimensional microfluidic applications. Lab on a Chip 10, 1983-1986.
Park, J.W., Vahidi, B., Taylor, A.M., Rhee, S.W., Jeon, N.L. (2006). Microfluidic culture platform for neuroscience research. Nature Protocols 1, 2128-2136.
Sundberg, S.A. (2000). High-throughput and ultra-high-throughput screening: solution- and cell-based approaches. Current Opinion in Biotechnology 11, 47-53.
Sung, J.H., Kam, C., and Shuler, M.L. (2010). A microfluidic device for a pharmacokinetic–pharmacodynamic (PK–PD) model on a chip. Lab on a Chip 10, 446-455.
Whitesides, G.M. (2006). The origins and the future of microfluidics. Nature 442, 368-373.
Wlodkowic, D., Cooper, J.M. (2010). Tumors on chips: oncology meets microfluidics. Current Opinion in Chemical Biology 14, 556-567.
Yeo, L.Y., Chang, H., Chan, P.P.Y, Friend, J.R. (2011). Microfluidic devices for bioapplications. Small 7, 12-48.
Yu, L., Chen, M.C.W., Cheung, K.C. (2010). Droplet-based microfluidic system for multicellular tumor spheroid formation and anticancer drug testing. Lab on a Chip 10, 2424-2432.

JULS REVIEWS

The pill that doesn't stop giving: exercise as a novel therapeutic intervention in bipolar disorder

Benedict Y. Cheung[a], Roger S. McIntyre[b]

[a]Department of Human Biology, University of Toronto, Toronto, ON Canada
[b]Mood Disorders Psychopharmacology Unit, University Health Network, University of Toronto, Toronto, ON, Canada

Abstract

Exercise has an attenuating effect on the symptoms of bipolar disorder (BD). While exercise has been shown to regulate general mood in BD, the underlying molecular mechanisms of this regulation have been elusive. Recent studies have found an imbalance of inflammatory cytokines (e.g. interleukins (IL), tumour necrosis factor (TNF)-α, etc.) salient to the pathophysiology of BD. Inflammatory molecules also seem to have a role in the regulation of neurotransmitters. Though causal mechanisms are unclear, attenuation of inflammatory markers in BD seems to be in part mediated by exercise. Meanwhile, studies have also focused on the molecular regulations of BD by way of neurotrophins, particularly brain-derived neurotrophic factor (BDNF), which has been associated with exercise. Whereas BDNF levels are reduced in bipolar patients, BDNF levels have been shown to increase after exercise, having implications on neurogenesis. Furthermore, there is new evidence for a state-dependent relationship of BDNF levels in BD patients. Collectively, the recent association of an inflammatory network and neurotrophins with BD has opened up avenues for therapeutic development. Rather than relying solely on classical pharmaceutical intervention, exercise should be explored as an adjunctive treatment for BD.

Introduction

"It is exercise alone that supports the spirits, and keeps the mind in vigor" (Marcus Cicero, 65 BC). Exercise has long been known to have a wide range of health benefits. Particularly, exercise has implications on brain health and might delay cognitive deficits associated with aging or neurodegeneration. However, it has only recently been implicated that exercise may have an attenuating effect on the symptoms of bipolar disorder (BD).

Affecting an estimated 1% of the world's population(Merikangas and Yu, 2002), BD is a debilitating mental illness marked by a characteristic elevation in mood or mania and is in almost all cases, accompanied by an episode of depression. In many ways opposite to the more familiar symptoms of depression, mania symptomatology varies in severity and is often characterized with elation, overactivity with a decreased need for sleep, and delusions of grandeur (see Table 1).

Because of the nature of the disease, treatment regimens for BD can be very complicated. Typically, a combination pharmacological treatment centered on mood stabilizers like lithium is prescribed for patients with BD (Azorin and Kaladjian, 2009). However, many side effects such as weight gain are often associated with this multi-drug approach (Bond et al., 2010; Correll, 2007). Given that exercise holistically improves the well-being of a person, recent efforts have been made to elucidate the role of physical activity in patients with BD. This review will examine possible mechanisms mediated by cytokines and neurotrophins salient in the pathophysiology of BD, while also exploring implications exercise may have on these inflammatory and neurotrophic alterations.

Cytokines in bipolar disorder

Recent findings on cytokines have explored the potential association between inflammation and BD (Goldstein et al., 2009). While alteration in inflammation is salient in major depressive disorder (MDD) (Raison et al., 2006) and other neuropsychiatric illnesses such as Alzheimer's disease (McGeer et al., 2006), the role of inflammation in BD remains to be elusive and inconclusive. Nevertheless, there is preliminary evidence that both manic and depressive episodes are generally associated with an increase in proinflammatory markers (PIMs), particularly tumour necrosis factor-alpha (TNF)-α (Kim et al., 2007a; O'Brien et al., 2006a; Ortiz-Domínguez et al., 2007). Furthermore, inflammation may have a regulatory role on neurotransmitters related to BD.

Proinflammatory markers and their association with BD

TNF-α, a proinflammatory molecule, is a persistent marker in both mania and depression in BD and is more recently, shown to be significantly greater in late-stage patients (diagnosed for at least 10 years) than early-stage patients (within first 3 years of first manic episode) (Kauer-Sant'Anna et al., 2009). This suggests that TNF-α may be upregulated as a consequence of the development of BD pathology. Though TNF-α can induce neuronal damage

Table 1: Definition and symptoms of mania and depression.

Mania	Depression
Definition: A period of elevated, irritable, or expansive mood for more than one week accomplished by at least 3 of the following: ❖ Inflated self-esteem or grandiosity ❖ Decreased need for sleep ❖ Increased talkativeness or pressured speech ❖ Racing thoughts or flight of ideas ❖ Distractability ❖ Increased activity or psychomotor agitation ❖ Excessive involvement in pleasurable activities that have high potential for painful consequences	Definition: A period characterized by depressed or irritable mood or diminished interest or loss of pleasure in most activities plus at least 4 of the following: ❖ Feelings of worthlessness or inappropriate guilt ❖ Sleep disturbance (increased or decreased amount) ❖ Fatigue or loss of energy ❖ Decreased concentration or indecisiveness ❖ Appetite or weight disturbances (failure to meet expected weight gains in children or loss of 5% of body weight in 1 month) ❖ Psychomotor agitation or retardation ❖ Suicidal ideation or thoughts of death

(Suzumura et al., 2006; Takeuchi et al., 2006), it has been proposed that this upregulation may be an adaptive response to the pathogenesis of BD. By contrast, the macrophage theory of depression postulates that proinflammatory cytokines can be depressogenic, commonly eliciting depressive symptoms in multiple sclerosis (Heesen et al., 2006), coronary artery disease (Appels et al., 2000; Pizzi et al., 2008), and cancer (Cleeland et al., 2003; Myers, 2008). Collectively, there has been substantial evidence for a bidirectional causal mechanism perhaps as a feedback network in the association of inflammation and disease states.

Inflammation impacts monoamine neurotransmitters

A general state of inflammation had been shown to activate indoleamine 2,3-dioxygenase (IDO), an enzyme that degrades tryptophan and serotonin (Babcock and Carlin, 2000). This degradation of serotonin and its precursor, tryptophan, may be the underlying explanation for the reduction of serotonergic neurotransmission in depression (Muller and Schwarz, 2007). In addition to the consumption of serotonin and tryptophan, the production of tryptophan catabolites such as quinolinic acid, is stimulated. Quinolinic acid, a potent N-methyl-D-aspartate (NMDA) receptor agonist, can cause neuroexcitotoxic effects in the brain (Schwarcz et al., 1983; Stone and Perkins, 1981), while elevating glutamatergic transmission by inhibiting glutmate uptake into astrocytes (Tavares et al., 2002). These processes by way of a proinflammatory state have been suggested to be related to acute mania in bipolar patients (Myint et al., 2007).

Neurotrophins in bipolar disorder

Neurotrophins such as brain-derived neurotrophic factor (BDNF), vascular endothelial growth factor (VEGF), and insulin-like growth factor -1 (IGF-1) play an important role in the pathophysiology of BD. It has been found that treatments for BD, for example, lithium can alter growth factors like VEGF (Guo et al., 2009). Drawing another example from the neurotrophin family, IGF-1 has been found to enhance BDNF signalling (McCusker et al., 2006). Of the myriad molecules involved with the growth factor cascades, BDNF seems to be crucial in the pathogenesis of BD. A dysfunctional BDNF-signalling system in BD has been supported by evidence that BDNF is implicated in: i) adult neurogenesis, ii) the action of antidepressant medication, iii) a genetic polymorphism in a subpopulation of BD patients, and iv) the affective status of BD patients.

BDNF on neurogenesis in bipolar disorder

BDNF is generally expressed in the hippocampus and other limbic structures and is responsible for neuronal functions such as axonal outgrowth, cell survival and synaptic plasticity (Huang and Reichardt, 2001). Direct evidence of a BDNF-mediated pathway to neurogenesis has been shown through BDNF infusion studies (Scharfman et al., 2005). BDNF infused into the hippocampus in rodents has led to an increase in neurons in the granule cell layer. Along with correlations between cognitive deficits and low levels of BDNF in BD, these alterations in the hippocampal cytoarchitecture support the idea that an increment in BDNF may have therapeutic value in modulating behavioural and cognitive deficits in BD patients.

BDNF mediates the effects of antidepressants

Enhancement of antidepressants has been speculated to feature a positive feedback mechanism involving BDNF (i.e. BDNF is upregulated by antidepressant medication) (Hashimoto, 2010) and works to enhance this medication in animal models (Shirayama et al., 2002). In one study, BDNF levels have been found to be significantly higher in both normal patients and depressed patients on antidepressants compared to those not on medications (Shimizu et al., 2003).

Val66Met polymorphism on the BDNF gene in bipolar disorder patients

Genetic associations with BD have been long sought for as it would lead to avenues for therapeutic development. The Val66Met polymorphism on the BDNF gene has been the primary candidate in efforts in unraveling genetic correlation in BD (Sklar et al., 2002). This polymorphism involving a valine for methionine amino acid substitution has been associated with many cognitive deficits, though not entirely exclusive to BD. However, while it has also been associated with schizophrenic patients, this polymorphism may be the best source of genetic correlation we may have for BD; it has been mainly seen in rapid cycling (Green et al., 2006) and in early onset BD (Tang et al., 2008a). Regardless, the Val66Met polymorphism has been more commonly linked with cognitive deficits and has a significant role in memory formation. For example, it has been shown that subjects with the Val66Met polymorphism have a poorer episodic memory, as well as abnormal hippocampal activation, than those without the polymorphism (Egan et al., 2003). A more recent study (Matsuo et al., 2009) looked at the gray matter variations with respect to having Val66Met polymorphism. Using MRI to collect brain images, the Val66Met polymorphism in BD patients seem to correlate with smaller gray matter volumes in areas known to be associated in the pathogenesis of BD and cognitive deficits (e.g. anterior cingulated cortex, hippocampus, dorsal lateral prefrontal cortex). There is a growing body of evidence that has linked this polymorphism on the BDNF gene with cognitive symptoms in BD, thus validating the importance of BDNF in the pathogenesis of BD.

Table 2: Summary of key molecular markers in bipolar disorder. Each arrow indicates a significant between-group differences found from previous studies (Cunha et al., 2006; Kim et al., 2007b; Liu et al., 2004; Machado-Vieira et al., 2007; Neeper et al., 1995; O'Brien et al., 2006b; Ortiz-Dominguez et al., 2007). A ↑ denotes a relative increase whereas ↓ denotes a relative decrease.

Molecular Markers	Mania vs. Control	Depression vs. Control	Late- vs. Early- stage	Effect of Exercise
TNF-α	↑	↑	↑	↓
IL-1RA	↑			↑
IL-4	↑			
IL-6	↑	↑	↓	↑
IL-10	↑	↑	-	↑
BDNF	↓	↓	↓	↑

State-dependent relationship of BDNF and bipolar disorder

BDNF levels have been generally demonstrated to be reduced in patients with BD when compared to healthy subjects (Lin, 2009). In a meta-analysis, subjects were pooled from fifteen studies and a differential BDNF serum level was found among the affective statuses of the patient. Particularly, the manic and depressive states were associated with a significant reduction in the BDNF levels but not in the euthymic state. In other words, BDNF levels seem to be adjusted and modulated when the mood was stabilized (i.e. in euthymic state). Interestingly, as demonstrated in another study, BDNF was found also to be negatively correlated with the duration of illness (Kauer-Sant'Anna et al., 2009). The collective evidence has suggested that BDNF may be a biomarker for the affective status and duration of illness in BD patients, confirming its importance in the disease progression of BD.

Implications of Exercise for Bipolar Disorder

Exercise on Inflammation

Exercise has been speculated to induce an anti-inflammatory state (Fallon et al., 2001; Geffken et al., 2001; Starkie et al.). Counterintuitive to traditional views, it was found that the concentration of proinflammatory cytokine, IL-6, markedly increased (Drenth et al., 1995; Pedersen et al., 2003) in response to exercise. Shown to be secreted by contracting muscles (Steensberg et al., 2002), IL-6 have inhibitory effects on the potent proinflammatory cytokine, TNF-α (Starkie et al., 2003), while also stimulating the production of IL-10 and interleukin 1 receptor alpha (IL-1RA), both of which exert anti-inflammatory effects (Steensberg et al., 2003).

Exercise on Neurotrophins

While evidence amounts to show that BDNF levels may be central in BD, exercise has been shown to increase BDNF levels in humans (Tang et al., 2008b). A recent review examined fifteen studies that investigated on the effects of exercise on serum levels of BDNF (Knaepen et al., 2010). Across the fifteen studies, it has been found that low to moderate intensity aerobic exercise increased BDNF concentration in 83% of the subjects with a disease or disability. Moreover, larger increases in BDNF concentrations were observed in these studies when subjects underwent a higher-intensity exercise protocol than a lower-intensity exercise protocol, thus showing a dose-response relationship. Collectively, there is strong evidence that exercise increases BDNF levels in humans.

Other growth factors such as insulin growth factor-1 (IGF-1) and vascular endothelial growth factor (VEGF) have been shown to act in concert with BDNF in mediating exercise-related benefits in brain health, particularly the cognitive and behavioural deficits associated in BD (Ding et al., 2006). While VEGF seems to orchestrate the proliferation of neuronal precursors, IGF-1 enhances BDNF signalling by increasing tyrosine kinase type 2 receptor (TrkB) expression in hippocampal cells (McCusker et al., 2006). Moreover, blocking IGF-1 abolishes BDNF-mediated action in the induction of synaptic proteins, such as synapsin, implicated in synaptic plasticity. Together, these results demonstrate that IGF-1 is an important modulator of BDNF signalling, and ultimately, may play a role in regulating the effect of exercise on hippocampal plasticity and learning. The facilitation of learning and memory via an exercise-induced increase of BDNF may have therapeutic implications in BD.

Clinical data and significance

While exercise may have significant inflammatory and neurotrophic effects in BD, a pilot study has demonstrated that exercise can facilitate mood and cognitive improvement in BD (Ng et al., 2007). BD patients participated in a nurse-led walking group for 40 minutes on a regular basis. Compared to non-participants, patients who were regular participants of the walking group significantly scored better on both the Cognitive Global Impression Severity (CGI-S) and Improvement (CGI-I) scales, and on the Depression Anxiety Stress Scale (DASS) at the time of discharge, which was on average 19.3 days post-admission. Despite methodological limits, the results of this study is consistent with a previous study looking at the benefits of exercise in depression (Dunn et al., 2005) and the general consensus that exercise improves cognition (Hillman et al., 2008).

Conclusion

In the past decade, there has been an accumulation of evidence for an underlying network of biological mediators of exercise. Particularly, exercise seems to help regulate cytokines and neurotrophins in disease states. In this light, exercise may be an appealing adjunctive psychosocial intervention for adolescents with BD, who are less responsive to medication (McElroy et al., 1997) and prone to weight gain (Bond et al., 2010; Correll, 2007). Interestingly, the peak onset of BD is between the ages 15 to 19 (Merikangas et al., 2007; Post et al., 2008) and an early onset of BD is predictive of a chronic course of illness (Carlson et al., 2000). Future randomized controlled trials should focus on the more vulnerable adolescent population. Moreover, these studies should compare subjects with and without bipolar disorder under a structured exercise on varying levels of exercise intensity. Regardless, the potential of exercise as an adjunctive intervention, however, is evident.

References

Appels, A., Bar, F.W., Bar, J., Bruggeman, C., and de Baets, M. (2000). Inflammation, depressive symptomtology, and coronary artery disease. Psychosom Med 62, 601-605.
Azorin, J.M., and Kaladjian, A. (2009). An update on the treatment of bipolar depression. Expert Opin Pharmacother 10, 161-172.
Babcock, T.A., and Carlin, J.M. (2000). Transcriptional activation of indoleamine dioxygenase by interleukin 1 and tumor necrosis factor alpha in interferon-treated epithelial cells. Cytokine 12, 588-594.
Bond, D.J., Kauer-Sant'Anna, M., Lam, R.W., and Yatham, L.N. (2010). Weight gain, obesity, and metabolic indices following a first manic episode: prospective 12-month data from the Systematic Treatment Optimization Program for Early Mania (STOP-EM). J Affect Disord 124, 108-117.
Carlson, G.A., Bromet, E.J., and Sievers, S. (2000). Phenomenology and outcome of subjects with early- and adult-onset psychotic mania. Am J Psychiatry 157, 213-219.
Cleeland, C.S., Bennett, G.J., Dantzer, R., Dougherty, P.M., Dunn, A.J., Meyers, C.A., Miller, A.H., Payne, R., Reuben, J.M., Wang, X.S., et al. (2003). Are the symptoms of cancer and cancer treatment due to a shared biologic mechanism? Cancer 97, 2919-2925.
Correll, C.U. (2007). Weight gain and metabolic effects of mood stabilizers and antipsychotics in pediatric bipolar disorder: a systematic review and pooled analysis of short-term trials. J Am Acad Child Adolesc Psychiatry 46, 687-700.
Cunha, A.B., Frey, B.N., Andreazza, A.C., Goi, J.D., Rosa, A.R., Goncalves, C.A., Santin, A., and Kapczinski, F. (2006). Serum brain-derived neurotrophic factor is decreased in bipolar disorder during depressive and manic episodes. Neurosci Lett 398, 215-219.
Ding, Q., Vaynman, S., Akhavan, M., Ying, Z., and Gomez-Pinilla, F. (2006). Insulin-like growth factor I interfaces with brain-derived neurotrophic factor-mediated synaptic plasticity to modulate aspects of exercise-induced cognitive function. Neuroscience 140, 823-833.
Drenth, J.P., Van Uum, S.H., Van Deuren, M., Pesman, G.J., Van der Ven-Jongekrijg, J., and Van der Meer, J.W. (1995). Endurance run increases circulating IL-6 and IL-1ra but downregulates ex vivo TNF-alpha and IL-1 beta production. J Appl Physiol 79, 1497-1503.
Dunn, A.L., Trivedi, M.H., Kampert, J.B., Clark, C.G., and Chambliss, H.O. (2005). Exercise treatment for depression: efficacy and dose response. Am J Prev Med 28, 1-8.
Egan, M.F., Kojima, M., Callicott, J.H., Goldberg, T.E., Kolachana, B.S., Bertolino, A., Zaitsev, E., Gold, B., Goldman, D., Dean, M., et al. (2003). The BDNF val-66met polymorphism affects activity-dependent secretion of BDNF and human memory and hippocampal function. Cell 112, 257-269.
Fallon, K.E., Fallon, S.K., and Boston, T. (2001). The acute phase response and exercise: court and field sports. Br J Sports Med 35, 170-173.
Geffken, D.F., Cushman, M., Burke, G.L., Polak, J.F., Sakkinen, P.A., and Tracy, R.P. (2001). Association between Physical Activity and Markers of Inflammation in a Healthy Elderly Population. American Journal of Epidemiology 153, 242-250.
Goldstein, B.I., Kemp, D.E., Soczynska, J.K., and McIntyre, R.S. (2009). Inflammation and the phenomenology, pathophysiology, comorbidity, and treatment of bipolar disorder: a systematic review of the literature. J Clin Psychiatry 70, 1078-1090.
Green, E.K., Raybould, R., Macgregor, S., Hyde, S., Young, A.H., O'Donovan, M.C., Owen, M.J., Kirov, G., Jones, L., Jones, I., et al. (2006). Genetic variation of brain-derived neurotrophic factor (BDNF) in bipolar disorder: case-control study of over 3000 individuals from the UK. Br J Psychiatry 188, 21-25.
Guo, S., Arai, K., Stins, M.F., Chuang, D.M., and Lo, E.H. (2009). Lithium upregulates vascular endothelial growth factor in brain endothelial cells and astrocytes. Stroke 40, 652-655.
Hashimoto, K. (2010). Brain-derived neurotrophic factor as a biomarker for mood disorders: An historical overview and future directions. Psychiatry and Clinical Neurosciences 64, 341-357.
Heesen, C., Nawrath, L., Reich, C., Bauer, N., Schulz, K.H., and Gold, S.M. (2006). Fatigue in multiple sclerosis: an example of cytokine mediated sickness behaviour? J Neurol Neurosurg Psychiatry 77, 34-39.
Hillman, C.H., Erickson, K.I., and Kramer, A.F. (2008). Be smart, exercise your heart: exercise effects on brain and cognition. Nat Rev Neurosci 9, 58-65.
Huang, E.J., and Reichardt, L.F. (2001). Neurotrophins: roles in neuronal development and function. Annu Rev Neurosci 24, 677-736.
Kauer-Sant'Anna, M., Kapczinski, F., Andreazza, A.C., Bond, D.J., Lam, R.W., Young, L.T., and Yatham, L.N. (2009). Brain-derived neurotrophic factor and inflammatory markers in patients with early- vs. late-stage bipolar disorder. Int J Neuropsychopharmacol 12, 447-458.
Kim, Y.-K., Jung, H.-G., Aye-Mu, M., Kim, H., and Park, S.-H. (2007a). Imbalance between pro-inflammatory and anti-inflammatory cytokines in bipolar disorder. Journal of affective disorders 104, 91-95.
Kim, Y.K., Jung, H.G., Myint, A.M., Kim, H., and Park, S.H. (2007b). Imbalance between pro-inflammatory and anti-inflammatory cytokines in bipolar disorder. J Affect Disord 104, 91-95.
Knaepen, K., Goekint, M., Heyman, E.M., and Meeusen, R. (2010). Neuroplasticity - exercise-induced response of peripheral brain-derived neurotrophic factor: a systematic review of experimental studies in human subjects. Sports Med 40, 765-801.
Lin, P.Y. (2009). State-dependent decrease in levels of brain-derived neurotrophic factor in bipolar disorder: a meta-analytic study. Neurosci Lett 466, 139-143.
Liu, H.C., Yang, Y.Y., Chou, Y.M., Chen, K.P., Shen, W.W., and Leu, S.J. (2004). Immunologic variables in acute mania of bipolar disorder. J Neuroimmunol 150, 116-122.
Machado-Vieira, R., Dietrich, M.O., Leke, R., Cereser, V.H., Zanatto, V., Kapczinski, F., Souza, D.O., Portela, L.V., and Gentil, V. (2007). Decreased plasma brain derived neurotrophic factor levels in unmedicated bipolar patients during manic episode. Biol Psychiatry 61, 142-144.
Matsuo, K., Walss-Bass, C., Nery, F.G., Nicoletti, M.A., Hatch, J.P., Frey, B.N., Monkul, E.S., Zunta-Soares, G.B., Bowden, C.L., Escamilla, M.A., et al. (2009). Neuronal correlates of brain-derived neurotrophic factor Val66Met polymorphism and morphometric abnormalities in bipolar disorder. Neuropsychopharmacology 34, 1904-1913.
McCusker, R.H., McCrea, K., Zunich, S., Dantzer, R., Broussard, S.R., Johnson, R.W., and Kelley, K.W. (2006). Insulin-like growth factor-I enhances the biological activity of brain-derived neurotrophic factor on cerebrocortical neurons. J Neuroimmunol 179, 186-190.
McElroy, S.L., Strakowski, S.M., West, S.A., Keck, P.E., Jr., and McConville, B.J. (1997). Phenomenology of adolescent and adult mania in hospitalized patients with bipolar disorder. Am J Psychiatry 154, 44-49.
McGeer, P.L., Rogers, J., and McGeer, E.G. (2006). Inflammation, anti-inflammatory agents and Alzheimer disease: the last 12 years. J Alzheimers Dis 9, 271-276.
Merikangas, K., and Yu, K. (2002). Genetic epidemiology of bipolar disorder. 2, 127-141.
Merikangas, K.R., Akiskal, H.S., Angst, J., Greenberg, P.E., Hirschfeld, R.M., Petukhova, M., and Kessler, R.C. (2007). Lifetime and 12-month prevalence of bipolar spectrum disorder in the National Comorbidity Survey replication. Arch Gen Psychiatry 64, 543-552.
Muller, N., and Schwarz, M.J. (2007). The immune-mediated alteration of serotonin and glutamate: towards an integrated view of depression. Mol Psychiatry 12, 988-1000.
Myers, J.S. (2008). Proinflammatory cytokines and sickness behavior: implications for depression and cancer-related symptoms. Oncol Nurs Forum 35, 802-807.
Myint, A.M., Kim, Y.K., Verkerk, R., Park, S.H., Scharpé, S., Steinbusch, H.W.M., and Leonard, B.E. (2007). Tryptophan breakdown pathway in bipolar mania. Journal of affective disorders 102, 65-72.
Neeper, S.A., Gomez-Pinilla, F., Choi, J., and Cotman, C. (1995). Exercise and brain neurotrophins. Nature 373, 109.
Ng, F., Dodd, S., and Berk, M. (2007). The effects of physical activity in the acute treatment of bipolar disorder: a pilot study. J Affect Disord 101, 259-262.
O'Brien, S.M., Scully, P., Scott, L.V., and Dinan, T.G. (2006a). Cytokine profiles in bipolar affective disorder: Focus on acutely ill patients. Journal of affective disorders 90, 263-267.
O'Brien, S.M., Scully, P., Scott, L.V., and Dinan, T.G. (2006b). Cytokine profiles in bipolar affective disorder: focus on acutely ill patients. J Affect Disord 90, 263-267.
Ortiz-Dominguez, A., Hernandez, M.E., Berlanga, C., Gutierrez-Mora, D., Moreno, J., Heinze, G., and Pavon, L. (2007). Immune variations in bipolar disorder: phasic differences. Bipolar Disord 9, 596-602.
Ortiz-Domínguez, A., Hernández, M.E., Berlanga, C., Gutiérrez-Mora, D., Moreno, J., Heinze, G., and Pavón, L. (2007). Immune variations in bipolar disorder: phasic differences. Bipolar Disorders 9, 596-602.
Pedersen, B.K., Steensberg, A., Fischer, C., Keller, C., Keller, P., Plomgaard, P., Febbraio, M., and Saltin, B. (2003). Searching for the exercise factor: is IL-6 a candidate? J Muscle Res Cell Motil 24, 113-119.
Pizzi, C., Manzoli, L., Mancini, S., and Costa, G.M. (2008). Analysis of potential predictors of depression among coronary heart disease risk factors including heart rate variability, markers of inflammation, and endothelial function. European Heart Journal 29, 1110-1117.
Post, R.M., Luckenbaugh, D.A., Leverich, G.S., Altshuler, L.L., Frye, M.A., Suppes, T., Keck, P.E., McElroy, S.L., Nolen, W.A., Kupka, R., et al. (2008). Incidence of childhood-onset bipolar illness in the USA and Europe. Br J Psychiatry 192, 150-151.
Raison, C.L., Capuron, L., and Miller, A.H. (2006). Cytokines sing the blues: inflammation and the pathogenesis of depression. Trends Immunol 27, 24-31.
Scharfman, H., Goodman, J., Macleod, A., Phani, S., Antonelli, C., and Croll, S. (2005). Increased neurogenesis and the ectopic granule cells after intrahippocampal BDNF infusion in adult rats. Exp Neurol 192, 348-356.
Schwarcz, R., Whetsell Jr, W.O., and Mangano, R.M. (1983). Quinolinic acid: An endogenous metabolite that produces axon-sparing lesions in rat brain. Science 219, 316-318.
Shimizu, E., Hashimoto, K., Okamura, N., Koike, K., Komatsu, N., Kumakiri, C., Nakazato, M., Watanabe, H., Shinoda, N., Okada, S., et al. (2003). Alterations of serum levels of brain-derived neurotrophic factor (BDNF) in depressed patients with or without antidepressants. Biol Psychiatry 54, 70-75.
Shirayama, Y., Chen, A.C., Nakagawa, S., Russell, D.S., and Duman, R.S. (2002). Brain-derived neurotrophic factor produces antidepressant effects in behavioral models of depression. J Neurosci 22, 3251-3261.
Sklar, P., Gabriel, S.B., McInnis, M.G., Bennett, P., Lim, Y.M., Tsan, G., Schaffner, S., Kirov, G., Jones, I., Owen, M., et al. (2002). Family-based association study of 76 candidate genes in bipolar disorder: BDNF is a potential risk locus. Brain-derived neutrophic factor. Mol Psychiatry 7, 579-593.
Starkie, R., Ostrowski, S.R., Jauffred, S., Febbraio, M., and Pedersen, B.K. Exercise and IL-6 infusion inhibit endotoxin-induced TNF-α production in humans. The FASEB Journal.
Starkie, R., Ostrowski, S.R., Jauffred, S., Febbraio, M., and Pedersen, B.K. (2003). Exercise and IL-6 infusion inhibit endotoxin-induced TNF-alpha production in humans. FASEB J 17, 884-886.
Steensberg, A., Fischer, C.P., Keller, C., Moller, K., and Pedersen, B.K. (2003). IL-6 enhances plasma IL-1ra, IL-10, and cortisol in humans. Am J Physiol Endocrinol Metab 285, E433-437.
Steensberg, A., Keller, C., Starkie, R.L., Osada, T., Febbraio, M.A., and Pedersen, B.K. (2002). IL-6 and TNF-alpha expression in, and release from, contracting human skeletal muscle. Am J Physiol Endocrinol Metab 283, E1272-1278.
Stone, T.W., and Perkins, M.N. (1981). Quinolinic acid: A potent endogenous excitant at amino acid receptors in CNS. European Journal of Pharmacology 72, 411-412.
Suzumura, A., Takeuchi, H., Zhang, G., Kuno, R., and Mizuno, T. (2006). Roles of glia-derived cytokines on neuronal degeneration and regeneration. Ann N Y Acad Sci 1088, 219-229.
Takeuchi, H., Jin, S., Wang, J., Zhang, G., Kawanokuchi, J., Kuno, R., Sonobe, Y., Mizuno, T., and Suzumura, A. (2006). Tumor necrosis factor-alpha induces neurotoxicity via glutamate release from hemichannels of activated microglia in an autocrine manner. J Biol Chem 281, 21362-21368.
Tang, J., Xiao, J., Shu, C., Wang, G., Liu, Z., Wang, X., Wang, H., and Bai, X. (2008a). Association of the brain-derived neurotrophic factor gene and bipolar disorder with early age of onset in mainland China. Neurosci Lett 433, 98-102.
Tang, S.W., Chu, E., Hui, T., Helmeste, D., and Law, C. (2008b). Influence of exercise on serum brain-derived neurotrophic factor concentrations in healthy human subjects. Neurosci Lett 431, 62-65.
Tavares, R.G., Tasca, C.I., Santos, C.E.S., Alves, L.B., Porciúncula, L.O., Emanuelli, T., and Souza, D.O. (2002). Quinolinic acid stimulates synaptosomal glutamate release and inhibits glutamate uptake into astrocytes. Neurochemistry International 40, 621-627.

Pharmacology & Toxicology
UNIVERSITY OF TORONTO
http://www.pharmtox.utoronto.ca

JULS REVIEWS

ADHD in Adulthood: Is it Mere Persistence? A Whorfian Dilemma.

Maryam Demian

Department of Psychology, University of Toronto at Scarborough, 1265 Military Trail, Toronto, ON, Canada M1C 1A4

Abstract

The present review seeks to examine evidence for the validity of Attention-Deficit/Hyperactivity Disorder (ADHD) diagnoses in adults. Several main concerns are discussed, including the controversy surrounding ADHD diagnoses in childhood, and the disorder's inconsistent manifestations across different developmental points in the patient's lifespan. Specifically, these inconsistencies include the disappearance of hallmarks as well as varying symptoms and epidemiology. Other problems rendering an adult-ADHD diagnosis problematic include ADHD's poor diagnostic specificity, high sensitivity and the use of a retrospective diagnosis. This review offers several hypotheses to explain ADHD's apparent persistence into adulthood: it could be the manifestation of ADHD characteristics left over from the disorder in childhood; an ADHD comorbidity; or ADHD's transformation into a non-ADHD disorder. It is concluded that adult-ADHD fulfills all requirements for validity, except for it being an independent disorder.

ADHD in Adulthood: Is it Mere Persistence? A Whorfian Dilemma.

Attention-Deficit/Hyperactivity Disorder (ADHD) is a neuro-developmental disorder that was first diagnosed in 1902. Sir George Frederick Still is credited for recognizing ADHD as a disorder. From the moment when Still noticed that some children were significantly more inattentive or hyperactive than others, the conceptualization of an ADHD diagnosis has undergone several amendments (Figure 1) (Mayes et al., 2008; Mayes and Rafalovich, 2007). With each subsequent DSM publication, the diagnostic criteria have been widened to include more children in having ADHD (Searight and McLaren, 1998).

Today, ADHD affects approximately 5% of school-aged children (Wilens et al., 2002) and presents itself as a burden to both sufferers and society (Biederman, 2005). Children with ADHD experience difficulties in getting along with family and friends, as reflected in their poor educational performance and in their interpersonal distress (Biederman, 2005). Moreover, ADHD remains one of the most controversial DSM-IV diagnoses largely because it is the most widely diagnosed disorder in minors; in the United States, on average, one in every twelve children is diagnosed with ADHD, and one in every 22 children receives stimulant medication (Mayes et al., 2008). Efforts towards understanding ADHD, specifically its provenance and manifestations across developmental lifespan, is thus necessary in order to fully resolve such issues and better help individuals diagnosed with ADHD. This review will discuss several differences between ADHD in childhood and adulthood with the aim of clarifying the nature of the disorder's apparent persistence into adulthood.

Diagnosis of ADHD

In Children

According to the American Psychological Association in the DSM-IV-TR, the child must present current features of either inattention and/or hyperactivity that have lasted for at least six months and that surpass those observed in age and gender-matched individuals (American Psychological Association [APA], 2000). The symptoms must have occurred before the age of seven and must interfere with developmentally appropriate functioning across at least two life domains (e.g. school, family, and social life) (APA, 2000). Finally, the complete constellation of symptoms must not be better explained by another disorder (APA, 2000). Given that these criteria are met, a child will meet the diagnostic criteria for one of three types of ADHD: i) predominately inattentive, by presenting at least six symptoms of inattention; ii) predominately hyperactive-impulsive, by presenting at least six symptoms of hyperactivity-impulsivity; or iii) combined, by presenting six symptoms of both inattention and hyperactivity-impulsivity (APA, 2000).

In Adulthood

ADHD is not merely a childhood disorder (Wilens et al., 2002). In about 50 to 75% of all children diagnosed with the disorder, ADHD symptoms will persist into adolescence. In a smaller proportion – 40 to 60% of these children – ADHD endures into adulthood (Wilens et al., 2002).

For an ADHD diagnosis to be made in adulthood, the patient exhibiting ADHD-like symptoms must have had childhood-onset ADHD (i.e. occurring before the age of 7) (Karam et al., 2009). The symptoms must both manifest themselves at the time of the diagnosis and endure into adulthood (Wilens et al., 2002). However, controversy over the age of ADHD-onset has made late-onset ADHD (in which criteria fulfillment occurs before the age of 12 rather than 7) a valid diagnosis (Karam et al., 2009; Kieling et al., 2010). This controversy arose because in some individuals who fulfilled all ADHD-criteria, symptoms could not be traced to as far back as 7 years of age (Applegate et al., 1999 as cited in Karam et al., 2009). Furthermore, studies that conducted an exhaustive search for intergroup differences between early and late-onset ADHD found none, apart from the age of onset (Rohde et al., 2000 as cited in Karam et al., 2009).

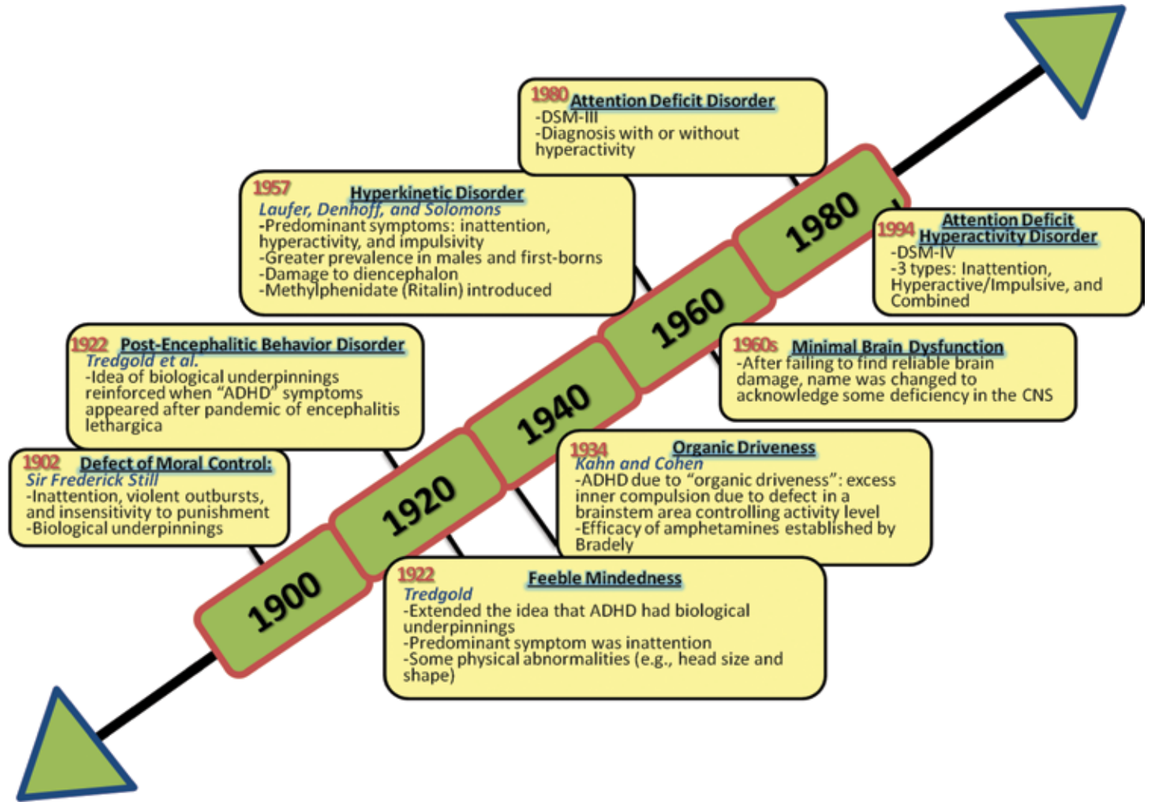

Figure 1: Evolution of ADHD timeline. The evolution of ADHD beginning from its initial recognition by Still (1902), to when it was first recognized in its current form (1980), and finally to its present state as it appears in the DSM-IV (1987). Each milestone contains the label believed to represent ADHD at that time, a description of common beliefs, and the names of those who contributed to its advancement.

Three factors predict the continuation of ADHD into adulthood: i) familial history of ADHD, ii) psychiatric comorbidity, and iii) adverse living factors (Biederman, 2005; Wilens et al., 2002). In Biederman and colleagues' 1995 study, ADHD was more likely to endure into adulthood in those individuals who endorsed more "adversity indicators" such as marital discord, living in a large family, or being placed in foster care (as cited in Biederman, 2005).

Symptoms of ADHD in adulthood may include inattention, distractibility, or lower efficiency as compared to age-matched individuals (Wilens et al., 2002). These adults have difficulties organizing tasks, which leads to problems at work and home, understandably contributing to the development of emotional disorders (Schmidt and Petermann, 2009). Additionally, due to the presence of comorbid disorders, there is no single, uniform developmental pathway in adult ADHD (Schmidt and Petermann, 2009).

Controversy Surrounding a Diagnosis of ADHD

In Children

A universal argument presented by both the learned and the lay concerns the observation that children – by virtue of their nature – fulfill criteria of inattentiveness and hyperactivity (Mayes et al., 2008). Furthermore, skepticism exists because ADHD's symptoms overlap with those of several childhood psychiatric disorders – such as conduct, oppositional defiance, anxiety, mood and learning disorders – contributing to the diagnosis' poor specificity (Searight and McLaren, 1998). The inherent subjectivity in deciding what denotes excessive inattention, hyperactivity or impulsivity presents another problem (Mayes et al., 2008). Studies have also been conducted to discern whether stimulant medications have suppressive effects on children's growth and development. However, there is little consensus over this issue since some studies have pointed out stimulants' heightened suppressive effects, while others have contradicted these findings, attributing them instead

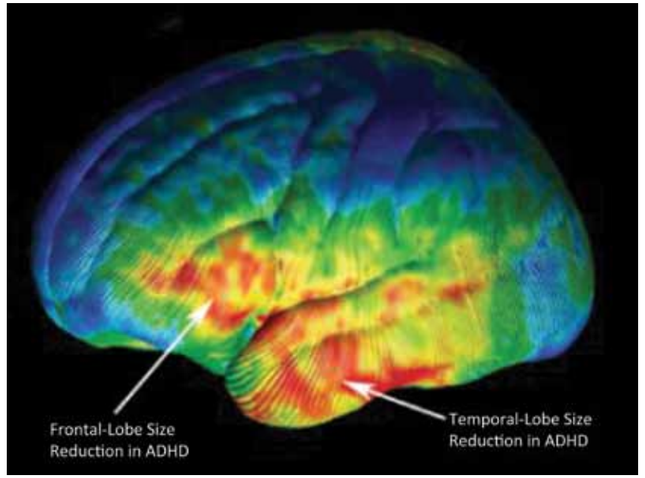

Figure 2: Brain size reductions in ADHD. Reductions in frontal and temporal lobe size in children and adolescents with ADHD as found in Sowell and colleagues' (2003) study.

to the disorder itself (Wilens et al., 2002). Nevertheless, the claim that our society has become more and more comfortable with medicalizing non-optimal behaviors, such as poor social skills, is of continual concern (Searight and McLaren, 1998). Although a discussion of childhood-ADHD is beyond the scope of this review, if adult-ADHD is to be a valid and widely accepted diagnosis, there should first be strong evidence for the diagnosis in childhood.

In Adults

The disappearance of hallmarks. Surprisingly, the hallmarks of childhood ADHD – impulsivity, hyperactivity and inattention – are not as prominent in an adult diagnosed with the disorder (Schmidt and Petermann, 2009; Wright, 2005). An adult presenting with ADHD displays less hyperactive and externalized symptoms (Klassen et al., 2009). In fact, these symptoms are subtle to the extent that the patient does not complain about them. In addition, they are masked by other behavioral presentations such as poor judgment, behavioral difficulties, forgetfulness and difficulties in reading and calculation (Wright, 2005).

Inconsistencies in symptoms. Why, then, is an assortment of symptoms clearly distinct from that present in childhood-ADHD labeled as ADHD? Such inconsistencies do not occur for other diagnoses. The DSM-IV, for instance, does not mention that anxiety disorders manifest differently across the developmental lifespan (APA, 2000). For ADHD, however, the constellation of symptoms differs in childhood and adulthood. For example, behavioral problems persist into adulthood in only 40-60% of all childhood cases (Schmidt and Petermann, 2009), with the greater majority of continuing symptoms being those of the inattentive rather than the hyperactive/impulsive type (Millstein et al., 1997).

Inconsistencies in epidemiology. Epidemiological studies have revealed differences in the prevalence and causation of child and adult ADHD diagnoses. Prevalence rates of ADHD are 3 to 15% in childhood, while in adulthood they are 1 to 7% (Schmidt and Petermann, 2009). This can be explained by the 40 to 96% rate of remission in all cases of childhood ADHD (Schmidt and Petermann, 2009). It may also point to the under-diagnosis of ADHD in adulthood because of its highly comorbid nature and unique expression during adulthood (Schmidt and Petermann, 2009). Similarly, while boys are two to four times more likely than girls to have ADHD in childhood, this difference disappears in adulthood (Schmidt and Petermann, 2009).

Finally, an exhaustive amount of research has been conducted to link ADHD to genetic or neurological underpinnings, the lion's share being in children (Konrad et al., 2010). This has clear implications on the present issue: we cannot be sure that an adult-ADHD diagnosis is valid until research demonstrates that a similar causal agent exists in both adults and children diagnosed with ADHD. To elaborate on this point, if children with ADHD constantly present with smaller frontal and temporal lobes (Sowell et al., 2003), then adults with ADHD – preferably those who have never been medicated – should also exhibit such abnormalities.

Researchers have identified genes common to both the childhood and adulthood forms of the disorder. These include the genes coding for the dopamine receptor D4 (Faraone, 2004) and the brain derived neurotrophic factor (Kebir et al., 2009; Lanktree et al., 2008), though findings are inconsistent over the latter's involvement (Sanchez-Mora et al., 2009 as cited in Müller et al., 2010).

Although there is evidence for a common genetic link, studies have not confirmed a common neurological factor. Recent research conducted by Konrad and colleagues investigated the differences in white matter tracts in never-medicated adults with ADHD and compared them to those in children (Konrad et al., 2010). Unfortunately, their results contradicted findings in children (Konrad et al., 2010), meaning that a common neurological etiological factor was not identified. Other research which utilized innovative diffusion tensor imaging (a technique used to examine white matter tracts), found differential selectivity of water diffusion (fractional anisotropy) in brain regions of children, adolescents and adults diagnosed with ADHD (Konrad et al., 2010). While these differences were attributed to inconsistencies in the type of subjects and methodology used (Konrad et al., 2010), the field of neuropsychology still awaits a common neurological etiological factor, in addition to confirmed genetic involvement.

Alternative Explanations for ADHD Persistence

It is difficult for ADHD's unique presentation in adulthood to not foment further inquiry into its nature. To be sure, there appear to be two clearly distinct entities – one in childhood and one in adulthood – each possessing unique symptoms, neurological underpinnings, and prevalence, but which nevertheless are subject to the same diagnosis and all related consequences. The issue is not merely a problem of a name or label, but concerns the more serious issue of a diagnosis' utility. An accurate diagnosis facilitates disorder conceptualization as a unique entity requiring specific assessments and interventions (First and Westen, 2007). This, in turn, aids in communicating about the disorder's specific nature and predicting its future course (First and Westen, 2007).

Thus, I have come up with several hypotheses that could help explain ADHD's inconsistent manifestation in adulthood: adult-ADHD could be a mere manifestation of disorders that are comorbid with ADHD, a result of a childhood lived with ADHD, or a transformation of ADHD into a novel and distinct disorder in adulthood.

Comorbidities

The adult diagnosed with ADHD may also present various concomitant disorders. These include substance abuse, depressive, bipolar, and anxiety disorders, as well as anti-social and borderline personality disorders (Klassen et al., 2009; Schmidt and Petermann, 2009). A common neurobiological factor may tie these disorders together, resulting in their simultaneous manifestation (Schmidt and Petermann, 2009). Thus, it is conceivable that ADHD, as it is currently known, is a disorder confined to childhood, and that the symptoms of an adult diagnosed with ADHD are actually a constellation of a comorbid disorder. In other words, since ADHD's hallmarks either diminish or disappear in adulthood, a child diagnosed with ADHD at the age of 7, who now presents with an adult-ADHD assemblage, might very well have another disorder.

Result of a childhood with ADHD

Yet another factor accounting for the disorder's apparent persistence could be that the child's learnt behaviors and thoughts leave behind a characteristic "adult-ADHD signature". For instance, it is understandable that the adult's reading and calculation difficulties may be a result of childhood ADHD symptoms that interfered with his or her reaching their full potential. Likewise, poor judgment in the adult could be the consequence of the child's learned impulsivity that interfered with careful consideration of situations and prudent decision-making. The same could be said for each of the symptoms an adult with ADHD presents. Long-term consequences of childhood-ADHD have already been established: poor performance in educational and work-related domains is common in adults who have had ADHD as children (Wilens et al., 2002).

Transformation into a non-ADHD disorder

Another explanation for ADHD-like symptoms persisting into adulthood could be that childhood-ADHD manifests itself differently along a child's lifespan. This is similar to the case of gender identity disorder (GID) and homosexuality (keeping in mind that the latter is not a disorder). About two-thirds of all boys diagnosed with GID are homosexuals in adulthood (Corbett, 1998), and a more recent study conducted by Wallien and Cohen-Kettenis (2008) concluded that homosexuality and bisexuality were the most probable outcomes for children with gender-dysphoric disorder. Here, GID transforms into an entirely novel entity, homosexuality, and is no longer what it originally was. Therefore, the phenomenon of disorder transformation exists and is not uncommon for a disorder whose adulthood presentation is dissimilar to that in childhood.

Symptoms of adult ADHD without childhood ADHD

As previously mentioned, disagreement does exist regarding the age-of-onset diagnostic criteria for ADHD. By making the age-of-onset criteria more lenient, the diagnosis is widened to account for 18% and 43% more of combined and inattentive ADHD cases, respectively (Applegate et al., 1999 as cited in Karam et al., 2009). Thus, on the one hand, while the field of psychiatry has adjusted to account for cases with a later onset, we remain tied to an onset that is no later than 12 years. A relevant conundrum would be the case of the patient who presents with an adult-ADHD symptom constellation, but whose past is not one that could be labeled with ADHD. Surely there exist patients who exhibit poor judgment, behavioral difficulties, forgetfulness, minimal hyperactivity and/or distractibility, but whose ADHD hallmarks did not appear before the age of 7 or did not affect performance in at least two areas of life. In such a case, it is unclear whether this adult would now be diagnosed as having another disorder or would be said to be suffering from a disciplinary, behavioral, or perhaps even a personality disorder.

Conclusion and Implications

To conclude, an assessment should be conducted to lend support to the validity of an adult-ADHD diagnosis. To be classified as a valid psychiatric diagnostic entity, the disorder must: i) provide a prognosis, ii) be related to neurobiology, iii) predict treatment response, and iv) be independent of other disorders (Degenhardt et al., 2010). Adult-ADHD successfully fulfills each of these conditions, save for being independent of other disorders.

Specifically, research has shown that a label of adult-ADHD does predict the outcome or course of the disease. For instance, since it is known that most adults with ADHD present the inattentive subtype, predictions can be made regarding what behaviors they will exhibit in certain situations (Millstein et al., 1997). Such adults are likely to have difficulties staying on task or sustaining attention (Millstein et al., 1997). In addition, an adult-ADHD diagnosis has been shown to predict treatment response, with approximately 80% of cases reporting relief from stimulants (Wilens et al., 2002). Adverse medication effects in adults taking stimulants can also be predicted, one of which is hypertension (Wilens et al., 2002). In keeping with ADHD's heterogeneous profile, neurobiological correlates are also diverse (Biederman, 2005). However, it is acknowledged that abnormalities in frontal lobe functioning and connections to subcortical structures are at the base of this disorder (Biederman, 2005).

It is true that the problem of comorbidities permeates psychiatric disorders and is not specific to ADHD. However, when it comes to demonstrating the independence of adult-ADHD from other disorders, the case is weak. The reader by this point might have already become aware of the non-specificity and high sensitivity of ADHD symptoms. The aforementioned symptoms typical of an adult with ADHD are often overlooked as being a distinguishable disorder. Although an early study conducted by Milberger et al. (1995) concluded that ADHD was not an artifact of symptoms of comorbid disorders, newer studies consistently run into the problem of ADHD's non-specific symptoms. For example, Klassen and colleagues found that in adults with ADHD and bipolar disorder, a diagnosis of ADHD was often overlooked because its symptoms were attributed to bipolar disorder (Klassen et al., 2010). Likewise, in a study conducted by Gray and others, nicotine-dependent adolescent participants who had ADHD were more likely to concomitantly endorse symptoms of a withdrawal syndrome than nicotine dependent non-ADHD adults, due to overlap in the symptoms of the two conditions (Gray et al., 2010). Furthermore, the case of adults whose symptoms could not be traced back to seven years

of age demonstrates that there exists a constellation of symptoms that, although resembling ADHD, do not meet its diagnostic criteria (Karam et al., 2009; Kieling et al., 2010). As a result, it was concluded that clinicians should be less stringent when diagnosing adult-ADHD to prevent underdiagnosis (McGough and Barkle, 2004). If diagnostic criteria cannot even be agreed upon, and the current DSM-IV's condition of age-of-onset being before seven lacks empirical support, then a diagnosis of ADHD in adults will always be questionable.

This is all aside from the fact that because the adult must have manifested childhood-onset symptoms, the diagnosis itself becomes questionable. Time and again, concern has been expressed regarding retrospectively diagnosed conditions, mild traumatic brain injury being one example. The clinician and adult must now delve into the past, retrieve old report cards, and ask around, to discover whether childhood-ADHD is a reality. Such procedures are problematic in that they are often subject to a confirmation bias. Moreover, the difference in the method of diagnosing ADHD in childhood and adulthood may contribute to informant bias. In childhood parental and teacher rating scales are used, while in adults self-report is the primary method.

Future studies should address the nature of ADHD's persistence into adulthood, and determine whether the adult's ADHD-like assembly is indeed a result of childhood-ADHD persistence. Importantly, research should reliably differentiate adult-ADHD as a separate and independent disorder with symptoms that are not accounted for by comorbidity. The idea of adult-ADHD being a manifestation of characteristics left over from the disorder in childhood should also be considered. Once common and reliable neural and genetic correlates have been identified for the childhood and adulthood forms of ADHD, the reason for the disorder's differing manifestation across the patient's lifespan should be investigated. For instance, if reliable neural and genetic correlates are found, studies can examine the role of changing gene expression, or maturation of the implicated neural systems on these differences.

Acknowledgements

I would like to thank Simon Beshara, Diana Demian, and the editors for their help and advice during the writing process.

References

American Psychiatric Association. Task Force on, D.-I. and A. American Psychiatric, Diagnostic and statistical manual of mental disorders: DSM-IV-TR. Vol. 4th , text revision. 2000, Washington, DC: American Psychiatric Association.

Biederman, J. (2005). Attention-deficit/hyperactivity disorder: a selective overview. Society of Biological Psychiatry *57,* 1215-1220.

Corbett, K. (1998). Cross-gendered identifications and homosexual boyhood: toward a more complex theory of gender. American Journal of Orthopsychiatry *68*, 352-360.

Degenhardt, L., Bruno, R., and Topp, L. (2010). Is ecstasy a drug of dependence? Drug and Alcohol Dependence *107*, 1-10.

First, M.B., and Westen, D. (2007). Classification for clinical practice: how to make ICD and DSM better able to serve clinicians. International Review of Psychiatry *19*, 473-481.

Gray, K., Baker, N., Carpenter, M., Lewis, A., and Upadhyaya, H. (2010). Attention-deficit/hyperactivity disorder confounds nicotine withdrawal self-report in adolescent smokers. The Journal on American Additions *19,* 325-331.

Karam, R. G., Bau, C. H. D., Salgado, C. A. I., Kalil, K. L. S., Victor, M. M., Sousa, N. O., Vitola, E. S., Picon, F. A., Zeni, G. D., Rohde, L. A., Belmonte-de-Abreu, P., and Grevet, E. H. (2009). Late-onset ADHD in adults: Milder, but still dysfunctional. Journal of Psychiatric Research *43*, 697-701.

Kebir, O., Taabane, K., Sengupta, S., and Joober, R. (2009). Candidate genes and neuropsychological phenotypes in children with ADHD: Review of association studies. Journal of Psychiatry & Neuroscience *34*(2), 88-101.

Kieling, C., Kieling, R. R., Rohde, L. A., Frick, P. J., Moffitt, T., Nigg, J. T., Tannock, R., and Castellanos, F. X. (2010). The age at onset of attention deficit hyperactivity disorder. The American Journal of Psychiatry *167*, 14-16.

Klassen, L., Katzman, M., and Chokka, P. (2010). Adult ADHD and its comorbidities, with a focus on bipolar disorder. Journal of Affective Disorders *124*, 1-8.

Konrad, A., Dielentheis, T. F., El Masri, D., Bayerl, M., Fehr, C., Gesierich, T., Vucurevic, G., Stoeter, P., and Winterer, G. (2010). Disturbed structural connectivity is related to inattention and impulsivity in adult attention deficit hyperactivity disorder. European Journal of Neuroscience *31*, 912-919.

Lanktree, M., Squassina, A., Krinsky, M., Strauss, J., Jain, U., Macciardi, F., Kennedy, J., and Muglia, P. (2008). Association study of brain-derived neurotrophic factor (BDNF) and LIN-7 homolog (LIN-7) genes with adult attention-deficit/hyperactivity disorder. American Journal of Medical Genetics. Part B: Neuropsychiatric Genetics *147B*(6), 945-951.

Mayes, R., Bagwell, C., and Erkulwater, J. (2008). ADHD and the rise in stimulant use among children. Harvard Review of Psychiatry *16,* 151-166.

Mayes, R., and Rafalovich, A. (2007). Suffer the restless children: the evolution of ADHD and paediatric stimulant use, 1900–80. History of Psychiatry *18*, 435-457.

McGough, J. J., and Barkley, R. A. (2004). Diagnostic controversies in adult attention deficit hyperactivity disorder. The American Journal of Psychiatry *161*, 1948-1956.

Milberger, S., Biederman, J., Faraone, S. V., Murphy, J., and Tsuang, M. T. (1995). Attention deficit hyperactivity disorder and comorbid disorders: Issues of overlapping symptoms. The American Journal of Psychiatry *152*, 1793.

Millstein, R., Wilens, T., Biederman, J., and Spencer, T. (1997). Presenting ADHD symptoms and subtypes in clinically referred adults with ADHD. Journal of Attention Disorders *2*, 159-166.

Müller, D., Chiesa, A., Mandelli, L., De Luca, V., Ronchi, D., Jain, U., Serretti, A., Kennedy, J. (2010). Correlation of a set of gene variants, life events and personality features on adult ADHD severity. Journal of psychiatric research *44*(9), 598-604.

Schmidt, S., and Petermann F. (2009). Developmental psychopathology: attention deficit hyperactivity disorder (ADHD). BMC Psychiatry *9*.

Searight, H., and McLaren, A. (1998). Attention-defict hyperactivity disorder: the medicalization of misbehavior. Journal of Clinical Psychology in Medical Settings *5*, 467-495.

Sowell, E. R., Thompson, P. M., Welcome, S. E., Henkenius, A. L., Toga, A. W., and Peterson B.S. (2003). Cortical abnormalities in children and adolescents with attention-deficit hyperactivity disorder. The Lancet *362*, 1699-1707.

Wallien, M. S. C., and Cohen-Kettenis, P.T. (2008). Psychosexual outcome of gender-dysphoric children. Journal of the American Academy of Child and Adolescent Psychiatry *47*, 1413-1423.

Wilens, T., Biederman, J., and Spencer T. (2002). Attention deficit/hyperactivity disorder across the lifespan. Annual Review of Medicine *53*, 113-131.

Wright, R. (2005). Attention deficit hyperactivity disorder: what it is and what it is not. In R. P. Halgin (Eds.), *Taking sides: Clashing views in abnormal psychology* (5th ed., pp.144-153). New York: McGraw-Hill.

Addendum

JULS Online

JULS RESEARCH

Molecular effects of Noonan syndrome-associated RAF1 mutants with increased or decreased kinase activity

Jenny H. Hong[1,2], Xue, Wu[1,3], and Benjamin G. Neel[1,3]

[1]Department of Medical Biophysics, University of Toronto, Toronto, ON, Canada
[2]Ontario Cancer Institute, University Health Network, Toronto, ON, Canada
[3]Campbell Family Cancer Research Institute, Ontario Cancer Institute and Princess Margaret Hospital, University Health Network, Toronto, ON, Canada

ABSTRACT

Noonan syndrome (NS) is one of several autosomal dominant "RASopathies" caused by germline mutations in several components of the RAS-RAF-MEK-MAPK pathway. Raf1 (encoding the serine-threonine kinase RAF1) mutations account for 3-5% of NS, and unlike other NS alleles, Raf1 mutations that confer increased kinase activity are highly associated with hypertrophic cardiomyopathy (HCM). It remains unclear how these Raf1 mutations cause NS, and why some mutant Raf1 proteins induce HCM. To address these questions, two lines of "knock-in" mice were generated: kinase-activated (L613V) and impaired (D486N) Raf1 mutants. Similar to NS patients, L613V/+ mice showed key NS phenotypes and developed HCM. In contrast, D486N/+ mice did not develop HCM and showed only some of the NS phenotypes. Phosphorylation status of signaling molecules associated with Raf1's kinase-dependent-functions (Mek, Erk) and Raf1's kinase-independent (Akt, Jnk, p38) functions in mouse embryonic fibroblasts (MEFs) were determined through immunoblotting. Unexpectedly, both Raf1 mutants enhanced Mek and Erk activation relative to WT, but to different degrees and through different kinetics. Enhanced Mek and Erk activation may therefore be critical in causing NS, and the level and duration of Mek and Erk activation may be responsible for evoking different cardiac and NS phenotypes. Inhibitors targeted to the Raf/Mek/Erk pathway may ameliorate the cardiac and other manifestations of NS, offering a potential treatment to NS patients with specific Raf1 mutations.

INTRODUCTION

Cardiac hypertrophy is a major way by which cardiomyocytes respond to enhanced hemodynamic demand, and it is a clinical hallmark of hypertrophic cardiomyopathy (HCM) (Heineke and Molkentin, 2006; Lorenz et al., 2009). There are two types of cardiac hypertrophy: 1) physiological, which is associated with exercise and pregnancy; and 2) pathological, which stems from genetic factors or from secondary factors (such as hypertension). In contrast to physiological stimuli, interstitial fibrosis and fetal-gene expression are induced by pathological stimuli of cardiac hypertrophy and lead to myocardial stiffness and decrease in cardiac output, all of which eventually result in heart failure, arrhythmia and sudden death (Lorenz et al., 2009).

The RAS-RAF-MEK-ERK (RAS/MAPK) pathway has an important but controversial role in mediating cardiac hypertrophy. Some data has suggested that enhanced activation of the RAS/MAPK pathway causes HCM, whereas other data suggest it is only involved in physiological rather than pathological hypertrophy (Bueno and Molkentin, 2002, Lorenz et al., 2009). In response to multiple agonists, including growth factors (e.g. EGF, PDGF), G-protein coupled receptor agonists, and physical stimuli in cardiomyocytes and other cell types, the RAS/MAPK pathway becomes activated and controls many fundamental cellular processes including cell proliferation, differentiation and growth (McCubrey et al., 2007). Following receptor stimulation, activated RAS recruits RAF proteins (serine/threonine kinases) to the cell membrane, where it subsequently phosphorylates and activates MEK1/2. Activated MEK1,2 then phosphorylates and activates ERK1/2, inducing ERK1,2's translocation into the nucleus to stimulate gene expression programs (Muslin, 2005; Yamazaki et al., 1998). In mammals, there are three isoforms of RAF: A-RAF, B-RAF, and C-RAF (RAF1). RAF1 was the first one to be studied and it is ubiquitously expressed in all cell types (Leicht et al., 2007). Other pathways that contribute to pathological hypertrophy include calcineurin/NFAT, PI3K/AKT/MTOR, GSK3b and SAPK pathways (JNK and p38) (Dorn and Force, 2005; Liang and Molkentin, 2003; Lorenz et al., 2009; Malumbres and Barbacid, 2003). The aberrant activation of which of the pathways evoke hypertrophy remain unclear.

Noonan syndrome (NS) is a common autosomal dominant disorder caused by germline mutations in several components of the RAS/MAPK pathway (Aoki et al., 2008; Bentires-Alj et al., 2006). Cardiovascular abnormalities occur in a majority of affected individuals with primarily pulmonary valvularstenosis, septal defects and hypertrophic cardiomyopathy (HCM) (Chan et al., 2008). About 50% of NS patients have mutations in the PTPN11 gene, encoding the tyrosine phosphatase SHP-2 (Tartaglia et al., 2001). Missense mutations in RAF1 account for ~3-5% of NS cases. Unlike the other germline mutations, RAF1 mutations that show increased in vitro kinase activity are highly associated with HCM (95%, compared with 18% prevalence in NS patients overall), whereas RAF1 mutations with decreased in vitro kinase activity are not highly associated (Pandit et al., 2007). Our laboratory has since generated two lines of "straight knock-in" mice expressing kinase-activating (L613V) and impaired (D486N) Raf1 mutations respectively. All mice were obtained at the expected Mendelian ratios at weaning. Like NS patients, L613V/+ (LV/+) mice showed key NS features, including short stature, craniofacial abnoramlities, and aberrant myeloid progenitors in bone marrow. LV/+ mice also developed progressive HCM, accompanied by chamber dilation and fibrosis. DN/+ mice showed some of the key NS phenotypes but they did not develop cardiac hypertrophy. It remains to be established how these two types of Raf1 mutations cause NS and how mutant Raf1 protein induce HCM.

In this study, we began to examine the molecular effects of the Raf1 mutations in vivo in order to understand the molecular basis of NS and HCM. Our biochemical data show that through different kinetics, both LV and DN mutants enhance the level of activation of Mek and Erk. The level of increase in Mek and Erk activations also differ between the mutants. Enhanced Mek/Erk activity may therefore be critical for causing Raf1-mutant NS phenotypes. The differences in the effects of Ras/MAPK pathway may contribute to the differences in the syndromic phenotypes observed in the mouse models.

MATERIALS AND METHODS

Primary MEF preparation and cell treatments

MEFs were prepared from E.13.5 embryos and cultured in DMEM with 10% FBS, along with 100 mg/ml penicillin, and 100µg/ml streptomycin. For growth factor stimulation, MEFs were starved for 20 h in serum-free DMEM, and then stimulated with 10ng/ml EGF, or 50ng/ml PDGF. For inhibitor studies, cells were starved as indicated above, and then incubated with MEK inhibitor CI-1040, PD0098059 (2 µM) for 30 minutes before and during stimulation with 10ng/ml EGF. A matched concentration of empty vehicle (DMSO) was used as a control.

SDS-PAGE and protein analysis

Cells were washed twice with cold PBS and incubated in RIPA buffer (50mM Tris.HCL pH 7.5, 150 mM NaCl, 1% NP40, 2mM EDTA, 0.5% Na Deoxycholate, 0.1% SDS, 10 mMNaF, 10 mMβ-glycerophosphate, 1 mM Na3VO4, 2 ug/mL PMSF, 20 µg/ml aprotinin, 20 µg/ml leupeptin, 10µg/ml antipain, and 2µg/ml pepstatin) for 15 min at 40C. Cell lysates were cleared by centrifugation at 13,200 rpm for 20 min at 40C and total protein concentrations were determined using the Bradford assay (at 595nm). Immunoblotting was performed by a previously described method (Zheng et al., 2000). With Shp2 used as a loading control, membranes were probed with the following antibodies from Cell Signaling Technology: anti-Akt1 (2H10), anti-phosphoAkt (Ser 473), anti-phospho SAPK/JNK (Thr183/Tyr185), anti-phospho p38 MAPK (Thr180/Tyr182), anti p38 MAP kinase, anti-phospho MEK1/2 (Ser217/221), and anti-MEK1/2. Anti-SHPTP2 (C-18), anti-ERK 2 (D-2) antibodies were purchased from Santa Cruz Biotechnology INC., and anti-c-Raf mouse antibody was from BD Transduction Laboratories. Dilutions used for each antibody used varied from 1 in 200 to 1 in 1000. Goat anti-mouse IRDye800CW and goat anti-rabbit IRDye680 secondary antibodies (LI-COR) were used depending on the primary antibody. The results were visualized and quantified by Li-COR system and Odyssey v3.0 program.

Statistical Analysis:

For sample sizes equal to or greater than 3, results are shown as mean +SD. Paired experimental groups were analyzed using the two-tailed Student's t-test. For three or more experimental groups, ANOVA was used to analyze the data. $p<0.05$ was considered statistically significant.

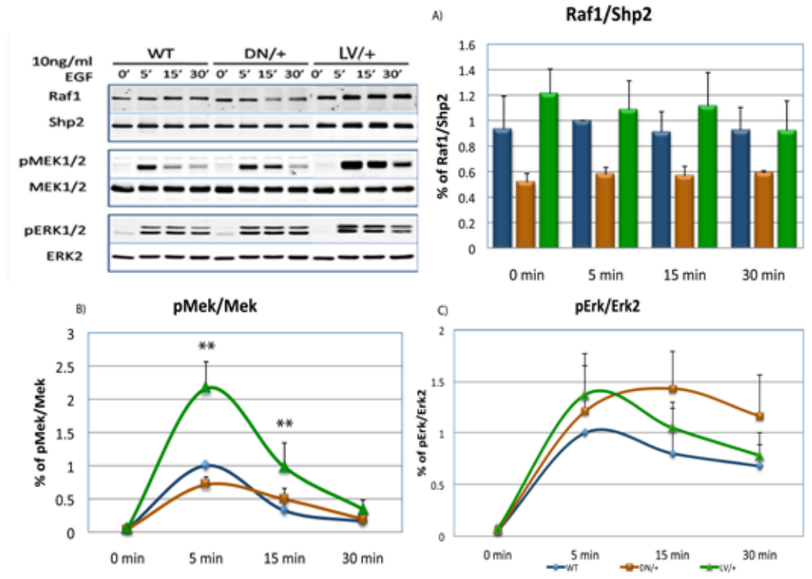

Figure 1: The effects of NS Raf1 D486N and L613V Mutants on Mek/Erk activation in response to EGF. WT, Raf1D486N/+ and Raf1L613V/+ MEFs were stimulated with EGF and lysed at indicated times. Lysates were blotted with the indicated antibodies. The quantified ratios of Raf1/Shp2 (a), pMek/Mek (b) and pErk/Erk (c) are shown in the right panel (n=4). **: p<0.001. Error bars indicate +SD. Delayed Mek activation, and sustained Erk activation were observed in DN/+ MEFs. However, in LV/+ MEFs, the kinetics for Mek and Erk activation followed that of WT. MEK activation was significantly enhanced in LV/+ MEFs.

RESULTS

DN and LV mutant enhance Mek and Erk activation

To investigate the molecular effects of RAF1 mutations on the RAS/MAPK pathway in vivo, MEFs were prepared from the mouse models and stimulated with growth factors. Relative to the WT MEFs, the level of Mek and Erk activation was enhanced at later time points in DN/+ MEFs (Figure 1 b, c), even though

the level of Raf1 expression was only 60-70% of the expression level seen in WT (and LV/+) cells (Figure 1 a). Relative to WT MEFs, the level of Mek and Erk activation were also enhanced in LV/+ MEFs, with a significantly higher Mek activation at 5 minute and 15 minute ($p<0.001$, Figure 1b). Although both types of Raf1 mutations seem to enhance the kinase activity of Raf1 (gain-of-function), the signaling kinetics is different between the mutant cell lines. The activation of Mek was delayed in DN/+ MEFs, peaking at 15 minutes, as opposed to at 5 minutes in both WT and LV/+ MEFs. The kinetics for Erk activation in DN/+ MEFs also differed from that of WT and LV/+ MEFs. As opposed to a subsequent decline after 15 minutes, Erk activation in DN/+ MEFs was sustained from 5 minutes and onwards (Figure 1 c) Together these data show that both DN and LV mutant evoke enhanced Mek and Erk activation following EGF stimulation although via different kinetics of activation.

MEFs were then stimulated with PDGF to determine whether the increases in Mek and Erk activation are also observed in response to others stimuli. In comparison to EGF stimulation, PDGF stimulation induced enhanced levels of Mek and Erk activation to a lesser degree in both DN and LV mutants (Figure 2). Moreover, the kinetics of Mek and Erk activation in the mutant MEFs followed the same trend as that in the WT MEFs. Interestingly, the stability of Raf1DN/+ protein was not affected upon PDGF stimulation. The data suggest that, depending on the stimulus, the effects of Raf1 mutants on the RAS/MAPK pathway may vary.

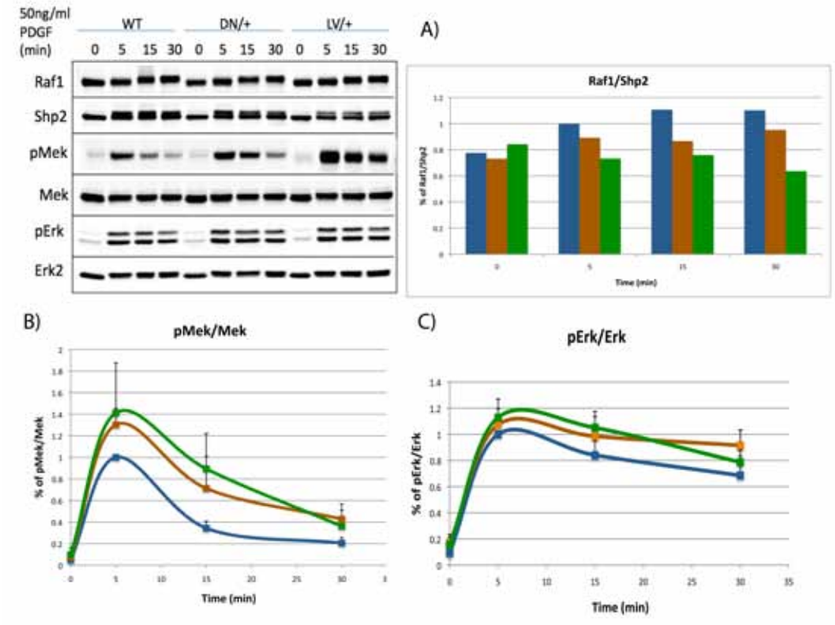

Figure 2: The effects of NS Raf1 D486N and L613V Mutants on Mek/Erk activation in response to PDGF. WT, Raf1D486N/+ and Raf1D486N/D486N MEFs were stimulated with PDGF and lysed at indicated times. Lysates were blotted with the indicated antibodies. The quantified ratios of Raf1/Shp2 (n=2) (a), pMek/Mek (b) and pErk/Erk (c) are shown in the right panel (n=3). Mutant Raf1 proteins evoked increase in Mek and Erk activation relative to WT protein.

Raf1 LV/+ mutant evokes a higher Jnk activation upon PDGF stimulation

To delineate between the pathways that evoke cardiac hypertrophy, the level of activation of other mediators of pathological hypertrophy (i.e. PI3K/Akt, Jnk and p38) were investigated.

Upon EGF stimulation, the levels of Akt, Jnk, and p38 activation were comparable between the WT and mutant MEFs (Figure 3). In response to PDGF, the level of Akt activation was again unaffected in all cell types. However, in DN/+ MEFs, p38 activation was sustained for a longer period of time (up to 15 minutes) relative to the other cell types (Figure 4b); and in LV/+ MEFs, there was a two-fold increase in Jnk activation at 5 and 15 minutes relative to WT and DN/+ MEFs ($p<0.05$, Figure 4c). Together, these data suggest that DN and LV mutants do not affect Akt, Jnk, and p38 activation upon EGF stimulation. However, upon PDGF stimulation, Raf1 mutant proteins evoke dissimilar increases in Jnk and p38 pathways.

CI-1040 effectively inhibits Erk activation in WT and mutant MEFs

Since both DN and LV mutants enhance activation of the Ras/MAPK pathway, inhibitors targeted to this pathway may be able to reverse the syndromic phenotypes seen in the mice models. As a result, inhibitor studies were carried out in MEFs using the Mek inhibitor, CI-1040 to test whether CI-1040 can effectively inhibit Erk activation. After incubating MEFs with CI-1040, the drug was able to completely inhibit Erk activation in both the mutant and WT MEFs (Figure 5 and 6). CI-1040 was less effective at inhibiting Mek activation.

DISCUSSION

Effects of DN and LV mutant on Mek and Erk activation

In the adult heart, MAPK pathways are important mediators of pathological cardiac hypertrophy. To better understand the role of RAS/MAPK pathway in HCM, we have generated two mouse models, bearing two different RAF1 mutations, one that is highly associated with HCM (L613V) in NS patients and one that is not associated with HCM (D486N) in NS patients.

Despite the lower level of Raf1 protein observed in DN/+ MEFs, both DN and LV mutants evoke increased Mek and Erk activation upon EGF stimulation. This opposes the results shown in Pandit et al (2006), where DN and LV mutants were over-expressed in COS1 cell-lines. The in vitro studies showed that LV mutant has increased kinase activity and enhanced ERK activation, whereas DN mutant has decreased kinase activity and reduced ERK activation. Over-expression studies may therefore not be able to accurately predict the molecular basis of NS features caused by NS mutations. Since the DN mutant is kinase-impaired, it is likely to enhance Mek activation by increasing the activity of BRaf and/or ARaf through heterodimerization (Rushworth et al., 2006). RAF1 has been shown to have a scaffolding role in enhancing BRAF's kinase activity (or vice versa) by heterodimerizing with BRAF. Heterodimers also have increased kinase activity compared to respective homodimers or monomers (Rushworth et al., 2006). Indeed, our Preliminary Data suggest that relative to WT Raf1, both Raf1 mutants increased heterodimerization with BRaf upon EGF stimulation (data not shown). Since Raf1 LV mutant is kinase-activating, it is likely to enhance Mek and Erk activation as homodimers, or heterodimers with ARaf, BRaf and/or Ksr (Rajakulendran et al., 2009). Therefore, although DN is kinase impaired, it acts as a gain-of-function (enhanced kinase activity) mutant when expressed under endogenous promoter control. Together these data may explain why both DN and LV mutations cause NS, since both mutants are able to hyperactivate the RAS/MAPK pathway.

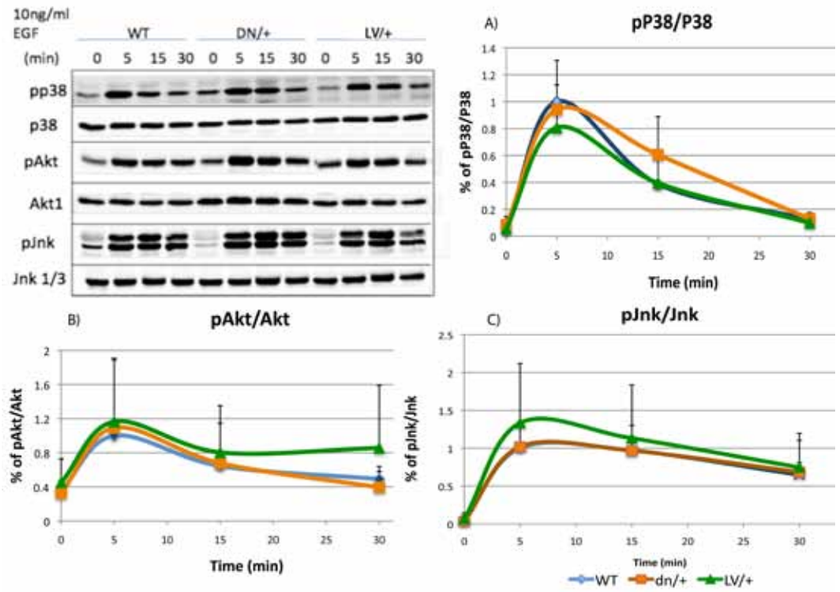

Figure 3: The effects of NS Raf1 D486N and L613V Mutants on Akt, Jnk and p38 activation in response to EGF. WT, Raf1D486N/+ and Raf1L613V/+ MEFs were stimulated with EGF and lysed at indicated times. Lysates were blotted with the indicated antibodies. The quantified ratios of pp38/p38 (a), pAkt/Akt (b), and pJnk/Jnk (c) are shown in the right panel (n=3). Error bars indicate +SD. The levels of activation of p38, Akt, and Jnk were similar between the three cell types, WT, DN/+ and LV/+.

The kinetics and magnitude of Mek and Erk activation

Although both DN and LV mutants enhanced Ras/MAPK signaling, distinct signaling profiles were found in comparison to each other and relative to the WT. In DN/+ MEFs, Mek activation was delayed upon EGF stimulation, peaking at 15 minutes (Figure 1 b). Moreover, Erk activation was sustained in DN/+ MEFs (Figure 1 c). Because the biological outcome is dependent on the duration of Ras/MAPK pathway (Marshall, 1995), the differences in kinetics of Erk activation between DN/+ and LV/+ MEFs may account for the differences in NS phenotypes and the different degree of cardiac hypertrophy seen in the two mouse models.

Variations in the activation kinetics were also stimulus dependent. The kinetic of Mek and Erk activation was comparable between the different MEFs upon PDGF stimulation, but deviated significantly in response to EGF (Figures 1,3). Stimuli-induced feedback regulation at the level of Raf1 may account for the different kinetic effects. Preliminary data showed that the kinetic of Raf1 phosphorylation at S338 is different upon EGF and PDGF stimulation (data not shown). S338 is a key, activating residue that is necessary for Raf1 activation (Dhillon et al., 2002). In contrast to PDGF stimulation, the phosphorylation level at S338 was prolonged and sustained in LV/+ MEFs upon EGF stimulation. The differential phosphorylation kinetics of S338 and perhaps other regulator residues of Raf1 are likely to explain why the stability of Raf1DN/+ protein varies depending on the stimulus.

The magnitudes of Mek and Erk activation were also different between DN/+ and LV/+ MEFs. The DN mutant evoked a higher Erk activation relative to LV/+ mutant, whereas the LV mutant evoked a higher Mek activation relative to DN mutant (Figures 2 b, c). The different magnitudes of Erk activation evoked by DN/+ and LV/+ mutants may be responsible for causing the distinct cardiac phenotypes observed in the mouse models. Whether levels of Erk activation are critical for HCM needs to be further examined by genetic and pharmacological approaches.

Effects of DN and LV mutant on other signaling pathways

Increasing evidences over the years indicate that Raf1 not only acts as a kinase, but has kinase independent functions as well, most notably for its anti-apoptotic functions. For instance, Raf1 regulates the activities of Jnks and p38 kinases through its physical interaction with the pro-apoptotic kinase, ASK1 (Chen et al., 2001; Yamaguchi et al., 2004). Raf1 also interacts with Akt to enhance the PI3K pathway to promote cell survival (Zimmermann and Moelling, 1999). From our mouse models, it was found that depending on the stimulus, DN and LV mutants differentially enhanced p38 and Jnk activation (Figures 3 and 4). This may be because of the different feedback regulation involved in response

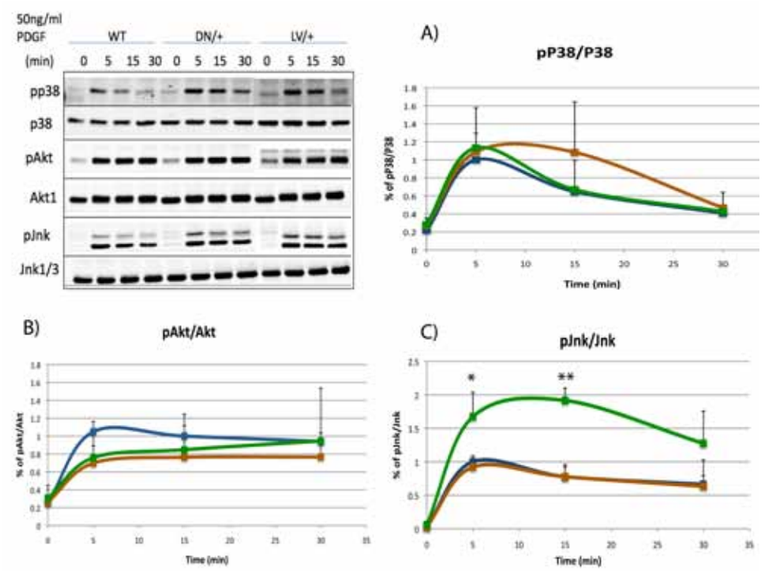

Figure 4: The effects of NS Raf1 D486N and L613V Mutants on Akt, Jnk and p38 activation in response to PDGF. WT, Raf1D486N/+ and Raf1L613V/+ MEFs were stimulated with PDGF and lysed at indicated times. Lysates were blotted with the indicated antibodies. The quantified ratios of pp38/p38 (a), pAkt/Akt (b), and pJnk/Jnk (c) are shown in the right panel (n=3). Error bars indicate +SD. *: p<0.05, **: p<0.001.In DN/+ MEFs, the activation of p38 was delayed. In LV/+ MEFs, the activation of Jnk was significantly enhanced at 5 and 15 minutes.

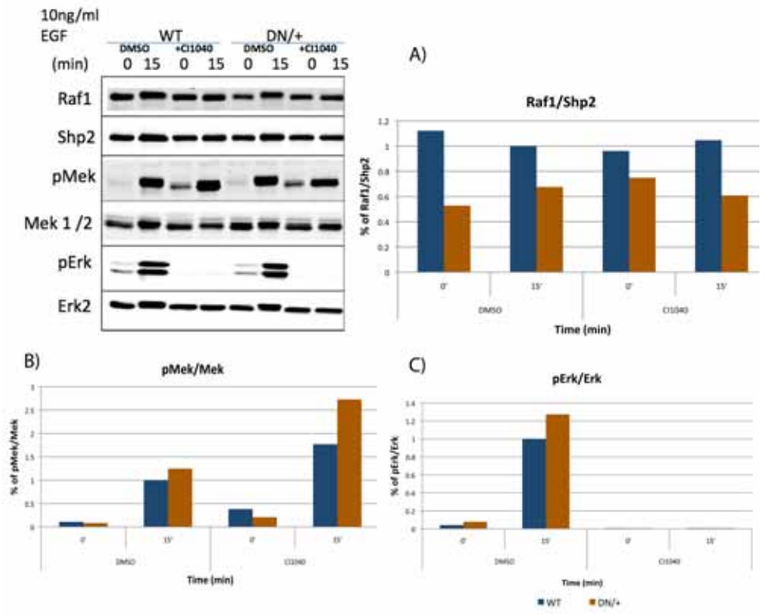

Figure 5: The effect of the Mek inhibitor (CI-1040) in WT, and Raf1D486N MEFs . WT, and DN/+ MEFs were incubated with CI-1040 (2 μM) for 30 minutes prior to stimulation with EGF. Cells were lysed at the indicated times, and lysates were blotted with the indicated antibodies. The quantified ratios of Raf1/Shp2 (a), pMek/Mek (b) and pErk/Erk (c) are shown in the right panel (n=2). CI-1040 completely inhibited Erk activation in WT, DN/+, and LV/+ MEFs.

to EGF and PDGF. Further investigation in understanding the feedback regulation is needed.

Enhancement in p38 and Jnk activation may also have phenotypic implications for the mouse model. Constitutive activation of Jnk or p38 in the mouse heart has been shown to promote dilated cardiomyopathy and heart failure (Liang and Molkentin, 2003). This is consistent with the cardiac phenotypes observed in LV/+ mice. Although DN/+ mice did not develop cardiac hypertrophy, increased gene dosage evoked cardiac hypertrophy (unpublished data). Progression to HCM in DN/DN mice is unclear. Together these data suggest that DN and LV mutants induce NS-associated phenotypes through different molecular mechanisms, possibly through different pathways.

Effects of CI1040 on Mek and Erk activation in MEFs

Since our data suggested that hyperactivation of the Ras/MAPK pathway may account for causing NS and the genesis of HCM, therapeutics targeted to components of this pathway would be useful in ameliorating NS and abnormal cardiac phenotypes. Genetic ablation of Erk1/2 (Araki et al., 2009; Krenz et al., 2008) or pre-natal treatment with a MEK inhibitor (Barrett et al., 2008; Nakamura et al., 2009) has been shown to prevent some NS phenotypes. CI-1040 was one of the first to be tested clinically (Barrett et al., 2008; Halilovic and Solit, 2008). At 2μM, CI-1040 completely inhibited Erk activation in WT and mutant MEFs (Figures 5 and 6). The reason for the inefficiency toward Mek may be a result of its protein dissociation constant, or a consequence of its toxicity and inhibitory effects on kinases that may negatively regulate Mek1/2 (Barrett et al., 2008). Since the completion of this study, CI-1040 has been administered to LV/+ mice and was successful in rescuing the NS and cardiac phenotypes (Wu et al., 2011).

CONCLUSION

The knock-in mouse models of NS-associated RAF1 mutations can serve as a way to examine the role of RAS/MAPK in inducing pathological cardiac hypertrophy. In this study, two types of NS-associated RAF1 mutations, D486N and L613V, were shown to enhance the

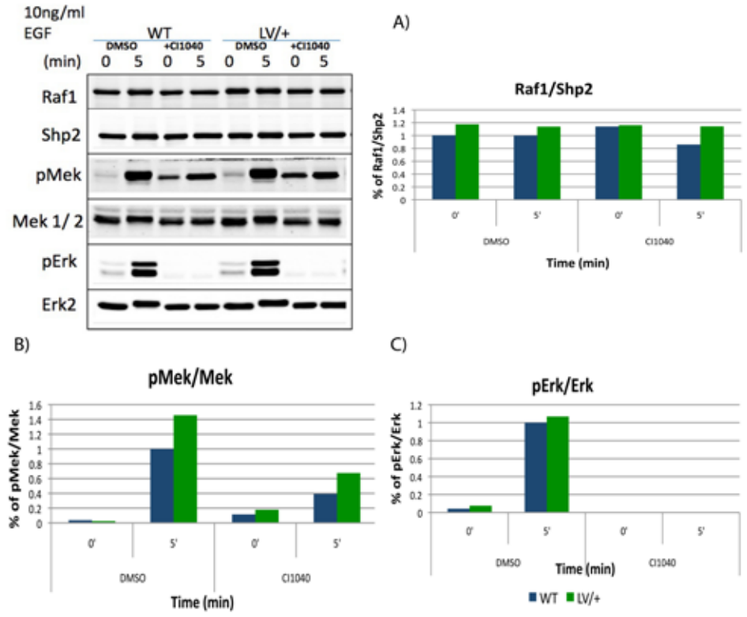

Figure 6: The effect of the Mek inhibitor (CI-1040) in WT, and Raf1L613V/+ MEFs. WT, and LV/+ MEFs were incubated with CI-1040 (2 μM) for 30 minutes prior to stimulation with EGF. Cells were lysed at the indicated times, and lysates were blotted with the indicated antibodies. The quantified ratios of Raf1/Shp2 (a), pMek/Mek (b) and pErk/Erk (c) are shown in the right panel (n=2). CI-1040 completely inhibited Erk activation in WT and LV MEFs.

level of Mek and Erk activation. In comparison to other pathways, hyperactivation of Erk appears to be an important mediator of NS phenotypes. Differences in the kinetics and magnitude of Erk activation between the two mutants may help to explain the different cardiac phenotypes observed in the mouse models. The Mek inhibitor (CI-1040) appears to be an effective drug in inhibiting Erk activation evoked by the Raf1 mutants. To better understand the molecular basis of NS, it is important to examine, in the future, the effects of DN and LV mutants in heart cell-types, such as cardiomyocytes and cardiac fibroblasts.

ACKNOWLEDGEMENTS

I would like to thank Xue Wu and Dr. Benjamin Neel for their guidance on this project. I would also like to thank Dr. Neel for giving me the opportunity to work in his lab. I would also like to thank the other lab members for their supervision and guidance as well.

REFERENCES

1. Aoki, Y., Niihori, T., Narumi, Y., Kure, S., and Matsubara, Y. (2008). The RAS/MAPK syndromes: novel roles of the RAS pathway in human genetic disorders. Hum Mutat 29, 992-1006.
2. Araki, T., Chan, G., Newbigging, S., Morikawa, L., Bronson, R.T., and Neel, B.G. (2009). Noonan syndrome cardiac defects are caused by PTPN11 acting in endocardium to enhance endocardial-mesenchymal transformation. Proc Natl Acad Sci U S A 106, 4736-4741.
3. Barrett, S.D., Bridges, A.J., Dudley, D.T., Saltiel, A.R., Fergus, J.H., Flamme, C.M., Delaney, A.M., Kaufman, M., LePage, S., Leopold, W.R., et al. (2008). The discovery of the benzhydroxamate MEK inhibitors CI-1040 and PD 0325901. Bioorg Med Chem Lett 18, 6501-6504.
4. Bentires-Alj, M., Kontaridis, M.I., and Neel, B.G. (2006). Stops along the RAS pathway in human genetic disease. Nat Med 12, 283-285.
5. Bueno, O.F., and Molkentin, J.D. (2002). Involvement of extracellular signal-regulated kinases 1/2 in cardiac hypertrophy and cell death. Circ Res 91, 776-781.
6. Chan, G., Kalaitzidis, D., and Neel, B.G. (2008). The tyrosine phosphatase Shp2 (PTPN11) in cancer. Cancer Metastasis Rev 27, 179-192.
7. Chen, J., Fujii, K., Zhang, L., Roberts, T., and Fu, H. (2001). Raf-1 promotes cell survival by antagonizing apoptosis signal-regulating kinase 1 through a MEK-ERK independent mechanism. Proc Natl Acad Sci U S A 98, 7783-7788.
8. Dhillon, A.S., Meikle, S., Yazici, Z., Eulitz, M., and Kolch, W. (2002). Regulation of Raf-1 activation and signalling by dephosphorylation. EMBO J 21, 64-71.
9. Dorn, G.W., 2nd, and Force, T. (2005). Protein kinase cascades in the regulation of cardiac hypertrophy. J Clin Invest 115, 527-537.
10. Halilovic, E., and Solit, D.B. (2008). Therapeutic strategies for inhibiting oncogenic BRAF signaling. Curr Opin Pharmacol 8, 419-426.
11. Heineke, J., and Molkentin, J.D. (2006). Regulation of cardiac hypertrophy by intracellular signalling pathways. Nat Rev Mol Cell Biol 7, 589-600.
12. Krenz, M., Gulick, J., Osinska, H.E., Colbert, M.C., Molkentin, J.D., and Robbins, J. (2008). Role of ERK1/2 signaling in congenital valve malformations in Noonan syndrome. Proc Natl Acad Sci U S A 105, 18930-18935.
13. Leicht, D.T., Balan, V., Kaplun, A., Singh-Gupta, V., Kaplun, L., Dobson, M., and Tzivion, G. (2007). Raf kinases: Function, regulation and role in human cancer. Biochimica et Biophysica Acta 1773, 1196-1212.
14. Liang, Q., and Molkentin, J.D. (2003). Redefining the roles of p38 and JNK signaling in cardiac hypertrophy: dichotomy between cultured myocytes and animal models. J Mol Cell Cardiol 35, 1385-1394.
15. Lorenz, K., Schmitt, J.P., Schmitteckert, E.M., and Lohse, M.J. (2009). A new type of ERK1/2 autophosphorylation causes cardiac hypertrophy. Nat Med 15, 75-83.
16. Malumbres, M., and Barbacid, M. (2003). RAS oncogenes: the first 30 years. Nat Rev Cancer 3, 459-465.
17. Marshall, C.J. (1995). Specificity of receptor tyrosine kinase signaling: transient versus sustained extracellular signal-regulated kinase activation. Cell 80, 179-185.
18. McCubrey, J.A., Steelman, L.S., Chappell, W.H., Abrams, S.L., Wong, E.W., Chang, F., Lehmann, B., Terrian, D.M., Milella, M., Tafuri, A., et al. (2007). Roles of the Raf/MEK/ERK pathway in cell growth, malignant transformation and drug resistance. Biochim Biophys Acta 1773, 1263-1284.
19. Muslin, A.J. (2005). Role of raf proteins in cardiac hypertrophy and cardiomyocyte survival. Trends Cardiovasc Med 15, 225-229.
20. Nakamura, T., Gulick, J., Pratt, R., and Robbins, J. (2009). Noonan syndrome is associated with enhanced pERK activity, the repression of which can prevent craniofacial malformations. Proc Natl Acad Sci U S A 106, 15436-15441.
21. Pandit, B., Sarkozy, A., Pennacchio, L.A., Carta, C., Oishi, K., Martinelli, S., Pogna, E.A., Schackwitz, W., Ustaszewska, A., Landstrom, A., et al. (2007). Gain-of-function RAF1 mutations cause Noonan and LEOPARD syndromes with hypertrophic cardiomyopathy. Nat Genet 39, 1007-1012.
22. Rajakulendran, T., Sahmi, M., Lefrancois, M., Sicheri, F., and Therrien, M. (2009). A dimerization-dependent mechanism drives RAF catalytic activation. Nature 461, 542-545.
23. Rushworth, L.K., Hindley, A.D., O'Neill, E., and Kolch, W. (2006). Regulation and role of Raf-1/B-Raf heterodimerization. Mol Cell Biol 26, 2262-2272.
24. Tartaglia, M., Mehler, E.L., Goldberg, R., Zampino, G., Brunner, H.G., Kremer, H., van der Burgt, I., Crosby, A.H., Ion, A., Jeffery, S., et al. (2001). Mutations in PTPN11, encoding the protein tyrosine phosphatase SHP-2, cause Noonan syndrome. Nat Genet 29, 465-468.
25. Wu, X., Simpson, J., Hong, J.H., Kim, K., Thavarajah, N.K., Backx, P.H., Neel, B.G., and Araki, T. (2011). MEK-ERK pathway modulation ameliorates disease phenotypes in a mouse model Noonan syndrome associated with the Raf1L613V mutation. J Clin Invest doi:10.1172/JCI44929.
26. Yamaguchi, O., Watanabe, T., Nishida, K., Kashiwase, K., Higuchi, Y., Takeda, T., Hikoso, S., Hirotani, S., Asahi, M., Taniike, M., et al. (2004). Cardiac-specific disruption of the c-raf-1 gene induces cardiac dysfunction and apoptosis. J Clin Invest 114, 937-943.
27. Yamazaki, T., Komuro, I., and Yazaki, Y. (1998). Signalling pathways for cardiac hypertrophy. Cell Signal 10, 693-698.
28. Zheng, X.M., Resnick, R.J., and Shalloway, D. (2000). A phosphotyrosine displacement mechanism for activation of Src by PTPalpha. EMBO J 19, 964-978.
29. Zimmermann, S., and Moelling, K. (1999). Phosphorylation and regulation of Raf by Akt (protein kinase B). Science 286, 1741-1744.

Targeting NMDARs: A Treatment for Inflammatory and Neuropathic Pain

Kelly Jamieson

When faced with the problem of treating chronic pain, researchers have been halted in their tracks by the glutamate receptors known as N-methyl-D-aspartate receptors, or NMDARs.

These receptors are responsible for facilitating communication between neurons in the Central Nervous System, which is the source of hypersensitivity to chronic pain [2]. In the past, treatment of chronic pain using drugs that block NMDARs hindered the other vital functions of the NMDARs such as breathing and locomotion [1].

However, Professor Michael W. Salter and his team at the University of Toronto Center for the Study of Pain have designed a peptide that prohibits the interaction of proteins inside the NMDARs without being detrimental to the NMDARs' other functions. NMDARs are multiprotein complexes made up of four subunits: two NR1 subunits and two NR2A-2D subunits which form the ion channel conductance pathway [1]. The newly developed peptide, referred to as Src40-49Tat, is composed of amino acids 40-49 of Src joined to the protein transduction domain of the HIV Tat protein [1]. The peptide functions by specifically blocking tyrosine kinase Src, an imperative regulatory hub within the NMDARs, from interacting with NADH dehydrogenase subunit 2 (ND2) which is an adaptor protein that anchors Src in the NMDARs [1]. By inhibiting this anchoring process, the Src40-49Tat selectively prevents the amplification of the NMDARs. Without being anchored, the Src is released from the NMDARs which removes the enzymes from the substrate, thus inhibiting the catalytic function of Src required for the upregulation of the NMDARs [1]. Src40-49Tat therefore blocks the functions of the NMDARs and Src with regards to chronic pain without eliminating either of them completely and without compromising their other functions.

Src40-49 was developed by synthesizing a series of overlapping 10-amino-acid peptides spanning the region vital for Src-ND2 interaction [1]. Other peptides such as Src45-54 or Src49-58 were synthesized but were unable to bind to ND2.1, the interacting domain of ND2 [1]. Since Src40-49 is predicted to be membrane impermeable, using it alone would be ineffective so Michael W. Salter and his team fused the protein transduction domain of the HIV Tat protein to the Src40-49 peptide to form Src40-49Tat [1]. The testing phase of the research included injecting the Src40-49Tat into rodent models 45 minutes before dilute formalin was injected to cause inflammatory pain [1]. The Src40-49Tat injections significantly reduced flinching, biting, or licking behaviours when compared with saline vehicles, Tat-protein transduction domain, and other controls [1,2]. Other tests yielded similar results, Complete Freund's Adjuvant and nerve induced pain behaviours were both reversed with Src40-49Tat [1].

These findings are significant in that the disruption of Src-ND2 interaction could treat a wide variety of chronic pain disorders. Inflammatory and neuropathic pain are both dependent on Src and this common characteristic creates a common target for treatment. Having a single treatment for both types of pain is very convenient as distinguishing between inflammatory and neuropathic pain can often be problematic. Also, in neurodegenerative disorders, such as epilepsy and stroke, it has been implicated that NMDARs are involved instead of basal receptor function [1]. Thus, targeting Src may be useful in future research into other NMDAR-dependent Central Nervous System pathologies [1].

References

1. Liu, X. J., J. R. Gingrich, et al. (2008). "Treatment of inflammatory and neuropathic pain by uncoupling Src from the NMDA receptor complex." Nature Medicine 14(12): 1325-1332.
2. Wolfe, C. J. and M. W. Salter (2000). "Neuronal Plasticity: Increasing the Gain in Pain." Science Magazine 288(5472): 1765-1768.

Sponsors

The Journal of Undergraduate Life Sciences would like to thank the following sponsors for supporting the production of this year's issue.

UNIVERSITY OF TORONTO
FACULTY OF MEDICINE

Biochemistry
Laboratory Medicine and Pathobiology
Molecular Genetics
Immunology
Pharmacology and Toxicology

Western Schulich MEDICINE & DENTISTRY

University College, Toronto
UNIVERSITY OF TORONTO

UNIVERSITY OF TORONTO LIBRARIES

McMaster University

ISSN 1911-8899 | University of Toronto Journal of Undergraduate Life Sciences (Print)
| juls.sa.utoronto.ca
| jps.library.utoronto.ca/index.php/juls

DISCOVERY @ utoronto

Graduate studies in biomedical research: Training leaders of tomorrow

www.facmed.utoronto.ca

cancer

endocrinology

biochemistry

stem cells

proteomics

medical imaging

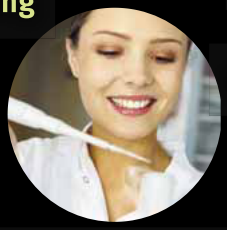

structural, molecular & cell biology

neuroscience

reproduction

immunology

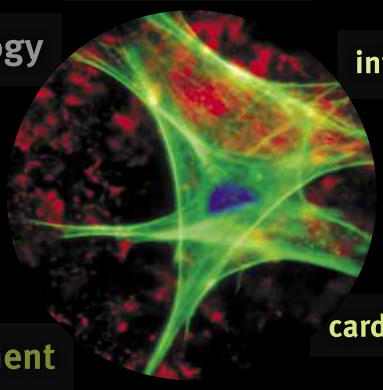

infection & immunity

genetics

nutrition

pharmacology & toxicology

cardiovascular sciences

development

- Eight basic science departments in the Faculty of Medicine
- A community of internationally renowned researchers
- State-of-the-art facilities on campus and at affiliated hospitals and institutes
- Guaranteed financial support

UNIVERSITY OF TORONTO
FACULTY OF MEDICINE